Multiscale modeling of thermochemical conversion of bio-oils

Chourouk Nait Saidi

INSTITUT POLYTECHNIQUE DE PARIS

NNT : 2020IPPAE010

Thèse de doctorat

Modélisation de la conversion thermique de carburants verts de type bio-huiles

Thèse de doctorat de l'Institut Polytechnique de Paris
préparée à l'école nationale supérieure de techniques avancées

École doctorale n°626 de l'Institut Polytechnique de Paris (IP Paris)
Spécialité de doctorat : Biologie et Chimie (Génie des procédés et énergétique)

Thèse présentée et soutenue à Palaiseau, le 14 décembre 2020, par

CHOUROUK NAIT SAIDI

Composition du Jury :

Christophe Coquelet Professeur, Mines ParisTech (CTP)	Président
Christelle Miqueu Maitre de conférences (HDR), UPPA (LCFR)	Rapportrice
Jean Philippe Passarello Professeur, Université Paris 13 (LSPM)	Rapporteur
Amparo Galindo Professeur, Imperial College of London (CPSE)	Examinatrice
Pierre Millet Professeur, Université Paris-Sud (ICMMO) - AREVA H2Gen	Examinateur
Patrice Paricaud Professeur, ENSTA Paris (UCP)	Directeur de thèse
Julian Garrec Enseignant-Chercheur, ENSTA Paris (UCP)	Co-directeur de thèse

Multiscale Modeling of Thermochemical Conversion of Bio-oils

Dr. Chourouk NAIT SAIDI

“He Who created from a green tree a fire for you,
a fire to light your stoves with”

The Quran, (36:80)

الَّذِي جَعَلَ لَكُم مِّنَ الشَّجَرِ الْأَخْضَرِ نَارًا فَإِذَا أَنتُم مِّنْهُ تُوقِدُونَ
(سورة يس: آية 80)

“If you want to find the secrets of the universe,
think in terms of energy, frequency and vibration.”

Nikola Tesla (1856-1943)

Dédicace

À ceux qui m'ont toujours épaulé et aimé inconditionnellement. À ceux qui ont toujours cru en moi,

À toi ma chère maman Amel Mahai,

À toi mon cher papa Nacer Nait Saidi,

À mes sœurs adorées Wiam et Nada,

À mon cher frère Islem,

Sans vous je n'aurais pas connu l'amour, sans vous je n'aurais jamais réussi à aller de l'avant. J'aurais beau essayer de trouver les mots pour vous remercier d'être la meilleure famille que l'un peut avoir. J'aurais beau essayer, je ne pourrais vous exprimer ma grande affection et ma profonde reconnaissance. Les mots m'échappent alors je préfère simplement vous dire je vous aime infiniment.

À toi ma chère tante Hamida Mahai, tu es bien plus qu'une tante pour moi, tu es une maman à mes yeux et je ne saurais te remercier pour le soutien moral que tu m'as apporté cette année.

À ceux que j'aime, à mes amis, merci d'avoir cru en moi et d'avoir été patient durant ces 3 années d'aventure. Vous êtes à la fois une richesse et une bénédiction.

Je vous dédie ce travail humblement. Puisse Dieu vous protéger, vous accorder la santé et une longue vie remplie de Bonheur.

Chourouk

Acknowledgments

First, I would like to thank the committee for accepting to evaluate this work. In particular, my reviewers Professor Jean Philippe Passarello from Université Paris 13 and Doctor Christelle Miqueu from Université de Pau et des Pays de l'Adour (UPPA) for accepting to review my thesis. I also thank all committee members, Professor Christophe Coquelet from Mines Paris, Professor Pierre Millet from Université Paris-Sud and Professor Amparo Galindo from Imperial College of London for their interest in this topic.

I would like to thank my supervisor, Professor Patrice Paricaud whose expertise was invaluable in formulating the research methodology. A deep gratitude goes to Doctor Julian Garrec for his insightful feedback that pushed me to sharpen my thinking and brought my work to a higher level. A special thanks to Professor Laurent Catoire as the laboratory head of UCP for his help and advice.

All my gratitude goes to my colleagues Doctor Detlev Conrad Mielczarek and Doctor Boyang Xu which without them this research study could not be done. This research was funded by Institut Polytechnique de Paris.

I am also thankful to Professor Eliseo Ranzi from Politecnico di Milano, Doctor Antony Dufour from LRGP - CNRS and Professor Andreas Klamt from Regensburg University for the valuable discussion that I had with each one of them.

I would also like to thank the one who encouraged and advised me before my presentation, the wonderful doctor Assia Asrir.

My appreciation also extends to my laboratory researchers and colleagues, Professor Johnny Deschamps, Doctor Diévart Pascal, Doctor Kerim Mansour Dolè, Fincias-Aguilera Nicolas, Belblidia Naila-Besma and Brialix Kévin for their help and encouragement during the last three years.

Contents

List of Figures

List of Tables

Nomenclature

θ_i	Normalized surface fraction
$\Delta G^{\infty}_{i,solv}$	The solvation gibbs free energy of a solute i at infinite dilution
ΔG_{solv}	The solvation gibbs free energy
ΔH^{0}_{solv}	The enthalpy of solvation at standard pressure 1 atm
$\Delta W\left(\sigma_m, \sigma_n\right)$	Exchange energy, kcal/mol
γ_i^{∞}	Activity coefficient of solute i at infinite dilution
Λ_i	The thermal De Broglie wavelength of a molecule i
μ_i^l	The chemical potential of a solute i in the solution l
μ_i^{*ig}	The pseudochemical potential of a solute i in the ideal gas phase
μ_i^{*l}	The pseudochemical potential of a solute i in the solution l
μ_i^{ig}	The chemical potential of a solute i in the in the ideal gas phase
ϕ_i	Normalized volume fraction
ρ_i^l	The density of solute i in the solution l
ρ_i^{ig}	The density of solute i in the ideal gas phase ig
σ	Averaged or "apparent" Surface-segment charge-density distribution, $e/\text{Å}^2$
σ^*	The screening charge density from the COSMO output, $e/\text{Å}^2$
σ_{hb}	The sigma-value cutoff for hydrogen bonding, $e/\text{Å}^2$

φ_i	Fugacity coefficient of component i, dimensionless
A_i	The total cavity surface area
a_{eff}	The surface area of a standard surface segment
c	The empirical correction factor
c_{hb}	Constant for hydrogen bonding
D_i	The diffusivity of a species i
d_{mn}	The distance between segments m and n
f_i	Fugacity of component i, Pa
h	The Planck constant
k_B	The Boltzmann constant
k_{diff}	Rate of diffusion
k_{gas}	Kinetic rate of the reaction in the gas phase
k_{solv}	Kinetic rate of the reaction in the liquid phase
K_{vs}	The gas-solvent partition coefficient of a solute at 298 K
P	Pressure, Pa
$p_i(\sigma)$	The sigma profile for a molecule i
P_i^{sat}	Saturation pressure or vapor pressure of solute i, Pa
$p_s(\sigma)$	The sigma profile for a mixture
q_i	Normalized surface-area parameter
R	The ideal gas constant
r_i	Normalized volume parameter
r_n	The radius of segment n
r_{eff}	The radius of a standard surface segment

T Temperature, K

x_i Molar fraction of component i in a liquid system, dimensionless

Z The compressibility factor, dimensionless

z Coordination number

AAD Absolute average deviation

B3LYP Becke's 1988 exchange functional, 3-parameter, with the correlation functional by Lee, Yang and Parr

BP86 Becke's 1988 exchange functional and the gradient-corrected correlation functional Perdew 1986

CCSD(T) Coupled Cluster Single-Double and perturbative Triple where the triple excitation is calculated using perturbation theory.

CPCM The conductor-like polarizable continuum model

D3BJ DFT-D3 damping model with Becke and Johnson damping

DFT Density functional theory

HEAT High accuracy Extrapolated Ab initio Thermochemistry method

HPC High Performance Computing

M06-2X Minnesota Global hybrid functional

msd mean square deviation

RI Resolution of Identity approximation (also called density fitting)

Context and Scope

The world is currently going through its hottest years and serious health crises, this is the result of an over-consumption lifestyle and an impending demographic crunch that induce a migration towards more hospitable places, an urbanization and mobility growth along with a massive energy demand. The world energy needs are constantly increasing while oil resources are not inexhaustible and the combustion of fossil fuels generates more and more greenhouse gas emissions. These facts lead us to think and act for not only a geopolitical but also a civilizational change to save humanity.

As an illustration, the global population was 1.6 billion a century before (1900), 2.5 billion fifty years later, and more than 7 billion human beings today. This demographic crunch is expected to grow faster in the next decades. On the other hand, energy consumption was less than 1 billion tons of oil equivalent at the beginning of the century and went to more than 13.9 billion tons of primary energy today. More than half of our energy comes from fossil fuels, approximately 32% come from oil exploitation, 22% come from natural gas exploitation and 27% come from coil exploitation (IEA Data of 2017)[1] as illustrated by the pie chart in Figure 1.

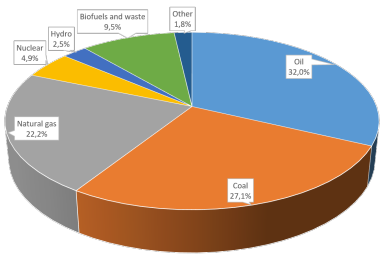

Figure 1: World total primary energy supply by sources in 2017[1].

To limit this global warming problem, ensure energy demand and reach the Paris agreement and Kyoto objectives, it is necessary to reduce energy consumption, to establish energy efficiency in all possible processes and to limit and capture greenhouse gas emissions. Today, fossil fuels constitute the bulk of our energy source consumption, the greenhouse gas emissions released from their thermal conversion; mainly from their combustion; accumulate in the atmosphere, absorb the sun counter radiation and emit it back towards the Earth leading to an increase of global tem-

peratures or what we commonly call global warming. For example, the residential sector in France, represents 43% of the national energy consumption and 25% of greenhouse gas emissions. In order to maintain the international climate protection process, including the specific target of limiting global warming to well below 2 °C, novel bio process and renewable sources are in development to enhance the change in the field of energy and tomorrow mobility. This study discusses the improvement of biomass thermo-degradation process "pyrolysis" using multi-scale approaches to better understand the chemical mechanism and estimate thermochemical data. Biomass is formed from living species like plants and animals, or species that are now alive or were a short time ago. This characteristic allows biomass to develop or regenerate quickly; some of biomass plants take not more than 5 years; unlike fossil fuels that take millions of years to develop, for that, it is considered renewable. Lignocellulosic biomass (plant biomass) is an interesting raw material for the production of fuels and chemicals, with it prodigious potential owing to its renewable character, widespread distribution, abundance and low price. There are multiple sources of biomass as schematized in Figure 2, we can cite:

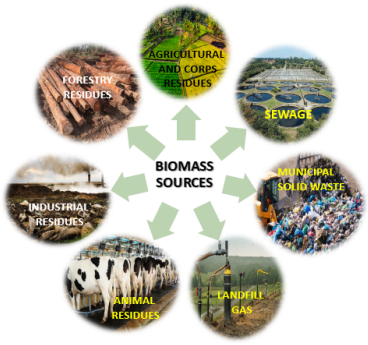

Figure 2: Biomass resources.

- Agricultural: food grain, cotton, "bagasse" (crushed sugarcane), corn stalks, straw, seed hulls, nutshells, and manure from cattle, poultry, and hogs.
- Forest: trees, wood waste, wood or bark, sawdust, timber slash, and mill scrap.
- Municipal: sewage sludge, food waste, waste paper, and yard clippings;
- Energy: poplars, willows, switch grass, prairie blue stem, corn, and soybean, canola, and other plant oils;
- Biological: animal waste, aquatic species, biological waste.

In this context, biomass thermal conversion has significant potential to expand in the production of heat, electricity, and fuels for transport. There are three main thermal biomass conversion processes: combustion, gasification, and pyrolysis. The comprehensive description of these thermal degradation of biomass processes is a very complex and challenging problem at several levels[23]:

- Multicomponent problem: Biomass needs to be properly characterized. It is a complex mixture of mainly organic components and also inorganic components. It usually reduced to the three main polymers: cellulose, hemicellulose, and lignin.
- Multiphase problem: The solid biomass reacts in a condensed phase and a gas phase for secondary reactions. This biomass thermal decomposition results in the formation of released products at different phases: a solid (char or biochar), a liquid (bio-oil), and a gas.
- Multiscale problem: The transport phenomena in the gas and solid phases, and between the solid and gas phases need to be considered both at the reactor scale and at the particle scale to define local temperature profile, concentrations of intermediate and final species and consequent reactivity.

A deep understanding of the kinetics of biomass pyrolysis is very important to maximize the bio-oil yield, improve the quality of the bio-oil and optimize the process parameters. Detailed chemical kinetic modeling is a valuable tool to understand and optimize the conditions of such a complex chemical system. In our work we will try to add new chemical kinetic modeling aspects of biomass pyrolysis in order to improve existing mechanisms and to complete existing thermochemical data. The pyrolysis process may be divided into different stages according to the heating rate, as described by Basu[24]. The first step is the drying of biomass: during this step the biomass is heated to a temperature around 100 °C, and the release of free moisture is observed. Afterwards, the pyrolysis process starts at temperatures between 100 and 300 °C, and the exothermic dehydration of the biomass takes place with the release of water and low-molecular-weight gases like CO and CO_2. At this stage a liquid phase can be observed. The primary pyrolysis step occurs in the temperature range 200 °C to 600 °C, and most of the condensable compounds are produced. To our knowledge, no modeling study of the rate of reactions in the liquid phase has been proposed for biomass pyrolysis.

The investigation of liquid phase reactions of such complex systems requires a good knowledge of solvent effects. It is often assumed that the solvent does not participate in the reaction via atom bonding or transfer, and the solvent is treated as a continuum that induces electrostatic interactions and modifies the solution phase energies of the reactants, transition states and products[25]. This leads to the following question: how can one estimate this solvent contribution to the kinetic rates in liquid phases?

Green and coworkers[26] proposed an approach that has mainly been used to study the liquid phase oxidation of surrogate fuels[27–29]. Depending on the solvent, the rate

of reaction is impacted as the pathways and product distribution change. The two different effects that can be observed are: (1) an increase or decrease of the activation energy E_a and (2) the competition between diffusion and reaction rates. According to Green[26], one can estimate the liquid phase kinetics based on the gas phase kinetics and solvation free energies.

Therefore a reliable kinetic study in the liquid phase requires accurate values for both gas phase properties and solvation free energies. Solvent molecules surround the other solute molecules and they rearrange to form a cage. The solute molecules find themselves trapped and this phenomenon becomes important when we are in presence of strongly hydrogen-bonded effect. Due to this limiting space in the liquid phase, solute molecules "reactants, products and transition states" find themselves in constant collision with each other or with solvent molecules and hence they can exchange kinetic energy with reactants.

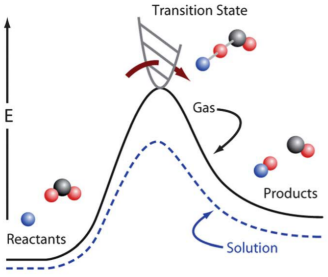

Figure 3: Influence of solvent on potential energy surface (PES) for a reaction in the gas phase and in solution (reprinted from Fleming 2012[2]).

This energy exchange influence the barrier energy of the reaction as can be seen in Figure 3. There are some limited cases where diffusion limit will l control the kinetics of reactions. It is considered that reactions with activation energies of less than 4 kcal are diffusion limited. This happens when the gas phase reaction rate is very fast thus the liquid phase reaction rate will resume to the rate of diffusion. Most of the radical recombination reactions are diffusion limited. Solvent effects have been studied with lots of attention due to their role in free radical polymerization. The experimental works of Ingold et al.[30–33] on Hydrogen abstraction reactions are one of the most cited works of kinetic solvent effects on free radical reactions. Other works are also done to investigate the solvent effects on free radical reactions as β-scission of alkoxy radicals[34,35], addition of radicals to alkenes[36,37] and decarbonylation of acyl radicals[35]. In Chapter 3 of this PhD thesis, we will discuss in detail the solvation energy predictive methods and propose an ab initio method based on activity coefficient prediction . On other hand, the accurate prediction of thermochemical properties is of crucial importance for many industrial applications such as the design of reactors, engines or combustion chambers. While chemists use accurate methodologies to predict molecular properties and reaction energetics, engineers are generally interested in enthalpies of formation, heat capacities and Gibbs free energies. However, these properties may not be known for chemical species encountered in the decomposition of biomass. As a result, it is highly

desirable to obtain an efficient and versatile method by which these values can be calculated, ideally in a black box tool for engineers, while still maintaining the full range of control desired by computational chemists. The calculation of properties at reasonable cost has been a consistent theme in the computational chemistry community and can be traced back to the earliest methods[38]. This has traditionally led to the development of more complex and complete schemes which were designed to provide higher accuracy results, often in conjunction with larger basis sets[39,40]. Predictive methods based on ab initio calculations[16,17,41] can be very accurate for predicting gas phase thermochemical properties and are usually more versatile than group contribution methods. An extension of ab initio prediction method of Paulechka and Kazakov[16] was proposed by Detlev et al.[42] and used for biomass compounds. This work is part of this PhD thesis, and will be presented in detail in Chapter 2.

Given these explanations, it is clear that the availability of a reaction model, composed of elementary reaction steps, for the biomass pyrolysis process would be of tremendous value to engineers who try to make this technique economically feasible. However, despite many research studies in biomass pyrolysis, such a model has not yet emerged due to the complexity and variety of components found in biomass material. Although we only consider three major components of biomass: cellulose, hemicellulose and lignin, the pyrolysis process is still not well understood, because the relative compositions of these three different components vary substantially in different biomass sources. Besides, these components are not well-defined molecules but macro molecules with varying degrees of polymerization. Not all reactions in a given mechanism can be described by rate estimation methods. We will provide examples for reaction systems of expected importance in biomass liquid phase chemistry. We will present calculations related to the initial formation of tar compounds via the condensation reactions of some lignin-related compounds at relatively low pyrolysis temperature.

The first Chapter of this manuscript presents the state of the art and a literature review of the biomass decomposition process, theory of the kinetic modeling and calculation methods used in this study.

The second Chapter presents the prediction of enthalpies of formation and heat capacities based on the performance of the method proposed by Paulechka and Kazakov[16] and by expanding the test set to cover more elements. Then, we propose a method to estimate solvation energies, based on activity coefficients predicted from ab initio calculations using the COSMO model.

In the last Chapter 4, a multi-scale methodology developed to generate a kinetic model for biomass lignin surrogate reactions in the liquid phase is presented.

Chapter 1

Literature Review

1.1 Biomass

Biomass is a composed word first recorded between the years 1930 and 1935. It is formed with the prefix "bio" which refers to a living matter and "mass". So from an ecological point of view, biomass can be defined as the amount of living matter in a given habitat, expressed either as the volume of organisms per unit volume of habitat or as the weight of organisms per unit area. And from an energy point of view, biomass is a potential energy source, as it is an organic matter that can be converted to fuel. According to this definition, biomass can resume to all kinds of materials that were directly or indirectly derived from photosynthesis reactions, such as vegetal matter, agricultural and agro−industrial by−products, animal by-products and human organic wastes.

Biomass as a potential energy source can be converted into heat and electricity or into fuels (charcoal, oil or gas) by both thermochemical and biochemical conversion technologies. Biochemical conversion technologies include fermentation for alcohol production and anaerobic digestion for production of methane enriched gas. On the other hand, thermochemical conversion of biomass is one of the most promising methods for the production of various chemicals and bio-oil to replace fuels obtained from the processing of fossil resources. We have four thermochemical conversion processes. The first is combustion and is the most developed and most frequently applied. The second is gasification of biomass and it converts biomass into a combustible gas mixture by the partial oxidation of biomass at high temperature, in the range 800 °C to 1100 °C. The third is liquefaction: in this process liquid is obtained by thermochemical conversion at low temperature (250 °C to 350 °C) and high pressure (100 bar to 200 bar) using a catalyst in the presence of high hydrogen partial

pressure. It is an expensive process and the product has a higher calorific value and lower oxygen content.The fourth and the best suited process for conversion of biomass to liquid fuel is pyrolysis. Different pyrolysis process types exist according to the heating rates, time reaction, type of reactor and the use of catalysis. We find four different types: slow pyrolysis, fast pyrolysis, flash pyrolysis and catalytic biomass pyrolysis.

The formed biomass conversion products can be divided into solid, gaseous and liquid fractions. Bio-oil is the liquid product. Unlike fossil fuels, bio-oil exhibits characteristics such a high oxygen concentration, high viscosity, high acidity, high moisture content, low calorific value, water and solid content, and a very poor stability that changes its physical and chemical properties[14]. This restricts its application and use as a possible fuel.

The biomass characterization relies on elemental, proximate and biochemical analysis, but they are usually unavailable, uncertain or incomplete. The hard part of biomass characterization is due to its complexity and heterogeneity.

Biomass is a mixture of a wide variety of organic and inorganic components. Hence it is very useful to use modeling tools for the characterization of biomass starting from basic information, as the elemental analysis of its materials.

Thus, biomass characterization is reduced to the definition of the composition of a limited number of selected models or reference compounds[23]. The three elemental natural polymers components of biomass are cellulose, hemicellulose and lignin, together with minor pectins, proteins, and minerals called extractives as presented in figure 4.

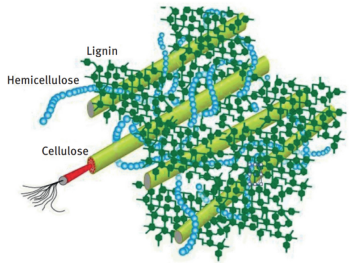

Figure 4: Cellulose, hemicellulose and lignin plant cells (reprinted from Wang et al.[3]).

- **Cellulose**, is a linear macro molecular polysaccharide that consists of a long chain of glucose units linked by $\beta - 1,4-$glycosidic bonds. Cellulose is the most abundant organic polysaccharide on the planet. Woody biomass contains approximately 45% cellulose. Its amount varies from 90% (by weight) in cotton to 33% for most other plants[5]. The chemical formula of cellulose is often denoted as $(C_6H_{10}O_5)_n$,where n is the degree of polymerization. The average degree of polymerization for woody fiber is at least 9000 to 10,000 and possibly as high as 15,000. The glycosidic bonds linking the glucose units in cellulose are not strong and tend to cleave under acid or high temperature conditions. Therefore, the cellulose structure degrades sharply during the initial stages of

fast pyrolysis with the reduction of degree of polymerization due to the cleavage of glycosidic bonds. Cleavage of $\beta-1,4-$glycosidic bonds contributes largely to the formation of furans and levoglucosan[43].

- **Hemicellulose**, is the second most abundant component of lignocellulosic biomass, accounting for 20–35$wt.\%$ of dry biomass. Hemicelluloses are defined as a group of cell wall polysaccharides that are not classified as either cellulose or pectin[5]. Hemicellulose presents an amorphous and branched structure composed of short chain heteropolysaccharides. Although the shape of the polysaccharide chain is similar to that of cellulose, the degree of polymerization of hemicellulose is approximately 200 on average. The functional groups of hemicellulose include pentoses (xylose and arabinose), hexoses (mannose, glucose, and galactose), hexuronic acids ($4-O-$methyl-Dglucuronic acid, galacturonic acid, and glucuronic acid), small amounts of rhamnose and fucose, and acetyl groups. These functional groups can assemble into a range of various hemicellulose polysaccharides, such as xylans, mannans, xyloglucan, $\beta-1,3;1,4-$glucans, and galactans, with diverse structures from linear to highly branched.

- **Lignin**, is the most complex of the three major biomass polymers. Lignin is known as a protective cell components, it reinforces the plant cell walls by bonding with cellulose and enhances the water proof nature of plant cell walls because of its hydrophobicity, thus allowing the efficient transport of water in the vascular tissues of plants. Lignin is also deposited in wounds as a barrier against attack by insects. In contrast to the carbohydrates structure of cellulose and hemicellulose, lignin has an aromatic matrix. The lignin content varies among species of biomass and even among morphological parts of a plant.

  Important structure and functionality distinctions between softwood lignin, hardwood lignin, and herbaceous crop lignin are observed. For example, soft wood lignin accounts for $25-35\%$ of the total plant mass, while hardwood and grass lignin accounts for $20-25\%$ and $10-15\%$, respectively. The complex structure of lignin contains numerous ether linkages, OH groups, and methoxy groups as shown in figure 5. Lignin is mainly anamorphous tridimensional cross linked phenolic polymer composed of three basic monomers, $p-coumaryl(4-hydroxycin-namyl)$, coniferyl $(3-methoxy4-hydroxycinnamyl)$ and sinapyl $(3,5-dimethoxy4-hydroxycinnamyl)$ alcohols, which are also known as p-hydroxyphenyl (H), guaiacyl (G) and syringyl (S) units, arranged in a hyper branched topology with no regular repeating structure. These units are interconnected through various cross-linkages and $C-C$ inter unit linkages in

macro molecular lignin. The most abundant is the ether linkage, representing about $50 - 65\%$ of all inter-sub unit bonds[44].

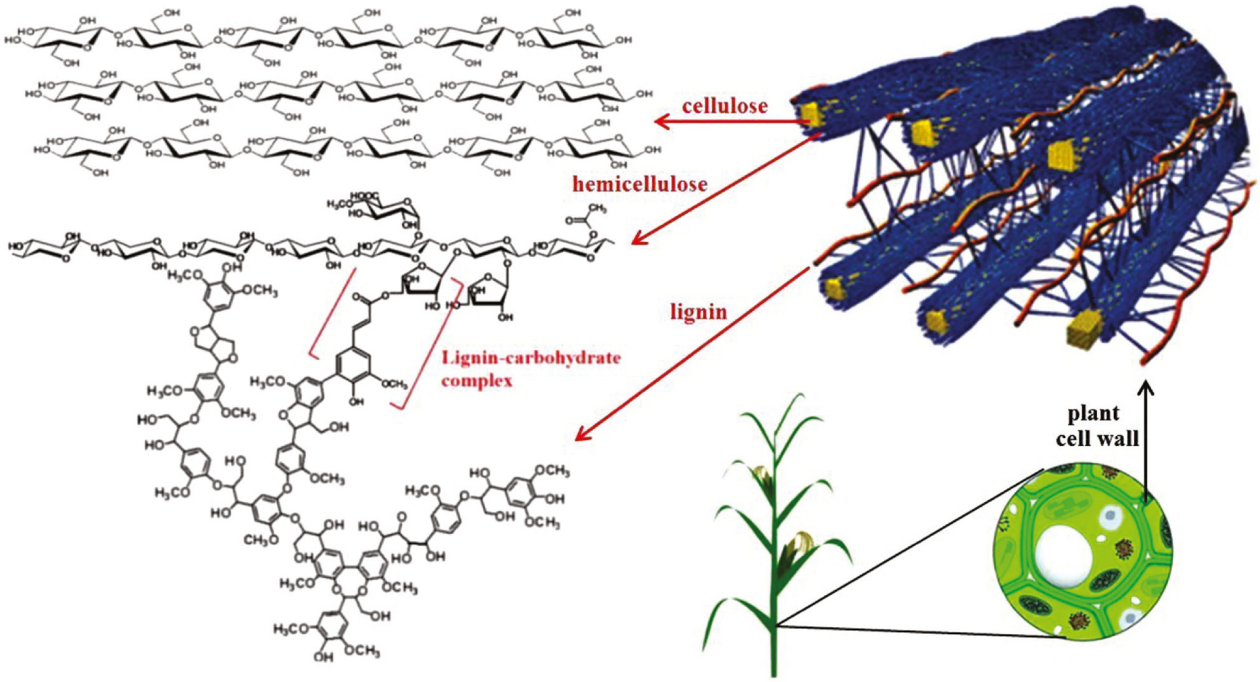

Figure 5: Structure of cellulose, hemicellulose and lignin linkages on plant cells (reprinted from Bohdan et al.[4]).

1.2 Biomass thermal conversion

Burning of biomass in wildfires has been a natural process on earth since humans discovered fire. Nowadays bioenergy can be converted from biomass via two main types of processes: thermochemical and biochemical or biological processes. Thermochemical conversion processes are more efficient than biochemical processes in terms of the lower reaction time required (a few seconds or minutes for thermochemical processes vs. several days, weeks or even longer for biochemical processes). For example, lignin materials are typically considered to be non fermentable and thus cannot be completely decomposed via biological approaches, whereas they are decomposable via thermochemical approaches. The different biomass conversion processes and products are schematized in figure 6. In the following section we will define the different conversion processes and compare them to the promising pyrolysis process.

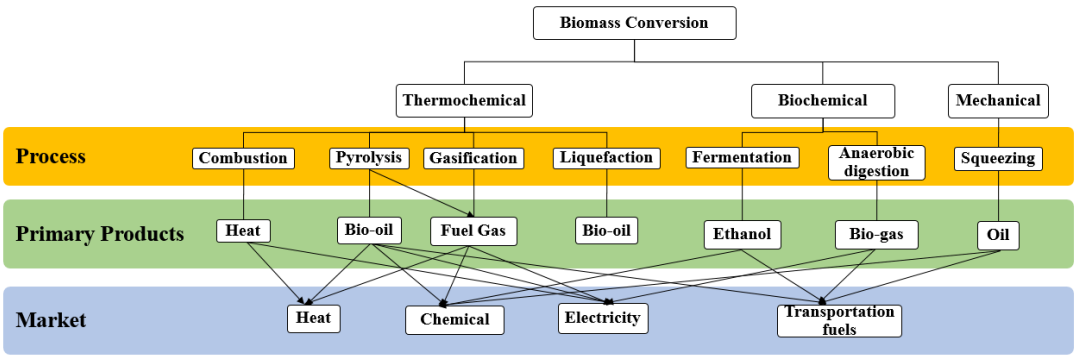

Figure 6: Biomass conversion processes and products.

1.2.1 Combustion

Combustion is considered as one of the first chemical reactions controlled by humans. It occurs between a fuel and an oxidizing agent; oxygen most of the time; to produce heat, energy and light in the form of flames. Combustion intrigued philosophers and scientists from earliest times. Every civilization had its own explanation for them. The Greeks first interpreted combustion in terms of a certain inflammable principle contained in all combustible bodies and this principle escaped when the body was burned to react with air. This was one of the Greeks philosophical doctrines at that time, but the first scientific approximation was posited by the French chemist Antoine-Laurent Lavoisier in 1772. The first experimental studies on combustion were conducted by the English chemist Sir Humphry Davy from 1815 to 1819. Sir Humphry Davy investigated measurements of flame temperatures, the effect on flames of rarefied gases, the dilution with various gases; and also discovered the oxidation of combustibles on a catalytic surface "catalytic combustion"[45]. During the 19th century, the kinetic theory of gases that took place based on the motions of molecules and atom. This ended up by the development of kinetic modeling and automatic reaction mechanism generations, a promising tool to simplify the complexity problems of combustion process as pyrolysis, a process with multicomponent problem.

Combustion is the most used biomass conversion process. It contributes to over 97% of bioenergy production in the world. Combustion is considered as a proven low cost, but highly reliable technology, besides it is relatively a well understood process and commercially available. But on a large scale, combustion of biomass is still a

complex process with technical challenges due to the biomass fuel characteristics, types of combustors, and the of co-firing process problems[46]. Moreover, it is to be noted that biomass combustion power plants differ mainly in the areas of fuel composition, boiler designs, and environmental regulations. Based on that, we can define three different combustion systems, fixed bed, fluidized bed, and dust combustion system.

1.2.2 Gasification

Gasification is the conversion process of solid feedstock like biomass or liquid feedstock in the presence of an externally supplied oxidizing agent into combustible gases (e.g. H_2, CO, CO_2, and CH_4) with a convenient heating value. These gases are used for the production of energy or value added chemicals. When the employed oxidizing agent is air or oxygen (O_2) gasification is similar to combustion, but considered as a partial combustion (typically 35% of the O_2 demand for complete combustion).
Gasification is optimized with respect to a maximum gas yield while pyrolysis is optimized with respect to a maximum char or tar yield. The operation temperature range of gasification is between 800 °C to 1100 °C[47].
The gasification, process may typically include the following steps: the biomass drying; the thermal decomposition or pyrolysis; partial combustion of some gases; vapors and chars; and the gasification of the decomposed products.

The use of a medium like air, steam/oxygen, water/oxygen or pure oxygen is essential for the gasification process. During this process, the molecular structure of the feedstock rearrange to convert the non decomposed carbon char (non-volatile) from pyrolysis into gases (syngas). According to that, the main difference between pyrolysis and gasification is that pyrolysis partially removes carbon from the feedstock at a temperature range 200 °C to 800 °C without any oxidizing agent, while gasification uses a fraction of oxidizing agent to convert the pyrolysis product at higher temperature range to produce syngas. Gasification can add hydrogen to the products, which is not the case for pyrolysis.

1.2.3 Pyrolysis

Pyrolysis is the term given to the thermal degradation (depolymerization) of organic matter in the absence of an externally supplied oxidizing agent like oxygen. It is globally an endothermic process. The rapid heating of biomass in such an inert atmosphere results in the production of organic vapor composed of fragments of cellulose, hemicellulose, and lignin polymers, tar and carbonaceous charcoal. Biomass

type and composition, temperature, pressure, heating rate and reaction time are all variables that affect the amounts and properties of the products formed. Pyrolysis will be discussed in more details in the following Section 1.3.

1.2.4 Liquefaction

Liquefaction is another thermochemical conversion process that gives rise to an oily liquid phase at low temperatures 250 °C to 350 °C and high pressures 100 bar to 200 bar. Liquefaction usually takes place in presence of a high hydrogen partial pressure and a catalyst to enhance the rate of reaction and improve the selectivity of the process. In comparison with pyrolysis, liquefaction gives a higher bio-oil yield with a higher calorific value and lower oxygen content [47].

Liquefaction can be classified into different reaction paths and conditions according to Chornet et al. [48], solvolysis, thermal decomposition under reducing atmosphere, aqueous medium (acidic hydrolysis, basic hydrolysis, neutral hydrolysis) and organic medium.

1.3 Pyrolysis

Pyrolysis is a thermal decomposition process that takes place in the absence of oxygen to convert biomass into solid charcoal, liquid (bio-oil), and gases at elevated temperatures. Pyrolysis is considered to be an industrially realized process for biomass conversion. The pyrolysis products are mainly tars and carbonaceous charcoal, and low molecular weight gases. In addition, CO and CO_2 can be formed in considerable quantities, especially from oxygen-rich fuels, such as biomass. Pyrolysis of biomass starts at 350 °C to 550 °C and goes up to 700 °C.

1.3.1 Pyrolysis operating parameters

The decomposition of biomass through pyrolysis process can be controlled by several parameters. Though an optimized process conditions are needed, it is still very difficult to control the pyrolysis process and obtain the desired products at a high yield. In this section, we will try to overview the different pyrolysis operating parameters.

- **Temperature** The most important and significant parameter is the reaction temperature. Many research groups investigated the effect of temperature on biomass pyrolysis yield products [24,49]. The pyrolysis temperature increase causes a reduction in char yields and enhances gas yields at temperature over

600 °C. These observations suggest that secondary reactions of the liquid fraction and further char decomposition reactions are promoted with an increase of temperature. They concluded that the oil-yield reaches a maximum at temperature in the range of 500 °C to 550 °C[24,49].

- **Heating rate** The effect of heating rate of biomass particles has an importance on pyrolysis product yields. As for the temperature, the increase of heating rate enhances liquid yields and decreases char yields, which suggests that optimum heating rate prevents secondary reactions. Lower heating rate is not favorable for bio-oil production, as it causes longer residence time for volatiles which enable the re-polymerization reactions forming char. If lower heating rates run for several days, the main pyrolysis product is char[49]. Thus a higher heating rate is recommended as it favors the fast formation of volatiles. Adjusting the heating rate to an optimum level results in a maximum bio-oil yields.

  The pyrolysis process may be divided to different stages according to the heating rate as described by Basu[24].
  Drying (~100 °C). During this step the biomass is heated at lower temperature to release free moisture.
  Initial stage 100 °C **to** 300 °C**.** In this stage, exothermic dehydration of the biomass takes place with the release of water and low-molecular-weight gases like CO and CO_2. In this stage a liquid phase is present.
  Intermediate stage (> 200 °C)**.** The primary pyrolysis step occurs in the temperature range of 200 °C to 600 °C. Most of the condensable vapor is produced at this stage.
  Final stage (~600 °C **to** 900 °C). In this stage, the secondary cracking reactions of volatiles into char and non-condensable gases occur.

- **Particle size**

  The biomass particle size directly affects heat transfer, which in turn influences residence time of pyrolysis reactions and volatile matter. This influences bio-oil yield and properties. It is well known that particle size feedstock influences the heat and mass transfer rate. As reported by Basu[24] when the biomass pyrolysis feedstock consists of large particles, the yield of obtained gaseous fraction was higher. Researchers explained that with the residence time increase of volatile matter favoring secondary cracking reactions of tar. So using smaller particle size enhances obtained bio-oil yield. During pyrolysis, heat transfers from the particle's outer surface by radiation and convection, then transfers by conduction and pore convection to the interior of the particle. With low heat

transfer rate, the temperature inside the larger particle is lower than expected, thus causing pyrolysis process to be incomplete and resulting in lower bio-oil yields. Moreover, in larger biomass particles mass transfer resistance is higher resulting in an increase of char yields[49].

- **Residence time and sweeping gas flow rate** Residence time of volatiles is influenced by the sweeping gas flow rate and thus influences the yield of gaseous products. As observed by[49–51] sweeping gas flow rates affected the bio-oil product yield, they have shown that higher sweeping gas flow rate favors vapors removal from the reaction medium, which end by reducing secondary reactions (repolymerization, recondensation) and char formation.

- **Catalyst effect** The catalyst effect has been widely investigated for lignocellulosic biomass thermal conversion. Several studies have shown that the use of a good catalysis improved not only the bio-oil yield but also the quality, stability, acidity and viscosity of the bio-oil product. This was explained by the influence of catalysts on the selectivity of lignocellulosic biomass reactions during thermal conversion, the application of heterogeneous catalysts as zeolites enhanced the reactivity of selective reactions. The catalyst effect in biomass pyrolysis process has also been investigated with different biomass sources.

- **Biomass composition** In biomass, cellulose is generally the largest fraction followed by hemicellulose, lignin and ash[52]. The biomass pyrolysis products are very affected by the biomass feedstock sources. We can note many differences in pyrolysis products and operating parameters according to the type and composition of biomass feedstock. One can first observe the influence of the biomass hydrogen-to-carbon (H/C) ratio on the heating rate. This led us to a preferred temperature range for each one of the three elemental biomass polymers, cellulose in a temperature range of 275 °C to 350 °C, hemicellulose in a temperature range of 150 °C to 350 °C and lignin in a temperature range of 250 °C to 500 °C. On the other hand, the biomass source composition influences the pyrolysis product chemical constitution and distribution, for example an important amount of lignin in biomass feedstock will end by an important amount of tar and char product. Lignin is known as the most difficult part of biomass to decompose and its reactivity is less understood than cellulose and hemicellulose. Recently, many researchers are working on finding a valorization pathways for lignin polymer.

1.3.2 Pyrolysis type

Slow pyrolysis

Slow biomass pyrolysis is mainly used to produce biochar through fixed bed reactors. It occurs at slow heating rate range from 5 K/ min to 80 K/ min. Slow pyrolysis is generally carried in the absence of medium and a liquid phase is observed during the conversion process. Carbonization process is an example of slow biomass pyrolysis process but with a very long residence time, usually the production of charcoal takes days. The conventional biomass slow pyrolysis residence time is on the order of minutes and during this process the three types of biomass pyrolysis products are present: gas, liquid, tar and char.

Fast Pyrolysis

Fast biomass pyrolysis is used for bio-oil production as it produces a higher yield of desirable liquid product. It has been studied since 1970. It involves rapid heating rate but not as fast as flash pyrolysis. The heating rate of fast biomass pyrolysis is higher than 1000 °C/ sec within a temperature range 400 °C to 700 °C, but if bio-oil is the product of interest, the peak temperature should be below 650 °C. Fast biomass pyrolysis process can operate with most of fluidized bed reactors as they offer high heating rates, easy control and easy product collection. Biomass fast pyrolysis liquids cannot be used as transportation fuels directly without prior upgrading due to their high oxygen ($40-50$ $wt\%$) and water content ($15-30$ $wt\%$) and the low H/C ratios. Their limited stability under storage conditions due to the presence of unsaturated compounds and their minor miscibility with conventional liquid fuels are additional obstacles[53].

Flash pyrolysis

The reaction time in this process is of only several seconds or even less. The heating rate is very high. This requires special reactor configuration, the two most appropriate reactors are entrained flow reactor and the fluidized bed reactor. Another important factor to optimize biomass flash pyrolysis is a fairly small particle size, approximately 105 µm to 250 µm[52]. We can distinguish four types of flash pyrolysis:

1. **Flash hydro-pyrolysis.** Hydro-pyrolysis is a flash pyrolysiscarried out in hydrogen atmosphere at a pressure up to 20 MPa.

2. **Rapid thermal process.** It is a heat transfer process with very short heat residence times between 30 m sec and 1.5 sec. Rapid thermal process occurs

in a temperature range between 400 °C to 950 °C, where biomass craking and de-polymerization reactions take place. The advantage of this process is giving a product with comparable viscosity to diesel oil, in fact, a rapid heating eliminates the side reactions thus char and tar formation.

3. **Vaccum flash pyrolysis.** In this process, pyrolysis takes place under vaccum. The vaccum limits the secondary decomposition reactions and facilitates the removal of the condensable products from the hot reaction zone, which in turn gives high oil yield.

4. **Solar flash pyrolysis.** Flash pyrolysis can be performed using concentrated solar radiation. This process is still under experimentation.

Catalytic biomass pyrolysis

According to the literature, one of the most popular processes of bio-oil production from lignocellulosic biomass is catalytic upgrading of pyrolysis vapors. It consists on using a solid catalyst during the initial decomposition of biomass feedstock. Then, the formed intermediate pyrolysis products are upgraded. Using catalysts in biomass pyrolysis influences the decomposition behavior of biomass and composition and quality of the produced oil. The obtained oil does not require costly pre-upgrading process involving condensation and re-evaporation. Various catalysts exist as $ZSM-5$ zeolite, transition metal catalysts (Fe/Cr), aluminas ($\alpha, \gamma - Al_2O_3$) and FCC catalysts[52,54]. The most important factors impacting the catalyst performance are the acidity, the surface area and porosity of the catalyst. It is also known that slow pyrolysis and catalytic pyrolysis occur in a liquid phase. Also different studies investigated the effect of catalyst with different biomass sources.

1.3.3 Pyrolysis reactors

Pyrolysis reactor designs are fixed beds, moving beds, entrained feed solid reactor, suspended and fluidized bed reactors and inclined rotating kilns reactors. As an illustration for the used reactors, we have circulating fluid bed reactor, ablative pyrolysis reactor, bubbling fluid bed reactor, rotating cone reactor, vacuum pyrolysis reactor and ultra pyrolysis entrained flow reactor[52].

1.3.4 Pyrolysis products

Biomass pyrolysis produces both condensable and non-condensable gaseous as well as solid residues called char. According to Yang et al.[55] great differences are found

among pyrolysis decomposition behaviors of the three main polymers (cellulose, hemicellulose and lignin). Hemicellulose started its decomposition easily with a weight loss mainly happened at 220 °C to 315 °C. It exhibits the maximum mass loss rate (0.95 wt.% $°C^{-1}$) at 298 °C, and there was still −20 % solid residue left even at 900 °C. Cellulose pyrolysis is carried out at a higher temperature range with the maximum weight loss rate (2.84 wt.% $°C^{-1}$) attained at 355 °C. When temperature was higher than 400 °C, almost all cellulose was pyrolyzed with a very low solid residue (−6.5 wt %/°C) left. Among the three biomass polymers, lignin was the most difficult one to decompose. Its decomposition happened slowly under the whole temperature range from ambient to 900 °C, but at a very low mass loss rate (<0.14 wt %/°C). The solid residue left from lignin pyrolysis (−45.7 wt %) was the highest. The maximum in all the tar production curves occur at or near 400 °C. At higher temperatures tar yields fall with temperature, while increases in vapor residence times result in greater loss of condensable product.

Solid char, Tars and Ash

The solid part of biomass pyrolysis products is the most useless part induced from the secondary decomposition, re-polymerization and condensation reactions. Its reactivity is also the less understood. As solid char part, we mainly have charcoal and bio-char depending on biomass feedstock type.

The tars are defined as a mixture of condensable hydrocarbons, including aromatic compounds with up to five rings (which can be oxygenated) as well as Polycyclic Aromatic Hydrocarbons (PAHs)[56]. However, according to the meeting about tar measurement protocol carried out in Brussels in the Spring of 1998, between the International Energy Agency (IEA), the Directorate General for Energy of the European Commission and the Energy Department of the United States, has been agreed to define tars as all hydrocarbons with molecular weight higher than benzene[57].

The ashes are more investigated due to their catalytic effect during pyrolysis as they decrease the bio-oil selectivity. In fact, they can interact with inorganic compounds of the solid phase. An accurate biomass pretreatment can reduce ash content but this will decrease the catalytic effect of inorganic salts on biomass products yields. Ranzi et al.[7] proposed a global Ash Factor (AF) to account ash catalytic effect on fast biomass pyrolysis kinetic mechanism.

Gaz

The non condensable gaseous products include H_2, CO, CO_2, and light hydrocarbons such as CH_4, C_2H_6, and C_3H_8.

Bio-oil

The condensable gaseous products include H_2O, aldehydes, low molecular weight alcohols, acids, furans, anhydrosugars, phenols, and aromatics. These products are referred as liquid phase product or bio-oil. Bio-oil is the main product of biomass pyrolysis process. It is obtained from the two step condensation of pyrolysis condensable gaseous products (vapors) Bio-oil is considered as a key renewable energy alternative, but due to its unstable properties during storage, shipment and use, it is still not widely used. Bio-oil is not a thermodynamically stable product, as it is produced with short a reaction time a rapid cooling from the pyrolysis temperature. This produces a condensate that is not at thermochemical equilibrium at storage temperature. Bio-oil is a very complex mixture composed of water, char and hundreds of organic oxygenated compounds : phenols, aromatics, aldehydes, ketones, acids, alcohols, ethers and sulfur compounds, with a wide range of molecular weights.

These compounds can react during storage to produce oligomers and polymers that have a high viscosity and reduced solubility in the bio-oil. Some patterns of reactions that can occur are as follows:

- Acids and alcohols react to form esters and water;
- Aldehydes react with water to form hydrates;
- Aldehydes react with alcohols to form hemiacetals, ethers and water;
- Olefins polymerize to form oligomers and polymers;
- Aldehydes react with phenols in the acidic bio-oil to form resins and water.

The potential reactions within bio-oil can be stabilized with solvents and hydrogenation. In order to investigate the complex chemistry of bio-oil a solvation model is needed to describe the solvent effects in liquid phase oxidation and on the kinetic of bio-oil decomposition.

Table 1.1: List of some components in Bio-oil mixture detected by GC/MS and HPLC and their quantitative concentrations (wt%).[14]

Compound	wt % Typical wood
Cellulose/hemicellulose derived compounds	
Acetic Acid	0.5-12.0
Glyoxal	0.1-1.1
Furfural	0.1-1.1
Furfuryl alcohol	0.1-5.2
Glycolaldehyde	0.9-13
Acetol	0.7-7.4
Levoglucosan	4.8-5.4
Lignin derived compounds	
Guaiacol	0.1-1.1
Isoeugenol	0.1-7.2
2-Methoxy-4-methylphenol	0.1-1.9
2,6-Dimethoxyphenol	0.7-4.8
Phenol	0.1-3.8

1.3.5 Biomass pyrolysis mechanisms

The kinetic modeling made a great progress at both global and micro-kinetic level to describe the thermal decomposition of biomass and its natural polymers, hemicellulose, lignin, and especially cellulose. Most of the kinetic models for biomass pyrolysis reported in the literature are global models. The first global kinetic scheme of cellulose pyrolysis was developed by Broido and his coworkers in 1975[58]. Broido's mechanism included two parallel pathways resulting in the formation of volatiles, char and gas as shown in figure 7.

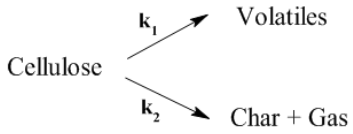

Figure 7: Broido and Nelson model for cellulose pyrolysis.

In 1979, Shafizadeh and coworkers[59] modified Broido's reaction scheme and reported the most generally accepted kinetic model for cellulose pyrolysis, known as

the Broido–Shafizadeh model (B-S model), as shown in figure 8, this model describes the formation of an intermediate species called “active cellulose”.

Figure 8: Broido–Shafizadeh model of cellulose pyrolysis.

Based on the pioneering work of Broido and Shafizadeh variety of kinetic schemes have been developed to describe the pyrolysis of cellulose and biomass, as well as the other two major components: hemicellulose and lignin. The global kinetic models of biomass pyrolysis can be broadly divided into single component models and three component models depending on whether biomass is modeled as a single component or the combination of three components. Models can also be categorized into one reaction/stage models and multi reaction/stage models. Most of these global kinetic models were based on the mass loss data from thermogravimetric analysis of biomass samples.

The simplest thermal decomposition model of biomass pyrolysis is the single component model. This model proposes a single reaction stage that forms directly gas, tar and char from biomass. The single reaction stage model describes the mass loss curve and the degradation rate of biomass during pyrolysis, but they cannot predict product yields from different biomass sources or from the same biomass feedstock under different pyrolysis conditions such as particle size, heating rate, and temperature. The one-stage models also do not include the secondary reactions of tar. The other type of global kinetic biomass pyrolysis model is the multi reaction or multi-stage model. This model describes the thermal decomposition of biomass feedstock by a series of consecutive and parallel reactions to account for both primary and secondary biomass pyrolysis reactions[5].

In 1983, Chan and Krieger[60] proposed a multistep reaction scheme for biomass pyrolysis including the evaporation of moisture as illustrated in figure 9. In Chan and Krieger’s model, the formation of primary gas competes with the formation of tar, which also undergo a secondary decomposition reaction, forming secondary gases and secondary tar, all of it in parallel with char formation. Besides, they account the evaporation of moisture and chemically bound water in biomass to produce vaporized and residual water during pyrolysis.

However, none of the mentioned kinetic models of biomass pyrolysis provide a

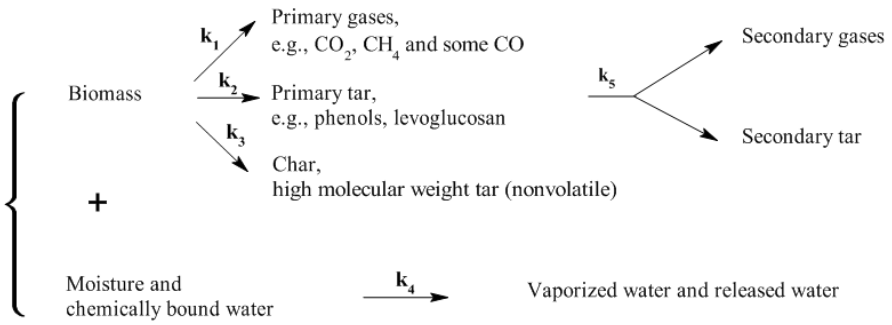

Figure 9: Kinetic scheme of biomass pyrolysis with the consideration of water evaporation proposed by Chan and Krieger (1983).

detailed product composition. Recently Ranzi and co-workers[6–8,61] reported the most applied semi-detailed biomass pyrolysis global kinetic model to predict the yields and lumped composition of gas, tar, and solid residue.

Ranzi et al. mechanism consists of individual biomass reference components; cellulose, hemicellulose, and lignin; decomposition with a multistep kinetic scheme. The biomass pyrolysis products are obtained from a linear combination of gas tar and char released from individual reference components decomposition. The strength of Ranzi's mechanism is that it accounts variations in feedstock composition. The model is able to describe the decomposition of three types of lignin molecules as shown in fig 11. Further, two types of hemicellulose are modeled; glucomannans and xylans, which makes it possible to account for compositional changes seen in various types of biomass like hardwood and softwoods biomass. Moreover, Ranzi's model includes the decomposition of extractives, the catalytic effects of inorganic ash and the secondary gas phase reactions of some of the important products. The biomass pyrolysis mechanism is thus the summation of all these individual reactions.

Moreover, the biomass pyrolysis global kinetic models simplifies data collection and analysis as well as the numerical modeling, which is of great interest for computational chemists and practical engineering applications.

However, there are still many weaknesses in this type of global model. For example, important product species that have been experimentally identified and quantified are not predicted and accounted such as methyl glyoxal, acetic acid, furfural, levoglucosan, furanose, anhydroxylose, dianhydroxylose, and many others. This can be explained by the use of over simplified structures for hemicellulose and lignin so that global models cannot capture the complexity of biomass structure. Also,

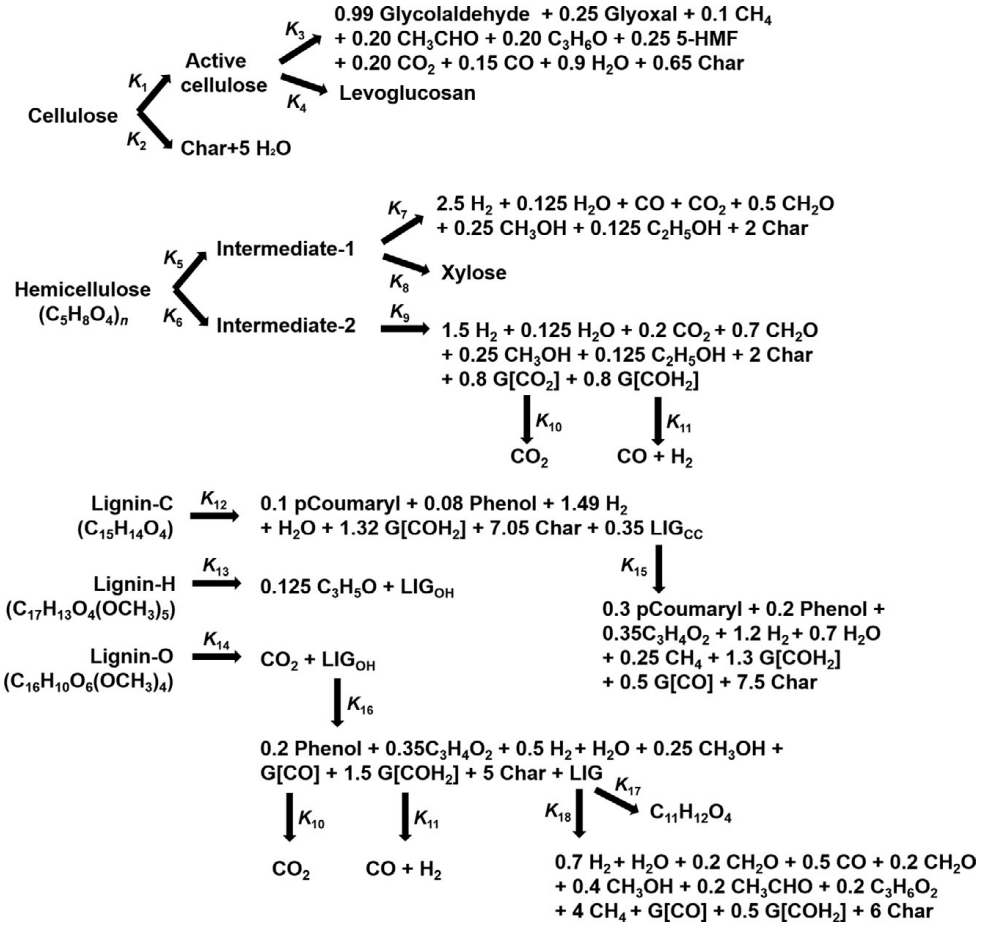

Figure 10: Semidetailed kinetic mechanism of biomass pyrolysis developed by Ranzi and coworkers (reprinted from Zhou et al.[5])

all these models did not discuss the pyrolysis first stage decomposition at low temperature 100 °C to 300 °C were reactions occurs in both gas and liquid phase as observed and mentioned by Nakamura et al.[24,62], especially the lignin monomer that decomposes partially and generates side reactions that produce char and tar with re-polymerization and re-condensation reactions.

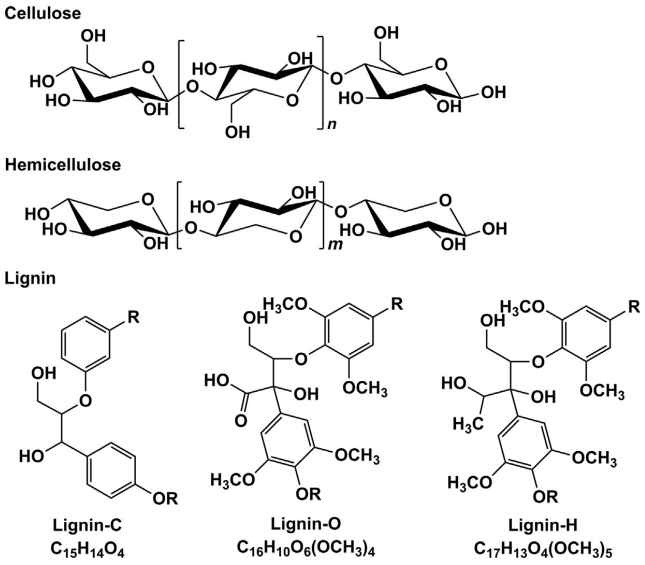

Figure 11: Structures of cellulose, hemicellulose and lignin used in the global kinetic model by Ranzi et al.[6–8]

Despite that, one can say that pyrolysis global kinetic models are able to explain experimental observations and promote an understanding of the kinetic of biomass pyrolysis to a certain extent.

1.4 Thermochemistry and Kinetic Modeling

Despite the fact that chemical kinetic is an old and traditional branch of physical chemistry, its importance is still of topical interest. New theoretical models, new complex and detailed kinetic mechanisms, and their applications are in progress. Over the past 50 years, numerous studies have been conducted to probe the kinetic and mechanism of pyrolysis of biomass and its major components. Pyrolysis kinetic is necessary and very important to maximize the bio-oil yield, improve the quality of the bio-oil and optimize the process parameters.

As we discussed in the previous Section 1.3.5 great progress in kinetic modeling at both the global kinetic level and the micro-kinetic level has been made to describe the thermal decomposition behavior of biomass and its natural polymers, hemicellulose, lignin, and especially cellulose.

Despite these research studies, very few multi-component (or multi-stage) mechanisms of biomass pyrolysis are available, that is, mechanisms for predicting the formation rates and the yields of reaction products or solid, liquid and gas-phase intermediates.

To discuss the kinetic decomposition of biomass surrogate components at the initial stage, one can assume that the solvent do not participate in the reaction. As a result, one can assume that the reactions that occur in the liquid phase are the same as those in the gas phase, even radical reactions. Green and co-workers[26] proposed an approach that has mainly been used to study the liquid phase oxidation of surrogate fuel[27–29]. Depending on the solvent, the rate of reaction is impacted as the pathways and product distribution change. The two different effects that can be observed are: (1) an increase or decrease of the activation energy E_a and (2) the competition between diffusion and reaction rates. According to Green, one can estimate the liquid phase kinetic based on the gas phase kinetic and solvation free energies. The kinetic rate k_{solv} of the reaction in the liquid phase can be estimated from the kinetic rate k_{gas} of the same reaction in the gas phase, as

$$\frac{1}{k_{solv}} = \frac{1}{k_{gas} \exp\left(\frac{-\Delta\Delta G^{*,\ddagger}_{solv}}{RT}\right)} + \frac{1}{k_{diff}}, \tag{1.1}$$

where k_{diff} is the rate of diffusion that can be calculated as[25,26],

$$k_{diff} = 4\pi \sum_i r_i \sum_i D_i \mathrm{N_A}, \tag{1.2}$$

where,

- r_i radii of a species i,
- D_i the diffusivity of a species i estimated using Stokes-Einstein relation

$$* \; D_i = \frac{k_B T}{6\pi\mu r_i}, \tag{1.3}$$

  k_B is the Boltzmann constant, T the temperature and μ the solvent viscosity.

- N_A=6.022 141 29 $\times 10^{23}\,\mathrm{mol}^{-1}$ the Avogadro number.

The term $\Delta\Delta G^{*,\ddagger}_{solv}$ is the difference between the solvation free energies of the transition state (represented by ‡) and the reactants. The symbol $*$ represents the Ben-Naim standard state at fixed concentration[63].

$$\Delta\Delta G^{*,\ddagger}_{solv} = \Delta\Delta G^{*,\ddagger}_{solv} = \Delta G^{*,\ddagger}_{solv} - \sum_i \Delta G^{*,Reactants}_{solv}, \tag{1.4}$$

The gas phase kinetic constant k_{gas} can be expressed with respect to the Arrhenius parameters as,

$$k_{gas} = AT^n \exp(\frac{-E_a}{RT}), \tag{1.5}$$

where R is the ideal gas constant.

1.4.1 Thermochemistry

In order to describe and understand the changes occurring during chemical reactions, not only the chemical composition change of products and reactants but also the change of physical transformation that reactions components undergo as vaporization, melting, sublimation or phase transition between two different states, we need a detailed knowledge of thermodynamic parameters of species. In chemical engineering modeling and physical chemistry calculation, we need a reliable, a consistent and with a high accuracy thermochemical data for a wide range of chemical species. As an example of process and application where a good knowledge of thermochemical data is needed, we have experimental and computational chemical kinetics and dynamics, construction of chemical reaction mechanisms, process designs at both experimental and industrial scale, the study of a single chemical reaction and as in our case the study of complex chemical systems that involve hundreds or even thousands of reactions and species, such as internal combustion engines, pyrolysis or the atmosphere environment. The need for available, reliable and accurate thermochemistry data in these models requires a predictive ability and to extend the actual models for a broad data range.

The majority of tabulated thermochemical data are extracted or inferred rather than being directly measured. As central and important group of thermochemical quantities we have enthalpies of formation; thermochemical quantities related to the partition function and its various derivatives, such as heat capacities, entropies, and enthalpies; and the Gibbs free energies. The prediction of thermochemical properties, such as enthalpies of formation and solvation Gibbs free energies, is of crucial importance in research and industrial applications. This applies especially to systems involving not well characterized molecules, such as biomass systems (bio-oils). It is thus desirable to obtain an efficient method by which these values can be predicted. Although most of the experimental techniques to determine these properties exist, experimental measurements methods can be expensive, difficult or time con-

suming. Different predictive models based on quantum calculations carried out on isolated molecules in a vacuum or in a cavity are widely used nowadays allowing the determination of thermochemical properties and phase equilibria. From 1970, we are now living what is called the "third age of quantum chemistry"[64]. Computational thermochemistry made an amazing progress since the development of electronic structure methods by John Pople[65] and Walter Kohn in 1998 (Nobel Prize), and modern high-level electronic structure theory is becoming capable of rivaling and sometimes even challenging experimental measurements methods. As state of the art of computational thermochemistry approaches, we have the Weizmann-n family (W3, W4[66–70] and W4-F12[69,70]), the Gn methods[16,71–74], the HEAT methods, DFT (Density Functional Theory) and the Group additivity approaches as the well known QSPR (Quantitative Structure-Property Relationship). More details about the electronic structures calculations will be provided in Section 1.4.4. An extension of the method proposed by Paulechka and Kazakov for prediction of enthalpies of formation and heat capacities will be presented in Chapter 2 and an improvement based on COSMO model methods for prediction of solvation Gibbs free energies will be discussed in Chapter 3.

1.4.2 Transition state theory

Let us start with a bit of history, Transition State Theory started its life as "Absolute Rate Theory" and has also been known as "Activated Complex Theory". It was first developed in 1935 by Henry Eyring and by Evans and polanyi[75,76]. Eyring's formulation of transition state theory is probably the one that had the most reaching influence and lasting value, for a bimolecular reaction, $A+B \rightarrow TS^{\ddagger} \rightarrow C$ this famous equation is as follows 1.6,

$$k = \kappa \frac{k_B T}{h} \frac{Q^{\ddagger}}{Q_A Q_B} \exp\left(\frac{-E}{RT}\right), \tag{1.6}$$

where E is the Gibbs energy of activation, κ is the transmission coefficient, k_B is Boltzmann's constant, h is Planck's constant and Q the partition functions. The transmission coefficient is often assumed to be equal to one, this assumes that the no-recrossing assumption of transition state theory holds perfectly.
A transition state is an unstable equilibrium structure which is at the maximum energy along the minimum-energy reaction path that connects two stable structures (the reactant and product). The energy difference between the transition state and the reactant structure is called the activation energy. Except under very special conditions, the structure of a transition state cannot, yet, be determined experimen-

tally. However, by studying chemical reactions at varying temperatures, activation energies can be measured by experiment. In order to overcome this experimental limit, computational chemistry methods can be used to calculate the structure of a transition state, which gives very useful insights into the mechanism of a chemical reaction as well as a predicted value for the activation energy.
Transitional state concepts have been used and investigated to demonstrate the feasibility of assigning rate rules. The advancement in computational chemistry and the increase of computational resources allow electronic structure rate constant calculations to be comparable and reviling to those measured experimentally. However, the high-level theoretical calculations that provide such accuracy are limited to some reactions and relatively small molecules.

As electronic structure calculations progressed (this is discussed in Section 1.4.4 below) to the point at which these TST results were sufficiently accurate to supplement experimental measurements, it became possible to use such calculations to predict rate constants for a series of reactions within a specific reaction class to generalize the results into a rate rule for this class. The potential to generate reasonable reaction class rate rules is based on the assumption that within the same reaction class, the geometries and energetics of the transition states are expected to be similar, thus leading to similar rate coefficients. The very large number of reactions needed in comprehensive reaction models for practical systems, such as those describing the pyrolysis/oxidation of hydrocarbon or oxygenated fuels, make it impractical to attempt to compute every elementary reaction. However, due to the similarity of the potential energy surfaces (PES) within the same reaction class we can use relatively high-level calculations to confirm that the rate constants follow an expected pattern for representative smaller or what we call surrogate components of this reaction class. Another advantage in pyrolysis and oxidation systems of our interest is that the number of reaction classes is limited. The following types of reactions are particularly important and are well discussed with transition state theory in the literature[77]:

- radical isomerizations,
- radical $\beta - scissions$,
- radical hydrogen abstractions,
- radical additions,
- radical recombinations.

1.4.3 Solvent effect

It is appreciated in the chemical kinetic and thermochemistry research sphere that changing the solvent do change reaction rates and sometimes the change can be dramatic. As mentioned by Jalan et al.[78] and Slakman et al[25] many cases are known where the gas phase rate coefficients differ by several orders of magnitude from liquid phase rate coefficients. During the last decades ab initio computation were widely used to calculate gas phase thermochemistry and rate coefficients, and they gave a high accuracy compared to well known experimentally data that gas-phase kinetic data are confidently based on ab initio methods. However, these types of calculation are still not widely used for reactions in solution "liquid phase". This gap between gas phase and liquid phase computation is mainly due to the lack of relevant and reliable estimation methods of solvent effects and also to the lack of direct experimental estimation methods of solvation energies. Predicting the liquid phase rate coefficients of chemical reactions in the absence of experimental data is a challenging task. However, for our system of interest like combustion, pyrolysis and fuel oxidation; common reaction families occur in both gas phase and liquid phase; for example, gas phase combustion of hydrocarbon fuels is dominated by hydrogen abstraction reactions, same thing occur at low temperature. Since these reactions are most of the time well studied in the gas phase or can be well estimated with ab initio computational method in the gas phase, it can be advantageous to modify these known gas phase reaction rates rather than predicting the solution phase kinetic rate directly and this was proposed by Green and co-workers[26] as described in the beginning of Section 1.4.

Up to now, solvation effects are mostly treated with so-called continuum models which place a single molecular species in media with a non vacuum dielectric constant. This means placing the species of our concern in a perfectly screening medium or what we call an electric conductor. This method is known as the COnductor like Screening MOdel (COSMO) and has been developed by Klamt[79–81] and then revised with new parameterizations by Sandler and co workers[11,82,83] which became the COSMO-SAC model. A special case of screening medium around solvated species environments is those with an infinite dielectric constant ($\epsilon = \infty$).

A general conversion of liquid (l) reactants in the bulk or in solution treatment as describes with Green's approach and Deglmann et al.[9] is shown in Figure 12.

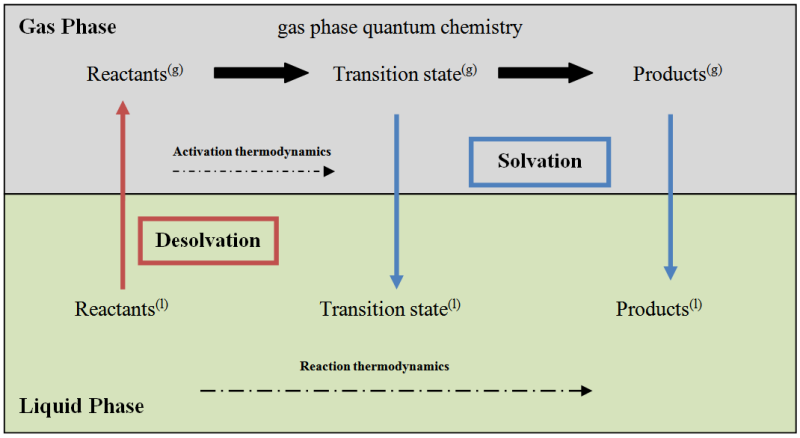

Figure 12: Computation of thermodynamics for chemical reactions in the condensed phase as a circular process involving desolvation and solvation as well as the actual chemical reaction in the gas phase[9,10].

To obtain the thermodynamic functions for the formation of the transition state TS or the products in the liquid phase, the following sequence of processes is considered as described by Deglmann et al.[9,10]:

- Vaporization of the reactants (i.e., computation of negative solvation enthalpies, entropies...),
- Chemical reaction in the gas phase, for which rather accurate quantum chemical methods can be used and thermodynamic functions can be derived from ab initio molecular partition functions (good separability of molecular degrees of freedom in the gas phase),
- Condensation (solvation) of the transition state or the products, which is done with the same equations as the initial vaporization.

The first application of COSMO models to chemical kinetic (activation barriers) was performed by Franke et al.[84] on isomerization reactions of phosphine ligands. Green and coworkers also describe the application of COSMO-RS to predict kinetic data for the oxidation of hydroxylamine by aqueous nitric acid. More recently Deglmann and coworkers[9,10] discussed the use of COSMO-RS model to predict chemical reaction kinetic in solution, and they obtained an accurate description. They reported that the accuracy of quantum chemical predicted Gibbs free energy of activation for radical addition reactions was around $6\,\mathrm{kJ\,mol^{-1}}$.

1.4.4 Electronic Structure Calculation

The total electronic energy of a molecule is a fundamental quantity in quantum chemistry. By virtue of the Born–Oppenheimer separation of nuclear and electronic motion, this total electronic energy is a function of the nuclear geometric configuration, thereby generating hyper surfaces of potential energy for electronically excited states as well as for the ground state. In order to obtain accurate thermochemistry and kinetic data, geometry optimizations and energy calculations of the optimized geometries are required. To reduce computational cost, a two-step approach is commonly assumed[85–87], with a low theory level for geometry investigation and then a higher theory level calculation for the optimized geometry. In some conditions, the gas phase geometries may correspond to the geometry with the lowest energy, while in other conditions, the solvent effect may change the energy level of the geometries. Thus, it is recommended to consider all initial geometries of the gas phase and identify a possible lower energy conformer. Energy barrier height may change due to the stabilizing effects of solvent, also the partition function may also be affected by the solvent effect. Finally, electronic energies are calculated and standard formation enthalpies and solvation energies are predicted with suitable methods.

Ever since the inception of quantum chemistry in the late 1920s, a large body of expertise and experience has been built up on the accurate and efficient calculation of molecular total electronic energies. Today, a variety of quantum chemical methods are available, ranging from semi-empirical methods, like AM1 and PM3, to full configuration interaction. This wide range of powerful techniques are of varying computational time and accuracy. Various models for the electronic wave function and various functional of the electronic density can be employed as well as other less standard techniques such as the quantum Monte Carlo method. The most used methods of present quantum chemistry are those of density functional theory (DFT). But, the reliability and accuracy are yet not sufficient. As a standard method, nowadays, coupled cluster methods, usually coupled cluster singles/doubles(triples) CCSD(T)[88], are applied for high precision calculations. However, coupled cluster methods CCSD(T)[88] are high computational demanding,and there use is limited to systems with less than 20 atoms if appropriate basis sets are used. As mentioned by Deglmann et al.[9] there is no hope that CCSD(T)[88] can be applied to condensed phase at present. For that, we usually use a combination of methods to account solvent effect and provide quantitative results for kinetic in solution.

In the following, we will provide a state of the art for different ab initio methods and density functional methods.

Semi-empirical Methods

So-called semi-empirical methods simplify calculations by using parameters for certain integrals and (or) ignoring certain terms in Hamiltonian. Since most of the calculation time in the ab initio calculation is devoted to the calculation of integrals, semi-empirical methods are much faster. Semi-empirical methods use experimental data or the results of ab initio calculations to perform some of their matrix element or to define their integrals. The most common semi-empirical methods are the MNDO, AM1 (Austin Model) and PM3 methods. The PM6 and PM7 methods are the most recent and correspond to other settings of the PM3 method.

Ab Initio Methods

Ab initio methods are predictive methods that use the complete Hartree-Fock/ Roothaan-Hall equations to describe the wave function as a function of the positions of the nuclei, from first principles without using experimental data. They are classified according to their level of theory and basis set. HF is the starting point in most cases; perturbation theory improves HF systematically, and so on, there is a hierarchy in methods with increasing accuracy. Ab initio methods calculation can be time consuming with high level of theory, for extended basis set, and for a molecule or a group of molecules with many atoms.

- Hartree-Fock (HF),
  It is a single determinant wave function method computationally cheap. However, it has the drawback that it does not take into account the electronic correlation. In the HF approach, electrons are assumed to move in a medium electrostatic potential due to other electrons and the instantaneous position of an electron is not influenced by the presence of other electrons. This leads to systematic errors that are not acceptable for chemical kinetics application. Although Hartree-Fock energetics are not accurate enough by themselves, almost all "higher correlated" methods are based on the Hartree-Fock reference wave function via an inclusion of further excited-state determinants into the ground state wave function.

- Perturbation theory in the formalism of Møller-Plesset (MP),
  This approach, is based on a perturbation method, in which Hamiltonian is expressed as the sum of Hamiltonian terms of zero order (where electron correlation is neglected) and the excited-state Slater-determinants and its energetic effect is treated via perturbation theory. MP[89,90] methods are much more accurate than the HF method, but there is not much difference between MP2[89]

and MP4[90] methods for most molecules. However, MP4[90] requires more calculation time if compared to explicitly setting up a multi-determinant wave function, in particular, MP2[89] (second-order perturbational treatment). Both MP2[89] and MP4[90] methods are much slower than the HF method, which is almost instantaneous but with a very low accuracy. In practice, it is common to use the MP2[89] method. A general problem of all MP methods is that they should not be applied to certain HF reference functions; in particular UHF (spin unrestricted HF) which leads to severe energetic artifacts. This limit makes the application of MP2[89] to radical chemistry calculation difficult, and even though, there is still the possibility to compute MP2[89] energies based on a spin-restricted open-shell HF reference (ROHF), but also this can lead to other errors. To reduce the computation time and avoid numerical errors, it is recommended to pre-optimize the geometry with another method such as a semi-empirical method or a Density Functional Theory method.

– G_n methods, MP modified methods,
The n-Gaussian (G_n) methods developed by Pople et al.[71–73] are procedures combining several ab initio methods and allowing an accurate estimation of various properties such as enthalpies of formation, atomization energies, ionization potentials, electronic affinities and protonic affinities. The most accurate methods currently available are G3[74] and G4[91]. G4[91] is the most expensive in computation time because it involves MP4 and couple-cluster methods. The G3[74] method use a defined sequence of calculations involving geometry optimization, first at the HF/6-31G level, then at the MP2/6-31G level. An energy calculation is then performed using the MP4[90] method. The main disadvantages of the n-Gaussian (G_n)[71–73,91] methods are time consuming and the fact that they have been developed based on small molecules. For large molecules, systematic deviations can be observed, especially for G2[73] and G3[74], and calculations can be extremely long. In practice, it may be recommended for large molecules to use ab initio method with a lower level of theory and to correct the results with empirical contributions depending on either the type of bond or the type of atom.

– Coupled cluster (CC) methods,
The CC (coupled cluster) method was developed by Coester and Kümmel[92] to study nuclear physics phenomena. The CC-type methods are part of the ab initio post Hartree-Fock methods, such as MP2 and MP4, and are considered to be the most precise methods for energy calculation, but also a high computational time demanding. The best known method among the post Hartree-Fock

is the "coupled cluster single double (triple)" CCSD(T)[88] method.

Density Functional Methods

In Hartree-Fock-type approaches (HF, MP2[89], ...), the multiple electron N-wave function is expressed in the form of a Slater determinant constructed from a set of N-wave functions to an electron. The HF theory then calculates the complete wave function of the N electrons. In the DFT approach, single electron functions are also taken into account, but the complete wave function of N electrons is not calculated. In the DFT method, only the distribution of the electronic density is calculated. The Density Functional Method is based on the theorem of Hohenberg and Kohn stating that the exact ground-state energy of any molecular system can be computed from one particle electron density. Hohenberg and Kohn demonstrated that the energy of the ground state and some other properties were determined solely by the electron density $\rho_e(r)$ which is a function of the position vector r. The Schrödinger equation can then be rewritten as the sum of electronic density functions. Thus they introduced a one particle functional, despite the fact that it has been shown that such a functional exists, its form is still unknown. Then, Kohn and Sham proposed different approximations to express the different energy terms in the Schrödinger equation, and the equations are resolved by determining $\rho_e(r)$ using an iterative substitution procedure. All current variants of functional within the local density approximation or the generalized gradient approximation (GGA), meta-GGAs or hybrid functional are guesses or approximations to this functional. The two very popular DFT methods are BP86[93,94] and B3LYP[95,96] represent a GGA "generalized gradient approximation" and a hybrid-GGA functional, respectively.The VWN-PB method[97] used in DMol3 packager for generation of cosmo cavities files in the COSMO-SAC[11,13,19,82,83,98] approach is a combination of the Becke exchange term and the Vosko, Wilk and Nusair correlation term. As we will see in Chapter 2 BP86 is very fast and predicts an accurate energies for aromatic compounds, thus we used it as a reference method for biomass components. Practically, DFT methods are widely used nowadays. They provide a good compromise between accuracy and computational effort but the accuracy is usually not sufficient for quantitative predictions. Also there is no possible systematic improvements for DFT methods like what we have seen for perturbation theory as in the case of HF methods. This is because the Hamiltonian in DFT methods is approximated. There are G_n methods that use DFT methods instead of MP approaches. The advantage of these approaches is that DFT calculations are much faster than MP methods and generally lead to good prediction of molecular geometries.

From all mentioned methods in this brief review, only DFT methods are computationally affordable for real chemical applications. In addition, for a quantum chemical treatment of molecules in the condensed phase (solvent effects) all calculations are typically based on DFT methods.

1.5 Modeling tools

1.5.1 Reaction Mechanism Generator (RMG)

In order to model the rates and products yields in a reacting system, we first have to construct a reaction mechanism. In the case where reacting system involve a small number of species and reactions, it is a common practice to construct detailed kinetic mechanism by hand, one have to be careful with this hand procedure with tracking of all species with possible reactions and incorporating relevant chemistry. But, even though it is possible to handle small reaction mechanism construction by hand, it is often a tedious and error-prone work, requiring expert and a very good understanding of chemistry. However, the challenges associated with hand constructed models are easily handled by computers. This insight led to the emergence of several automatic reaction mechanism generation codes, some are open-source software and others are proprietary including MAMOX, NetGen, REACTION, and EXGAS.
The open-source software package RMG (Reaction Mechanism Generator) was developed in the Professor William H. Green Group at MIT to make modeling of physical and chemical processes much easier for researchers with an automatic mechanism generation. RMG[99] uses known chemistry data, as atoms adjacency, thermochemical data and rate kinetic data stored in databases along with parameter estimation methods to generate detailed chemical kinetic mechanisms. These mechanisms can be used as inputs to a third party reactor kinetic solver like Cantera or Chemkin software to model specific conditions. The output list of species and their thermochemistry parameters, and reactions with their respective rate parameters are called a "reaction mechanism" and is reported as a CHEMKIN format file or Cantera format file. RMG[99] generates elementary reactions from chemical species using an extensible set of 58 reaction families. Individual rate rules are defined for a set of functional group-based reaction sites through a temperature dependent kinetic parameter $k(T)$ described by the modified Arrhenius expression for gas phase eq.1.7:

$$k(T) = AT^n \exp\big(-\frac{E_a}{RT}\big) \tag{1.7}$$

where A is the pre-exponential factor, n is the temperature exponential factor, R is the gas constant, T is the temperature and E_a the activation energy.

For the reversible reactions, thermodynamic consistency is maintained through the following relation 1.8 between the forward and the reverse reaction rate:

$$K_{eq} = \frac{k_f}{k_r} = \left(\frac{RT}{P^\circ}\right)^{-\Delta n} \exp\left(\frac{-\Delta G^\circ(T)}{RT}\right) \tag{1.8}$$

where K_{eq} is the equilibrium constant of the reaction, T is the reaction temperature, R is the gas constant, P° is the standard pressure (1bar), $\Delta G^\circ(T)$ is the standard reaction free energy, and Δn is the change in moles in the reaction. The reverse kinetics are calculated through the relation 1.8 using the thermodynamic parameters estimated for the reaction species and the forward rate constant estimated with the Arrhenius expression 1.7 within RMG[99] or the third party reactor software. RMG[99] can also estimate transport and solvation properties based on the QSPPR group contribution group methods to compute a liquid phase rate kinetic calculation. The generated reaction mechanisms are only approximations to reality, and their numerical predictions are often less accurate than we desire. All code lines of RMG are written in Python and it can be used on linux systems. RMG[99] is still under development, new corrections and new capabilities are added.

In this study, we used RMG[99] 2.1.8 version to predict a first guess mechanism for reactions involved in the lignin surrogate compounds decomposition. We then investigated the most relevant reactions with quantum chemistry calculations.

1.5.2 Gaussian/ ORCA

The main goal of quantum chemistry calculations is to obtain solutions to atomic and molecular Schrodinger equations. Based on the fundamental laws of quantum mechanics, Gaussian software allows as to predict the energies, molecular structures and vibration frequencies of complex molecular systems, and thus to approximate their chemical properties. Wide range of conditions can be used for example molecules and reactions can be studied in a wide range of temperature and with different methods. Also not only stable species or complex compounds can be studies but also transient intermediates or transition states. To be useful to chemists, such solutions must be at a tolerable computational cost and must be reasonably accurate. Gaussian 09W (G09)[100] and ORCA[101] are both a computational quantum chemistry packages capable of predicting many properties of atoms, molecules, and reactive systems such as structures, electronic energies, vibrational frequencies. They both use a variety of methods such as ab initio, density functional theory, semi-empirical, molecular

mechanics, and hybrid methods. The mathematical models used in Gaussian calculation are the Final Element Method and Simplex method. Gaussian is the widely used software for electronic structure calculations, it was originally available through the Quantum Chemistry Program Exchange, then licensed out of Carnegie Mellon University. Since 1987, Gaussian[100] has been developed and licensed by Gaussian, Inc this makes it a non open source software. On other hand, ORCA[101] is a freely available quantum chemistry program, for academic use, developed at the Centre for Energy Conversion at the Max Planck Institute in Mülheim and der Ruhr, Germany by the research group of Professor Frank Neese.

1.5.3 KiSThelP

Kinetic and Statistical Thermodynamical Package (KiSThelP) is a cross platform free open-source program developed by the research group Professor Eric Henon at Université de Reims Champagne-Ardenne. KiSThelP[102] use statistical mechanics equations to estimate molecular and reaction properties based on electronic structure calculations[102].

KiSThelP[102] has been designed to perform statistical mechanics calculations from ab initio quantum chemistry. The starting point for calculation of statistical and thermochemical data is the partition function $Q_i(V,T)$ for component i. The individual partition function equations used to calculate the translational, electronic, rotational, and vibrational contributions in the canonical ensemble are given in the following equations 1.9, 1.10, 1.11 and 1.12 respectively[103]:

$$q_{trans} = \Big(\frac{2\pi m k_B T}{h^2}\Big)^{\frac{3}{2}} V \tag{1.9}$$

$$q_{elect} = g_{elect}^{ground} = -(\epsilon_{elect,1} + \frac{1}{2} hc\omega) \tag{1.10}$$

where g_{elect}^{ground} is the ground-state electronic degeneracy, that means the energy involved in bond formation (bond dissociation energy at 0 K).

$$q_{rot} = \frac{T}{\sigma \Theta_r} \tag{1.11}$$

where σ, the symmetry number has a value of 1 for heteronuclear molecule, and 2 for a homonuclear molecule; and Θ_r, the rotational temperature is equal to $\Theta_r = \frac{h^2}{8\pi^2 I k_B}$ with I the moment of inertia.

$$q_{vib} = \prod_i \frac{1}{1 - \exp\left(-\frac{hc\omega_i}{k_B T}\right)} \tag{1.12}$$

where ω_i is the wave number in units of cm^{-1} and c is the speed of light. h, k_B and m are the Planck constant, the Boltzmann constant and the mass respectively. Thus the total partition function of a molecule in its ground state is calculated as the product of all partition functions as follows:

$$Q_{tot} = q_{trans} \times q_{rot} \times q_{vib} \times q_{elect} \tag{1.13}$$

This calculation results in the computation of molecular thermodynamic properties, thermal equilibrium constants, transition state theory, rate coefficients, and RRKM rate constants. One dimensional tunneling and variational effects are also incorporated in the TST calculations. All KiSThelP code lines are written in the programming language Java, which makes it available on different operating systems. Conventional TST requires information only for the saddle point and reactant(s). The equation usually presented for the conventional TST is 1.14 for n reactants,

$$\mathbf{k}^{\mathrm{TST}}(\mathrm{T}) = \kappa \frac{k_B T}{h} \frac{Q^{\ddagger}}{\prod_i^n Q_i} \exp\left(\frac{-E_a}{RT}\right), \tag{1.14}$$

1.5.4 Cantera

Cantera is an open-source chemical kinetics suite of object-oriented software tools for problems involving chemical kinetics, thermodynamics, and/or transport processes. Cantera can be used from both Python and Matlab interfaces, or in C++ applications and Fortran 90. It was developed by Professor Dave Goodwin from Division of Engineering and Applied Science of California Institute of Technology.

Chapter 2

Prediction of Enthalpies of Formation

2.1 Introduction

In many important areas of modern physico-chemical science, the energy needed to form a compound out of its elementary constituents, plays a central role. The enthalpy of formation (ΔH_f) of a chemical compound, a key property in thermochemistry, is defined as the change in enthalpy that accompanies the chemical reaction formation of a compound from its constituent elements. Thus, the standard enthalpy of formation (ΔH_f°) of a compound is the change in enthalpy that accompanies the formation of 1 mole of that substance from its elements, with all substances in their standard states at 298 K (25 °C, or standard "room temperature") and 1 atmosphere of pressure. ΔH_f of a compound, if negative, determines ranges of chemical potentials of its elementary constituents within which the examined compound is thermodynamically stable. To predict accurately the enthalpies of reactions required for chemical reactions to occur, we need to know the enthalpy of formation ΔH_f values of all chemical compounds involved. However, these basic properties have been experimentally measured and reported only for a minority of compounds. Therefore, the development of theoretical capabilities to aid in the prediction of physico-chemical properties of compounds is essential.

The majority of tabulated thermochemical data are extracted or inferred rather than being directly measured. The enthalpies of formation as other thermochemical data is not directly measured, it is most of the time a not amenable thermochemical property for direct experimental determinations. The few rare exceptions where enthalpies of formation could be measured experimentally are with direct calorimetric

measurements of the combustion of hydrogen in oxygen to form liquid water, the combustion of graphite in oxygen to form carbon dioxide, or the combustion of graphite in fluorine to form tetrafluoro methane[64]. Consequently, the thermodynamic data from which enthalpies of formation are extracted belong to the group of species interrelating data, such as constants of equilibria, various reaction enthalpies, adiabatic ionization energies or electron affinities, proton affinities, gas phase acidities. One of the most used predictive methods of the physico-chemical properties is the quantitative structure property relationship technique (QSPR). This technique tries to produce correlations that relate the important physical and chemical properties of compounds to the simplest molecular structure-based parameters, called molecular descriptors. The group additivity method for predicting thermochemical properties of compounds as sums of the properties of their component part, is similar to the development of QSPR methods. Group additivity method was initially developed and utilized by Benson and co-workers[104–107]. Predictive capabilities of these types of correlations are verified by many statistical methods. Therefore, these correlations can help us to predict the physico-chemical properties of a desired molecule with some limitations. The limitations are mainly related to diversity of the data set and the number of components used to develop the model.

Up to now, a large number of models have been presented to estimate or predict the ΔH_f of pure components[16,104–124]. However,the majority of these correlations have been obtained for specific families of components.

The calculation of properties at reasonable cost has been a consistent theme in the computational chemistry community and the prediction of enthalpies of formation at 298 K has long been a goal of computational chemistry. This led to the development of more complex and complete schemes to provide higher accuracy results as described before in Section 1.4.4. Amongst the better known high accuracy methods are triple excitations in coupled cluster theory (CCSD(T))[88], which is generally considered to provide very accurate results with sufficiently large basis sets, but take a very high computational cost. The G_n[71–74,91] compound methods implemented in Gaussian[100] offer a computationally more cost effective method relative to CCSD(T)[88] by using a weighted average across multiple methods for error minimization. Another group of high accuracy compounds methods are the Weizmann methods[66–68] as well as the more recent CCSD(T)-F12 methods[69,70]. The final well established method is the group of complete basis set approximations, of which CBS-QB3[125] is commonly used.

In general, the Gn methods[16,71–74] together with CBS-QB3[125] can be considered to be "budget methods" which provide good results and are applicable to both smaller and larger molecules[40,126,127]. In contrast, the Wn methods[66–70] as well as CCSD(T)-

F12[69,70] are computationally much more expensive and thus only used for small molecules[39,40,127].

While computationally expensive, these methods have been regularly assessed and have been gradually expanded to include larger molecules with the improvement in available computational resources. In a 2015 evaluation[126], G3 and G4 were shown to provide the best results over the chosen test set relative to reference calculations. The issue of computational cost becomes apparent when we consider largest molecules in the test set. A different large scale study in 2016[127] treated molecules with up to 47 heavy atoms using the "budget methods" with the assistance of a high performance computing center. For application to real multicomponent systems, a faster method is imperative, both to investigate larger molecules as well as systems such as reaction mechanisms which require calculations for many species.

Local Pair Natural Orbital LPNO[128] and Domain-based Local Pair Natural Orbital DLPNO[129,130] methods offer an attractive solution to the problem, by providing an efficient approximation scheme through which the ideal CCSD(T))[88] solution is approached in an efficient manner[131,132]. A key advantage of the DLPNO-CCSD(T)[129,130] method is the use of a single method for the calculation of the electronic energy, which thus avoids the issue of requiring empirical weighing for the numerical results, as applied in the popular compound method G4[91]. In addition, the computational cost of DLPNO-CCSD(T)[129,130] methods is extremely competitive which makes it suitable for larger scale studies, both larger molecules or large numbers of smaller molecules[131,133].

Different methods exist for the calculation of formation enthalpies, such as atomization, isodesmic reactions or regression parameters. The atomization approach requires the calculation of very accurate energies and thus relies on the use of high accuracy methods that quickly become prohibitively expensive[134]. A second technique that is also known to offer a high accuracy is isodesmic reactions[134–138]. In this case, an artificial, or real, reaction is proposed, in which ideally the same type of bond is broken and formed[135–138]. As this method looks at relative energies, good results can be obtained at the DFT-level. However, the method is limited to compounds where reactions with accurately measured or calculated reference species are available, which excludes the calculation of non tabulated compounds. A third method is the use of regression coefficients[16,17,41,139,140], which is a modification of the atomisation approach. Further proposed calculation methods employed with high accuracy computational schemes HEAT[141], NEAT[142], the "method of Fishtik[143]" or ATOMIC[144–146].

In the case of the use of regression coefficients, calculations are carried out for a known set of species and regression parameters are fitted to the elements in the

test set to minimize the error in the calculated formation enthalpy. This fitting is intended to compensate for errors in the functional and has been shown to offer good results in the past[17,147]. This method has been recently modified to employ DLPNO-CCSD(T)[129,130] for the electronic energy calculation, while DFT is used for the geometry optimization and frequency calculation[16]. As Paulechka and Kazakov show, the standard deviation of the error is capable of rivalling with the well established G4 method[16], while offering a more direct approach to the calculation of formation enthalpies as the weighing of different methods employed in common compound methods is no longer required. To our knowledge, the DLPNO-CCSD(T)[129,130] method is only available in ORCA[148,149]. Originally introduced for closed shell molecules in ORCA 3[148], DLPNO-CCSD(T) has been recently developed further to be able to treat open shell molecules as well as to be more efficient[129,130].

In this work[42], we examine the performance of the method proposed by Paulechka and Kazakov[16] by expanding the test set to cover the elements hydrogen, carbon, nitrogen, oxygen, fluorine, silicon, phosphorous, sulfur, chlorine and bromine. In order to investigate a computationally low cost method for calculating the thermodynamic properties of compounds.

2.2 Methodology

2.2.1 Quantum chemistry method

We chose to employ B3LYP with D3BJ[150,151] for comparison purposes on a subset of the species, as it was used by Paulechka and Kazakov[16] as well as by Demenay et al.[17] Despite extensive criticism of B3LYP[152–159], the functional remains widely used and thus it is valuable to comment upon its performance. BP86 with D3BJ[150,151] is used for its speed, which makes it particularly suitable in cases with finite computational resources. ωB97X-D3 is used due to the good performance of the functional in benchmark studies[160] combined with reasonable runtime. The methodology employed follows the general outline of Osmont et al.[41,140] using the improved approach proposed by Paulechka and Kazakov[16] and consists of the following steps:

i) optimize the gas phase geometry of molecules with a DFT method such as B3LYP D3BJ, BP86 D3BJ[151], wB97X-D3. Where more than one conformer exists, all identified conformer are investigated and the conformer with the lowest electronic energy is kept.

ii) calculate frequencies using the same method with identical parameters.

iii) calculate the electronic energy, E_0, for the DFT-optimized geometry with DLPNO-CCSD(T).

The DFT functionals were employed with the def2-TZVP[161,162] basis set, the def2/J[163] auxiliary basis set as well as the RIJCSOX[164,165] approximation for a significant reduction of the required computational time. DLPNO-CCSD(T)[130] calculations were carried out at the normal PNO level using the def2-QZVP[161,162] basis set with the def2-QZVPP/C[166] auxiliary basis set and def2/J[163] auxiliary basis sets as well as the RIJCOSX[164,165] approximation, using the 2016 implementation of the DLPNO method available in ORCA 4.0.1.2[149]. Calculations were carried out with the tightscf convergence criteria in ORCA[149] with Grid4 which offers a slightly finer grid than the default. Hence, the input for the optimization and frequency calculation was as follows, with the geometry supplied in the xyz-file.

```
! BP86 D3BJ def2-TZVP def2/J RIJCOSX
! tightscf grid4
! opt freq
* xyzfile 0 1 geometry.xyz
```

While the DLPNO-CCSD(T) calculation of the electronic energy employed the following two combinations of keywords, assuming an optimized geometry being presented in the xyz-file.

```
! DLPNO-CCSD(T) def2-QZVP def2-QZVPP/C def2/J RIJCOSX
! tightscf grid4
* xyzfile 0 1 geometry.xyz
```

In order to study whether the result could be improved with a larger basis set, a geometry obtained with BP86 and the def2-TZVP basis set was tested using a basis set extrapolation in the DLPNO step as well as geometries and frequencies obtained with BP86 at the def2-QZVPP[167] level with a slightly finer Grid5 and a basis set extrapolation in the DLPNO step. The basis set choices mirror those suggested by Paulechka and Kazakov[16], except for the the basis set extrapolation as well as the auxiliary basis sets[163,166] and the RIJCOSX[164,165] approximation included to significantly reduce the required computational time. To compute the zero point vibrational energy as well as the thermal (enthalpic) contribution, the frequencies from the ORCA quantum chemistry calculation were used with and without scaling factors. We used scaling factors taken from literature as well as fitted scaling factors on the basis of known heat capacities. Calculations were performed with and without scaling factors, to assess their impact on the final predictions of formation enthalpies.

For B3LYP with the def2-TZVP[161,162] basis set, the scaling factors proposed by Paulechka and Kazakov[16] were used, which are 0.985 for frequencies from $1 \times 10^4\,\mathrm{m}^{-1}$ to $30 \times 10^4\,\mathrm{m}^{-1}$ and 0.96 for $30 \times 10^4\,\mathrm{m}^{-1}$ to $40 \times 10^4\,\mathrm{m}^{-1}$. The scaling factor for BP86 was taken from Kesharwani et al.[168], using the proposed values for the zero point vibrational energy, and is equal to 1.0192 over the entire frequency range for BP86. For ωB97X-D3, the scaling factor quoted by Kesharwani et al.[168] for ωB97X-D was used, and is equal to 0.9791. One problem with the ωB97X-group of functionals is, that very different scaling factors are quoted depending on the focus of the study, such as spectra, zero point vibrational energies or enthalpy. Finally, a set of heat capacity-derived scaling parameters, specific to every functional, was also used and is discussed in greater detail in the following Section 2.2.3. Where multiple conformers exist, this method considers only the lowest energy conformer. For molecules with multiple conformers, multiple geometries are used in the optimization process to identify the lower energy structure. The lowest energy structure is then chosen on the basis of the DLPNO-CCSD(T) calculation.

2.2.2 Mathematical Implementation of Regression Parameter Fitting

As presented by Osmont et. al[41,140] as well as Paulechka and Kazakov[16], the enthalpy of formation can be calculated as

$$\Delta Hf^\circ = E_0 + ZPVE + H_{tot}^T + RT + \sum_{i=0}^{N} n_i h_i \tag{2.1}$$

where E_0 is the electronic energy of the molecule, $ZPVE$ the zero point vibrational energy; H_{tot}^T consists of the vibrational, rotational and translation contributions to enthalpy; R is the ideal gas constant and T the temperature (298.15 K). Lastly, the number of atoms n_i of type i in the molecule is multiplied with the fitted regression parameter h_i. The zero point vibrational energy as well as the thermal enthalpy contributions are calculated from a frequency calculation and can be obtained either with or without scaling factors. As mentioned by Paulechka and kazakov[16], the equation 2.1 is mathematically equivalent to the derivation of ΔHf° using the enthalpy of atomization, and h_i can be formally defined via computed atomic electronic energies, reference enthalpies of formation, and reference enthalpy changes for individual atomic species.

The regression parameters were obtained by minimising the sum of the error squared

for all molecules with known reference values, with an objective function defined in Eq. (2.2) and using optimization tools in R[169].

$$error_{tot} = \sum \left(\Delta Hf^{\circ}_{ref} - \Delta Hf^{\circ}_{calc} \right)^2 \tag{2.2}$$

The zero point vibrational energy, $ZPVE$, is calculated by using the standard expression (2.3)[170,171].

$$ZPVE = 0.5 \times h \times c \times N_{av} \times \sum frequencies \tag{2.3}$$

$$H^T_{tot} = H^T_{vib} + H^T_{rot} + H^T_{trans} \tag{2.4}$$

where

$$\mu = \frac{h \times c \times frequencies}{k \times T} \tag{2.5}$$

$$H^T_{vib} = h \times c \times N_{av} \times \sum \frac{frequencies}{e^{\mu} - 1} \tag{2.6}$$

$$\begin{aligned} H^T_{rot} &= 1.0 \times R \times T \text{ (diatomic molecules)} \\ H^T_{rot} &= 1.5 \times R \times T \text{ (polyatomic molecules)} \end{aligned} \tag{2.7}$$

$$H^T_{trans} = 1.5 \times R \times T \tag{2.8}$$

The constants h, c and N_{av} are the Planck constant, the speed of light and Avogadro's number, while the frequencies are given in m^{-1} units. k is the Boltzmann constant and T is the temperature in Kelvin.

The regression fitting process consists of two steps. A first guess for the solution is obtained initially using the standard non linear minimisation available in R[169] and later using a re-implementation of the subplex algorithm[172,173]. For performance reasons, first guess integer rounded values are provided for H, C, N, O, F, Si, P S, Cl and Br in the regression fitting. This generally provides decent results, however it cannot be guaranteed that a local instead of a global minimum has been reached. In a second step, the results of the non-linear minimisation are employed as the starting condition for a controlled random search[174,175] with local mutation[176], as implemented in the NLopt library[172], which can be interfaced natively from C++ or from R using the nloptr package[177].

The method implemented in this algorithm creates a starting population of $10 \times (n+1)$

members by randomly varying the starting guess within the given bounds, where n is the number of variables under investigation, in this case, the number of elements and thus associated regression coefficients. The Figure 13 represent the algorithm that summarize the implemented methodology described above.

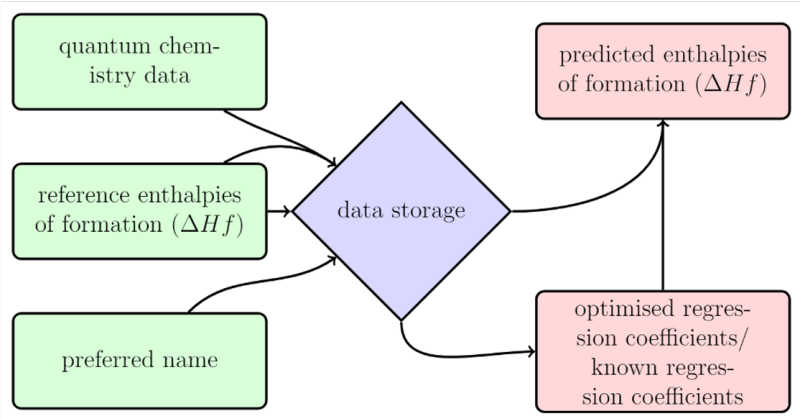

Figure 13: Algorithm of the implemented method to optimise regression coefficients and calculate predicted enthalpies of formation from reference and quantum chemistry input data.

In our case, we chose limits of $\pm 5\,\mathrm{kJ/mol}$ in the original R implementation and $\pm 10\,\%$ in the C++ implementation for the regression coefficient boundaries derived from a first minimization. The number of maximum iterations was set to 1.0×10^5 in R and 1.0×10^6 in C++, while the relative tolerance was set to 1×10^{-6} in R and 1×10^{-8} in C++ with all other parameters left at their default setting. Controlled random search with local mutation[174–176] was chosen, as it provided the lowest energy in a comparison with the global minimisation algorithms provided by NLopt[172]. After the optimization, the results are investigated for consistency and species with large errors are manually removed from the fitting set, to be discussed independently of the parameter optimization. We have chosen to use an error of $\pm 15\,\mathrm{kJ/mol}$ as a threshold value in the fit with BP86 D3BJ and def2-QZVPP as the boundary for compounds to be excluded from the fitting.

In this study a total of 210 compounds were considered. Excluding compounds for which a stable geometry was not found (imaginary frequencies present) or the calculation otherwise failed, such as in the case of the def2-QZVPP calculations for a number of nitrogenous compounds. The species counts employed in the final fitting are shown in Table 2.1. The initial set of reference (experimental) values of enthalpies of formation used to regress the element parameters h_i were taken from the publications of Paulechka and Kazakov[16]. This set comprises the elements hydrogen,

carbon, nitrogen and oxygen. We added the reference values of Demenay et al.[17] to consider the fluorine and chlorine elements.

Additional compounds were included in the fitted data set, to include bromine, sulfur, silicon and phosphorous elements with values taken from literature.

Thus the final fitting set includes 45 species for the elements hydrogen, carbon nitrogen and oxygen. A further 48 species for the inclusion of fluorine and chlorine and 13 bromine compounds. Sulfur is included in 54 species. 32 species cover silicon compounds and a final 14 species are used for phosphorous. Thus, in total 199 reference compounds have been considered in this study, of which 179 were included in the final fitting set.

Table 2.1: Overview of number of compounds included in fitting and filtered sets for individual methods. (Where numbers are lower, calculations either did not converge or produced no stable geometry).

opt & freq	B3LYP	ωB97X-D3	BP86		
basis	def2-TZVP				def2-QZVPP
E_0, DLPNO-CCSD(T)	def2-QZVP			def2(3,4) extr.	
O_2, F_2, Cl_2, Br_2	4	4	4	4	4
fitted					
H, C, N, O	45	45	45	45	41
F,Cl	48	48	48	45	47
Br	13	13	13	13	12
Si	19	19	19	19	19
P	7	7	7	7	7
S	47	47	47	47	47
filtered					
Si	13	13	13	13	13
P	7	7	7	7	7
S	7	7	7	7	5
Total:	210	210	210	207	202

2.2.3 Determination of Scaling Factors Based on Ideal Gas Heat Capacities

As the heat capacity of compounds is of interest to the engineering community, we have decided to employ the known heat capacities of a number of reference species to determine scaling parameters for the frequencies. This fitting set is comprised primarily of a number of hydrocarbons as well as halogenated (hydro)carbons for

which experimental data presenting the heat capacity at different temperature has been published. The full list of species is provided in Table 2.2. Ideal gas heat capacity for a polyatomic molecule is calculated from the vibrational frequencies as [171]

$$\mu = \frac{h \times c \times frequencies}{k \times T} \tag{2.9}$$

$$Cp = 4 \times R + R \times \sum \frac{\mu^2 \times e^{-\mu}}{\left(1 - e^{-\mu}\right)^2} \tag{2.10}$$

Similar to the fitting of the enthalpy of formation, the regressed scaling factors are determined by minimisation of the total error between experimental (reference) and calculated values. The objective function is the sum of the error squared, and is given by

$$error = \sum \left(Cp_{ref} - Cp_{calc}\right)^2 \tag{2.11}$$

The optimization is achieved using the non-linear optimizer available in the statistical package R[169]. Only a single scaling factor is used over the entire frequency range. The results obtained with these scaling factors are presented alongside the results obtained with both literature-derived scaling factors as well as no scaling factors for comparison.

For the heat capacity fitting of frequencies, reference heat capacities for 25 [15,178–198] compounds were used. All compounds used in the fitting of frequencies on heat capacities are also a part of the enthalpy of formation fitting set.

Table 2.2: Species used to determine C_p-based scaling parameters. Data taken from the Thermo Data Engine published by NIST[15].

Compounds Name	References
1-1-1-2-tetrafluoroethane	15,178,179
1-1-dichloro-1-fluoroethane	15,180
1-1-difluoroethane	15,179
2-2-dichloro-1-1-1-trifluoroethane	15,181
2-chloro-1-1-1-2-tetrafluoroethane	15,182
acetonitrile	15
anisole	15,183
benzene	15,184
chlorodifluoromethane	15,185–187
chlorotrifluoromethane	15,185
dichlorodifluoromethane	15,185
dichlorofluoromethane	15,185
difluoromethane	15,185
ethane	15
H_2O	15,188
iso-butane	15,186,189,190
methane	15,185,187,191
methanol	15,192,193
neopentane	15,194,195
nitrobenzene	15,196
propane	15,186,187,197
propyne	15,197
tetrafluoromethane	15,185,198
trichlorofluoromethane	15,185
trifluoromethane	15,185

2.3 Results & Discussion

As a large number of compounds were used with different family group, we first choose to begin with known compounds for which the method has shown to work. Then we include the additional compounds with bromine containing species as well as additional fluorinated and chlorinated compounds. As the prediction of sulfur compounds has a large effect on the regression coefficients. Same behavior was observed with silicon compounds, the silicon compounds group prediction are put in

the last group. Thus, the following section will be divided in frour groups. Compounds with an error greater than ±15 kJ/mol using BP86 def2-QZVPP geometries without scaling factors for the frequencies were excluded from the fitting. This choice was made to avoid any distortion in the accuracy of the fit due to very badly fitted compounds.

The investigation of this method covers the following main points:

- First the expansion of the method to encompass additional elements and compounds relative to the previous studies[16,17,41];
- secondly the influence of scaling factors in the context of calculating accurate enthalpies of formation.

A third question arose during the work, namely by which method one should determine the minimum energy structure where multiple conformers exist. Should preference be given to the lowest energy structure at the DFT level or at the DLPNO-CCSD(T) level, as the electronic energy can either be calculated from the DFT method used in the optimization, or from the DLPNO-CCSD(T) calculations, used in the final calculation. Given that the DLPNO-CCSD(T) calculation is considered to be more accurate with respect to electronic energies when compared to DFT methods, we have chosen to discuss the results obtained when selecting conformers based on the DLPNO-CCSD(T) electronic energy. For completion, the results for filtering conformers based on the DFT-derived electronic energy is provided in our published work[42].

2.3.1 H, C, N, O

The first test set to be considered, is the dataset presented by Paulechka and Kazakov[16], whose combined DLPNO-CCSD(T) with DFT methodology. Calculations were carried out using B3LYP with D3BJ using the latest 2016 DLPNO-CCSD(T) implementation available in ORCA 4.0.1.2[149]. The very fast BP86 with D3BJ and generally well performing ωB97X-D3 are also tested. Table 2.3 presents an assessment of the accuracy of the methods employed for scaled frequencies using literature values, reference heat capacities as well as unscaled frequencies, used as is from the quantum chemistry calculation. The values presented are the minimum and maximum error in the fitting set, the mean error to indicate potential bias in the fitting, the mean absolute error as well as the standard deviation. As can be seen from Table 2.3 the final error in the fitting is extremely similar irrespective of whether the frequencies are scaled or not, as well as across the different functional.

When comparing the results obtained in this work to the results obtained by Paulechka and Kazakov[16], it is found that the standard deviation for B3LYP with scaled frequencies, including the biphenyl outlier of $\sigma = 1.97$ is larger than the quoted standard deviation of $\sigma = 1.4$. The largest errors are observed for biphenyl ($-6.48\,\mathrm{kJ/mol}$) and urea ($-4.54\,\mathrm{kJ/mol}$). If these three compounds are removed, the standard deviation reduces to $\sigma = 1.6$ In addition, slightly larger maximum and minimum deviations are obtained when compared with the published medium scheme[16]. These are most likely attributable to the use of only tightscf criteria in the geometry optimization as well as the use of only normalPNO criteria for the DLPNO-CCSD(T) part. In contrast, Paulechka and Kazakov have employed verytightscf and tightPNO settings which are expected to provide higher accuracy. However, especially the tightPNO settings lead to a significant increase in the computational time required by a factor of up to four[101,129]. As Table 2.3 shows, the use of larger basis sets leads to a reduction in the error within the same method, in this case BP86. It was concluded that the obtained results are sufficiently similar to those obtained by Paulechka and Kazakov[16], but with the benefit of drastically reduced computational time.

As the results are remarkably similar between the individual functionals, with no major differences between B3LYP D3BJ, BP86 D3BJ and ωB97X-D3, it is very hard to recommend the use of a specific method, as consistent results can be obtained with all proposed methods. ωB97X-D3 appears to be the best performing method under identical input conditions for the group of H, C, N and O, in line with its performance in benchmarks [160,199–201]. Larger basis sets were only assessed for BP86, however a clear improvement in the obtained fitting can be observed with first the use of an extrapolated basis set for the DLPNO step only and then also the use of a larger basis set for the geometry optimization and frequency too. In combination with auxiliary basis sets and the RICOSX method, the performance of BP86 remains extremely competitive despite the large basis set. The favoured method in this study is BP86, mainly for its speed relative ωB97X-D3. B3LYP is employed mainly as a reference method, given its frequent use in the past.

As can be further seen from Table 2.3, whether the frequencies are scaled or not, has no large impact on the accuracy of the method. The use of an extrapolated basis set leads to a further small improvement with the species considered in the initial fitting set. While the observed errors with scaled frequencies are smaller in the initial fitting set, this advantage is lost as the fitting set is increased throughout this study. The use of unscaled frequencies is in so far attractive, as it allows the user to utilise the data from the quantum chemistry calculation without further manipulation of the data. Comparing the results with and without scaling factors,

Table 2.3: Overview of errors in kJ/mol obtained on the species presented by Paulechka and Kazakov[16] (Elements included are H, C, N and O). Frequencies were scaled using parameters from literature, not scaled or scaled to reproduce a selection of heat capacities. Values presented are largest errors (positive and negative), mean error, mean absolute error as well as the standard deviation.

opt & freq	B3LYP	ωB97X-D3	BP86		
basis	def2-TZVP				def2-QZVPP
E_0, DLPNO-CCSD(T)	def2-QZVP			def2(3,4) extr.	
unscaled					
mean	0.14	0.12	0.18	0.00	-0.06
mean absolute deviation	1.53	1.54	1.88	1.81	1.42
standard deviation	2.06	2.01	2.73	2.35	1.70
largest error +	4.08	4.3	6.79	6.46	3.38
largest error -	-6.43	-5.65	-8.05	-6.03	-3.70
scaled					
mean	0.15	0.15	0.16	-0.02	
mean absolute deviation	1.42	1.53	1.89	1.83	
standard deviation	1.97	2	2.74	2.36	
largest error +	3.74	4.34	6.93	6.59	
largest error -	-6.48	-5.65	-8.06	-6.03	
C_p-scaled					
mean	0.16	0.18	0.13	-0.05	-0.12
mean absolute deviation	1.52	1.52	1.91	1.87	1.51
standard deviation	2.05	2.00	2.75	2.39	1.77
largest error +	3.89	4.41	7.2	6.86	3.81
largest error -	-6.43	-5.66	-8.07	-6.04	-3.82

it can be observed that while the results are better for B3LYP and ωB97X-D3, the impact on BP86 can be described as negligible. Thus, it was concluded that while the use of scaling factors is advisable, it is not absolutely necessary, with respect to be aware of the slightly reduced accuracy. A problem that was observed with the def2-QZVPP basis set in conjunction with BP86 was the inability to optimize to a proper ground in some cases, with imaginary frequencies in the final geometry. For some molecules, this could be explained as low wave number rotations, however in the case of urea, the program failed to converge to a proper ground state using the employed settings. Compounds with imaginary frequencies are not used in the fitting which employs only stable ground state molecules. The list of reference species is shown in Supplementary Table A.1.

Contrary to the results presented by Paulechka and Kazakov[16], the largest error in our calculation was observed with the biphenyl molecule. References give an enthalpy of formation of ≈180 kJ/mol[16,202–209], with our calculation suggesting ≈187 kJ/mol. The lowest divergence is observed with BP86 and the def2-TZVP basis set using an extrapolated basis set in the DLPNO-CCSD(T) step. The calculation with the def2-QZVPP basis set failed to produce a geometry without negative frequencies.

A second important aspect in the application of this methodology is the reliable identification of minimum structures. In the case of z-butene, both B3LYP as well as ωB97X-D3 identify three minimum structures with no negative frequencies, while BP86 identify only one minimum structure without negative frequencies. This is insofar significant, as the lowest energy DFT-structure is not necessarily the lowest energy DLPNO-CCSD(T) structure, as found during this study and care must be taken to chose the correct geometry.

2.3.2 H, C, N, O, F, Cl, Br

From the work by Demenay et al.[17] we saw that prediction of enthalpies of formation method using regression coefficients can be employed for fluorinated and chlorinated compounds, but using DFT-only electronic energies. Knowing that fluorinated and chlorinated compounds are commonly used in refrigeration applications, we decided to expand the species considered in the previous section study 2.3.1 by the compounds published in Demenay et al.[17] paper as well as additional fluorinated and chlorinated compounds.
As industrial processes make use of brominated compounds which can benefit from the accurate calculation of thermochemical parameters, brominated compounds were also included.

The assembled set of published data for reference species from literature is shown in Supplementary Tables , A.3, A.2 and A.4 . The error statistic for the set is shown in Table 2.4.

The expansion of the method to encompass additional elements leads to a reduction in the overall accuracy of the method, however the observed errors remain acceptable. The largest errors are observed with the following 5 compounds, using the result from BP86 with a def2-QZVPP basis set, shown in Table 2.5.

As an independent reference point, we have decided to compare with the predicted values in a study by Ghahremanpour et al.[127], who used CBS-QB3, G2, G3, G4, W1BD and W1U in their calculations. For 1,1,1,2-tetrafluorethane, Ghahremanpour et al.[127] cite a reference value of −901.4(80) kJ/mol[210]. The calculations with G4 suggests a value of −908.4 kJ/mol[127], while G3 predicts −917.3 kJ/mol[127]. CBS-QB3,

Table 2.4: Overview of errors in kJ/mol obtained on the merged set of species presented by Paulechka and Kazakov[16] and Denemay et al.[17], adding additional fluorine, chlorine and bromine compounds to the fitting set (Elements included are H, C, N, O, F, Cl and Br).

opt & freq	B3LYP	ωB97X-D3	BP86		
basis	def2-TZVP				def2-QZVPP
E_0, DLPNO-CCSD(T)	def2-QZVP			def2(3,4) extr.	
unscaled					
mean	0.35	0.37	0.35	0.22	0.20
mean absolute deviation	3.65	3.76	3.75	3.65	3.66
standard deviation	4.80	4.91	4.92	4.85	4.83
largest error +	12.58	12.73	12.22	12.29	12.22
largest error -	-11.56	-11.83	-11.39	-12.00	-11.82
scaled					
mean	0.34	0.34	0.37	0.24	
mean absolute deviation	3.67	3.76	3.75	3.65	
standard deviation	4.83	4.91	4.92	4.84	
largest error +	12.69	12.8	12.18	12.25	
largest error -	-11.61	-11.83	-11.39	-12.01	
C_p-scaled					
mean	0.34	0.32	0.38	0.25	0.23
mean absolute deviation	3.65	3.77	3.75	3.64	3.65
standard deviation	4.80	4.92	4.92	4.84	4.82
largest error +	12.62	12.84	12.19	12.23	12.14
largest error -	-11.56	-11.83	-11.39	-12.01	-11.82

G2 as well as W1BD[211] and W1U[211] predict values lower than $-920\,\mathrm{kJ/mol}$[127]. A similar trend is observed with pentafluoroethane, where G4 predicts $-1113.9\,\mathrm{kJ/mol}$[127], with other methods predicting lower values and the W1U column left blank. In addition, an older reference value, compared to the one employed in this work, of $-1104.6(45)\,\mathrm{kJ/mol}$[212,213] is also available, which would lead to a smaller error in the prediction when used. For 1,3-dichlorobenzene, Ghahremanpour et al.[127] use a reference value of $25.6(1)\,\mathrm{kJ/mol}$[214] with predictions of $10.2\,\mathrm{kJ/mol}$ for CBS-QB3 and $25.7\,\mathrm{kJ/mol}$ to $19.5\,\mathrm{kJ/mol}$ for G2, G3 and G4[127]. 1,2,3,5-tetrachlorobenzene was not included in the study by Ghahremanpour et al.[127]. The final compound to discuss is 2,2-dichloro-1,1,1-trifluoroethane.

The reference value used is identical and the predictions range from $-782.5\,\mathrm{kJ/mol}$ with CBS-QB3 to $-753.8\,\mathrm{kJ/mol}$ for G4[127].

From this we can conclude that the results of our method is very similar to that of the popular G4 method when it comes to the estimation of enthalpies of formation. However in contrast, we do not rely on error cancellation between the individual methods and any systematic error will be compensated as part of the regression coefficient fitting procedure, an aspect previously discussed by Paulechka and Kazakov[16].No compounds were excluded for exceeding an error of 15 kJ/mol.

Table 2.5: Compounds with the largest error from calculations with BP86 and the def2-QZVPP basis set with unscaled frequencies. All values in kJ/mol.

Compound Name	CAS Number	ref. ΔH_f	calc. ΔH_f	error
1,1,1,2-tetrafluoroethane	811-97-2	-895.80[17,212]	-906.47	10.67
pentafluoroethane	354-33-6	-1100.40[17]	-1111.41	11.01
1,3-dichlorobenzene	541-73-1	28.10[215,216]	16.83	11.27
1,2,3,5-tetrachlorobenzene	634-90-2	-34.90[215,217]	-23.08	-11.82
2,2-dichloro-1,1,1-trifluoroethane	306-83-2	-743.90[17]	-756.12	12.22

2.3.3 H, C, N, O, F, Si, Cl, Br

Another important element is silicon, with its best known use in the semi-conductor industry, however it is also under investigation as, for example, a rocket propellant[218]. Experimental formation enthalpies are often obtained by combustion calorimetry, which poses a problem in the case of silicon-containing compounds. When combusted under oxygen, silcon-containing compounds such as silanes have been shown to self-passivate during the combustion process, as a layer of silicon oxide forms on the surface of the sample[218]. More sophisticated calorimetry methods[219], such as fluorine calorimetry[220–222] or reactions with hydrogen[223] have been developed to resolve the problem, nevertheless, there often remains a not insignificant margin of error in published experimental data[224,225]. This provides a problem when selecting appropriate values for the fitting set, as bad reference values will propagate into a bad fitting. As a result, it was decided to select the values that provide the most consistent fitting, with badly fitted species to be discussed independently. The statistics for the best fitting set are shown in Table 2.6.

The two largest errors in the silane fitting set are observed with dimethyl-silane (1111-74-6) with an error of -10.60 kJ/mol and silicon-tetrachloride (10026-04-07) with and error of 12.42 kJ/mol.

A further problem with the calculation of enthalpies of formation for silicon-compounds

Table 2.6: Overview of errors in kJ/mol for the set of species covering the elements H, C, N, O, F, Si, Cl and Br. Values presented are largest errors (positive and negative), mean error, mean absolute error as well as the standard deviation.

opt & freq	B3LYP	ωB97X-D3	BP86		
basis	def2-TZVP				def2-QZVPP
E_0, DLPNO-CCSD(T)	def2-QZVP			def2(3,4) extr.	
unscaled					
mean	0.30	0.31	0.29	0.12	0.10
mean absolute deviation	3.86	3.95	3.97	3.74	3.74
standard deviation	4.99	5.06	5.10	4.99	4.97
largest error +	12.97	13.01	12.57	12.75	12.42
largest error -	-11.57	-11.93	-11.48	-13.1	-12.77
scaled					
mean	0.28	0.29	0.31	0.14	
mean absolute deviation	3.82	3.93	3.98	3.74	
standard deviation	4.94	5.05	5.11	4.98	
largest error +	12.92	13.03	12.78	12.41	
largest error -	-11.83	-12	-11.42	-13.04	
C_p-scaled					
mean	0.28	0.27	0.32	0.15	0.13
mean absolute deviation	3.85	3.93	3.99	3.75	3.74
standard deviation	4.98	5.04	5.12	4.97	4.95
largest error +	12.97	13.04	12.88	12.24	11.86
largest error -	-11.61	-12.05	-11.38	-13	-12.66

is the absence of new, verified experimental data. Large errors are observed for a number of compounds for which the only reference consists of the JANAF tables[226], with a note indicating the last review of the data having taken place in the 1960ies[215]. The reference for the ethylsilanes[227] is newer, however unfortunately subject to not insignificant uncertainties of $\pm 20\,\mathrm{kJ\,mol^{-1}}$ in some cases. In addition, the authors discuss earlier measurements for some compounds such as for example $(C_2H_5)_4Si$, for which greatly deviating measurements exist. These are attributed to incomplete combustion, a problem they suggest to have solved using the described methodology[227]. Interestingly, the authors break down the published values into liquid phase and gas phase values, with the enthalpy of formation in the liquid phase at $\approx 276\,\mathrm{kJ/mol^{-1}}$ notably higher than in the gas phase at $\approx 235\,\mathrm{kJ\,mol^{-1}}$. A higher energy outlier is also presented for either case. The publication[227] then goes on to present the new mea-

surement of the gas phase enthalpy of formation as 297(5) kJ /mol^{-1}. Interestingly, the result of the calculation of the enthalpy of formation using regression coefficients aligns more closely with the cited older measurements for the gas phase compound, than the newer measurement. For the other compounds, only old JANAF table data is available[226]. As it is not clear how this data was obtained, we can only quote the value as well as our prediction.

Table 2.7: Compounds excluded from the fitting due to large errors between available reference data and calculations with BP86 and the def2-QZVPP basis set with unscaled frequencies. All values in kJ/mol.

Compound Name	CAS Number	ref. ΔH_f	calc. ΔH_f	error
tetramethyl-silane	75-76-3	-286.60[215,226]	-210.65	-75.95
ethyl-silane	2814-79-1	-84.00[227,228]	-31.46	-52.54
triethyl-silane	617-86-7	-217.50[227–229]	-173.72	-43.78
tetraethyl-silane	631-36-7	-297.00[227,228]	-246.92	-50.08
diethylmethyl-silane	760-32-7	-200.00[227]	-165.11	-34.89
dioxosilane	7631-86-9	-305.43[215,226]	-277.89	-27.54
fluorosilane	13537-33-2	-376.56[215,226]	-355.57	-20.99
trifluoromethyl-silane	373-74-0	-1232.71[215,226]	-1279.13	46.42
methyltrichlorosilane	75-79-6	-528.86[215,226]	-581.82	52.96
vinyl-trichlorosilane	75-94-5	-481.16[22,230] or -496.22[215,226]	-459.96	-21.20
chlorotrifluorosilane	14049-36-6	-1317.96[215,226]	-1373.42	55.46
trichlorofluorosilane	14965-52-7	-840.98[215,226]	-906.70	65.72
difluorooxosilane	14041-22-6	-966.50[215,226]	-898.70	-67.80

Referring again to the study of Ghahremanpour et al.[127] for tetramethylsilane, we find that they predict a value in the range of −216.3 kJ/mol to −224.2 kJ/mol. In addition, the authors suggest that the reference value of −286.60 kJ/mol may be incorrect and the value of −237.1(34) kJ/mol from Yaws et al.[210] is in better agreement with other sources. For fluorosilane, Ghahremanpour et al.[127] found −368.0 kJ/mol for CBS-QB3, −355.8 kJ/mol to −357.9 kJ/mol for G2, G3 and G4 as well as −367.4 kJ/mol and −367.8 kJ/mol for W1BD and W1U. Our result agrees well with the Gn results obtained by Ghahremanpour et al.[127]. For methyltrichlorosilane, Ghahremanpour et al.[127] cite a different reference enthalpy of formation of −571.812 kJ/mol[214], with the best results obtained using the Gn methods with enthalpies of formation around −570.6 kJ/mol to −575.7 kJ/mol[127]. CBS-QB3 gives −599.0 kJ/mol, while W1BD and W1U give −592.9 kJ/mol and −592.7 kJ/mol[127]. For vinyl-trichlorosilane, proposed values are with CBS-QB3 −475.0 kJ/mol, with

Gn $-446.3\,\mathrm{kJ/mol}$ to $-454.1\,\mathrm{kJ/mol}$ and $-469.2\,\mathrm{kJ/mol}$ for W1BD and W1U[127]. Once again, our result agrees well with the Gn values, while CBS-QB3 is closest to the reference value. The other compounds in the list were not investigated by Ghahremanpour et al.[127].

A similarity between the Gn methods and our approach is the use of DFT for geometry optimizations and thermochemistry calculations. In contrast, Weizmann theory uses post-SCF methods for the geometry optimization, however CBS-QB3 also employs a DFT geometry.

2.3.4 H, C, N, O, F, Si, P, Cl, Br

Phosphorous is essential in biochemistry, but also of interest in the context of industrial processes, such as for example silicon refining for applications such as solar cells[117,231]. Thus, it was decided to include a small subset of phosphorous compounds in the investigation.

As can be seen from Table 2.8, the errors observed remain low. Once again, a number of compounds are not well described, shown in Table 2.9. A problem with phosphorous compounds is the single data point[215] for these compounds consisting of the JANAF tables from Chase et al.[226] with no indication on how the data was originally obtained.

Table 2.8: Overview of errors in kJ/mol for the set of species covering the elements H, C, N, O, F, Si, P, Cl and Br. Values presented are largest errors (positive and negative), mean error, mean absolute error as well as the standard deviation.

opt & freq	B3LYP	ωB97X-D3	BP86		
basis	def2-TZVP				def2-QZVPP
E_0, DLPNO-CCSD(T)	def2-QZVP			def2(3,4) extr.	
unscaled					
mean	0.28	0.29	0.28	0.09	0.08
mean absolute deviation	3.82	3.91	3.95	3.73	3.8
standard deviation	4.94	5.02	5.10	4.97	4.98
largest error +	12.99	12.97	12.73	12.4	12.08
largest error -	-11.68	-12.11	-14.02	-13.37	-12.97
scaled					
mean	0.26	0.27	0.30	0.11	
mean absolute deviation	3.79	3.9	3.96	3.73	
standard deviation	4.89	5.01	5.12	4.96	
largest error +	12.91	12.97	12.75	12.06	
largest error -	-11.95	-12.19	-14.08	-13.3	
C_p-scaled					
mean	0.26	0.25	0.31	0.12	0.11
mean absolute deviation	3.81	3.89	3.97	3.73	3.79
standard deviation	4.93	5.00	5.13	4.95	4.95
largest error +	12.98	12.97	12.76	11.9	11.59
largest error -	-11.73	-12.24	-14.1	-13.27	-12.86

Table 2.9: Outlier in the fitting.

Compound Name	CAS Number	ref. ΔH_f	calc. ΔH_f	error
trimethyl phosphite	121-45-9	-699 ± 8 [117]	-677.84	-21.16
phosphorous-mononitride	17739-47-8	104.78 [215,226]	180.70	-75.92
phosphoryl-chloride-fluoride	13769-76-1	-765.67 [215,226]	-794.93	29.26
phosphoryl-tribromide	7789-59-5	-406.02 [215,226]	-379.62	-26.40
methinophosphide	6829-52-3	149.90 [215,226]	216.61	-66.71

The only problematic compound also covered by Ghahremanpour et al.[127] is phosphorous-mononitride, with a quoted reference enthalpy of 171.5 kJ/mol[214]. The results are given as 180.7 kJ/mol to 176.2 kJ/mol for CBS-QB3 and Gn as well as

187.0 kJ/mol and 185.4 kJ/mol for W1BD and W1U[127]. Our value agrees with the CBS-QB3 prediction and if the reference value from the CRC handbook were taken, the source used in the cited study, the error would be around 10 kJ/mol which would lead to inclusion in the fitting set.

2.3.5 H, C, N, O, F, Si, P, S, Cl, Br

Sulfur compounds are commonly found in fuels where they are nowadays considered contaminants due to the undesirability of sulfur oxides in exhaust streams. Other uses of sulfur compounds include their use in industrial products such as vulcanised rubber, scents as well as the semi-conductor industry.

Unfortunately, in the presented implementation, the prediction of sulfur compounds is only possible with the limitation that the oxidation number must be consistent. Thus, values are presented for sulfur (II), (IV) and (VI) independently. The main constituents of the sulfur (II) group are mercaptans which are a subgroup of organo-sulfurs which are generally well described in literature. However it equally includes sulfur difluoride and sulfur monoxide. Sulfur (IV) compounds most notably contain sulfite species and form the second fitting group. The third group consists of sulfur (VI) compounds, most notably sulfates as well as halogenated sulfurs.

As shown in Table 2.10, the errors observed with well fitting sulfur (II) compounds remain low, suggesting the method applicable.

The discrepancy in the data proved large for only one of the species amongst the mercaptans, namely dihydro-3-2H-thiophenone (1003-04-09) with a reference value of −135.30 kJ/mol for which an enthalpy of formation of around −168.65 kJ/mol is calculated. This may suggest a problem with the original data, which is a single reference only[232]. The result for the sulfur (IV) group is shown in Table 2.11. While we see a small increase in the mean deviation as well as mean absolute deviation as well as standard deviation, the overall performance of the method remains very similar suggesting that it is applicable to sulfur (IV) compounds when these are treated in isolation.

Amongst the selected sulfur (IV) compounds, only one exhibits a large deviation relative to the reference values, namely thionyl-fluoride (7783-42-8) with a reference value of −543.92 kJ/mol and a predicted value of −590.27 kJ/mol. Unfortunately, we were unable to locate any references for thionyl flouride beyond the JANAF tables[215,226], which precludes us from further commenting on the discrepancy observed between the reported and predicted enthalpy of formation. Sulfurous acid dimethyl ester(616-42-2) is predicted adequately in the sulfur (IV) only fitting with a refer-

Table 2.10: Overview of errors in kJ/mol for the set of species covering the elements H, C, N, O, F, P, Si, Cl and Br as well as sulfur (II) compounds. Values presented are largest errors (positive and negative), mean error, mean absolute error as well as the standard deviation.

opt & freq	B3LYP	ωB97X-D3	BP86		
basis	def2-TZVP				def2-QZVPP
E_0, DLPNO-CCSD(T)	def2-QZVP			def2(3,4) extr.	
unscaled					
mean	0.22	0.25	0.18	0.00	0.00
mean absolute deviation	3.54	3.66	3.68	3.51	3.54
standard deviation	4.74	4.88	4.91	4.77	4.76
largest error +	13.18	13.06	13.02	12.52	12.28
largest error -	-14.35	-15.16	-15.49	-13.79	-13.42
scaled					
mean	0.21	0.23	0.20	0.02	
mean absolute deviation	3.49	3.65	3.69	3.51	
standard deviation	4.69	4.87	4.93	4.76	
largest error +	13.11	13.06	13.04	12.19	
largest error -	-14.11	-15.09	-15.55	-13.71	
C_p-scaled					
mean	0.20	0.21	0.21	0.03	0.03
mean absolute deviation	3.54	3.64	3.69	3.50	3.52
standard deviation	4.73	4.86	4.94	4.75	4.74
largest error +	13.17	13.06	13.05	12.02	11.80
largest error -	-14.3	-15.04	-15.59	-13.67	-13.30

ence value of $-483\,\mathrm{kJ/mol}$ and a predicted value of $-469.27\,\mathrm{kJ/mol}$, resulting in an error of $-13.73\,\mathrm{kJ/mol}$. However in the case where all sulfur oxidation states are included in the fitting, the error increases to $-19.20\,\mathrm{kJ/mol}$ leading to this compound being excluded from the fitting set. At the same time, this further promotes the use of dedicated regression coefficients depending on the oxidation state of sulfur.

The last group of sulfur compound are the sulfur (VI) species, for which the error statistic is shown in Table 2.12. In absolute numerical terms, the errors are smaller than for sulfur (VI) and near identical to the results observed with the sulfur (II) compounds, again supporting the use of the method.

In the set of sulfur (VI) species, two compounds are in signicant disagreement

Table 2.11: Overview of errors in kJ/mol for the set of species covering the elements H, C, N, O, F, P, Si, Cl and Br as well as sulfur (IV) compounds. Values presented are largest errors (positive and negative), mean error, mean absolute error as well as the standard deviation.

opt & freq	B3LYP	ωB97X-D3	BP86		
basis	def2-TZVP				def2-QZVPP
E_0, DLPNO-CCSD(T)	def2-QZVP			def2(3,4) extr.	
unscaled					
mean	0.38	0.48	0.43	0.25	0.24
mean absolute deviation	3.92	4.03	4.05	3.85	3.88
standard deviation	5.02	5.14	5.17	5.04	5.05
largest error +	13.00	12.93	12.82	12.42	12.12
largest error -	-11.75	-12.21	-13.30	-13.46	-13.06
scaled					
mean	0.36	0.46	0.45	0.27	
mean absolute deviation	3.88	4.01	4.07	3.85	
standard deviation	4.97	5.12	5.2	5.03	
largest error +	12.92	12.93	12.84	12.09	
largest error -	-12.02	-12.29	-13.35	-13.39	
C_p-scaled					
mean	0.37	0.44	0.46	0.28	0.27
mean absolute deviation	3.91	4.00	4.08	3.85	3.88
standard deviation	5.01	5.11	5.21	5.03	5.03
largest error +	12.99	12.93	12.85	11.92	11.60
largest error -	-11.8	-12.34	-13.37	-13.35	-12.94

with literature data, namely disulphur-decafluoride (5714-22-7) with a reference value of $-2064.39\,\mathrm{kJ/mol}$, a calculated value of $-1873.33\,\mathrm{kJ/mol}$ and sulfur-chloride-pentafluoride (13780-57-9) with a reference value of $-1038.89\,\mathrm{kJ/mol}$ and a calculated value of $-988.25\,\mathrm{kJ/mol}$.

Disulfur decafluoride is a problematic molecule, with no clear reference data beyond Chase et al.[226] being available, a note stating values were last reviewed in 1977[215]. Irikura[233,234] suggests an enthalpy of formation of $1903(8)\,\mathrm{kJ\,mol^{-1}}$, but also suggests that an enthalpy of formation of $2073\,\mathrm{kJ\,mol^{-1}}$ has been suggested based on equilibrium measurements, while an enthalpy of $1891\,\mathrm{kJ\,mol^{-1}}$ is suggested based on reaction rate measurements. All these values conflict with Chase et al.[215,226] whose JANAF tables suggest an enthalpy of formation of $-2064.39\,\mathrm{kJ\,mol^{-1}}$. And finally,

Table 2.12: Overview of errors in kJ/mol for the set of species covering the elements H, C, N, O, F, P, Si, Cl and Br as well as sulfur (VI) compounds. Values presented are largest errors (positive and negative), mean error, mean absolute error as well as the standard deviation.

opt & freq	B3LYP	ωB97X-D3	BP86		
basis	def2-TZVP				def2-QZVPP
E_0, DLPNO-CCSD(T)	def2-QZVP			def2(3,4) extr.	
unscaled					
mean	0.25	0.25	0.24	0.05	0.01
mean absolute deviation	3.76	3.84	3.91	3.69	3.78
standard deviation	4.87	4.94	5.05	4.90	4.93
largest error +	13.11	13.05	12.95	12.30	12.01
largest error -	-11.72	-12.14	-14.26	-13.46	-13.03
scaled					
mean	0.22	0.23	0.26	0.07	
mean absolute deviation	3.72	3.83	3.92	3.68	
standard deviation	4.82	4.93	5.07	4.89	
largest error +	13.03	13.05	12.97	11.97	
largest error -	-11.98	-12.21	-14.31	-13.39	
C_p-scaled					
mean	0.23	0.21	0.27	0.08	0.05
mean absolute deviation	3.75	3.82	3.93	3.68	3.76
standard deviation	4.86	4.93	5.08	4.88	4.90
largest error +	13.10	13.05	12.98	11.86	11.72
largest error -	-11.77	-12.26	-14.33	-13.35	-12.92

by Pass[235] from 1969 suggests that the enthalpy of formation should be around 2037 kJ mol^{-1}. This wide discrepancy of reported data, which may not be an exhaustive list, makes a realistic assessment of the method for disulfur decafluoride impossible. Hence we present the calculated value as is. A similar lack of data exists for pentafluoru-trifluoromethyl-sulfur, with the only data given, being the JANAF tables of Chase et al.[215,226] While the compound has been researched previously[236], no other sources for the enthalpy of formation are available. Identified to be a powerful greenhouse gas, there has been some interest in the compound, unfortunately without any new data concerning the enthalpy of formation[237–239].

The final step was then to apply the method to the entire test set which includes sulfur (II), (IV) and (VI) compounds. The error statistic is shown in Table 2.13. Once again, the error statistic looks extremely similar to those presented earlier for

sulfur (II), (IV) and (VI). In contrast to the previous groupings, the error distribution for especially B3LYP shows significant broadening with a less well defined peak in the distribution. Conversely, ωB97X-D3 also shows a significant broadening of the peak, while BP86 fears better. All methods also exhibit an expanded error range on the x-axis, reinforcing the observation that the error range has increased.

Table 2.13: Overview of the errors in kJ/mol in the set covering the elements H, C, N, O, F, P, Si, Cl and Br as well as sulfur (II), (IV) and (VI) compounds.

opt & freq	B3LYP	ωB97X-D3	BP86		
basis	def2-TZVP				def2-QZVPP
E_0, DLPNO-CCSD(T)	def2-QZVP			def2(3,4) extr.	
unscaled					
mean	0.49	0.55	0.54	0.27	0.26
mean absolute deviation	4.17	4.30	4.52	4.02	3.99
standard deviation	5.37	5.48	5.84	5.28	5.26
largest error +	14.58	14.25	14.9	12.98	13.12
largest error -	-15.66	-15.19	-21.83	-14.44	-14.09
scaled					
mean	0.47	0.53	0.57	0.30	
mean absolute deviation	4.10	4.28	4.54	4.03	
standard deviation	5.30	5.46	5.86	5.27	
largest error +	14.49	14.24	14.92	13.01	
largest error -	-15.48	-15.02	-21.91	-14.37	
C_p-scaled					
mean	0.48	0.51	0.58	0.31	0.30
mean absolute deviation	4.16	4.27	4.55	4.03	3.98
standard deviation	5.36	5.45	5.87	5.27	5.24
largest error +	14.57	14.24	14.94	13.02	13.11
largest error -	-15.6	-14.91	-21.95	-14.34	-13.97

This observation can be explained by investigating the regression coefficients obtained in the optimization steps. For discussion and easy comparison, the regression coefficients for the best performing method, BP86 with def2-QZVPP, using unscaled frequencies are shown in Table 2.18 at the end of this section. As can be seen from Table 2.18, the addition of sulfur in just a single oxidation set does not lead to a large impact on the resulting regression coefficients with only small numerical changes being observed. However when all sulfur oxidation states are included in the fitting, the regression coefficient for oxygen changes by 3.889 kJ/mol. While the values for the

other elements change less, the variation is significantly larger than with just a single oxidation state for sulfur. A close look at the regression coefficient for sulfur reveals a difference of 13.826 kJ/mol between the largest and smallest regression coefficient.

Thus it can be concluded that one suitable approach would be to consider the different oxidation states of sulfur individually with dedicated regression coefficients. However it would be desirable to improve the method so that all oxidation states of sulfur can be treated efficiently within a single consistent framework. The work presented herein shows that the method can be applied without any problems to a single oxidation state, however is negatively affected by the presence of multiple oxidation states. Focussing only on the calculations carried out with BP86 for the geometry optimization and frequency step for the set of all sulfur oxidation states, one can observe how the use of the basis set extrapolation leads to a reduction in the error. The standard deviation and mean error for BP86 with the def2-TZVP basis set are 5.83 kJ/mol and −0.52 kJ/mol. Employing a basis set extrapolation for the DLPNO step reduces both values to 5.29 kJ/mol and 0.29 kJ/mol. However employing the larger def2-QZVPP basis set for the optimization and frequency calculation together with a basis set extrapolation in the DLPNO step leads to near identical results which are 5.26 kJ/mol and 0.24 kJ/mol. The weakest step in the method with respect to accuracy is the geometry optimization and frequency calculation. Future work may want to look at the best method to employ in these steps, however this work is beyond the scope of this study.

Indeed, the subject of the accuracy of DFT-derived geometries for halogenated sulfurs is discussed by Kozuch et al.[240]. The authors[240] further also raise an interesting problem, namely the observation that the use of the dispersion correction has a negative influence on the quality of the geometry when investigating sulfur halogen bonds. In the conclusion, the authors[240] recommend double hybrids for energies, while M06-2X[241] and ωB97XD[242] are also recommended for geometries. As the functionals such as M05[243] and M06[241] are highly parametrised and known to provide good results in benchmarks and assessments[201,244–246], their performance for molecules outside of their parametrisation is unknown. In addition, the functionals are known to be mesh dependent[201,247], which is not ideal for the fast and efficient calculation of parameters for new or novel compounds. In these cases, it is desirable to employ a method which has been shown to generally provide good results without being affected by computational aspects such as the mesh used by the quantum chemistry software.

Table 2.14: Regression coefficients h_i obtained for B3LYP D3BJ with the def2-TZVP basis set using unscaled frequencies in kJ/mol.

									diff, no S	diff
H	1524.965	1525.584	1525.582	1525.567	1525.568	1525.546	1525.567	1525.484	0.619	0.619
C	99904.602	99903.789	99903.806	99903.810	99903.875	99903.870	99903.812	99904.216	0.813	0.813
N	143604.778	143605.426	143605.530	143605.872	143605.878	143606.032	143605.803	143606.111	1.094	1.333
O	197130.144	197129.960	197129.766	197129.854	197129.204	197128.823	197130.105	197125.686	0.378	4.458
F		261704.437	261704.313	261704.288	261704.207	261704.293	261704.242	261703.753	0.149	0.684
Si			759047.682	759047.706	759047.761	759047.824	759047.702	759048.355	0.024	0.673
P				895139.910	895140.007	895139.998	895139.936	895140.774	0.000	0.864
S(II)					1044342.717					
S(IV)						11044326.779				
S(VI)							1044325.132			
S(II,IV,VI)								1044341.247	0.000	17.585
Cl		1207039.356	1207039.334	1207039.363	1207039.326	1207039.302	1207039.371	1207039.007	0.000	0.069
Br		6754952.986	6754952.277	6754952.284	6754952.244	6754952.254	6754952.286	6754952.087	0.000	0.742

Table 2.15: Regression coefficients obtained for ωB97X-D3 with the def2-TZVP basis set using unscaled frequencies in kJ/mol.

									diff, no S	diff
H	1524.679	1525.346	1525.355	1525.330	1525.306	1525.261	1525.339	1525.197	0.676	0.676
C	99904.268	99903.393	99903.393	99903.398	99903.453	99903.481	99903.390	99903.778	0.875	0.878
N	143604.237	143604.823	143604.938	143605.292	143605.349	143605.529	143605.233	143605.646	1.055	1.409
O	197129.639	197129.454	197129.258	197129.390	197128.852	197128.262	197129.612	197125.463	0.381	4.176
F		261704.367	261704.255	261704.240	261704.171	261704.265	261704.208	261703.786	0.127	0.581
Si			759047.712	759047.744	759047.826	759047.980	759047.714	759048.444	0.032	0.732
P				895140.046	895140.154	895140.205	895140.045	895140.889	0.000	0.844
S(II)					1044342.314					
S(IV)						11044326.629				
S(VI)							1044327.103			
S(II,IV,VI)								1044341.072	0.000	15.685
Cl		1207039.265	1207039.287	1207039.338	1207039.355	1207039.271	1207039.350	1207039.065	0.000	0.290
Br		6754953.393	6754952.572	6754952.587	6754952.575	6754952.578	6754952.587	6754952.446	0.000	0.000

Table 2.16: Regression coefficients obtained for BP86 D3BJ with the def2-TZVP basis set using unscaled frequencies in kJ/mol.

									diff, no S	diff
H	1525.617	1526.198	1526.193	1526.137	1526.167	1526.085	1526.130	1526.044	0.581	0.581
C	99904.960	99904.213	99904.226	99904.278	99904.365	99904.353	99904.282	99904.791	0.747	0.747
N	143602.700	143603.552	143603.666	143605.237	143605.154	143605.396	143605.114	143605.391	2.537	2.696
O	197130.106	197129.869	197129.693	197129.587	197128.859	197128.684	197130.095	197124.832	0.519	5.274
F		261704.041	261703.916	261703.845	261703.743	261703.825	261703.754	261703.126	0.196	0.915
Si			759047.335	759047.499	759047.522	759047.693	759047.504	759048.293	0.164	0.958
P				895139.659	895139.746	895139.818	895139.720	895140.757	0.000	1.098
S(II)					1044342.717					
S(IV)						11044323.725				
S(VI)							1044320.996			
S(II,IV,VI)								1044340.945	0.000	21.721
Cl		1207039.281	1207039.287	1207039.286	1207039.192	1207039.225	1207039.311	1207038.814	0.000	0.497
Br		6754952.997	6754952.274	6754952.262	6754952.187	6754952.249	6754952.273	6754952.009	0.723	0.723

Table 2.17: Regression coefficients obtained for BP86 D3BJ with the def2-TZVP basis set and an extrapolated basis set in the DLPNO step using unscaled frequencies in kJ/mol.

									diff, no S	diff
H	1526.674	1527.319	1527.271	1527.263	1527.319	1527.211	1527.277	1527.227	0.645	0.645
C	99921.554	99920.712	99920.697	99920.678	99920.734	99920.744	99920.661	99921.022	0.876	0.893
N	143629.046	143629.354	143629.604	143629.472	143629.418	143629.646	143629.389	143629.621	0.558	0.600
O	197166.046	197165.891	197165.795	197166.035	197165.249	197165.173	197166.385	197162.430	0.251	3.955
F		261752.554	261752.501	261752.507	261752.422	261752.516	261752.451	261752.022	0.053	0.532
Si			759064.621	759064.574	759064.486	759064.755	759064.519	759065.008	0.047	0.522
P				895164.183	895164.180	895164.311	895164.180	895164.851	0.000	0.671
S(II)					1044375.541					
S(IV)						11044361.353				
S(VI)							1044361.119			
S(II,IV,VI)								1044374.361	0.000	14.422
Cl		1207083.242	1207083.563	1207083.664	1207083.655	1207083.613	1207083.702	1207083.432	0.000	0.422
Br		6756148.328	6756148.683	6756148.711	6756148.639	6756148.703	6756148.716	6756148.526	0.000	0.383

Table 2.18: Regression coefficients obtained for BP86 D3BJ with the def2-QZVPP basis set using unscaled frequencies in kJ/mol.

									diff, no S	diff
H	1526.700	1527.468	1527.403	1527.432	1527.457	1527.379	1527.455	1527.347	0.768	0.768
C	99921.633	99920.568	99920.555	99920.492	99920.595	99920.563	99920.471	99920.926	1.141	1.162
N	143632.271	143632.713	143632.948	143631.025	143630.877	143631.069	143630.978	143630.645	1.923	2.303
O	197166.007	197165.983	197165.940	197166.292	197165.505	197165.406	197166.693	197162.806	0.352	3.887
F		261752.589	261752.551	261752.592	261752.482	261752.599	261752.532	261752.047	0.041	0.552
Si			759064.390	759064.213	759064.230	759064.403	759064.139	759064.830	0.177	0.691
P				895163.577	895163.687	895163.769	895163.540	895164.582	0.000	1.042
S(II)					1044375.478					
S(IV)						11044361.636				
S(VI)							1044361.710			
S(II,IV,VI)								1044374.367	0.000	13.842
Cl		1207083.467	1207083.758	1207083.887	1207083.833	1207083.829	1207083.923	1207083.557	0.420	0.456
Br		6756147.924	6756148.618	6756148.683	6756148.602	6756148.675	6756148.685	6756148.477	0.759	0.761

Table 2.19: Regression coefficients obtained for B3LYP D3BJ with the def2-TZVP basis set using scaled frequencies in kJ/mol.

									diff, no S	diff
H	1525.758	1526.404	1526.393	1526.382	1526.372	1526.364	1526.384	1526.293	0.646	0.646
C	99904.908	99904.063	99904.073	99904.074	99904.148	99904.130	99904.074	99904.481	0.845	0.845
N	143605.137	143605.735	143605.856	143606.109	143606.113	143606.264	143606.037	143606.336	0.972	1.199
O	197130.230	197130.043	197129.913	197130.020	197129.400	197129.008	197130.286	197125.950	0.317	4.336
F		261704.504	261704.397	261704.378	261704.294	261704.382	261704.333	261703.846	0.126	0.658
Si			759046.638	759046.647	759046.730	759046.755	759046.638	759047.305	0.009	0.667
P				895139.590	895139.707	895139.672	895139.612	895140.457	0.000	0.867
S(II)					1044342.586					
S(IV)						11044326.953				
S(VI)							1044325.227			
S(II,IV,VI)								1044341.124	0.000	17.359
Cl		1207039.340	1207039.383	1207039.418	1207039.379	1207039.358	1207039.425	1207039.064	0.078	0.361
Br		6754953.005	6754952.400	6754952.408	6754952.372	6754952.378	6754952.410	6754952.216	0.605	0.789

Table 2.20: Regression coefficients obtained for ωB97X-D3 with the def2-TZVP basis set using scaled frequencies in kJ/mol.

									diff, no S	diff
	H,C,N,O	H,C,N,O,F,Cl,Br	H-C-N-O-F-Si-Cl-Br	H,C,N,O,F,Si,P,Cl,Br	all+S2	all+S4	all+S6	all+S	0.000	0.000
H	1525.257	1525.928	1525.932	1525.908	1525.886	1525.840	1525.918	1525.779	0.675	0.675
C	99904.585	99903.705	99903.704	99903.707	99903.762	99903.789	99903.699	99904.084	0.881	0.886
N	143604.512	143605.080	143605.203	143605.509	143605.562	143605.742	143605.447	143605.854	0.997	1.342
O	197129.788	197129.606	197129.434	197129.580	197129.037	197128.467	197129.809	197125.682	0.354	4.127
F		261704.491	261704.384	261704.372	261704.302	261704.397	261704.340	261703.920	0.119	0.571
Si			759047.404	759047.430	759047.507	759047.663	759047.398	759048.118	0.026	0.720
P				895139.900	895140.004	895140.056	895139.898	895140.732	0.000	0.834
S(II)					1044342.317					
S(IV)						11044326.681				
S(VI)							1044327.237			
S(II,IV,VI)								1044341.077	0.000	15.636
Cl		1207039.290	1207039.334	1207039.388	1207039.404	1207039.322	1207039.400	1207039.118	0.000	0.286
Br		6754953.384	6754952.621	6754952.637	6754952.624	6754952.629	6754952.638	6754952.495	0.000	0.889

Table 2.21: Regression coefficients obtained for BP86 D3BJ with the def2-TZVP basis set using scaled frequencies in kJ/mol.

									diff, no S	diff
H	1525.103	1525.680	1525.680	1525.624	1525.651	1525.571	1525.616	1525.527	0.577	0.577
C	99904.687	99903.944	99903.958	99904.011	99904.098	99904.087	99904.016	99904.526	0.743	0.743
N	143602.472	143603.339	143603.445	143605.056	143604.976	143605.218	143604.934	143605.217	2.584	2.746
O	197129.983	197129.744	197129.546	197129.428	197128.705	197128.513	197129.930	197124.649	0.555	5.334
F		261703.938	261703.808	261703.734	261703.633	261703.714	261703.644	261703.014	0.204	0.924
Si			759047.615	759047.783	759047.811	759047.981	759047.790	759048.587	0.168	0.972
P				895139.792	895139.882	895139.954	895139.855	895140.898	0.000	1.106
S(II)					1044342.724					
S(IV)						11044323.700				
S(VI)							1044320.902			
S(II,IV,VI)								1044340.950	0.000	21.822
Cl		1207039.263	1207039.249	1207039.245	1207039.151	1207039.183	1207039.270	1207038.771	0.018	0.499
Br		6754953.011	6754952.235	6754952.222	6754952.148	6754952.209	6754952.233	6754951.970	0.789	1.041

Table 2.22: Regression coefficients obtained for BP86 D3BJ with the def2-TZVP basis set and an extrapolated basis set in the DLPNO step using scaled frequencies in kJ/mol.

									diff, no S	diff
H	1526.160	1526.801	1526.758	1526.750	1526.804	1526.697	1526.764	1526.711	0.641	0.644
C	99921.280	99920.443	99920.428	99920.410	99920.466	99920.477	99920.394	99920.757	0.870	0.886
N	143628.818	143629.142	143629.384	143629.292	143629.240	143629.468	143629.210	143629.447	0.566	0.650
O	197165.923	197165.766	197165.649	197165.876	197165.095	197165.002	197166.220	197162.247	0.274	3.973
F		261752.451	261752.393	261752.395	261752.311	261752.405	261752.340	261751.910	0.058	0.541
Si			759064.900	759064.857	759064.773	759065.042	759064.804	759065.301	0.043	0.528
P				895164.316	895164.316	895164.447	895164.315	895164.993	0.000	0.678
S(II)					1044375.547					
S(IV)						11044361.326				
S(VI)							1044361.025			
S(II,IV,VI)								1044374.366	0.000	14.522
Cl		1207083.224	1207083.526	1207083.623	1207083.614	1207083.571	1207083.661	1207083.390	0.399	0.437
Br		6756148.342	6756148.644	6756148.671	6756148.600	6756148.663	6756148.676	6756148.487	0.329	0.334

2.3.6 Deriving scaling parameters from Heat Capacities

As introduced in Section 2.2.3, we have investigated the possibility of obtaining scaling parameters, by fitting calculated heat capacities C_p to experimentally determined heat capacities in a number of reference compounds from literature. The obtained scaling factors are shown in Table 2.23.

Table 2.23: Heat capacity derived scaling parameters used in this work.

functional	scaling factor
B3LYP D3BJ, def2-TZVP	0.987
wB97X-D3, def2-TZVP	0.965
BP86 D3BJ, def2-TZVP	1.029
BP86 D3BJ, def2-QZVPP	1.0325

Full plots of the reference heat capacities and estimated heat capacities are shown in section B for the interested reader. An excellent description of experimental heat capacities for normal and iso alkanes as well as halogenated compounds (refrigerants) is obtained. Exceptions are benzene and anisole, where the predicted values show a significant divergence relative to experimental values with BP86 and ωB97X-D3. B3LYP manages to describe benzene well, however also exhibits problems for the heat capacity of anisole. Given the good fit of nitrobenzene, which is also an aromatic compound, the origin of the problem for benzene remains unknown. Detailed investigations into the quantitative calculation of heat capacities are beyond the scope of this document, and readers are recommended to refer to publications that have focussed in depth on the prediction of the heat capacity of compounds. For this discussion, readers are referred to for example large scale benchmark studies and the discussions contained within, such as the work by Mardirossian and Head-Gordon[248]. Amongst the other chosen reference species, no clear trend is discernible between better and worse fitted species, potentially owing to the small fitting set employed in this study.

2.4 Application to Bio-oil Compounds

To present the application of the method proposed by Paulechka and Kazakov[16], it was decided to re-evaluate a number of compounds whose enthalpy of formation were originally calculate and published by Catoire et al.[124] All calculations were carried out using the combination of BP86 with D3BJ for the geometry optimization and frequency calculation and DLPNO-CCSD(T) for the electronic energy, following the

methodology outlined in Section 2.2.1. No reference compounds were chosen for a fitting and instead the regression coefficients obtained for the H,C,N,O fitting set were used, with the numbers given in the Section "Final Regression Parameters" as part of the results overview of our published work[42] and represented in the Table 2.21 above.

The accurate prediction of thermochemical properties is of crucial importance to understanding and design pyrolysis reactors. The following settings were used to estimate Enthalpies of formation.

```
Frequency Calculation:
functional: BP86
basis:      def2-TZVP
auxiliary:  def2/J RIJCOSX D3BJ grid4 tightscf

Frequencies (in cm^-1) are scaled as follows:
            100 -- 4000    1.0192

Electronic Energy Calculation:
functional: DLPNO-CCSD(T)
basis:      def2-QZVP
auxiliary:  def2/J def2-QZVPP/C RIJCOSX grid4 tightscf

Statistics errors obtained in the fitting:
(All results are reported in kJ/mol).
                    mean:       0.12
mean absolute deviation:       1.90
                variance:       7.47
     standard deviation:       2.73
       largest error + :       6.98
       largest error - :      -8.04

Regression coefficients by element:
   H:        1526.160
   C:       99921.280
   N:       143628.81
   O:       197165.92
```

Table 2.24: Prediction of the gas phase enthalpy of formation for a number of compounds typically found in bio-oil or representative of compounds typically found in bio-oil.

Compound	CAS	ΔHf_{ref} (kJ/mol)		ΔHf_{paper} [124] (kJ/mol)	ΔHf_{calc} (kJ/mol)	diff. to ref (kJ/mol)
1-hydroxy-2-propanone	116-09-6	-370.1		-371.1	-372.32	2.22
3-hydroxypropanal	2134-29-4			-330.1	-336.53	
hydroxyacetaldehyde	141-46-8			-314.6	-304.80	
2,6-dimethoxyphenol	91-10-1			-390.4	-385.83	
2-acetylfuran	1192-62-7	-207.4	[249]	-217.57	-205.04	-2.36
3-furaldehyde	498-60-2	-151.9	[249]	-165.69	-152.10	0.20
methyl-pyruvate	600-22-6			-522.2	-497.54	
1,2-ethanediol	107-21-1	-394.4	[215,250]	-374.89	-391.18	-3.22
2,5-dimethylfuran	625-86-5	-128.1	[251]	-124.62	-117.33	-10.77
2-furaldehyde	98-01-1	-149.6	[215]	-165.69	-152.81	3.21
2-furfuryl-alcohol	98-00-0	-212	[215]	-208.32	-219.31	7.31
4-ethyl-guaiacol	2785-89-9			-293.7	-295.57	
4-vinyl-guaiacol	7786-61-0			-178.2	-190.30	
Guaiacol	90-05-1	-246.10	[252]		-255.07	-8.97
creosol	93-51-6	-291.90	[215]		-283.75	
acetic-acid	64-19-7	-432.8	[16,253]	-433.04	-429.79	-3.01
benzene	71-43-2	82.9	[16,254]	82.01	81.41	1.49
dihydro-2,5-furandione	4100-80-5	-528.0	[124,255]	-532.20	-524.65	-3.35
ethylene	74-85-1	52.5	[16,253]	51.46	52.76	-0.26
ethanedial	107-22-2	-212.0	[215,256]	-220.08	-215.05	3.05
formic-acid	64-18-6	-378.5	[16,253]	-378.65	-378.48	-0.02
furan	110-00-9	-34.7	[215,257]	-34.91	-34.93	0.23
homovanillin	5703-24-2			-373.6	-361.84	
oxirane	75-21-8	-52.6	[215,226,258]	-56.90	-52.31	-0.29
phenol	108-95-2	-96.4	[215,259,260]	-87.44	-93.04	-3.36
tetrahydrofuran	109-99-9	-184.2	[215,258]	-184.10	-184.34	-0.14
4-propyl-guaiacol	2785-87-7			-318.40	-305.70	
coniferyl-alcohol	458-35-5			-348.53	-343.53	
eugenol	97-53-0			-183.68	-196.23	
guaiacylacetone	2503-46-0			-421.75	-396.65	
propioguaiacone	1835-14-9			-440.99	-406.65	
benzaldehyde	100-52-7	-36.8	[124,215,261]	-42.68	-37.75	0.95
benzofuran	271-89-6	13.8	[124,262]	15.48	13.85	-0.05
benzophenone	119-61-9	49.9	[215,263]	63.60	53.88	-3.98
dibenzofuran	132-64-9	47.3	[215,264]	57.32	53.90	-6.60
dihydrobenzofuran	496-16-2	-46.4	[124,265]	-51.46	-48.64	2.24
methoxy-benzene	100-66-3	-70.8	[124,266]	-76.57	-70.52	-0.28
methyl-heptanoate	106-73-0	-516.7	[124,267]	-525.09	-513.49	-3.21
naphtalene	91-20-3	150.6	[16,254]	153.97	147.66	2.94
o-cresol	95-48-7	-128.5	[124,215,260]	-120.92	-126.410	-2.09
toluene	108-88-3	50.2	[124,215,254]	49.79	50.70	-0.50
1-methylnaphtalene	90-12-0	116.9	[215,268]		115.62	1.28

Additional reference values were also obtained from literature for an assessment of the calculation results. The results are presented in Table 2.24.

As can be seen from Table 2.24, the combined DFT + DLPNO-based method as proposed by Paulechka and Kazakov[16] generally performs better than the only

DFT-based method originally proposed by Osmont et al.[41,139,140] However, this observsation is not universally true, with 2,5-dimethylfuran, 2-furfuryl-alcohol and 4-methyl-guaicol predicted worse in this study than in the original work by Catoire et al.[124].

2.5 Conclusion

The method generally provides excellent results for both the species in the fitting set as well as species in the prediction set taken from a bio-oil study[124].

If geometries are selected based on the DLPNO-CCSD(T) energy, the method appears to be insensitive to the DFT-functional used for the optimization and frequency calculation which is unexpected, given the very different performance of the employed DFT-functional in benchmark studies. If minimum energy structures are selected based on the DFT-energies, the results for both BP86 and wB97X-D3 can be described as fairly similar.

So while the method is not sensitive towards the functional used in the optimization step, it is nevertheless sensitive to making the right choices with regards to the minimum energy conformer and use of the DLPNO energy is recommended.

The combination of DFT and DLPNO-CCSD(T) with the def2/J and def2-QZVPP/C auxiliary basis sets and the RIJCOSX approximation provides a computationally very efficient low cost path for the calculation of formation enthalpies. This makes the method suitable for desktop application without significant computational resources. Calculations in this work were run without the use of an HPC cluster with typical run-times on the scale of hours for the larger molecules. The main computational limitation was the I/O operations using the hard drive during the DLPNO step whose impact could be minimized by running DLPNO calculations in series rather than in parallel as can be done with more memory and CPU dependent DFT-based geometry optimizations and frequency calculations. The expansion to additional elements provides a promising method for the prediction of the formation enthalpy of species that are difficult to measure or where significant uncertainty in the measurement exists and offers the opportunity for additional investigations.

Chapter 3

Prediction of Solvation Energy

3.1 Introduction

The interaction of molecules with solvents is clearly capable of producing dramatic effects on structure, reactivity, biological activity, equilibrium and reaction rate constants and a host of other aspects which are of central interest to chemistry.

Predictive methods based on ab initio calculations[16,17,41] can be very accurate for predicting gas phase thermochemical properties and are usually more versatile than group contribution methods. In this work we investigate different predictive methods of free Gibbs solvation energies that can be used for the kinetic modelling of reactions in the liquid phase. COSMO-SAC approaches are found to be more accurate as long as the vapor pressures of the solutes are known. We propose an extension of COSMO-SAC models to CPCM cavities and reoptimized the universal parameters of different versions of COSMO-SAC, for both COSMO (DMOL3) and CPCM (ORCA) cavities. The reoptimized models, especially the reoptimized COSMO-SAC 2006, lead to accurate predictions of the reference data for a broad range of systems. We obtained a significant improvement of the predictions of the activity coefficients of alkanes in water. The main advantages of COSMO approaches compared to the PCM and Abraham models is the possibility to treat explicitly solvent mixtures and study multicomponent systems.

One can classify the predictive methods of solvation energies into different categories[269,270]: (1) quantum mechanical (QM) methods; (2) classical molecular simulations, (3) equations of state and activity coefficient models; and (4) empirical methods.

Solvent continuum models[271–274] (implicit) are now routinely used in quantum mechanical (QM) studies to calculate solvation effects on molecular properties. In

these models, the solvent is represented by a dielectric continuum surrounding the solute molecules, creating an electrostatic potential[269]. Using ab initio calculation, continuum solvation models are applicable to a wide variety of solutes, including neutral and ionic compounds, and even transient species such as reaction intermediates and transition states. Among implicit QM methods, one can mention the polarizable continuum model (PCM)[269,275–277].

Klamt and co workers proposed an alternative approach which reconsiders some features of the PCM model but which can be used to multicomponent systems of any composition. They proposed the conductor-like screening models for realistic solvation (COSMO-RS)[79,80,278] , which is a predictive thermodynamic activity coefficient model. Later, Lin and Sandler[11] developed a modified version of COSMO-RS denoted as COSMO-SAC, and different versions of COSMO-SAC were proposed in the literature[11,13,18,19]. Both COSMO-SAC and COSMO-RS approaches are predictive thermodynamic models based on COSMO quantum calculation. They have been extensively used for the predictions of free energies of solvation and phase equilibria.

Other kinds of predictive approaches for solvation energies are thermodynamic models based on group contribution methods. One can mention the predictive activity coefficient models such as the UNIFAC model[279–281]. Group contribution methods can also be combined with equations of state (EoS), such as the SAFT-γ Mie EoS[282] or the GC-PPC-SAF[283] equation of state (Group Contribution – Polar Perturbed Chain – Statistical Associating Fluids Theory) for vapor liquid equilibria predictions. Computations are very fast with EoS and activity coefficients models, and the main advantage compared to the PCM approach is the possibility to consider multicomponent mixtures of any composition. Recently Moine et al.[284] proposed a predictive method for the solvation Gibbs energies, which is based on the Peng-Robinson cubic equation of state combined with the UNIFAC predictive model.

Solvation Gibbs free energies can also be predicted with classical molecular simulations (Monte-Carlo or Molecular dynamics), by performing the Widom particle insertion or thermodynamic integration. These approaches allow for a detailed description of the interactions between solvent and solute molecules, but are rather demanding in terms of CPU time. The accuracy of such approaches relies on the parametrization of the classical force fields[134,285], which contain intramolecular terms to describe bond stretching, angle bending, torsions, intermolecular terms for repulsion and dispersion, and electrostatic charge-charge interactions[134,285]. More recently the GPU molecular dynamics platform were developed with a much more accurate force fields such as the polarizable AMOEBA[286], AMBER18[287]. Other classical force fields also improved their accuracy as Amber[287,288], CHARMM, GROMACS, and OPLS-AA[289]. The recent models reduced very much their CPU time but still

comparing to the solvent continuum models and equations of state model; that are very fast; the classical molecular simulations can not be used in kinetics calculation methods to estimate thermochemistry properties.

A last class of predictive methods are QSPR models[270,290]. These models are empirical functions of molecular descriptors such as topological indices, geometric, quantum mechanical, and thermodynamic quantities. One can mention models based on empirical group contribution methods, such as the linear solvation energy relationships (LSER), the linear free energy relationships (LFER) and the theoretical linear solvation energy relationships (TLSER). Among these methods, one can cite the Abraham solvation LSER[291,292] method, which is commonly used in Green's approach and is discussed in details in this work.

Moine et al.[12] recently published an extensive database (the CompSol database) of solvation energies for pure components and binary mixtures, based on experimental data of different kinds (activity coefficients at infinite dilution, vapor-liquid equilibrium data, Henry constants, ..). The CompSol binary system data-bank contains 14102 binary mixtures involving 865 different solutes and 775 different solvent (including ionic liquids that were not studied in this work). In total, 70 062 values of infinite dilution solvation chemical potential data expressed in (kcal/mol) at different temperatures (K) are reported in CompSol as well as 29 344 values of infinite dilution solvation enthalpy data expressed in (kcal/mol)[12]. One aim of this work is to compare the prediction capabilities of COSMO-SAC with those of the Abraham solvation model, by considering the CompSol database as the reference data. We then proposed a re-parametrization of these COSMO-SAC models that leads to much better predictions, and extend these models to CPCM cavities.

3.2 Solvation Energy

The term "solvation energy" has been used with a multitude of meanings, and there is no general agreement on its definition. Ben Naim defines the solvation process of a molecule s in a fluid l as the transfer of the molecule s from a fixed position in an ideal gas phase (ig) to a fixed position in the liquid phase l. The process is carried out at constant temperature T and pressure P, and the composition of the system remains unchanged[63].

The chemical potential[293] of a solute i in a solution l of density ρ_i^l at temperature T is given by

$$\mu_i^l = \mu_i^{*l} + RT \ln \rho_i^l \Lambda_i^3, \tag{3.1}$$

where μ_i^{*l} is the pseudochemical potential, k_B the Boltzmann constant, ρ_i^l the density of solute i in the solution l, Λ_i^3 the thermal De Broglie wavelength of molecule i; $\Lambda_i = h/\sqrt{2\pi m_i k_B T}$, where h and m_i are the Planck constant and the molecular mass of molecule i, respectively.

The expression for the pure solute in the ideal gas phase is similar and given by eq. 3.2

$$\mu_i^{ig} = \mu_i^{*ig} + RT \ln \rho_i^{ig} \Lambda_i^3. \tag{3.2}$$

The solvation Gibbs free energy of solute i, according to the Ben-Naim definition, is given by

$$\Delta G_{i,solv} = \mu_i^{*l} - \mu_i^{*ig}. \tag{3.3}$$

$\Delta G_{i,solv}$ corresponds to the work done in transferring solute i from a fixed position in the gas phase to a fixed position in solution l, and the solvent molecules rearrange themselves to accommodate the added solute particle. At equilibrium, $\mu_i^l = \mu_i^{ig}$ and the two phases are at the equal temperature and pressure. One can show that [63,294]

$$\Delta G_{i,solv} = RT \ln \left[\frac{\rho_i^{ig}}{\rho_i^l} \right]_{eq}. \tag{3.4}$$

According to Ben-Naim's definition, the solvation Gibbs energy is calculated from the solute densities in the two coexisting vapor and liquid phases. The pseudochemical potential (residual potential) can be expressed in terms of the fugacity [281] as

$$\mu_i^*(T,P,x) = RT \ln \frac{\varphi_i(T,P,x)P}{RT\rho(x,T,P)} = RT \ln \varphi_i(T,P,x)Z, \tag{3.5}$$

In the case of an ideal gas, $Z = 1$ and $\varphi_i^{ig} = 1$, thus the pseudochemical potential of an ideal gas is $\mu_i^{*ig} = 0$. This leads to the expression of the solvation energy for a liquid phase shown in eq. 3.6, which is similar to the expression of Moine et al. [12],

$$\Delta G_{i,solv}(T,P,x) = RT \ln \left[\frac{\varphi_{i,liq}(T,P,x).P}{RT\rho_{liq}(T,P,x)} \right], \tag{3.6}$$

where $\varphi_{i,liq}(T,P,x)$ is the fugacity coefficient of solute i in the liquid phase of composition x; $\rho_{liq}(T,P,x)$ is the density of the liquid phase, P the pressure and T the temperature.

3.2.1 Estimation of solvation energy from activity coefficients at infinite dilution

At infinite dilution of solute i in solvent j, the density of the liquid mixture tends to the density of pure solvent j, i.e., $\rho_{liq}(T,P,x) = \rho_{j,liq}(T,P)$. The fugacity of solute i, $f_{i,liq}(T,P,x)$ is related to its activity coefficient as

$$f_{i,liq}(T,P,x) = P.x_i.\varphi_{i,liq}(T,P,x) = x_i.\gamma_{i,liq}(T,P,x).f_{purei,liq}(T,P). \tag{3.7}$$

On the other hand, the density of a liquid phase does not significantly depend on pressure. Consequently, according to Moine et al.[12], by assuming that the pressure P is close to the vapor pressure P_i^{sat} of solute i ($|P_i^{sat}(T) - P| < 10\,\text{bar}$), thus the solvation energy can be estimated from the solute activity coefficient, saturation pressure and the density of the saturated liquid phase as shown in eq.3.8 and eq.3.9

$$\Delta G^{\infty}_{i,solv}(T,P) = RT \ln \left[\frac{P_i^{sat}(T).\gamma_i^{\infty}(T,P).\varphi_i^{sat}(T)}{RT.\rho_{j,liq}^{sat}(T).exp\left(\frac{P_i^{sat}(T)-P}{RT.\rho_{i,liq}^{sat}(T)}\right)} \right] \tag{3.8}$$

$$\Delta G^{\infty}_{i,solv}(T,P) = RT \ln \left[\frac{P_i^{sat}(T).\gamma_i^{\infty}(T,P)}{RT.\rho_{j,liq}^{sat}(T)} \right]. \tag{3.9}$$

The saturation pressure $P_i^{sat}(T)$ of solute i and the saturated-liquid density $\rho_{i,liq}^{sat}(T)$ can be estimated with thermodynamic correlations. In our study, the DIPPR[295] database (Design Institute for Physical Properties) has been used to generate $P_i^{sat}(T)$ and $\rho_{i,liq}^{sat}(T)$ using temperature-dependent correlations fitted to experimental data[295]. The constraint of the use of these correlations is the limited temperature range. In most of the cases the maximum temperature range $T_{max}^{P_i^{sat}} = T_{max}^{\rho_{i,liq}^{sat}} = T_{c,i}$, where $T_{c,i}$ denotes the critical temperature of the component i.

The enthalpy of solvation ΔH^0_{solv} at standard pressure (1 atm) can be obtained from the standard free energy of solvation G_{solv}, by applying the Gibbs-Helmholtz equation as

$$\left(\frac{\Delta(\frac{G_{solv}}{T})}{\delta T} \right)_P = -\frac{\Delta H^0_{solv}}{T^2}. \tag{3.10}$$

3.2.2 Abraham's model

Gibbs solvation free energy

The Abraham model is the most commonly used model in Green's approach to estimate solvation free energies. One of the reasons to choose the Abraham solvation model is it's low computational time. It is expressed in terms of the partition coefficient K_{vs} (also known as gas-solvent partition coefficient) of a solute between the vapor phase and a particular solvent at 298 K[78,291], as

$$\log_{10} K_{vs} = c + eE + sS + aA + bB + vV, \tag{3.11}$$

where (c, e, s, a, b) are the solvent coefficients and (E, S, A, B, V) are the solute descriptors[292]: E is the solute excess molar refractivity in units of $(cm^3/mol)/10$, S is the solute dipolarity/polarizability, A and B are the overall hydrogen bond acidity and basicity, and V is the McGowan characteristic volume in units of $(cm^3/mol)/100$[291]. The solvent coefficients were obtained by linear regression using experimentally determined partitions and solubilities of solutes with known Abraham descriptors. The Abraham model is used in the RMG code[99] to estimate ΔG which is related to the K_{vs} of a solute according to the following expression :

$$\Delta G_{solv} = -RT \ln K_{vs}. \tag{3.12}$$

Enthalpy of solvation (Mintz model)

The Mintz model[296] is based on the Abraham solvation model, and is used to estimate the enthalpy of solvation at 298.15 K by using solvent and solute descriptors. The descriptors of the Mintz and Abraham methods were taken from the database provided by RMG's official website[99]. The solvation enthalpy is given by eq. 3.13,

$$\Delta H^0_{solv} = c + eE + sS + aA + bB + vV, \tag{3.13}$$

where (c, e, s, a, b) are the solvent coefficients and (E, S, A, B, V) the solute descriptors, in a manner similar to the Abraham Gibbs solvation free energy model.

3.3 COSMO-SAC model

The COnductor like Screening MOdel (COSMO) is a dielectric solvation model that can predict the activity coefficients of chemical species in a multicomponent mixture, by using results from computational chemistry. All COSMO-SAC models are

based on the original COSMO-RS model proposed by Klamt[80,81]. Lin and Sandler later proposed the COSMO-SAC model[11]. Several versions of COSMO-SAC were then developed[13,18,19,83,98,297,298]. Some vapor–liquid equilibrium experimental data measurements have been done for biomass compounds mixtures and used to assess COSMO-SAC model predictions, one can cite the work of Nala et al.[299] for the systems $furan + n - hexane$ and $furan + toluene$ and the work of Pr. Coquelet et al.[300] for liquid-liquid equilibria of water + solutes (acetic acid/acetol/furfural/guaiacol/methanol/phenol/propanal) + solvents (isopropyl acetate/toluene) ternary systems for pyrolysis oil fractionation.

In all these models the excess Gibbs free energy can be expressed as a sum of different contributions: combinatorial term, charge + hydrogen bonding term and for some versions dispersion terms. The combinatorial part accounts for entropic effects and is restricted to contributions which arise from the differences in the size and shape of the molecules. The other terms account for the effects which arise from energetic interactions. The activity coefficient of chemical species i is given by

$$\ln \gamma_{i/s} = \frac{\Delta G_{i/s}^{*chg} - \Delta G_{i/i}^{*chg}}{RT} + \ln \gamma_{i/s}^{SG} + \ln \gamma_{i/s}^{disp} = \ln \gamma_{i/s}^{res} + \ln \gamma_{i/s}^{SG} + \ln \gamma_{i/s}^{disp}, \quad (3.14)$$

where j ($j = i$ for pure solvent i and $j = s$ for mixture s). The Staverman-Guggenheim combinatorial term is given by

$$\ln \gamma_{i/s}^{SG} = \ln \frac{\phi_i}{x_i} + \frac{z}{2} q_i \ln \frac{\theta_i}{\phi_i} + l_i - \frac{\phi_i}{x_i} \sum_j x_j l_j, \quad (3.15)$$

with $\theta_i = \frac{x_i q_i}{\sum_j x_j q_j}, \phi_i = \frac{x_i r_i}{\sum_j x_j r_j}, l_i = \frac{z}{2}(r_i - q_i) - r_i + 1$; x_i is the mole fraction of component i, r_i and q_i are the normalized volume and surface area parameters of species i and z is the coordination number, taken to be 10. In all COSMO-SAC models, the molecular volume and surface area are obtained from ab initio calculations and are normalized with a standard volume r_0 and surface area q_0. In the case of binary mixtures with infinite dilution conditions the normalized volume r_0 cancels internally in the equations above.

In this work, the COSMO-SAC methods have been implemented in a C++ code. For each COSMO-SAC version the universal model parameters are set to their original values by default. We explored the re-optimization of parameters by regressing experimental data and propose new universal constants. The procedure for a COSMO-SAC calculation consists of the following steps:

i) First, we perform ab initio calculation on isolated molecules, in order to com-

pute their sigma profiles. In the COSMO-SAC approach, the commonly used package is the DMol3 module based on density functional theory (DFT) employing the BP86[95,301] method and COSMO calculations with an infinite dielectric constant. Lin and Sandler in their paper[11] used the implementation of DMol3 from Cerius2 and Mullins used the implementation from Materials Studio. Both software lead to slightly different ab initio calculations. In this work we use the 2014 version of DMOL3 (BIOVIA Materials Studio). The initial molecule geometry needs to be drawn in material studio, in Avogadro, chemcraft or it can be taken from an online source as a mol or mol2 file. The "geometry optimization" is then performed in the gas phase, as recommended by Sandler and co workers. Next, we carry out the "COSMO Energy Calculation" to obtain surface screening charges and generate the cosmo file. The reader is referred to the following references[11,18,298] for further details regarding the options and parameters used in the input file of DMOL3.

In this work, we extend the approach by computing the sigma profile of molecules with the CPCM module and the DFT method implemented in ORCA 4[148,149]. This step includes all the geometry optimization calculation, conformer stability, frequency calculation if needed and finally the cavity generation.

ii) Once the cosmo cavity or the CPCM cavity is generated, we determine the sigma profile of the mixture using the sigma profile of each molecule eq 3.16. The analytical COSMO-SAC models can then be used to compute the activity coefficients and solvation free energies.

3.3.1 CPCM cavities

The conductor-like polarizable continuum model, CPCM[80,271,276,302] is an implementation of the conductor-like apparent surface charge method. In these models the solute is placed in a cavity of roughly molecular shape. The solvent reaction field is described by apparent polarization charges on the cavity surface, which are in turn determined by the solute. The CPCM[80,271,276,302] implementation in ORCA 4.01[148,149] was used in this work using the BP86[95,301] method with dispersion D3BJ[150,151] and def2-TZVP[161,162], def2/J[163] RIJCOSX[164,165] basis set to generate the cpcm cavities. ORCA is for academic use freely available software developed at the Max Planck Institute for coal research in Mulheim an der Ruhr, Germany. To compute the CPCM[80,271,276,302] cavities with ORCA, as for cosmo cavities we first draw the molecule in Avogadro. Then we optimise the gas-phase geometry of molecules with a DFT method such as B3LYP[94,95] D3BJ[150,151], BP86 D3BJ[150,151], wB97X-D3.

When more than one conformer exists, all identified conformers are investigated and the conformer with the lowest electronic energy is kept. The conductor-like polarizable continuum model[80,271,276,302] (CPCM), is implemented in ORCA[148,149] and is an efficient and simple way of accounting for solvent effects in quantum chemical calculations. The solvent is represented as a dielectric polarizable continuum and the solute is placed in a cavity of approximately molecular shape. The solvent reaction field is described by polarization charges on the surface of the cavity. The cavity is created by the GEPOL algorithm[303] using a solvent-excluding or solvent-accessible surface. In our work we choose the infinite dielectric constant to generate the CPCM surface charge distribution.

3.3.2 $\sigma-$profile

The screening charge densities on a standard surface segment, σ^* from COSMO (DMOL3) or CPCM output, are averaged to give the apparent charge density σ by using expression[11] shown in eq.3.16 :

$$\sigma_m = \frac{\sum_n \sigma_n^* \frac{r_n^2 r_{eff}^2}{r_n^2+r_{eff}^2} \exp\left(-c\frac{d_{mn}^2}{r_n^2+r_{eff}^2}\right)}{\sum_n \frac{r_n^2 r_{eff}^2}{r_n^2+r_{eff}^2} \exp\left(-c\frac{d_{mn}^2}{r_n^2+r_{eff}^2}\right)} \tag{3.16}$$

where σ_m is the averaged charge density of segment m and σ_n^* is averaged charge density of segment n, $n = A_i/a_{eff}$ is the number of segments in molecule i, a_{eff} is the surface area of a standard segment and $r_{eff} = (a_{eff}/\pi)^{0.5}$ the radius of a standard surface segment, c the empirical correction factor and d_{mn} the distance between segments m and n. The sigma profile contains 50 segments, 0.001 e/Å^2 wide, in the range of -0.025 e/Å^2 to 0.025 e/Å^2. For COSMO cavities, we used the VT-2005 database of COSMO files for most molecules, while the CPCM cavity calculation were performed in this work. When COSMO files of some molecules were missing in the VT-2005 database, we used DMOL3 (Materials Studio 2014) and followed the procedure proposed by Xiong et al.[298] to generate these COSMO files.

The sigma profile (σ-profile), $p(\sigma)$, is the probability of finding a surface segment with a charge density σ. For a mixture, the σ -profile is the weighted sum of the σ profiles of all the components[11,18] and is given by

$$p_s(\sigma) = \frac{\sum_i x_i n_i p_i(\sigma)}{\sum_i x_i n_i} = \frac{\sum_i x_i A_i p_i(\sigma)}{\sum_i x_i A_i}, \tag{3.17}$$

where x_i is the mole fraction of component i, and A_i the total surface area from all the segments of component i; $p_i(\sigma) = A_i(\sigma)/A_i$, where $A_i(\sigma)$ is the surface area with the charge density σ.

3.3.3 Hydrogen bonding

Hydrogen bonding is taken in account by a matrix commonly called $\Delta W(\sigma_m, \sigma_n)$ in COSMO-SAC papers. Two different expressions of ΔW can be found in the literature: one can first refer to the expression of Lin and Sandler[11] without explicit hydrogen bonding, which is given by

$$\Delta W(\sigma_m, \sigma_n) = 0.5\alpha'(\sigma_m + \sigma_n)^2 + c_{hb} max[0, \sigma_{acc} - \sigma_{hb}] \times min[0, \sigma_{don} + \sigma_{hb}], \tag{3.18}$$

where $\sigma_{acc} = max[\sigma_m, \sigma_n]$, $\sigma_{don} = min[\sigma_m, \sigma_n]$ and $\alpha' = \frac{0.64 \times 0.3 \times a_{eff}^{3/2}}{\epsilon_0}$, where $\epsilon_0 = 2.395 \times 10^{-4} \mathrm{e}^2\mathrm{mol}/(\mathrm{kcal\AA})$. σ_{acc} and σ_{don} are the larger and smaller values of σ_m and σ_n.

An alternative formulation for ΔW with explicit hydrogen bonding is given by

$$\Delta W(\sigma_m, \sigma_n) = c_{es}\left(\sigma_m^t + \sigma_n^s\right)^2 - c_{hb}\left(\sigma_m^t, \sigma_n^s\right) \times \left(\sigma_m^t - \sigma_n^s\right)^2, \tag{3.19}$$

Different formulations for c_{es} exist, as well as different criteria for the types of segments, denoted s and t.

In the COSMO-SAC 2007 version of by Wang et al.[297], c_{es} is defined as

$$c_{es} = f_{pol}\left(\frac{0.3 \times a_{eff}^{3/2}}{2\epsilon_0}\right), \tag{3.20}$$

In the COSMO-SAC 2010 version of Hsieh et al.[19,83], c_{es} is temperature dependent and is defined as follows:

$$c_{es} = A_{es} + \frac{B_{es}}{T^2}. \tag{3.21}$$

The term c_{hb} can also be calculated with different expressions. For Wang et al.[297] the following expression is used:

$$c_{hb}\left(\sigma_m^t, \sigma_n^s\right) = \begin{cases} c_{hb} & \text{if } s = t = \text{hb, and } \sigma_m^t \sigma_n^s < 0, \\ 0 & \text{otherwise.} \end{cases} \tag{3.22}$$

Hsieh et al.[19] proposed the following expression for c_{hb}:

$$c_{hb}\left(\sigma_m^t, \sigma_n^s\right) = \begin{cases} c_{OH-OH} & \text{if } s = t = \text{OH, and } \sigma_m^t \sigma_n^s < 0, \\ c_{OH-OT} & \text{if } s = \text{ OH },\, t = \text{ OT, and } \sigma_m^t \sigma_n^s < 0, \\ c_{OT-OT} & \text{if } s = t = \text{OT, and } \sigma_m^t \sigma_n^s < 0, \\ 0 & \text{otherwise.} \end{cases} \tag{3.23}$$

3.3.4 Dispersion term

To our knowledge, the COSMO-SAC models developed before the 2014 versions of Hsieh et al.[13] and Xiong et al.[298] do not include any dispersion term for the calculation of activity coefficients. A dispersion term was included to correct and improve the predictions, but this dispersion term introduced a significant number of additional parameters that depend on the type of atoms in the molecules. In a binary mixture the dispersion contribution proposed Hsieh et al.[13] is based on the one parameter Margules model and is given by

$$\ln \gamma_1^{dsp} = A x_2^2, \tag{3.24a}$$

$$\ln \gamma_2^{dsp} = A x_1^2, \tag{3.24b}$$

where x_i is the mole fraction of component i in the liquid phase and A a constant determined from the molecular dispersion parameters ϵ_1 and ϵ_2, as follows:

$$A = w.\left[1/2\left(\varepsilon_1 + \varepsilon_2\right) - \sqrt{\varepsilon_1 \varepsilon_2}\right], \tag{3.25}$$

where

$$w = \begin{cases} -0.275, & \text{if (a) water + hb-only-acceptor,} \\ & \quad \text{(b) COOH + nhb or hb-donor-acceptor,} \\ & \quad \text{(c) water + COOH,} \\ 0.275, & \text{otherwise.} \end{cases} \tag{3.26}$$

The default global atomic dispersion parameters used in this work are taken from Hsieh et al.[13] and are given in Table 3.5. A re-optimization of these parameters has been carried out in this work, and the results are presented in the following Section 3.3.5.

3.3.5 Parameter optimization

We have re-optimised some of the universal parameters of COSMO-SAC models in order to better predict solvation energies. The optimization is achieved by using the open source nonlinear optimization library NLopt developed by Steven G. Johnson. This library provides a common interface for a number of different free optimization routines available online[172].

The minimizing function is calculated as the mean square deviation msd between the calculated Gibbs free solvation energies and reference Gibbs free solvation energy data reported by Moine et al. database[12]. The msd is given by

$$msd = 1/M \sum_{j=1}^{M} \left(\frac{\Delta G_{solv,j}^{calc} - \Delta G_{solv,j}^{ref}}{T} \right)^2 \tag{3.27}$$

where M is the total number of data points; T and $\Delta G_{solv,j}$ are the temperature and the Gibbs free solvation energy of each system j, respectively.

The global optimization was performed using a controlled random search[174,175] with local mutation[176] as implemented in the NLopt library, using the NLopt Algorithms called
$NLOPT\_GN\_CRS2\_LM$[172]. The optimization was carried out for different COSMO-SAC versions[11,13,18,19] considering both the COSMO (VT-2005 database , DMOL3) and CPCM cavities. The initial values of the COSMO-SAC parameters used in the optimization were the original values corresponding to each COSMO-SAC model. The bound constraints chosen where, 0.1 of the relative original / initial values for the lower constraint and 2 of the relative original / initial values for the upper constraint. After the optimization, the results are investigated for consistency and systems/species with large errors are manually removed from the fitting set, to be discussed independently of the parameter optimization. After the optimization, the results are investigated for consistency and systems/species with large errors are manually removed from the fitting set, to be discussed independently of the parameter optimization. The Figure 14 represents the algorithm that summarize the implemented methodology described above. The optimised parameters can be found in the results and discussion Section 3.4.

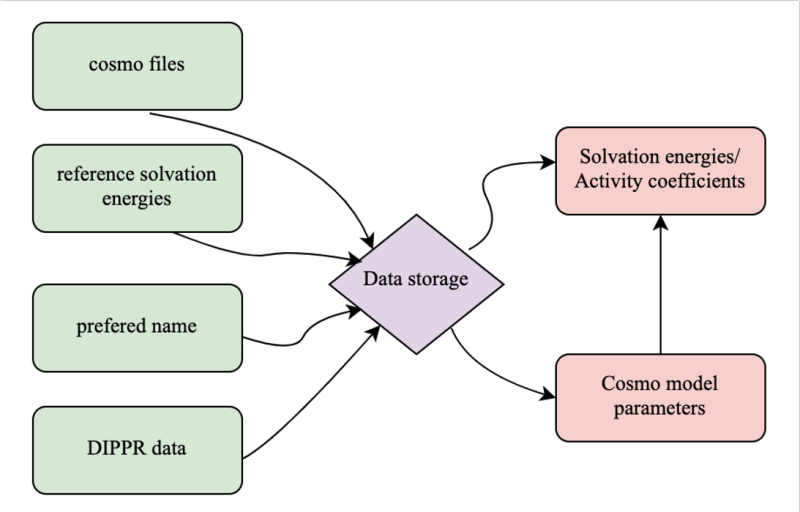

Figure 14: Algorithm of the implemented method to optimise activity coefficients and calculate predicted solvation energies at infinite dilution.

3.4 Results & discussion

First, one can compare the predictions of Abraham's model with those of the original COSMO-SAC 2002[11] and COSMO-SAC dsp (Hsieh 2014)[13] models .

As shown in Figure 15, the COSMO-SAC model predictions with COSMO cavities are much closer to the reference data (Moine et al. COMPSOL database[12]), in comparison to Abraham's model as the absolute deviation calculation shows; with an average absolute deviation (AAD) of the Gibbs free solvation energies for binary mixtures from Abraham's model to the reference data of 0.81 kcal/mol comparing to the AAD of the COSMO-SAC 2002 model estimated as 0.59 kcal/mol and the AAD with COSMO-dsp model that gives 0.72 kcal/mol. The results reported in the figure 15 (a) and (b) showed us the weakness of COSMO-SAC both models to describe the system with alkane solvent and water solute (ex: cyclohexane, hexane,heptane,octane,pentane, nonane). We also observed that systems with alcohol solute ex (ethanol, methanol) and water solvent gives important errors at a temperature range from 40 °C to 100 °C for further details see the supplementary data C.1 that shows the calculated values reported in the figure 15. These observations suggest that the cosmo models does not support temperature effect accurately. On the other hand, Abraham coefficients assume that groups always have the same contribution no matter the solvent effect or the neighbors where in the case of biomass compounds most of them are unknown. Therefore COSMO-SAC approaches seem

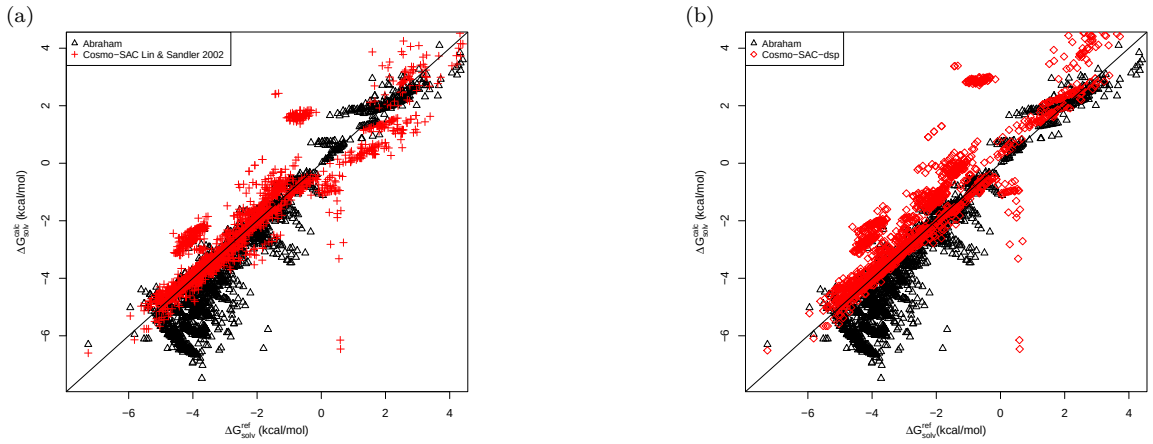

Figure 15: Prediction of Gibbs free solvation energies for binary mixtures: comparison between Abraham's model and COSMO-SAC models (VT-2005 database of COSMO-files). a) Abraham's model versus COSMO-SAC 2002 (Lin and Sandler's model[11]) compared to the reference data from the Moine et al.[12] COMPSOL database.b) Abraham's model versus COSMO-SAC dsp 2014 model[13] compared to the reference data from Moine et al.[12] database.

more suitable for the prediction of solvation energies of complex mixtures such as bio-oil. Moreover, COSMO-SAC models can be explicitly applied to multicomponent systems, while Abraham's model is dedicated to binary systems (one solute in one solvent) only. In the next following Sections 3.4.1,3.4.2 and 3.4.3, the universal parameters of COSMO-SAC models have been re-optimised in order to improve their accuracy.

3.4.1 Reoptimization of Lin and Sandler COSMO-SAC model

In this work, we have reoptimized some of the universal parameters of the original Lin and Sandler COSMO-SAC 2002 model[11], by minimizing the mean-square deviation between the calculated excess Gibbs free energy and the reference data taken from Moine et al. COMPSOL databank[12]. About 33800 reference data were considered to adjust only 3 universal parameters (a_{eff}, c_{hb} and σ_{hb}). For all the other parameters, we kept the original values from Lin and Sandler. Note that the standard volume r_0 does not have to be reoptimized as it cancels internally in the Staverman-Guggenheim combinatorial contribution for binary mixtures, as mentioned by Xiong and Sandler[298]. As a first step, a sensitivity analysis of the impact of the universal parameters a_{eff}, c_{hb} and σ_{hb} on the MSD of the solvation free energy was conducted. The results as presented in figure 16 show that we do have a minimum value of a_{eff} and c_{hb} that minimize the MSD error for Lin and Sandler COSMO-SAC 2002

model[11]. For σ_{hb} value, we conclude by saying that from a fixed limit the MSD will diverge, thus one must choose carefully this parameter. More details about the obtained optimised values will be given in the following section.

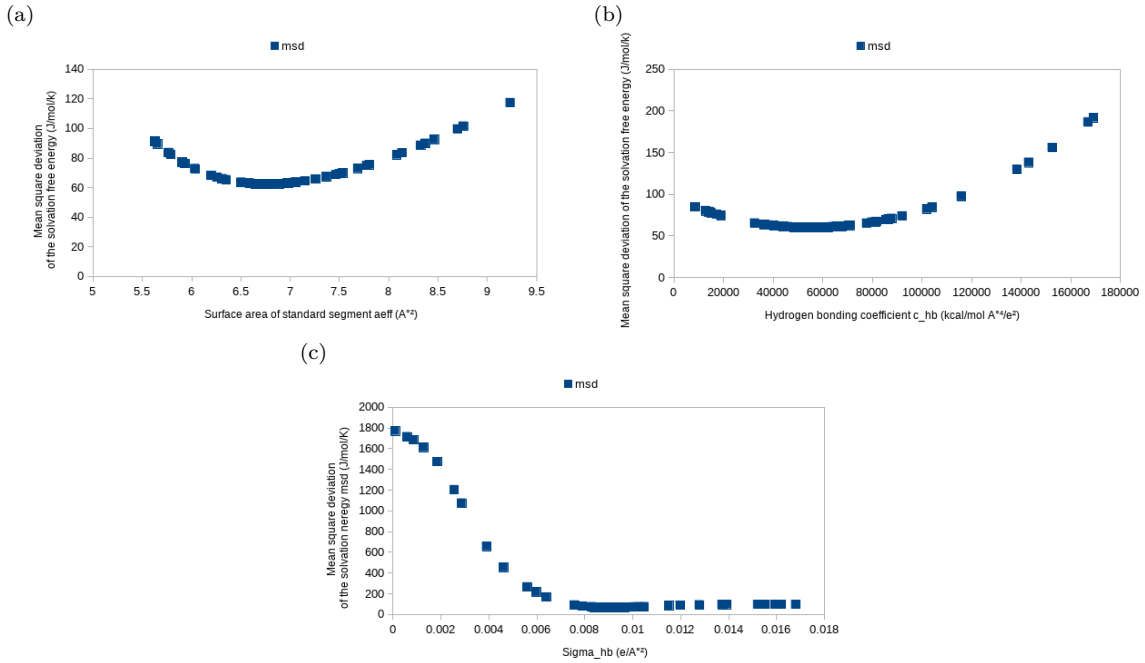

Figure 16: Sensitivity analysis results of the optimisation of the universal parameters a_{eff}, c_{hb} and σ_{hb} on the mean square deviation (MSD) of the solvation free energy calculated with error between Lin and Sandler COSMO-SAC 2002 model[11] and reference data[12]. (a) Sensitivity of a_{eff}. (b) Sensitivity of c_{hb}. (c) Sensitivity of σ_{hb}.

The new optimized parameters for COSMO (VT-2005 database, DMOL3) and CPCM cavities (ORCA) are reported in Table 3.1.

The reoptimized COSMO-SAC 2002 model has been used to predict infinite dilution activity coefficient data. The 50 solute compounds that we chose in this work are those used in Lin and Sandler's paper[11], and the solvents are water and Hexane. The activity coefficients at infinite dilution of somenalkane, alcohol and ketone solutes in water are presented in Table3.2 and in Figure 17, a comparison between experimental data and the COSMO-SAC prediction from Lin and Sandler 2002 model is given. One can show that the reoptimized version is much more accurate than the original one, especially for alkane-water systems. The original tends to underestimate the activity coefficients, while the bias error of the reoptimized model is much closer to

Table 3.1: Optimized parameters of the Lin and Sandler COSMO-SAC model.

Parameter cavities	description	Lin 2002 COSMO	Optimization COSMO	Optimization CPCM	Unit
a_{eff}	surface area of standard segment	7.5	6.78	6.22	$Å^2$
chb	Hydrogen bonding constant	85580.0	16654.3	42790	$(\text{kcal}\,Å^4)/(\text{mol}\,e^2)$
sighb	sigma cutoff for hydrogen bonding	0.0084	0.0046	0.00764	$e/Å^2$
Final error	mean square deviation error	75.59	45.77	50.28	J/(molK)

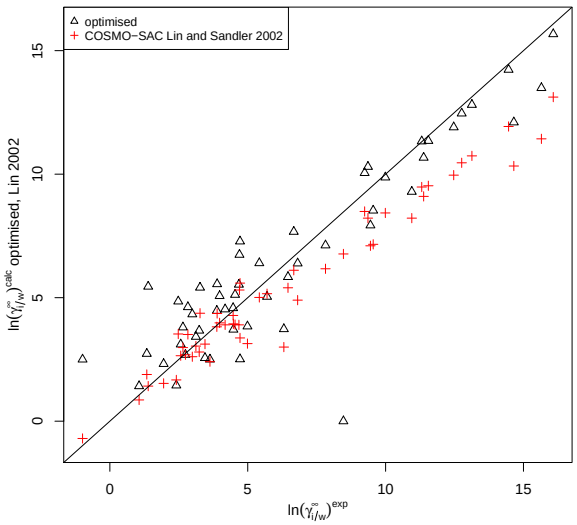

Figure 17: Prediction of activity coefficients at infinite dilution : comparison between the original Lin and Sandler[11] COSMO-SAC model and the reoptimized Lin and Sandler model. The reference of experimental data can be found in Ref.[11].

0.

The Gibbs solvation free energies were then estimated from these solutes activity coefficients, the saturation pressure of solutes and the density of solvent respectively using equations 3.9 or 3.8 depending on the pressure of the studied systems. The results were then compared to the work of Moine et al.[12] and are presented below in Tables 3.9 and 3.7 .

Table 3.2: Predictions of activity coefficients at infinite dilution in water, for solutes from different families: alkanes, alcohols and ketones: comparison between the original Lin and Sandler [11] COSMO-SAC model and the reoptimized Lin and Sandler model. The reference of experimental data can be found in Ref. [11].

		$\ln \gamma^{\infty}_{i/Water}$		
Solute	CAS	expt	Lin 2002[11]	Lin opt[w]
alkanes				
butane	106-97-8	9.99	8.34	9.87
pentane	109-66-0	11.55	9.53	11.35
hexane	110-54-3	13.13	10.74	12.81
heptane	142-82-5	14.46	11.93	14.23
octane	111-65-9	16.08	13.12	15.67
2,2-dimethylbutane	75-83-2	12.47	9.96	11.9
2-methylpentane	107-83-5	12.76	10.46	12.46
cyclohexane	110-82-7	11.31	9.48	11.33
alcohols				
ethanol	64-17-5	1.34	1.89	2.73
1-propanol	71-23-8	2.65	2.98	3.8
1-butanol	71-36-3	3.98	3.98	5.07
2-butanol	78-92-2	3.27	4.37	5.41
Tert-butyl alcohol	75-65-0	2.48	3.53	4.85
isobutanol	78-83-1	3.89	4.36	5.55
1-pentanol	71-41-0	5.42	5.01	6.4
1-hexanol	111-27-3	6.67	6.11	7.67
1-octanol	111-87-5	9.36	8.22	10.3
ketones				
acetone	67-64-1	1.95	1.53	2.32
2-butanone	78-93-3	3.24	2.8	3.67
2-pentanone	107-87-9	4.54	3.91	5.12
3-pentanone	96-22-0	4.68	3.9	5.53
AAD[*]			1.24	0.82

[*] $AAD = \frac{\sum_i^n \left| \ln \gamma^{\infty,calc}_{i/Water} - \ln \gamma^{\infty,exp}_{i/Water} \right|}{n}$

[w] Optimization done in this work

3.4.2 COSMO-SAC 2006

Mullins et al. [18] proposed different universal parameters from the original Lin and Sandler COSMO-SAC 2002 version, that we denote as COSMO-SAC 2006. They also proposed a new averaging of the apparent charge density, by using a new averaging radius and removing the correction factor with the following expression,

$$r_{eff} = r_{av} = 0.81764,$$

$$\sigma_m = \frac{\sum_n \sigma_n \frac{r_n^2 r_{av}^2}{r_n^2+r_{av}^2} exp\left(-\frac{d_{mn}^2}{r_n^2+r_{av}^2}\right)}{\sum_n \frac{r_n^2 r_{av}^2}{r_n^2+r_{av}^2} exp\left(-\frac{d_{mn}^2}{r_n^2+r_{av}^2}\right)}. \tag{3.28}$$

The re-optimised parameters of the COSMO-SAC 2006 are presented in Table 3.3. Note that we used an extended sigma profile range of [-0.05,0.05], instead of [-0.025, 0.025]. We maintain unchanged, the standard surface area and the standard volume as used in COSMO-SAC 2002.

Table 3.3: Optimized parameters of the COSMO-SAC 2006 (Mullins et al. model) for COSMO and CPCM cavities.

Parameter	description	Mullins 2006[18]	Optimization		unit
Cavities		COSMO	COSMO	CPCM	
a_{eff}	surface area of standard segment	7.5	6.48	6.805	$Å^2$
r_{av}	sigma averaging radius	0.81764	0.83235	0.69776	Å
c_{hb}	Hydrogen bonding constant	85580.0	21587.8	17731.9	$(\text{kcal}\,Å^4)/(\text{mol}\,e^2)$
σ_{hb}	sigma cutoff for hydrogen bonding	0.0084	0.00311	0.0027	$e/Å^2$
z	coordination number	10	10	10	-
q	standard area	79.53	79.53	79.53	$Å^2$
r	standard volume	66.69	66.69	66.69	$Å^3$
Final error	mean square deviation error	124.03	39.06	34.06	J/(molK)

The predicted activity coefficients at infinite dilution of alkanes, alcohol and ketones in water are reported in Table 3.4 and in Figure 17.

As shown in Figure 18 and in Table 3.4 the original COSMO-SAC 2006 version of Mullins et al. was not very well optimized compared to the other models. However, after the reoptimization of some universal parameters: a_{eff} the surface area of a standard segment, r_{av} the sigma averaging radius, c_{hb} the hydrogen bonding constant and σ_{hb} the sigma cutoff for hydrogen bonding (see eq. 3.18) using the extended sigma profile range [-0.05,0.05] , we found that the predictions were dramatically improved when c_{hb} the hydrogen bonding constant and σ_{hb} the sigma cutoff for hydrogen bonding were reduced as shown in Table 3.3.

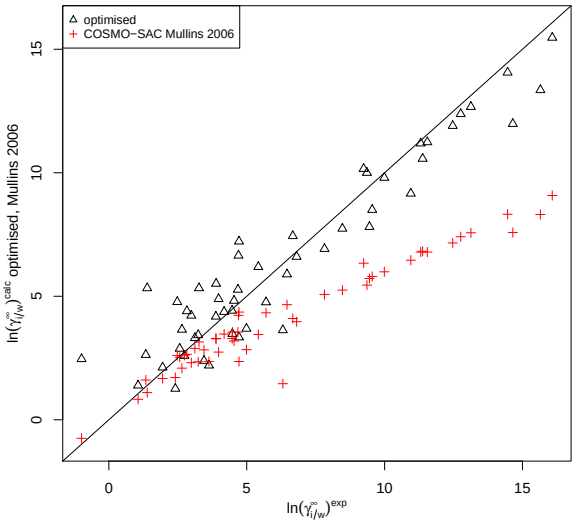

Figure 18: Prediction Activity Coefficients at infinite dilution: comparison between the original Mullins et al. 2006 COSMO-SAC model and the reoptimized Mullins et al. model in this work. The reference of experimental data can be found in Ref. [11].

Table 3.4: Prediction of activity coefficients at infinite dilution for solutes from different families: alkanes, alcohols and ketones in water. Comparison between the original COSMO-SAC 2006 model of Mullins et al. [18] and the reoptimized COSMO-SAC 2006 model (this work).

		$\ln \gamma^{\infty}_{i/Water}$		
Solute	CAS	exp	Mullins 2006[18]	Mullins opt[w]
alkanes				
butane	106-97-8	9.99	5.99	9.8
pentane	109-66-0	11.55	6.79	11.24
hexane	110-54-3	13.13	7.57	12.67
heptane	142-82-5	14.46	8.32	14.06
octane	111-65-9	16.08	9.08	15.47
2,2-dimethylbutane	75-83-2	12.47	7.16	11.9
2-methylpentane	107-83-5	12.76	7.41	12.38
cyclohexane	110-82-7	11.31	6.79	11.19
alcohols				
ethanol	64-17-5	1.34	1.61	2.63
1-propanol	71-23-8	2.65	2.09	3.65
1-butanol	71-36-3	3.98	2.74	4.89
2-butanol	78-92-2	3.27	3.15	5.33
Tert-butyl alcohol	75-65-0	2.48	2.6	4.77
isobutanol	78-83-1	3.89	3.28	5.51
1-pentanol	71-41-0	5.42	3.45	6.19
1-hexanol	111-27-3	6.67	4.1	7.44
1-octanol	111-87-5	9.36	5.45	10
ketones				
acetone	67-64-1	1.95	1.67	2.12
2-butanone	78-93-3	3.24	2.35	3.43
2-pentanone	107-87-9	4.54	3.19	4.82
3-pentanone	96-22-0	4.68	3.55	5.27
AAD[*]			2.75	0.74

[*] $AAD = \frac{\sum_i^n \left| \ln \gamma^{\infty,calc}_{i/Water} - \ln \gamma^{\infty,exp}_{i/Water} \right|}{n}$

[w] Optimization done in this work

3.4.3 Re-optimised COSMO-SAC 2010 and COSMO-SAC dsp

The universal parameters of the COSMO-SAC dsp[13] that have been re-optimised in this work are the atomic dispersion parameters given in Table 3.5, the hydrogen bonding parameters c_{hb} and c_{es}, the surface area of standard segment a_{eff}, and the Hydrogen bonding weighing charge σ_{hb}. Note that we used an extended sigma profile range of [-0.05,0.05], instead of [-0.025, 0.025] because sigma profile of charge density of some compounds (as an example one can cite Dipropylamine,Pyrocatecho, Heptylamine, Butylamine, 1,2,4-Benzenetricarboxylic anhydride, D-Sorbitol ...) exceeds [-0.025, 0.025] sigma profile range .

Table 3.5: Universal parameters of the COSMO-SAC dsp model: original parameters[13,19] via re-optimised parameters (this work) for COSMO cavities.

Parameters	Description	Original	optimised	Unit
a_{eff}	surface area of standard segment	7.25	7.00	$Å^2$
c_{es}	Electrostatic interaction coefficient	$6525.69 + \frac{1.4859e8}{T^2}$	$7963.66 + \frac{1.48968e7}{T^2}$	$\mathrm{kcal\,Å^4\,mol^{-1}\,e^{-2}}$
c_{OH-OH}	Hydrogen bonding interaction coefficient	4013.78	2026	$\mathrm{kcal\,Å^4\,mol^{-1}\,e^{-2}}$
c_{OT-OT}	Hydrogen bonding interaction coefficient	932.31	93.23	$\mathrm{kcal\,Å^4\,mol^{-1}\,e^{-2}}$
c_{OH-OT}	Hydrogen bonding interaction coefficient	3016.43	2044.25	$\mathrm{kcal\,Å^4\,mol^{-1}\,e^{-2}}$
Atomic dispersion	Atom type			
$\varepsilon_{C(sp3)}/k_B$	C (sp3)	115.7023	104.147	K
$\varepsilon_{C(sp2)}/k_B$	C (sp2)	117.4650	117.452	K
$\varepsilon_{C(sp)}/k_B$	C (sp)	66.0691	132.138	K
ε_{-O-}/k_B	-O-	95.6184	9.56184	K
$\varepsilon_{=O}/k_B$	=O	-11.0549	-22.1098	K
$\varepsilon_{N(sp3)}/k_B$	N (sp3)	15.4901	22.9095	K
$\varepsilon_{N(sp2)}/k_B$	N (sp2)	84.6268	8.46268	K
$\varepsilon_{N(sp)}/k_B$	N (sp)	109.6621	10.9662	K
ε_F/k_B	F	52.9318	26.4409	K
ε_{Cl}/k_B	Cl	104.2534	100.956	K
$\varepsilon_{H(OH)}/k_B$	H (OH)	19.3477	38.6954	K
$\varepsilon_{H(NH)}/k_B$	H (NH)	141.1709	49.4621	K
$\varepsilon_{H(water/COOH)}/k_B$	H (water/COOH)	58.3301	79.6663	K

As shown in figure 19 the optimized COSMO-SAC dsp model does not give significantly better predictions of infinite dilution activity coefficients than the original model of Hsieh et al.[13,19], probably because the original model was already well optimized. By considering the solvation Gibbs free energy of about 3000 binary mixtures from the COMPSOL database[12], we obtained a final mean square deviation of $51.4\,(\mathrm{kJ/mol\,K})^2$ with the new reoptimized model, which is smaller than $84.47\,(\mathrm{kJ/mol\,K})^2$ the deviation obtained with the original COSMO-SAC dsp model

(see Table 3.9).

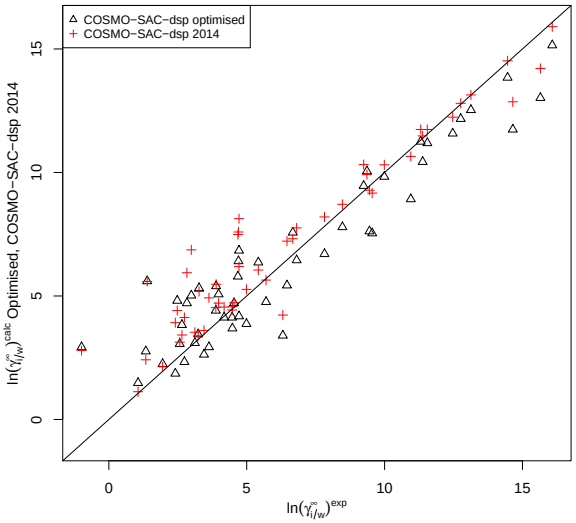

Figure 19: Prediction of activity coefficients at infinite dilution: comparison between the original COSMO-SAC dsp 2014 model and the reoptimized COSMO-SAC-dsp (this work). The reference of experimantal activity coefficients can be found in Ref. [11].

As for comparison we report the predictions of the COSMO-SAC 2010 model[19]. The main difference between COSMO-SAC 2010 and COSMO-SAC dsp is the use of a dispersion term in the latter model. he mean error obtained with the re-optimised COSMO-SAC 2010 model is close to that obtained with the COSMO-SAC dsp model[13] as shown in Table 3.9 with a final mean square deviation of $51.8\,(\mathrm{kJ/mol\,K})^2$ for the COSMO-SAC 2010. This result leads us to infer that the atomic dispersion does not add an important contribution to the model even though the relative error of the optimised atomic dispersion parameters is in most cases greater than 50%. The COSMO-SAC 2010[19] re-optimised parameters are given in Table 3.6.

Table 3.6: optimised parameters of the COSMO-SAC 2010 (Hsieh et al. model).

Parameter Cavities	description	COSMO-SAC 2010[19] COSMO	optimization COSMO	unit
a_{eff}	surface area of standard segment	7.25	6.88	$Å^2$
c_{es}	Electrostatic interaction coefficient	$6525 + \frac{1.4859e8}{T^2}$	$7901.92 + \frac{4.3889e7}{T^2}$	$kcal\,Å^4\,mol^{-1}\,e^{-2}$
c_{OH-OH}	Hydrogen bonding interaction coefficient	4013.78	1765.95	$kcal\,Å^4\,mol^{-1}\,e^{-2}$
c_{OH-OT}	Hydrogen bonding interaction coefficient	3016.43	1774.32	$kcal\,Å^4\,mol^{-1}\,e^{-2}$
c_{OT-OT}	Hydrogen bonding interaction coefficient	932.31	344.018	$kcal\,Å^4\,mol^{-1}\,e^{-2}$
σ_{hb}	sigma cutoff for hydrogen bonding	0.007	0.0079	$e/Å^2$
q	standard area	79.53	79.53	$Å^2$
r	standard volume	66.69	66.69	$Å^2$
Final error	mean square deviation error	76.77	51.8	$(J/mol\,K)^2$

All infinite dilution activity coefficients prediction in water $\ln \gamma^{\infty}_{i/Water}$ and hexane $\ln \gamma^{\infty}_{i/Hexane}$ for binary systems at 298.15 K with COSMO-SAC models before and after optimization are reported in supplementary data C.2.

The deviations from experimental data are similar for the optimised COSMO-SAC 2006 and the original COSMO-SAC dsp, although the latter model has significantly more universal parameters and is more costly in term of computation, due to the split of the sigma profile into different types of sigma profiles (non bonded, bonded OH, OO, ..). Thanks to the dispersion contribution, we expected to see a clear improvement for water systems and acidic binary system in the case of the COSMO-SAC dsp model but the results are quite similar to those obtained with COSMO-SAC 2002 and 2006. We observed that the original COSMO-SAC dsp model is more accurate than the other models for activity coefficients at infinite dilution.

The re-optimised COSMO-SAC 2006 model has the lowest mean square deviation error for solvation Gibbs free energies, with both COSMO and CPCM cavities, and is less computationally intensive. We thus consider it as the model of choice for the predictions of Gibbs free solvation energies and enthalpies of solvation.

The COSMO-SAC Lin and Mullins optimised models are found to be much more accurate. The average absolute deviation errors between ΔG^{∞}_{solv} reference of infinitely diluted binary systems and the one estimated with $\ln \gamma^{\infty}_{i/s}$ from COSMO-SAC models are given in Table 3.7. As shown in Table 3.7, the AAD obtained in this work for the re-optimised COSMO-SAC models (0.347 for lin and Sander 2002 and 0.321 for Mullins et al. 2006) are slightly lower than the AAD reported by Moine et al .[12] (group contribution model with AAD = 0.36 kcal/mol) for the same binary systems, although the number of optimised universal parameters is smaller for COSMO-SAC approaches compared to group contribution methods.

Table 3.7: Absolute Average Deviations (AAD) between predicted solvation Gibbs free energies and reference data from Moine et al.[12] The predictions were obtained with different models and COSMO (DMOL3) cavities.

Model	AAD before optimization (kcal/mol)	AAD after optimization (kcal/mol)
Lin and Sandler 2002	0.443	0.347
Mullins et al. 2006	0.625	0.321
Cosmo-dsp Hsieh et al.2014	0.37	0.367
Moine et al.[284]	0.36	-

We also compared the re-optimised COSMO-SAC model of Mullins et al with recent model published by Borhani et al.[270] and based on the QSPR approach. By considering the same binary systems as Borhani et al.[270], we obtained an average deviation of 0.37 kcal/mol, while Borhani et al. reported an AAD of 0.44 kcal/mol. Our re-optimised COSMO-SAC model is then rather accurate and can be used at any temperature and for multi-component systems. However its main drawback compared to the model of Borhani et al. is the need of correlations for the vapor pressure of the solute and the density of the solvent.

Activity coefficient prediction of ternary mixtures and comparison with experimental data are presented in Table 3.8. In this calculation The optimized Mullins model is used.

Table 3.8: Activity coefficient prediction of ternary mixtures.

Composition			$\gamma^{exp}_{i/mixture}$ [304]			$\gamma^{Cosmo-SAC}_{i/mixture}$		
x_1	x_2	x_3	γ_1^{exp}	γ_2^{exp}	γ_3^{exp}	γ_1	γ_2	γ_3
Ethanol(1)-benzene(2)- water(3)								
0.4565	0.0416	0.5019	1.21	11.70	1.52	1.19	7.9	1.79
0.272	0.027	0.701	1.6	25.89	1.14	1.73	23.33	1.34
0.878	0.018	0.104	1	4.51	2.55	1	2.71	2.82
0.397	0.5415	0.0615	1.43	1.57	7.07	1.15	1.38	10.49
Acetone(1)-acetonitrile(2)- water(3)								
0.081	0.0642	0.8548	1.02	1.15	2.79	3.3	2.26	1.05
0.0043	0.0507	0.945	7.83	7.11	0.99	6.24	2.97	1.00
0.0043	0.8834	0.1123	0.95	1.01	4.16	1.3	1.02	2.51
0.144	0.0455	0.8105	2.96	3.68	1.17	2.57	2.07	1.09
0.268	0.501	0.231	1.07	1.14	3.26	2.08	1.09	1.14

Table 3.9: Mean Square Deviations (msd) between predicted solvation Gibbs free energies and reference data from Moine et al. [10]. The predictions were obtained with original and re-optimised COSMO-SAC models: Lin and Sandler 2002, Mullins et al.2006 and COSMO-SAC dsp 2014 using COSMO(DMOL3) cavities and CPCM cavities. The msd is calculated with Eq.3.27.

Model	Cavity type	msd before opt $(J/mol\,K)^2$	msd after opt $(J/mol\,K)^2$
Lin and Sandler[11]	COSMO	75.59	45.77
Mullins et al.[18]	COSMO	164.03	39.06
Mullins et al.[18]	CPCM	-	34.06
Hsieh et al. hb[19]	COSMO	76.77	51.8
Hsieh et al. dsp[13]	COSMO	84.47	51.4

3.5 Application to Bio-oil compounds

In order to model a process using bio-oil it is important to have a surrogate bio-oil. The major problem of bio-oil is that such system contain hundreds of species so one of the solution is to substitute the major bio-oil/biomass components with a set of model compounds. Appropriate thermochemical and kinetic data are required to get a meaningful mechanism. After reviewing different work we found out that the most important compounds are[14,305,306]:

Table 3.10: Activity coefficients of a surrogae Bio-oil mixture prediction with Cosmo-SAC model.

Bio-oil surrogate						
Component	CAS	Wt %	$\gamma_{i/mixture}$ Cosmo-SAC model			
			Lin 2002	Dsp-opt	Mullins-opt	Mullins-cpcm
Water	7732-18-5	22	1.29	1.28	1.31	1.38
Acetic Acid	64-19-7	3.9	0.67	1.21	1.15	1.15
Ethylene Glycol	107-21-1	5.46	0.83	0.91	0.89	0.94
Glycol Aldehyde	141-46-8	5.46	1.81	1.29	1.59	1.50
Vanillin	121-33-5	17.94	1.44	2.24	3.07	2.52
Levoglucosan	498-07-7	29.64	0.77	0.99	0.96	1.11
2,5 Dimethylfuran	625-86-5	5.46	35.42	17.08	41.74	33.29

3.6 Conclusion

We have briefly outlined the parameterization of the COSMO-SAC solvation models, examined and compared the computational performance of these solvation models.

Understanding complex chemical systems requires detailed kinetic models, with each elementary reaction rate known or estimated. These models can be quite large; for example, a model for the liquid-phase oxidation of a biodiesel surrogates fuel blend contained 3 275 chemical reactions. Due to the size of these models, it is desirable to generate them automatically, but using quantum chemistry and transition state theory or direct dynamics to calculate thousands of liquid-phase reaction rates on-the-fly during mechanism generation would be computationally expensive. Jalan et al[86] automated the estimation of solvation thermochemistry using Abraham's model and diffusion limitations during automated mechanism generation and manually modified some reaction rates, on the basis of PCM calculations, to build solvent-sensitive models. We saw from our comparison that the COSMO-SAC models are much more accurate than Abraham's model to predict solvation energies that's why we presented in this work a reoptimization in order to predict data for biomass and bio-oil compounds. It had been demonstrated that solvent can impact both thermochemistry and kinetics of liquid phase auto oxidation and thus liquid phase of biomass pyrolysis. So to model the liquid phase we have to integrate solvent effects on both thermochemistry and kinetics. Experimental data are only available for certain reactions in some reaction families, most extensively for hydrogen abstraction family. It is hard to generalize effects to a whole family of reactions without both experimental and theoretical data and a variety of reactants and solvents tested, which would require a lot of experiments and/or calculations. Augmenting these data for reaction families beyond hydrogen abstraction would greatly benefit the kinetic community. The use of predictive COSMO-SAC models allow us to extend that to unknown or non-existent data of biomass compounds with a higher accuracy.

Next step is understanding how to systematically apply kinetic solvent effects to all the reactions with a higher accuracy and reducing human effort when building detailed kinetic models.

Chapter 4

Kinetic Modeling

4.1 Introduction

Biomass pyrolysis process is known as a potential cheapest route for renewable liquid fuel production. However, it poses a multi-scale problem starting from the complexity of the feedstock (raw biomass) characterization, then goes to the identification of products and reaction intermediate at molecular scales, and continues with the understanding of the complex chemical kinetic mechanism occurring in different reactor configurations.

These challenges make the study of a detailed kinetic mechanisms of pyrolysis and oxidation of biomass mixture very difficult to achieve. Also, from a thermodynamic point of view, we are in the presence of a multi-phase problem (solid-gas-liquid). The biomass feedstock characterizes the solid phase, and as discussed in Chapter 1, we may divide the pyrolysis process into three stages with respect to the Drying step occurring at a temperature range <100 °C. The boundaries between the pyrolysis stages are not sharp. As proposed by Basu[24], the pyrolysis process starts at a temperature between 100 °C to 300 °C where the exothermic dehydration of the biomass takes place with the release of water and low-molecular-weight gases like CO and CO_2 and tars. During this initial/first stage, a liquid phase is observed. Then the intermediate pyrolysis step occurs in the temperature range <200 °C to 600 °C, and most of the condensable compounds are produced.

When biomass is heated, molecular bonds break and induce the formation of smallest (gaseous) molecules, along with water and larger molecules that we can call primary tars. These primary tars are fragments of the original natural polymers components of biomass. Primary tars can react to secondary tars by further reactions such as re-polymerization and condensation reactions at the same temperature. The

reactivity of biomass tars is very important to the further development of biomass decomposition models, as tars are difficult to remove from pyrolysis reactors. We can define tar as a mixture of condensable hydrocarbons, including aromatic compounds with up to five rings as well as Polycyclic Aromatic Hydrocarbons (PAHs)[56]. Also, according to the meeting about tar measurement protocol carried out in Brussels in the Spring of 1998, between the International Energy Agency (IEA), the Directorate General for Energy of the European Commission and the Energy Department of the United States, they agreed to define tars as all hydrocarbons with molecular weight higher than benzene[57].

In this chapter we will focus on the thermal decomposition of one of the major three biomass cell wall polymers, the lignin. Lignin is a polymer of phenylpropane units containing three different aromatic ring substitution patterns: p-hydroxyphenyl, (H), guaiacyl ($4-hydroxy-3-methoxyphenyl$, G) and syringyl ($3,5-dimethoxy-4-hydroxyphenyl$, S) depending on the wood species. It is a complex structure with the most poorly understood kinetics. Primary pyrolysis reactions of lignin occurs over a wide temperature range from 200 °C to 400 °C. We investigated the initial pyrolysis stage kinetics of lignin at low temperature 250 °C based on the experimental work of Nakamura et al.[62] on condensation reactions of some lignin surrogate compounds: guaiacol, creosol, 2-methoxy-4-vinylphenol a $C_\alpha = C_\beta$ type of sidechain and the phenolic $C_\alpha - OH$ type hydroxyethyl-guaiacol. Nakamura et al.[62] obtained condensation products with creosol (4-methylguaiacol) at 250 °C. They proposed a quinone methide-based mechanism including a nucleophilic addition of the aromatic ring carbon or hydroxyl hydrogen to the C_α carbon of the quinone methide intermediate. After that, Kotake and co-workers[307] studied the pyrolytic reactivity of 4-O-methylconiferyl alcohol (a primary tar compound from lignin polymer) and ended by the conclusion that polymerization was a more important process than evaporation and sidechain conversion processes at low temperature range 250 °C to 300 °C. They also proposed a quinone methide and radical mechanism for the polymerization of coniferyl alcohol. Quinone methide intermediate was suggested to be an important intermediate for the condensation of coniferyl alcohol. This reactivity can be explained by the electro-positive carbon of quinone methide that tends to react with the electro-negative aromatic and double bond carbons of the vinyl guaiacol rather than the oxygen atoms of the sidechain and the phenolic groups. Given that the condensed (C-C) linkages have been reported to be much more stable than the ether linkages during the lignin pyrolysis process which tend to form solid product (char) more preferentially than cellulose and hemicellulose. In this study, we investigated pyrolysis mechanism reactions of lignin surrogate compounds at both macro level and molecular level.

As for combustion pyrolysis process is known to proceed through a free radical mechanism. Three reaction families can be distinguished: (i) hydrogen abstraction reactions, both intra-molecular and inter-molecular (hydrogen migration); (ii) carbon bond scission and radical recombination; and (iii) radical β-scission and the reverse radical addition to olefins. In order to study these reactions at the molecular level, the computational chemistry community commonly uses density functional theory (DFT) to calculate the potential energy surface (PES) and identify the electronic structures of reactants, transition states or intermediate compounds and products. From density functional theory (DFT) and potential energy surface (PES) investigations, it is known that generally carbon bond scission and radical recombinations reactions have no clear maximum barrier energy: these reactions cannot be studied with classical transitional state theory (TST) instead they are studied with variational transition state theory (VTST). On the other hand, for hydrogen abstraction reactions and free radical β-scission family most of their reactions have a clear barrier energy and thus can be proceeded through classical transitional state theory.

Free radical β-scission thermochemistry and reactivity have been studied through a variety of computational methods from semi-empirical ab initio methods to density functional theory and post Hartree Fock (post-HF) methods. It was found that free radical thermochemistry and reactivity calculations required post-HF methods and large basis set in order to obtain results with accuracy. But density functional theory (DFT) uses computationally less demanding methods as B3LYP, BP86 and MP062X and it predicts accurate kinetic and thermodynamic parameters[308].

Green and co-workers[26] proposed an approach that has mainly been used to study the liquid phase oxidation of surrogate fuel[27–29]. Depending on the solvent, the rate of reaction is impacted as the pathways and product distribution change. The two different effects that can be observed are: (1) an increase or decrease of the activation energy E_a and (2) the competition between diffusion and reaction rates. According to Green[26], one can estimate the liquid phase kinetics based on the gas phase kinetics and solvation free energies. Therefore, a reliable kinetic study in the liquid phase requires accurate values for both gas phase properties and solvation free energies. Solvent molecules surround the other solute molecules and they rearrange to form a cage. The solute molecules find themselves trapped and this becomes important when we are in presence of strongly hydrogen-bonded effect.

4.2 Methodology

In this work, a primary pyrolysis mechanism has been developed based on reaction mechanism generator "RMG"[99] prediction combined with a kinetic solver. Then, we

added reactions based on the experimental work of Nakamura et al.[309]. This step characterizes the macroscopic scale of the kinetic modeling approach. Then in order to improve the predicted mechanism at microscopic scale, we focus on key reactions where no literature data are available, and perform an atomic and molecular modeling approach.

4.2.1 Mechanism Generation

To investigate the reaction mechanism involved in the lignin surrogate components primary pyrolysis in the liquid phase, we used the RMG (reaction mechanism generation tool) software at a temperature of 250 °C and a pressure of 1 atm, for each compound separately. The selected surrogate compounds are based on the work of Nakamura et al.[62,309]. Thus the selected compounds are guaiacol, creosol, $4-(1-Hydroxyethyl)-guaiacol$ and $2-Methoxy-4-vinylphenol$ commonly called $4-vinyl-guaiacol$.

Mechanism was generated using the following kinetic families, hydrogen abstraction, radical recombination and intra-hydrogen migration, called isomerization, assuming that at this temperature polymerization reaction of free radicals generated from the surrogate components decomposition will occur according to the observations of Kawamoto et al.[62,309,310]. As reported by the experimental work of Nakamura et al.[309] the condensation process occurs at 200 °C to 250 °C followed substantial depolymerization and carbonization. Additionally, the phenolic α-ether, β-ether and β-aryl types of model compounds became reactive at the temperature where condensation of lignin related compounds was observed. The mechanism generation using RMG requires several iterations to get a relevant mechanism. As observed by Nakamura et al.[62] and suggested by Kotake et al.[307] the guaiacol, creosol, $4-(1-Hydroxyethyl)-guaiacol$ and $4-vinyl-guaiacol$ sidechain conversion process is a radical mechanism from the initiation reactions as described in Figure 20. The guaiacol and creosol will form different dimers due to the existence of various radical species and consequently a radical coupling reactions occur.

The reaction kinetics of the guaiacol radical coupling mechanism as described in Figure 21 is extracted from RMG calculation and added to the mechanism. Same sidechain conversion process was also predicted for creosol decomposition at 250 °C involving isomerization reactions and coupling of creosol radicals.

In RMG the thermochemistry libraries treatment used for the liquid phase generation concerns only the gas phase thermochemistry. Species thermochemistry parameters matching a thermo library are then corrected through the LSER method (Abraham method) to obtain the liquid phase parameters in the final mechanism.

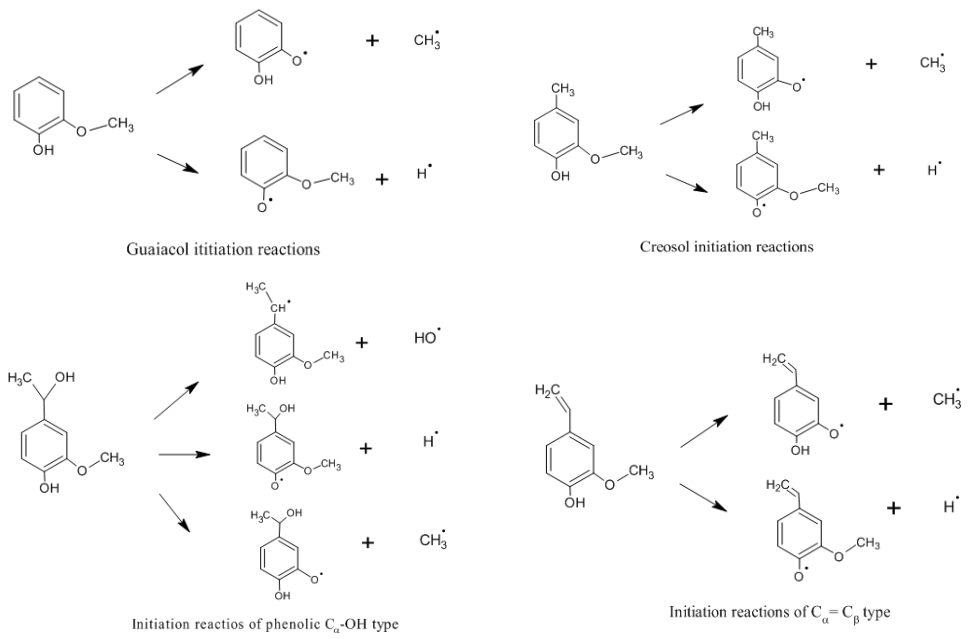

Figure 20: Initiation reactions of lignin surrogate components decomposition guaiacol, creosol, $4-(1-Hydroxyethyl)-guaiacol$, and $4-vinyl-guaiacol$ respectively at 250 °C.

Thus, the liquid phase thermochemical library cannot be used directly without applying a second correction on it. In our previous Chapter 3, we demonstrated from our comparison that the COSMO models are much more accurate than Abraham's model to predict solvation energies. But, the thermo data needed to compute cantera kinetic solver for the liquid phase reactor calculation or CHEMKIN kinetic solver for the gas phase reactor calculation with RMG are group additivity estimation with LSER method.

Table 4.1 summarizes the rate parameters range utilized in our mechanism. The majority of these parameters were taken from reaction families values that were developed for polystyrene pyrolysis mechanism of Levine and Broadbelt[20]. These literature rate parameters allow us to compare the predicted RMG parameters with experimental data to target important discrepancies such as missing species or inaccurate species profiles. Missing species and paths is the first problem to address with the reaction mechanism generator software RMG.

The rate constants for all individual elementary reactions presented in appendix E are extracted from RMG and expressed according to Arrhenius equation and with an estimation of diffusion limit for free radical reactions as suggested by the works

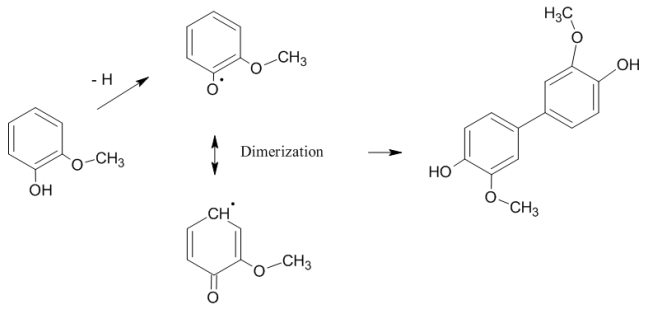

Figure 21: Isomerization mechanism and coupling of guaiacol radicals at 250 °C.

Table 4.1: Rate parameters for the various reaction types used in lignin pyrolysis model taken from Vinu et al.[20] study.

Reaction type	Frequency factor A (/ sec or L/mol/ sec)	Activation energy E_a (kcal/mol)
Alkoxy radical hydrogen abstraction	2.10×10^6	12
Benzyl radical hydrogen abstraction	2.10×10^6	11.9
Isomerization 1,4 H-shift and 1,3 H-shift	3.8×10^7 - 7.85×10^8	13.4 - 25.6
β-scission	10^{13} - 10^{14}	0.0 or 11.4
Elimination of H2O from alcohols	1.6×10^4	65.2
H-abstraction by CH3 from α-CH in alcohols		20.29

of Ingold et al.[30–33]. In our study, we observed that RMG predicted negative activation energies for some subset of reactions. These energies were also observed by Venu et al.[20] with the standard procedure of an E–P correlation and they came to the conclusion that the reactions were inactivated. Even though, these reactions are not removed from our mechanism, we assume that they are inactivated at the temperature range around 250 °C, but for consistency reasons they are maintained.

4.2.2 Microscopic scale improvement

As discussed above, the microscopic scale modeling is a must in this study, due to the lack of kinetic data for lignin surrogate compounds decomposition. After the prediction of reaction mechanism with RMG, if key reactions involved in condensation process according to experimental results and observations obtained from Nakamura et al.[62,309] are not found we perform a potential energy surface (PES) calculations. Thus, we investigated with quantum chemistry the dehydration reaction of $4-(1-Hydroxyethyl)$-guaiacol as an initiation reaction to form $4-vinyl-guaiacol$, the $C-\alpha = C_\beta$ type, as proposed by Nakamura et al.[62]. The studied dehydration reaction is presented in Figure 22. As a second reaction, we studied the condensation reaction step of the formed $4-vinyl-guaiacol$ (23).

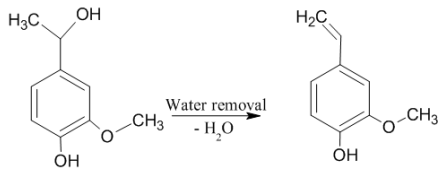

Figure 22: Vinyl formation 250 °C.

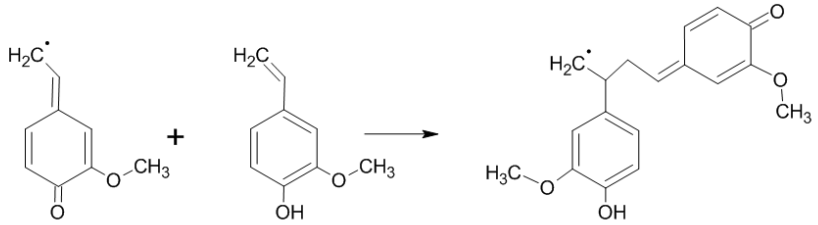

Figure 23: Vinyl condensation mechanism of the $C_\alpha = C_\beta$ at 250 °C.

Once the electronic structures of the liquid phase species (reactant, transition state/intermediate and products) are identified with quantum chemistry calculations, we estimate the kinetic. The estimation of the liquid phase kinetics is based on the Pr William H. Green approach[78]. It is mainly a solvent correction applied to the gas phase kinetic. The kinetic rate k_{solv} of the reaction in the liquid phase can be estimated from the kinetic rate k_{gas} of the same reaction in the gas phase as,

$$\frac{1}{k_{solv}} = \frac{1}{k_{gas} \exp\left(\frac{-\Delta\Delta G^{*,\ddagger}_{solv}}{RT}\right)} + \frac{1}{k_{diff}}, \tag{4.1}$$

where k_{diff} is the rate of diffusion that can be calculated as[25,26],

$$k_{diff} = 4\pi \sum_i r_i \sum_i D_i \mathrm{N_A}, \tag{4.2}$$

It is considered that reactions with activation energies of less than 4 kcal are diffusion limited. This happens when the gas phase reaction rate is very fast thus the liquid phase reaction rate will resume to the rate of diffusion. Most of the radical recombination reactions are diffusion limited. Solvent effects have been studied with lots of attention due to their role in free radical polymerization. For our case

the estimated barrier energies of our studied reactions were higher than 4 kcal, so we removed the diffusion kinetic contribution. Thus, the final liquid phase kinetic expression is summarized in the following equations 4.3, 4.4 and 4.5, as

$$k_{solv} = k_{gas} \exp\left(\frac{-\Delta\Delta G^{*,\ddagger}_{solv}}{RT}\right), \tag{4.3}$$

The term $\Delta\Delta G^{*,\ddagger}_{solv}$ is the difference between the solvation free energies of the transition state (represented by $\ddagger$) and the reactants. The symbol $*$ represents the Ben-Naim standard state at fixed concentration[63].

$$\Delta\Delta G^{*,\ddagger}_{solv} = \Delta G^{*,\ddagger}_{solv} - \sum_i \Delta G^{*,Reactants}_{solv}, \tag{4.4}$$

The gas phase kinetic constant k_{gas} can be expressed with respect to the Arrhenius parameters as,

$$k_{gas} = A \exp(\frac{-E_a}{RT}), \tag{4.5}$$

Electronic structures generation

Electronic structure calculation allows us to evaluate important thermochemical properties. They are based on the theories and laws of Quantum Mechanics (QM) and predict molecules structures, energies, vibrational frequencies and reactions pathways of a variety of chemical compounds (stable or transition structures). To perform these calculations, the algorithm is solving the time-independent Schrödinger equation to find the different stationary states of the considered species and to compute the potential energy surface of the molecular system.

In equation $H\psi(x) = E\psi(x)$, ψ is the wave function (whose squared norm represents the probability of presence), H is the Hamiltonian operator and E the energy of the particle. This equation is analytically not solvable for poly electronic systems, thus modeling approaches are required. As described in the review Chapter 1, there are two main classes of methods to approach a solution of Schrödinger equation. Mainly we have semi-empirical methods and ab initio and DFT methods.

Many software are available in literature to perform electronic structures calculations. Due to their availability, Gaussian 09[100] was selected to perform all low theory levels calculations and ORCA[101] was selected to perform higher theory levels calculations.

To reduce computational cost, a two-step approach is commonly used, with a low theory level calculation for geometry investigation and then a higher theory

calculation once an optimized geometry has been identified. In our work, after a potential energy surface investigation using density functional theory (DFT) method B3LYP and M062X with the standard basis set 6-31G(d,p), the structures of the stationary points on the reaction potential energy surfaces (PES) of the identified reactants, intermediate, transition state and products were fully optimized using M062X/ 6-31G(d,p) basis set with Gaussian 09[100] then at a higher level with BP86 D3BJ and def2-TZVP def2/J RIJCOSX basis set with ORCA[101]. M06-2X is a Global hybrid functional with 54% HF exchange. It is the top performer within the 06 functional for main group thermochemistry, kinetics and non-covalent interactions[311]. Moreover, to approach the complete basis set, new theoretical approximation are often used; it is to be noted that the complete basis set (CBS) limit is not a basis set but an extrapolated estimate of a result obtained with an infinitely large basis set as the def2-TZVP basis set. However, this is a very demanding calculation, and we chose at a first step to proceed with the 6-31G (d, p) basis set. 6-31G means that the central orbit is described by a contraction of six primitive Gaussian functions, and that the valence orbit is described by 2 contractions: 1 containing 2 gaussians and another having 1 Gaussian. The increase in the number of Gaussian functions do not always lead to better predictions, because the functions are centered on the atoms. In some cases, the electronic cloud can be deformed: this deformation may correspond to a mixture of s-type and p-type orbitals leading to an hybrid orbit sp. Similarly, the d orbital introduces asymmetry into the p orbitals. The solution to this problem consists in introducing polarizable functions, denoted by the letter p or an asterisk (*). Thus, the 6-31G (p) basis set refers to a base 6-31G with a polarization function on heavy atoms (other than H), and the 6-31G (d, p) basis set indicates the use of polarization functions also on hydrogen atoms. Then, at a second theory level, we chose the balanced polarized triple-zeta basis set def2-TZVP with def2/J RIJCOSX approximations coupled with the BP86 density functional method which usually gives fairly converged energies and geometries.

Transition State Theory

Transition state theory (TST) is the most widely used theory for calculating rates reactions occurring in the gas phase and in condensed phases. There are different types of transition state theory according to the investigated reaction families. The simplest one is the conventional TST. It requires information only for the saddle point and reactant(s). The equation usually presented for the conventional TST is the Eyring equation for a reaction with i reactants 4.6,

$$\mathbf{k}^{\mathrm{TST}}(\mathrm{T}) = \kappa(\mathrm{T}) \times \frac{k_B T}{h} \frac{Q^{\ddagger}}{\prod_i^n Q_i} \exp\left(\frac{-E_a}{RT}\right), \tag{4.6}$$

For low energy barriers reactions, a specific treatment based on the Multi Path Transition State Theory (MP-TST) and Multi Structural Transition State Theory (MS-TST) is required. And for carbon bond scissions and radical recombinations reactions as they have no clear maximum barrier energy, these reactions are studied with the variational transition state theory (VTST).

In our case, the potential energy surface (PES) investigation of the $4-(1-Hydroxyethyl)-guaiacol$ dehydration reaction and the $4-vinyl-guaiacol$ condensation reaction exhibit a clear barrier energy, so the classical transitional state theory can be considered. On the other hand, the quinone methide formation PES investigation did no exhibit any clear maximum barrier energy, so it should be studied via the variational transition state theory (VTST): we leave this study in future works.

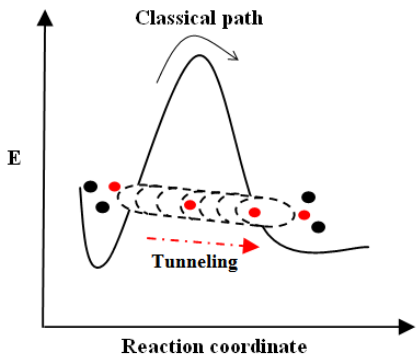

Figure 24: Quantum tunneling effect through the Potential Energy barrier.

Another aspect that we took into account is the quantum tunneling effect. Quantum tunneling refers to the quantum mechanical phenomenon where particles with a small amount of probability pass or tunnels through a finite potential energy barrier that it would not normally be able to surmount. This phenomenon is schematized in Figure 24.

A formulation for incorporating the effect of tunneling is the Wigner transmission coefficient (1932)[312] approach. This one-dimensional quantum mechanical effects on reaction coordinate motion (tunneling and non-classical reflections) is incorporated by a multiplicative transmission coefficient $\kappa^W(\mathrm{T})$. This approach is called the classical Transition State Theory (TS located at the first-order saddle point) including Wigner tunneling correction and it is expressed as follows,

$$\kappa^W(\mathrm{T}) = 1 + \frac{1}{24}\left(\frac{\mathrm{h\,Im}\left(\mathrm{v}^{\ddagger}\right)}{\mathrm{k_b T}}\right)^2 \tag{4.7}$$

and

$$\mathbf{k}^{\mathrm{TST}}(\mathrm{T}) = \kappa^{W}(\mathrm{T}) \times \frac{k_B T}{h} \frac{Q^{\ddagger}}{\prod_i^n Q_i} \exp\left(\frac{-E_a}{RT}\right) \tag{4.8}$$

In this relative simple treatment, the imaginary frequency characterizing the reaction mode is used to compute the Wigner tunneling correction.

Another quantum tunneling correction is the Eckart tunneling correction where a one-dimensional quantum mechanical tunneling treatment through an unsymmetrical Eckart (1930)[313] potential energy barrier is involved. This methodology requires no ab initio calculations at points other than reactants, products, and saddle point. The analytic form proposed by Eckart can model a variety of physically reasonable shapes (involving unsymmetrical forms) and admits an analytical solution of the corresponding Schrödinger equation and then for the probability p(E) of transmission through the corresponding 1-D barrier at energy E.

For our kinetic estimation, all gas phase kinetic parameters calculations were performed with the KiSThelP[102,314] package that includes all equations of quantum tunneling correction. In this study, the classical Transition State Theory (TS located at the first-order saddle point) including Wigner tunneling correction is considered.

Estimation of Gibbs Free Energy of Solvation

To take into account the solvent effect on the liquid phase, and to add the solvent contribution or more precisely the solvation energy correction to the gas phase kinetics, the following approach is used as described in Section 1.4.3 and illustrated in Figure 12.

After the identification of the electronic structures of the stationary points of reactants, intermediate, transition state and products from the reaction potential energy surfaces (PES); we extracted the optimized geometries from Gaussian[100] calculation. A second optimization step with higher calculation level using BP86 method coupled with def2-TZVP basis set with def2/JRIJCOSX approximations from ORCA[101] . The optimized geometries were then used to generate the COSMO files using TURBOMOLE[315] package rather than DMOL3 (BIOVIA Materials Studio) and then we computed the boiling point and solvation energies with COSMOtherm[21].

TURBOMOLE[315] is a computational chemistry program based on ab initio methods that implement various quantum chemistry methods based on density functional theory (DFT) employing the BP methods and COSMO cavity calculations with an infinite dielectric constant.

The cosmo cavities are generated from the optimized geometries as described in Figure 25 The solvation energies were then computed with COSMO-RS[80,81] model

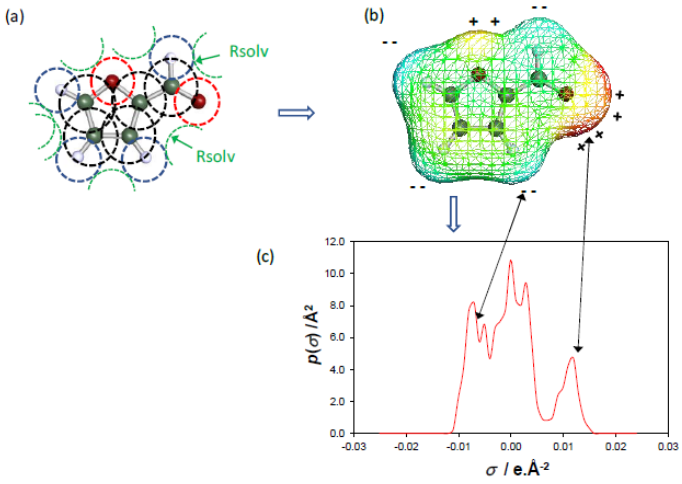

Figure 25: Definition of the cavity surrounding furfural geometry for a cosmo calculation. (a) The cavity is formed by the intersection of spheres surrounding each atom. A solvent radius R_{solv}, is taken into account. (b) The surface of the cavity is cut into segments having a certain surface and charges. (c) Sigma profile of furfural (distribution of surface charges on the cavity).

using COSMOtherm[21]. The solvation corrections reactants and transition states solvation energies at 250 °C is then applied to the predicted gas phase kinetic.

4.3 Results & Discussion

4.3.1 Mechanism generation

For many large mechanisms as combustion and pyrolysis, the identification of surrogate compounds to characterize the global aspects is of crucial importance. In this work, we consider five lignin surrogate compounds: guaiacol, creosol, $4-(1-Hydroxyethyl)-guaiacol$, anisole and $4-vinyl$-guaiacol to investigate and reproduce the global lignin decomposition at low temperature (liquid phase). Often a surprisingly small number of reactions really govern the conversion mechanism and selectivity of product formation. We first predicted the liquid phase decomposition of each compound separately with RMG. Then, we refined the predicted RMG surrogate mechanism pathways, based on the gas chromatography/mass spectroscopy (GC/MS) measurements of chemical structures of pyrolysis products of lignin at 250 °C taken from Kawamoto et al.[62,309] work.

The reactor conditions are first set to P=1 atm and T=250 °C. We choose the

reaction families to be used according to our reactants linkages and to our product estimations. The following RMG[99] reaction families were used: hydrogen abstraction, radical recombination, 1,2 carbene insertion, intra-hydrogen migration, and intra OH migration. These were accompanied by the rate rules kinetic estimator and with primary ThermoLibrary and GRI-Mech3.0 for thermochemistry data and seed mechanisms. The maximum radical electrons number was set to 2. For the solvent choice, as the RMG solvent parameter library is restricted to only 25 solvents, we chose the most representative one with solvent effects close to creosol. The solvent used was toluene.

Two other solver parameters must be set : *rtol* (relative tolerance) and *atol* (absolute tolerance). These parameters influence the mechanism size (number of reactions) as mentioned by Chatelain[29]: for a given input file, the size of the final mechanism may diverge by setting too low solver parameters. According to those results, the *atol* parameter has to be set below 10^{-16} if we want to avoid a huge number of reactions. Since *rtol* parameter has no significant effect on the mechanism size, a value between 10^{-6} and 10^{-10} seems reasonable. We choose the following solver parameters setting: $atol = 10^{-16}$ $rtol = 10^{-8}$. The reactant concentrations were taken from the experimental work of Nakamura et al.[62,309].

The kinetic parameters were estimated with rate rules and Arrhenius law. For most reaction families in RMG, the rates are defined in the forward direction. The reverse kinetics are calculated through the relation $k_r = k_f/K_{eq}$ using the thermodynamic parameters estimated for the reaction species. The cage diffusion effect governing the radical reactions kinetic and solvent activation energies corrections are directly integrated into the rate constant in the RMG[99] kinetic solver. The solvation energy corrections are estimated with LSER parameters of Abraham group additivity method[291,292].

The constants used in this work are given in the following Table 4.2.

Table 4.2: Constants used in the kinetic modeling.

Constant	Value	Unit
Bohr radius (a_0)	5.29177211E-11	m
Atomic mass unit (amu)	1.6605389E-27	kg
Planck's constant (h)	6.6260696E-34	J s
Avogadro's number (N_a)	6.0221413E23	mol^{-1}
Speed of light in vacuum (c)	2.99792458E8	$m\,s^{-1}$
Boltzman constant (k_B)	1.380649E-23	$J\,K^{-1}$

Finally, once the mechanism generation is completed, it can be used in a kinetic solver like Cantera or CHEMKIN software to model specific reactor conditions. The second step of the work consists in validating the obtained mechanism against ex-

perimental data, by using a 0-D reactor model based on Cantera formalism. The mechanisms can be improved by regenerating the mechanism with new conditions or using the molecular scale improvement.

Then, when the agreement is satisfactory, the generated model can be used. The kinetic simulation results of our generated mechanism are presented in Figures 26 and 28.

The Table in Appendix E.1 reports the kinetic parameters of some reactions families computed from the decomposition of each surrogate compound separately with RMG in the liquid phase (toluene solvent). The kinetic of initial decomposition reactions of each model compound are shown in Figure 20.

Guaiacol

As observed in Figure 26, the guaiacol recovery yield is around 100% which is in total agreement with the experimental results of the work of Nakamura et al.[62].

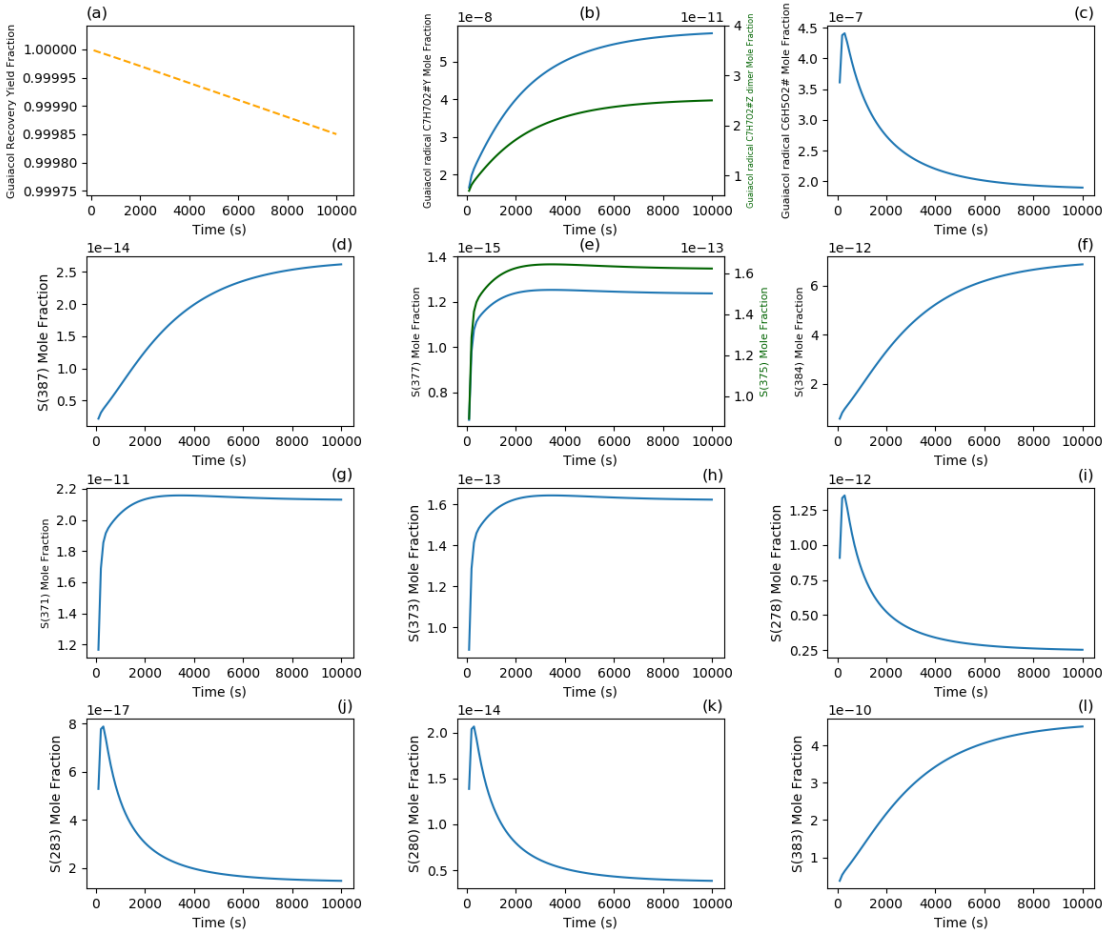

Figure 26: Yield profile of guaiacol decomposition and its condensation products from the radical dimers. Kinetic simulation run with Cantera at 250 °C and 1 atm with a Zero-Dimensional Reactor Networks. (a) Fraction of guaiacol recovery. (b) Molar fraction of Guaiacol radical $C_7H_7O_2^{\#}$Y and its isomer $C_7H_7O_2^{\#}$Z. (c) Molar fraction of Guaiacol radical $C_6H_5O_2\#$. (d) Molar fraction of radical $C_7H_7O_2^{\#}$ coupling product with index S(387). (e) Molar fraction of radical $C_7H_7O_2^{\#}$ coupling with radical $C_6H_5O_2^{\#}$ product with index S(377) and its conformer S(375). (f) Molar fraction of radical $C_7H_7O_2^{\#}$ coupling product with index S(384). (g) Molar fraction of radical $C_7H_7O_2^{\#}$ coupling product with index S(371). (h) Molar fraction of radical $C_7H_7O_2^{\#}$ coupling product with index S(373). (i) Molar fraction of radical $C_7H_7O_2^{\#}$ coupling product with index S(278). (j) Molar fraction of radical $C_7H_7O_2^{\#}$ coupling product with index S(283). (k) Molar fraction of radical $C_7H_7O_2^{\#}$ coupling product with index S(280).(l) Molar fraction of radical $C_7H_7O_2^{\#}$ coupling product with index S(383).

Moreover, we also predicted the decomposition of guaiacol and the isomerization

reaction via the intra-hydrogen migration kinetic library. This result give us the kinetic of the produced dimers $C_7H_7O_2^{\#}$Y and $C_7H_7O_2^{\#}$Z. All the coupling products structures indexed in the predicted mechanism are reported in the supplementary data appendix E. We also observed the formation of intermediate radical coupling product as we see in Figures 26 (i), (j) and (k) these intermediate species are unstable and end up breaking down to their first reactants or they are involved in isomerization reactions and some radical coupling reactions. The S(283) and S(278) represent the coupling product of a quinone methide which is in agreement with the proposed quinone methide intermediate.

After an identification of the quinone methide intermediate, we suggest the pathway of an active quinone methide radical, which is described in Figure 27.

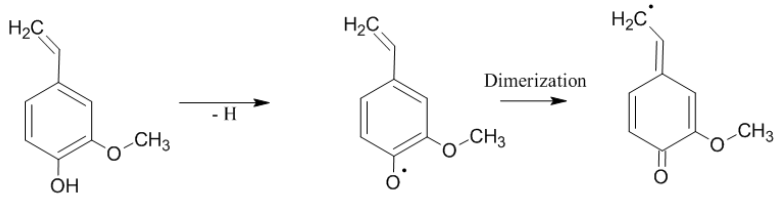

Figure 27: Quinone methide formation from vinyl H-abstraction reaction at 250 °C.

Hydroxy-ethyl guaiacol and Vinyl-guaiacol

The identified products of hydroxy-ethyl guaiacol decomposition in presence of 20 mol equivalent of creosol at 250 °C from the experimental work of Nakamura et al.[62] are vinyl-guaiacol with almost a yield of 50 mol% and 9 mol% of vinyl polymer.

The generated RMG mechanism for Hydroxy-ethyl guaiacol did not predict the presence of vinyl guaiacol. Thus, we investigated this reaction at molecular level and added the estimated kinetic to the generated mechanism. Details about the molecular scale modeling are discussed in the following Section 4.3.2. For more consistency, the generated vinyl-guaiacol decomposition mechanism was assembled with the generated mechanism for hydroxy-ethyl guaiacol.

We observed vinyl polymer in the vinyl-guaiacol decomposition mechanisms, which is not the case for the hydroxy-ethyl guaiacol mechanism. The structures of the identified polymer (dimer) products are reported in the supplementary data appendix E.

As shown in Figure 28 the hydroxy-ethyl guaiacol recovery yield is around 100% which is in disagreement with the experimental results from Nakamura et al.[62] work.

This leads us to investigate the kinetic at molecular scale in order to predict accurate mechanism for hydroxy-ethyl guaiacol decomposition.

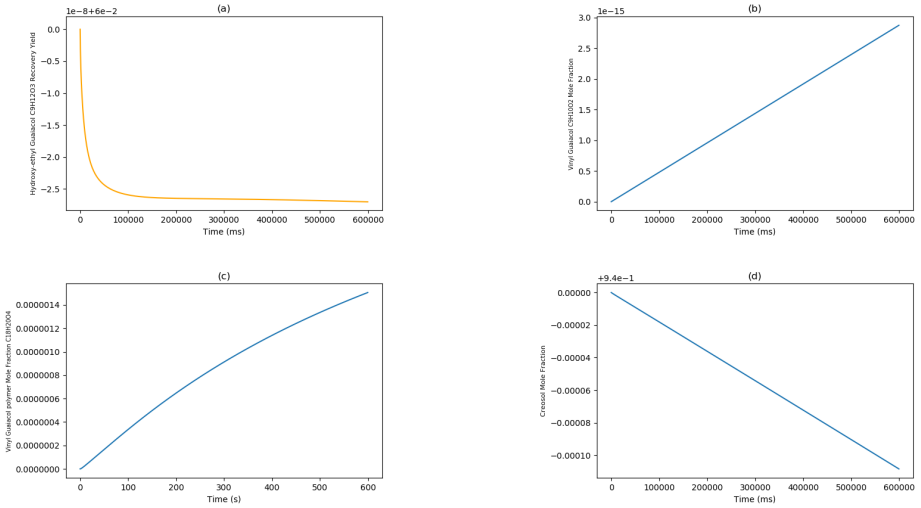

Figure 28: Yield profile of hydroxyethyl guaiacol decomposition and its condensation products from the radical dimers. Kinetic simulation run with Cantera at 250 °C and 1 atm with a Zero-Dimensional Reactor Networks. (a) Molar fraction of hydroxyethyl guaiacol recovery. (b) Molar fraction of vinyl guaiacol.(c) Molar fraction of vinyl guaiacol radical coupling $C_18H_20O_4$. (d) Molar fraction of creosol.

4.3.2 Kinetic improvement from molecular scale modeling

In this work, the vinyl-guaiacol formation from dehydration of $4-(1-Hydroxyethyl)$-guaiacol and the condensation reaction of the formed vinyl-guaiacol via a quinone methide intermediate are investigated with transition state theory. All potential energy surface calculations were performed using Gaussian 09 package [100]. Electronic energies, optimized geometries and frequencies were first obtained at the M062X/6-31G(d,p) level of theory. Then at a higher level with BP86 D3BJ and def2-TZVP def2/J RIJCOSX basis set with ORCA [101]. The optimized geometries and frequencies of the identified compounds of interest are reported in appendix D.

The predicted free solvation energies at 250 °C and boiling points of the compounds of interest (including the transition states and intermediate compounds found from DFT calculations) are reported in Table 4.3. The cosmo cavities were generated with the method described in Section 4.2.2. We predicted the boiling points of the compounds with COSMO-RS, as solvation free energies are related to vapor pres-

sures (and boiling points) of the compounds. A good agreement with experimental data is obtained for the following compounds: toluene, styrene and hydroxyethyl guaiacol, with an absolute average deviation of <5 °C. For water, creosol, anisole and vinyl-guaiacol, the deviations are higher and around 10 °C.

For guaiacol and furfural conformers, the deviation is rather high, but we could not find a clear pattern to explain it. Concerning the solvation correction kinetic modeling, the involved compounds are vinyl guaiacol and hydroxyethyl-guaiacol. The solvation energies of transition states and intermediate compounds are fictive solvation energies as these compounds are unstable compounds.

Table 4.3: Solvation energies estimated with COSMO-RS[21] along with boiling point data and its absolute deviation to literature reference data.

Compound		Solvation Energy	Boiling point (K) at (1 atm)		
Name	CAS	$\Delta G^{solv}(T)$ (kcal/mol) at 250 °C	$T_{eb}^{COSMO-RS}$	$T_{eb}^{literature}$ [215]	diff. to ref
$4-Vinyl-guaiacol$	7786-61-0	0.26	523.9	518	5.9
Creosol	93-51-6	-10.086	506.6	495	11.6
Guaiacol	90-05-1	0.48	504.5	478.2	26.3
Toluene	108-88-3	3.13	383.15	383.8 ±0.2	-0.6
Anisole	100-66-3	1.94	436.2	427.0 ±0.9	9.2 ±0.9
Styrene	100-42-5	2.15	417.8	419 ±2	-1.2
$4-(1-Hydroxyethyl)$-guaiacol	2480-86-6	-1.43	595.7	594.5	1.2
Furfural	98-01-1	1.35	457.9	434.7 ±0.4	23.2
3-Furfural	498-60-2	1.62	445.9	417.2	28.7
H_2O	7732-18	16.0162	364.93	373.15	-8.22
Transition state and intermediate compounds					
TS vinyl-guaiacol formation	-	-3.58	652.5	-	
Vinyl Polymer	-	-8.29	920.8	around 703 for polystyrene	
TS vinyl-guaiacol condensation	-	-8.33	921.5	-	
Quinone Methide	-	0.65616	526.1	-	

The gas phase kinetic parameters of the reactions investigated with quantum chemical calculation were performed using the KiSThelP tool. The classical transitional state theory approach is considered Winger tunneling corrections. The derived thermodynamic parameters of quantum chemistry calculation (DFT calculations) were used to compute the gas phase rate constant within the canonical transition state theory tool KiSThelP.[102,314] The computed kinetic parameters according to the recipe from Section 4.2.2 above, using the DFT calculations and using the solvation correction estimated from predicted solvation energies (Table 4.3) are given in Table 4.4.

As shown in Figure 29, the tunneling effect correction on the vinyl formation reaction increases as the temperature is increased. This result suggests that for a temperature above 250 °C the reactant or intermediate transition state can tunnel (pass through) the barrier energy of the reaction. Although the correction due to Winger tunneling effect slightly increases with an increase of temperature, it affects

(a) (b)

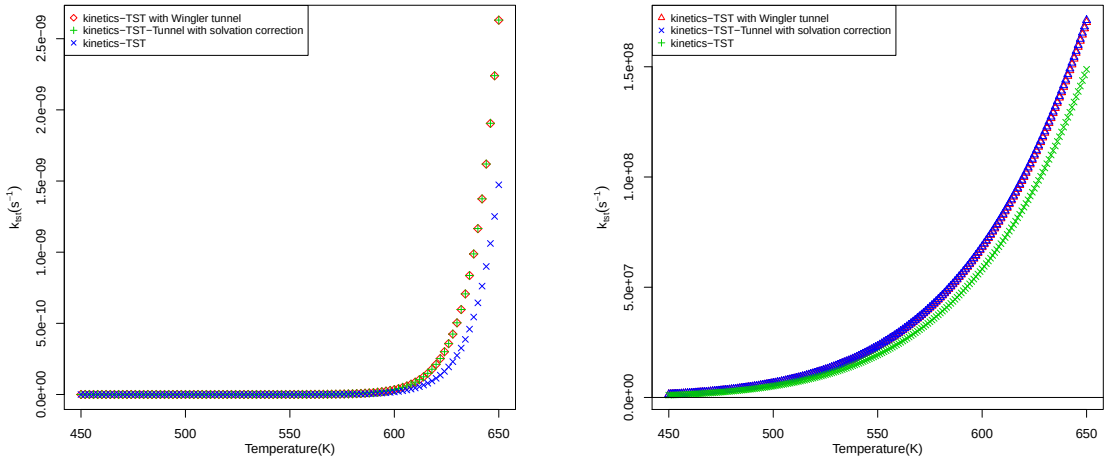

Figure 29: Kinetic rate with transitional state theory via classical transitional state theory with winger tunneling effect corrections from the processed DFT calculation data with KiSThelP tool. a) Kinetics of Vinyl phenol formation from the phenolic $C_\alpha - OH$ type. b) Kinetics of the condensation reaction of the phenolic $C_\alpha - C_\beta$ type from quinone methide intermediate addition on vinyl.

the kinetic over all the temperature range 250 °C to 300 °C.

From the kinetic parameters presented in Table 4.4, the activation energy of the vinyl formation reaction from the dehydration of 4-(1-Hydroxyethyl)-guaiacol is about 63.35 kcal/mol with solvation correction. The obtained result is in agreement with literature as reported by Carstensen and Dean[316] calculation and Zhou et al.[5] work for the intrinsic energy barrier of elimination of H_2O from alcohols for the Elementary Steps in the thermal conversion of biomass polymers: the suggested energy was 65.2 kcal/mol. This value obtained by Carstensen and Dean[316] was predicted for the CBS-QB3 basis set extrapolation and the B3LYP method, with an average deviation of ±3 kcal/mol.

From the DFT investigation of the condensation mechanism of the Phenolic $C_\alpha - C_\beta$ type (2-Methoxy-4-vinylphenol) we confirmed the presence of the quinone methide intermediate involved as the second reactant of the polymerized product, as suggested by Nakamura et al.[62] and Kotake et al.[307]. The polymerized product is a starting point of a polymerization chain that induces the formation of heavy molecular weight lignin (HMWL), as reported by Ranzi et al.[6–8] concerning the primary biomass pyrolysis composition products.

Table 4.4: Gas phase kinetic parameters estimated from DFT calculation with transition state theory and solvation energies correction estimated with COMSO-RS for vinyl formation reaction and vinyl condensation reaction.

Reaction	Reactants	Product	Rate constants		
			A (/ sec)	E_a (kcal/mol)	$\Delta\Delta G^{*,\ddagger}_{solv}$ (kcal/mol)
Kinetics with TST					
Vinyl Formation	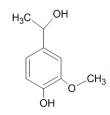	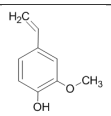	1.027E14	67.7	- 2.307
Polymerization	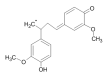	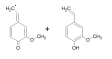	9.954E12	30.59	-3.736
Kinetics with TST and Wigner tunneling correction					
Vinyl Formation	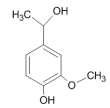	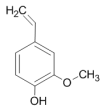	7.867E13	65.5	-2.15
Polymerization	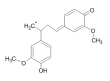	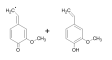	8.6249E12	30.11	-3.736

Note that this kinetic study represents a preliminary work, as it would be necessary to perform some experimental measurements to validate and refine the kinetic mechanism. The identified species from the generated mechanisms confirms the available global mechanisms must be completed with the initial stage reactions.

4.4 Conclusion

A better understanding of lignin pyrolysis reactions is important to limit the formation of tar in pyrolysis reactors. It is important to develop a reliable and detailed model for the kinetic mechanisms of pyrolysis and oxidation of biomass.

The modeling of the thermochemical conversion of lignin polymer is also important to design processes where lignin is used as a raw material for the production of biochemicals, biomaterials, and biofuels. However, much research work still must be done to deeply understand lignin pyrolysis and gasification processes. Recently, many theoretical studies[317] have been conducted to estimate the BDEs of linkages in lignin and propose reaction mechanism.

Our modeling study does not take into account (i) diffusion into the liquid and (ii) products migration out of the system. The kinetic mechanism predicted in this work are in good qualitative agreement with the chemical species observed experimentally during the pyrolysis process. This underlines the consistency of the mechanisms and highlights the requirement of a more precise reactor model with well-defined structures and kinetic data. While the generated models do not quantitatively reproduce all experimental conditions, they qualitatively reproduce the overall phenomenology of (i) the temperature, (ii) the chain length and (iii) the branching effect. Although further mechanism developments are still required, the present results underline the requirement of a liquid phase reactor to model the lignin primary pyrolysis. However, there is a particular need of experimental data to effectively our predictions.

The current reactor model represents only the homogeneous liquid phase part of the system and omits the gas phase. Solvent properties do not evolve during the oxidation and are fixed by the input file. A proper way to account for solvent effects is to incorporate the solvation free energy method with a temperature dependence in the kinetic solver.

General Conclusions and Perspectives

The aim of this study was a deep understanding of thermochemical conversion of biomass "pyrolysis" kinetic from a macro scale to a molecular scale. The first challenges encountered in our work were the lack of experimental data for biomass decomposition reactions and thermochemistry data of the compounds involved in biomass conversion. We wanted to understand the decomposition at low temperature where a multi-phase and multi-component problems are encountered. These ended by structuring our work in three parts:

First, we proposed an extension of the Paulechka and Kazakove method to predict the ideal heat capacities and enthalpies of formation for compounds containing the following elements: H, C, N, O, F, Cl, Br, Si, P and S. This approach is fully predictive and based on ab initio calculation. The ab initio method combines DFT calculation (geometry optimization) and DLPNO-CCSD(T) calculation (energy), with the def2/J and def2-QZVPP/C auxiliary basis sets and the RIJCOSX approximation. This approach provides accurate predictions of enthalpies of formation and more computationally efficient than the well-known G3 and G4 methods especially for long molecules.

In a second part of this work, we reviewed the COSMO-SAC models and proposed a re-parametrization for each one of them, by adjusting the solvation free energies of hundreds of binary systems. It is found that COSMO models are much more precise than Abraham's model that is commonly used to predict solvation energies in reactive systems. These models based on ab initio methods make them suitable for desktop application without significant computational resources and thus give us the possibility to handle a large set of compounds. While COSMO models provide good predictions for oxygenated organic molecules, they are not suitable for small gaseous compounds. The small gaseous compounds are a common issue for COSMO models and we suggest that they need a proper investigation with a different approach. Concerning free radical compounds, we could not estimate solvation energies using

COSMO-SAC models due to the lack of vapor pressure data for these compounds. We decided to use the COSMO-RS model (COSMOTherm Software) to overcome this problem and predict "pseudo vapor pressure data" for radicals. It would be very useful for future studies, to develop our own tool for vapor pressure predictions, based on COSMO-SAC.

Another promising route is the combination of atomistic molecular dynamics and machine learning to predict self-solvation free energies. This innovative approach was introduced in the work of Julia Gebhardt[318] and co-workers employing COSMO-RS model and UNIFAC group additivity model. Their promising results open a new novel research topic that can simplify the thermodynamic data predictions in the future.

In the third part of this study, we tried to investigate the complex process of biomass pyrolysis at low temperature, by only considering the liquid phase. Further improvements of the proposed liquid phase mechanism would consist in studying experimentally the kinetic of lignin surrogate compound mixture and identifying their product yield profile. The experimental data would then be necessary to have a full validated mechanism.

In order to develop a reliable and precise kinetic mechanism for the pyrolysis process at low temperature, one would need a specific multiphase reactor (solid, liquid and gas). In this case, the multiphase reactor should consider both the gas phase species and their interactions with the liquid and solid phase species. Depending on the application and the complexity of the system, each phase could then be modeled with its proper kinetic model. There is also a need to investigate and include in the kinetic modeling, at first, the competition between chemical and physical kinetics via for example Stokes-Einstein theory and then the dynamic vaporization via Hertz-Knudsen theory.

Finally, one can say that a research work is never finished and each time we try to reach the end we will end by discovering the beginning of a new challenge, but isn't it the most exciting part of research work?

Appendix A

Reference species for Enthalpies of formation predictions

A.1 H, C, N, O

[H] Name	CAS	ΔHf(kJ/mol)
1-3-butadiene	106-99-0	110[16,319]
1-butyne	107-00-6	165.4[16,253]
1-naphthol	90-15-3	-27.5[16,320–322]
2-methyl-propan-2-ol	75-65-0	-312.5[16,319]
2-propanol	67-63-0	-272.8[16,253]
acetic-acid	64-19-7	-432.8[16,253]
acetonitrile	75-05-8	74[16,319]
ammonia	7664-41-7	-45.56[16,253]
aniline	62-53-3	87.1[16,323–327]
anisole	100-66-3	-69.9[16,183,266,328–330]
benzamide	55-21-0	-99.8[16,262,323,324,331–334]
benzene	71-43-2	82.9[16,254]
benzoic-acid	65-85-0	-294.1[16]
biphenyl	92-52-4	180.2[16,202–209]
CO2	124-38-9	-393.51[16,335]
cyclohexane	110-82-7	-123.3[16,319]
cyclohexene	110-83-8	-5[16,336–338]
dimethyl-ether	115-10-6	-184[16,253]
E-2-butene	624-64-6	-11.2[16,253]

ethylene	74-85-1	52.53[16,253]
ethanal	75-07-0	-165.5[16,253]
ethane	74-84-0	-83.78[16,253]
ethanol	64-17-5	-234.6[16,253]
ethyne	74-89-2	228.32[16,253]
formic-acid	64-18-6	-378.5[16,253]
H2O	7732-18-5	-241.83[16,335]
iso-butane	75-28-5	-135.1[16,339–341]
methanal	50-00-0	-109.16[16,253]
methane	74-82-8	-74.53[16,253]
methanol	67-56-1	-200.7[16,253]
naphthalene	91-20-3	150.6[16,254]
n-butane	106-97-8	-125.8[16,253]
neopentane	463-82-1	-168[16,319]
nitrobenzene	98-95-3	66[16,327,342,343]
norbornene	498-66-8	81.9[16,344–346]
phenol	108-95-2	-95.7[16,259,347–351]
piperidine	110-89-4	-47.3[16,352–356]
propane	74-98-6	-104.6[16,253]
propanone	67-64-1	-216.1[16,253]
propene	115-07-1	20.3[16,253]
propyne	74-99-7	185.1[16,357,358]
pyridine	110-86-1	140.4[16,319]
styrene	100-42-5	148[16,319]
urea	57-13-6	-237.8[16,359–367]
Z-2-butene	590-18-1	-7.3[16,253]

Table A.1: List of known formation enthalpies, including source citation, used in this study for H, C, N, O species. All values taken from Paulechka and Kazakov[16], including the original references.

A.2 H, C, N, O, F, Cl

Table A.2: List of species containing the elements H, C, F and Cl. Species taken from Demenay et al.[17], with additional compounds from Green and Perry et al.[22] an other literature with references given in the table.

Name	CAS	ΔHf(kJ/mol)	
fluoromethane	593-53-3	-234.3[17,109]	
difluoromethane	75-10-5	-450.6[17]	-452.2[368,369]
fluoroethane	353-36-6	-264.4[17]	-276.6[368],−262[109], -284.2[213]
fluoroethene	75-02-5	-140.1[368,369]	
hydrogen-fluoride	7664-39-3	-273.3[22,230]	
1,1-difluoro-ethane	75-37-6	-500.8[213,368,369]	
1,2-difluoro-ethane	624-72-6	-447.7[22,230]	
chloroethene	25085-46-5	23[368,369]	
trifluoromethane	75-46-7	-697.1[17]	696.7[368,369]
tetrafluoromethane	75-73-0	-933.2[17,368,369]	
pentafluoroethane	354-33-6	-1100.4[17]	-1104.6 ± 4.5[212,213]
tetrafluoroethylene	116-14-3	-658.6[17,212]	
hexafluoroethane	76-16-4	-1343.9[17]	
hexafluoropropylene	76-16-4	-1151.7[17]	−1147.7 to −1148.4[370]
hydrogen-chloride	7647-01-0	-92.31[22,230]	
chloromethane	74-87-3	-81.96[22,230]	
chloroethane	75-00-3	-112.26[22,230,368,369]	
1,1-dichloro-ethane	75-34-3	-129.41[22,230]	-130.1[368,369]
1,2-dichloro-ethane	107-06-2	-129.979[22,230]	-126.8[368,369]
trichlorofluoromethane	75-69-4	-288.7[17]	
1-1-1-2-3-3-3-heptafluoropropane	431-89-0	-1552[17]	
1-1-1-2-3-3-hexafluoropropane	690-39-1	-1333[17]	
1-1-1-2-tetrafluoroethane	811-97-2	-895.8[17,212]	
1,1-dichloro-1-fluoroethane	1717-00-6	-339.7[17]	
1-chloro-1,1-difluoroethane	75-68-3	-529.7[17]	
2-2-dichloro-1-1-1-trifluoroethane	306-83-2	-743.9[17]	
2-chloro-1-1-1-2-tetrafluoroethane	2837-89-0	-924.7[17]	
chlorodifluoromethane	75-45-6	-481.[17]	-481.6[368]
chlorotrifluoromethane	75-72-9	-707.9[17]	-710.0[368]
dichlorodifluoromethane	75-71-8	-491.6[17,368]	
dichlorofluoromethane	75-43-4	-283.3[17,368]	

Table A.3: Aryl halides containing the elements H, C, F and Cl.

Name	CAS	ΔHf(kJ/mol)
1,2-difluoro-benzene	367-11-3	-283.0 ± 0.92[215,371]
1,3-difluoro-benzene	372-18-9	-309.2 ± 1.0[215,371]
1,4-difluoro-benzene	540-36-3	-306.7 ± 1.0[215]
1,2,4,5-tetrafluoro-benzene	327-54-8	-646.8 ± 3.4[215]
pentafluorobenzene	363-72-4	-806.0 ± 1.4[215,372]
hexafluorobenzene	392-56-3	-1015[215,373]
		-956.0 ± 1.2[215,372]
chloro-benzene	108-90-7	54.42[215,217]
1,2-dichloro-benzene	95-50-1	33[215,216]
1,3-dichloro-benzene	541-73-1	28.1[215,216]
1,4-dichloro-benzene	106-46-7	24.6[215,216]
1,2,3-trichloro-benzene	87-61-6	8.2 ± 1.8[215,374]
		3.78[215,375]
1,2,4-trichloro-benzene	120-82-1	4.9 ± 1.6[215,374]
		-8.05 kJ/mol[215,217]
1,3,5-trichloro-benzene	108-70-3	-2.6 ± 1.4[215,374]
		-13.36[215,217]
1,2,3,4-tetrachloro-benzene	634-66-2	-25.4[215,217]
1,2,3,5-tetrachloro-benzene	634-90-2	-34.9[215,217]
1,2,4,5-tetrachloro-benzene	95-94-3	-32.62[215,375]
pentachlorobenzene	608-93-5	-40.0 ± 8.7[215,376]
hexachlorobenzene	118-74-1	-44.7[215,375]

A.3 H, C, N, O, F, Cl, Br

Table A.4: List of known formation enthalpies, including source citation, used in this study for H, C, N, F, Br species. Individual references given in the table.

Name	CAS	ΔHf(kJ/mol)	
hydrogen-bromide	10035-10-6	-36.29[22,215,226,230,377]	
bromomethane	74-83-9	-34.3[215,378–380]	-37.7[22,230]
bromoethane	74-96-4	-63.6[22,215,230,378,381–383]	-64[109,368]
1,1-dibromo-ethane	557-91-5	-40.8[22,230]	-36.3 ± 7.8[384]
1,2-dibromo-ethane	106-93-4	-38.9[22,230]	-43.6[109,368]
bromoethene	593-60-2	79.2[109,215,267,368,385]	74.01 ± 0.59[384]
1-bromopropane	106-94-5	-82.93[215,386,387]	
2-bromopropane	75-26-3	-95.6[215,267,386–388]	
3-bromo-1-propene	4392-24-9	47.7[215,389,390]	
1-bromobutane	109-65-9	-107[215,391]	
bromotrifluoromethane	75-63-8	-648.94[215,226,267,392,393]	
cyanogen-bromide	506-68-3	186.19[215,226,267,394]	180.62 ± 0.73[384]
tribromo-methane	75-25-2	55.4[215,395]	

A.4 H, C, N, O, F, S, Cl, Br

Table A.5: List of known formation enthalpies, including source citation, used in this study for H, C, O, S species. References for individual values provided in the table.

Name	CAS	ΔHf(kJ/mol)
1,1-diMethyl-1-Propylthiol	1679-09-0	-126.9[215,396]
1,2-Ethanedithiol	540-63-6	-9.3[215,397]
1,3-Propanedithiol	109-80-8	-29.8[215,397]
1-Heptanethiol	1630-09-4	-149.5[215,398]
1-Hexanethiol	111-31-9	-129.3[215,398]
1-Pentanethiol	110-66-7	-109.7[215,399,400]
2-Butanethiol	513-53-1	-96.11[215,401]
1-propanethiol	107-03-9	-68.58[215,402]
2-Methyl-1-butanethiol	1878-18-8	-114.7[215,403]
2-Methyl-1-propanethiol	513-44-0	-96.48[215,401]
2-Propanethiol	75-33-2	-76.94[215,402]
3-Methyl-1-butanethiol	541-31-1	-114.6[215,403]
3-Methyl-2-butylthiol	2084-18-6	-121[215,403]
3-methyltetrahydrothiophene	4740-00-5	-60.54[215,403,404]
benzyl-mercaptan	100-53-8	93.1[215,267,403,405]
cyclohexanethiol	1569-69-3	-95.73[215,403,406]
cyclopentyl-mercaptan	1679-07-8	-47.78[215,407]
dihydro-3-2H-thiophenone	1003-04-9	-135.3[215,232]
ethanethiol	75-08-1	-46.15[215,408]
methanethiol	74-93-1	-22.8[215,409]
S-ethyl-ethanethioate	625-60-5	-227.8[215,410]
tert-butylmercaptan	75-66-1	-108.7[215,399,401,411]
tetrahydro-2-methyl-thiophene	1795-09-1	-63.89[215,403]
tetrahydrothiophene	110-01-0	-33.6[215,399,400,412]
thiophene	110-02-1	116.4[215,400,413–416]
Thiophenol	108-98-5	112.4[215,267,417]

Table A.6: List of known formation enthalpies, including source citation, used in this study for H, C, O, F, Cl, S species. References for individual values provided in the table.

Name	CAS	ΔHf(kJ/mol)
carbon-disulfide	75-15-0	116.94[215]
diethyl-sulfate	64-67-5	-756[215]
diethyl-sulfite	623-81-4	-552[215]
dimethyl-sulfate	77-78-1	-687[215]
dimethyl-sulfide	75-18-3	-37.5[215]
dimethyl-sulfoxide	67-68-5	-150.5[215]
dipropyl-ester-sulfurous-acid	623-98-3	-588[215]
disulfur-monoxide	20901-21-7	-56.48[215]
disulphur-decafluoride	5714-22-7	-2064.39[215]
ethyl-methyl-sulfite	10315-59-0	-524[215]
fluorosulfuric-acid	7789-21-1	-753.12[215]
hydrogen-sulfide	7783-06-4	-20.5[215]
pentafluoru-trifluoromethyl-sulfur	373-80-8	-1717.05[215]
sulfur-chloride-pentafluoride	13780-57-9	-1038.89[215]
sulfur-dichloride	10545-99-0	-17.57[215]
sulfur-difluoride	13814-25-0	-296.65[215]
sulfur-dimer	23550-45-0	128.6[215]
sulfur-dioxide	7446-09-5	-296.81[215]
sulfur-hexafluoride	2551-62-4	-1220.47[215]
sulfuric-acid	7664-93-9	-735.13[215]
sulfur-monochloride	10025-67-9	-16.74[215]
sulfur-monoxide	13827-32-2	5.01[215]
sulfurous-acid-dimethyl-ester	616-42-2	-483[215]
sulfur-tetrafluoride	7783-60-0	-763.16[215]
sulfur-trioxide	7446-11-9	-395.77[215]
sulfuryl-dichloride	7791-25-5	-354.8[215]
sulfuryl-fluoride	2699-79-8	-758.56[215]
thionyl-fluoride	7783-42-8	-543.92[215]

A.5 H, C, N, O, F, Si, S, Cl, Br

Table A.7: List of known formation enthalpies, including source citation, used in this study for H, C, O, F, Cl, Si species. References for individual values provided in the table.

Name	CAS	ΔHf(kJ/mol)	
silane	7803-62-5	34.31 ± 2[215,224–226,418]	
Si_2H_6	1590-87-0	79.76[218,419]	
Si_3H_8	7783-26-8	120.95[218,419]	
methyl-silane	992-94-9	-29.1 ± 4[22,224,230]	
dimethyl-silane	1111-74-6	-94.7 ± 4[22,224,230,418]	
Tert-methyl-silane	75-76-3	-233.2 ± 3.2[224,418]	
bromosilane	13465-73-1	-78.24[215,226]	-64.0152[225]
chlorosilane	13465-78-6	-141.84[215,226]	-135.5616[225]
fluorosilane	13537-33-2	-376.56[215,226]	
dibromosilane	13768-94-0	-190.37[215,226]	-180.7488[225]
dichlorosilane	4109-96-0	-320.49[215,226]	-315.0552[225]
tribromosilane	7789-57-3	-302.92[215,226]	-303.34[225]
trichlorosilane	10025-78-2	-496.22[215,226]	-499.1512[225]
trifluorosilane	13465-71-9	-1200.81[215,225,226]	
silicon-tetrabromide	7789-66-4	-415.47[215,225,226]	
silicon-tetrachloride	10026-04-7	-662.75[225]	
silicon-tetrafluoride	7783-61-1	-1614.94[215,226,377]	-1615.024[225]
methyltrichlorosilane	75-79-6	-528.86[215,226]	−584.9232[420]
silicon-monoxide	10097-28-6	-100.42[215,226]	
trichlorofluorosilane	14965-52-7	-840.98[215,226]	
ethyl-trichlorosilane	115-21-9	-595.4[22,230]	
methyl-chlorosilane	993-00-0	-215[22,230]	−251.8768[420]
methyl-dichlorosilane	200-877-1	-402[22,230]	−414.216[420]
vinyl-trichlorosilane	75-94-5	-481.16[22,230]	
$(C_2H_5)_1SiH_3$	2814-79-1	-84[227,228]	
$(C_2H_5)_3SiH_1$	617-86-7	-217.5[227–229]	
$(C_2H_5)_4Si$	631-36-7	-297[227,228]	
$CH_3(C_2H_5)_2SiH$	760-32-7	-200[227]	
chlorotrifluorosilane	14049-36-6	-1317.96[215,226]	
difluoro-oxosilane	14041-22-6	-966.5[215,226]	
dioxosilane	7631-86-9	-305.43[215,226]	
trifluoromethyl-silane	373-74-0	-1232.71[215,226]	

A.6 H, C, N, O, F, Si, P, S, Cl, Br

Table A.8: List of known formation enthalpies, including source citation, used in this study phosphorous compounds. References for individual values provided in the table

Name	CAS	ΔHf	(kJ/mol)
thiophosphoryl tribromide	3931-89-3	-281.05	[215,226]
phosphorus chloride	17167-55-4	129	[215,226]
phosphoryl tribromide	7789-59-5	-406.02	[215,226]
phosphoryl chloride fluoride	13769-76-1	-765.67	[215,226]
phosphenothious fluoride	55753-39-4	-172.27	[215,226]
methinophosphide	6829-52-3	149.9	[215,226]
phosphoryl fluoride	13478-20-1	-1254.25	[215,226]
phosphorus mononitride	17739-47-8	104.78	[215,226]
phosphorus trifluoride	7783-55-3	-958.44	[215,226]
phosphorus trichloride	7719-12-2	-288.7	[215,226]
phosphine	7803-51-2	5.47	[215,226]
trimethyl-phosphor	594-09-2	-101.1 ± 5.2	[117]
dimethyl-phosphor	676-59-5	-62.8 ± 5	[117]
methyl-phosphor	593-54-4	-19.5 ± 5	[117]
tricyanophosphine	1116-01-4	470 ± 10	[117]
trimethyl phosphite	121-45-9	-699 ± 8	[117]

Appendix B

Heat capacities Plots: Fitting Results

Plots of the heat capacities C_p of a number of reference species, with experimental data. Values are shown for the experimental data, the calculation of the heat capacity without scaling factors as well as the final result obtained with scaling factors for the frequencies.

- B3LYP D3BJ

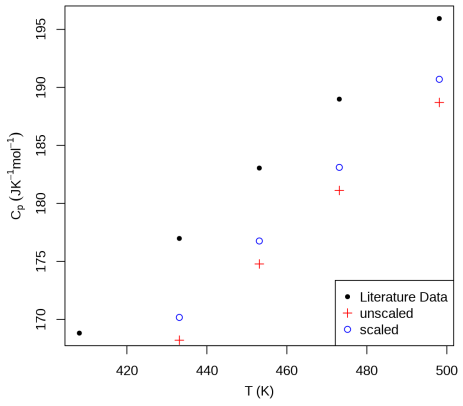

(a) anisole

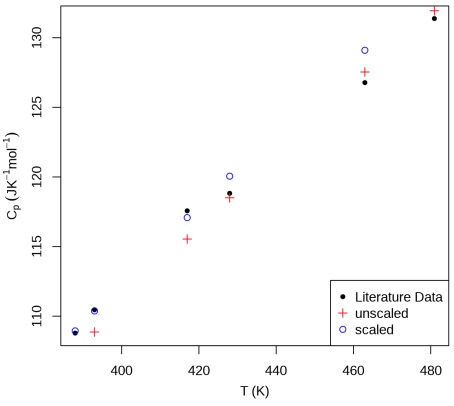

(b) benzene

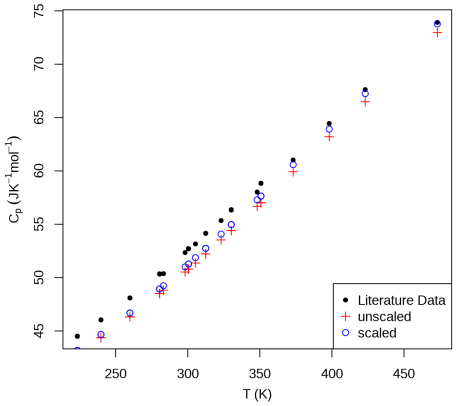

(a) ethane

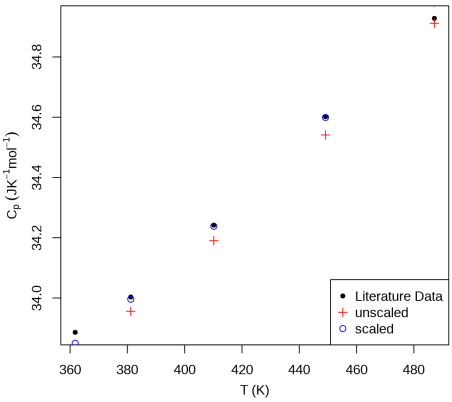

(b) H2O

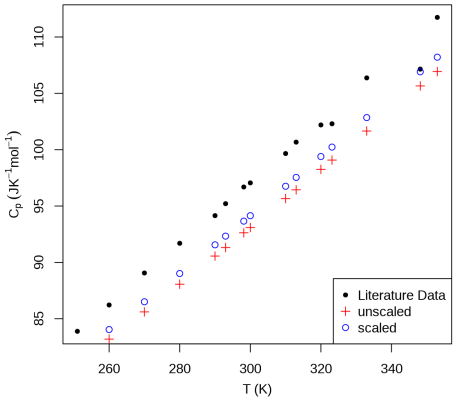

(c) iso-butane

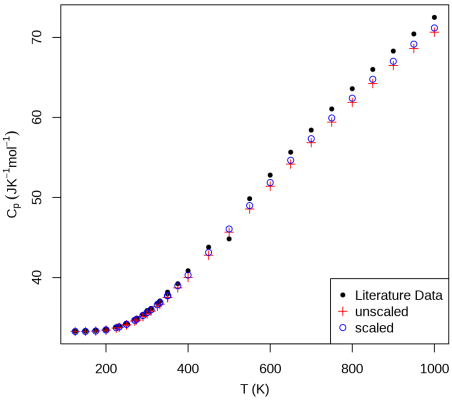

(d) methane

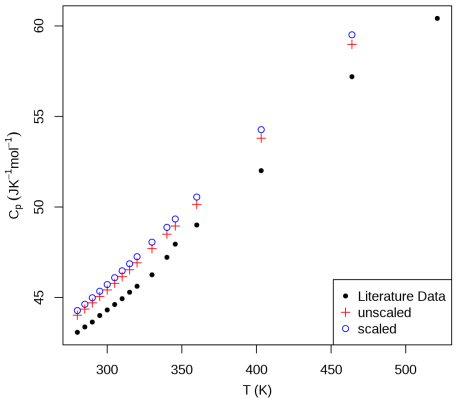

(a) methanol

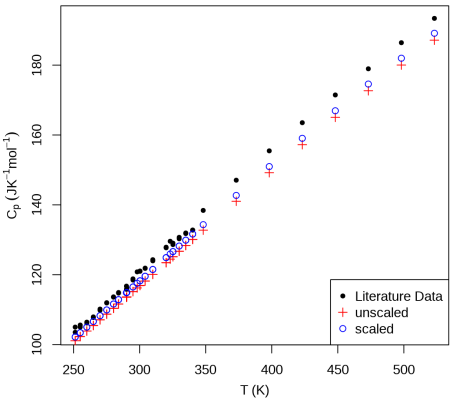

(b) neopentane

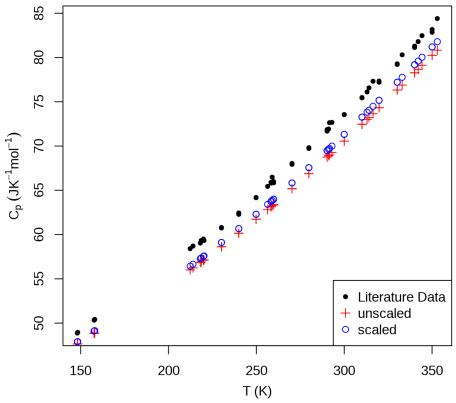

(c) propane

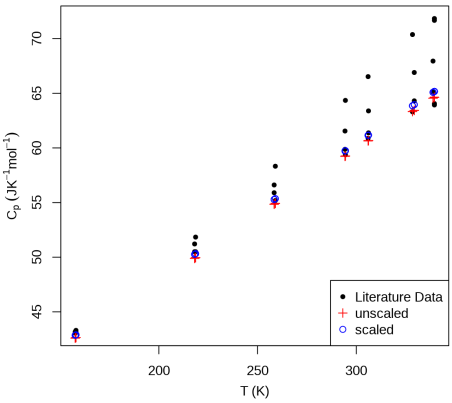

(d) propyne

- BP86 D3BJ

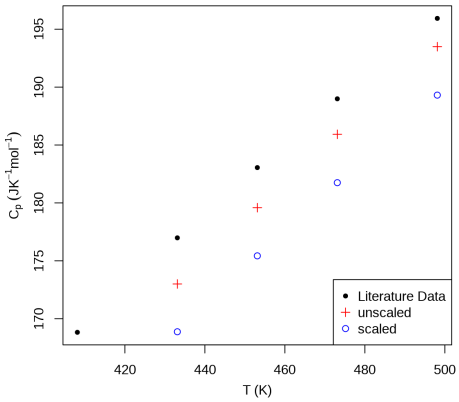

(a) anisole

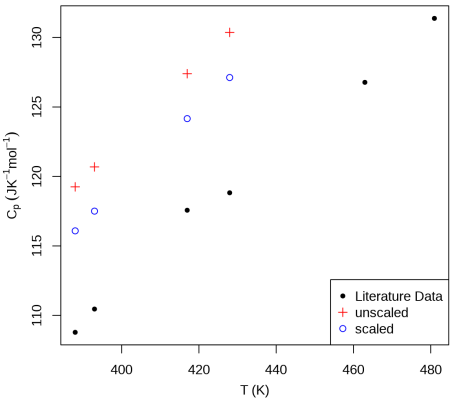

(b) benzene

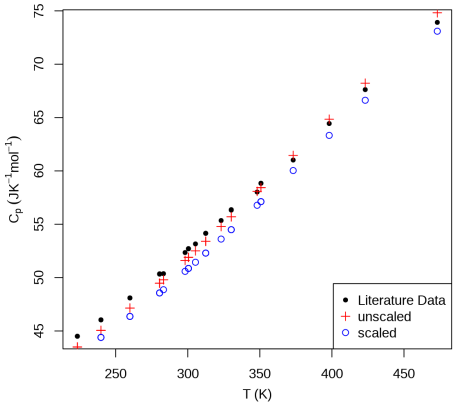

(c) ethane

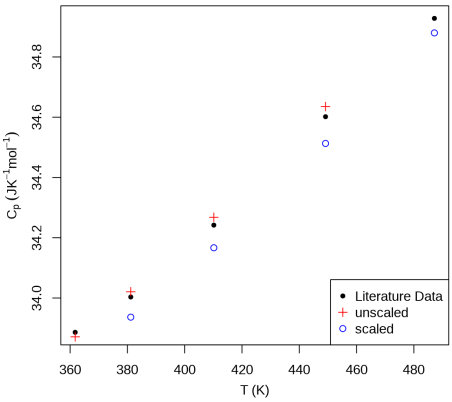

(d) H2O

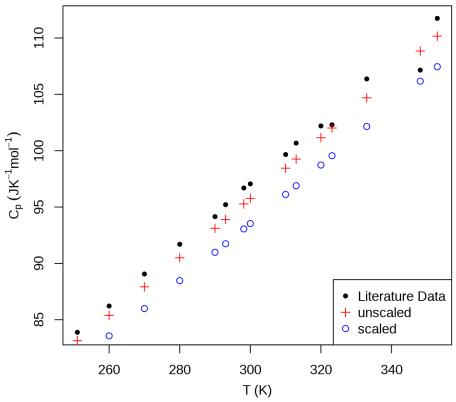

(e) iso-butane

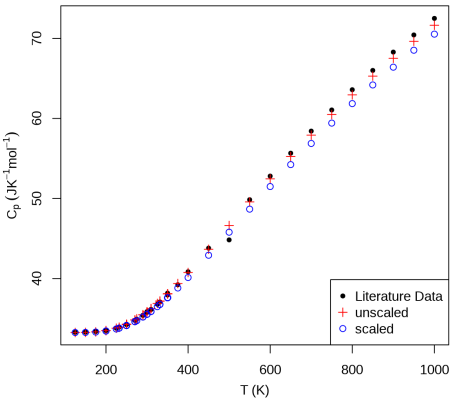

(f) methane

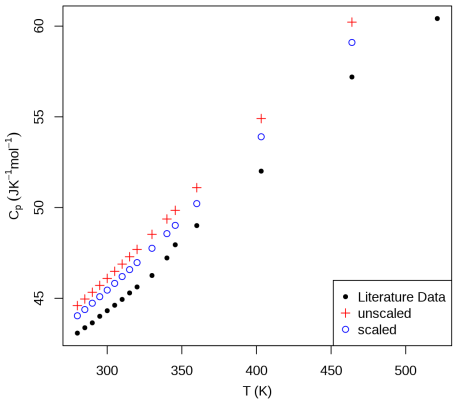

(g) methanol

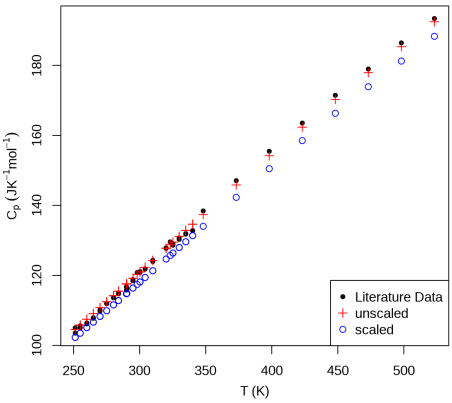

(h) neopentane

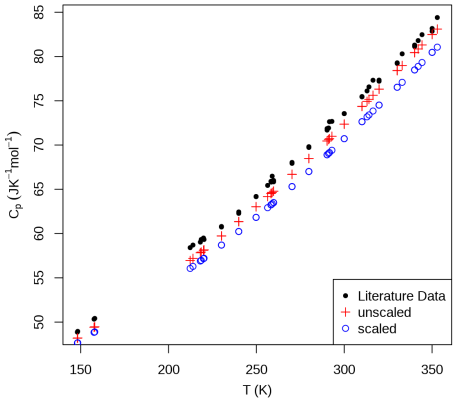

(i) propane

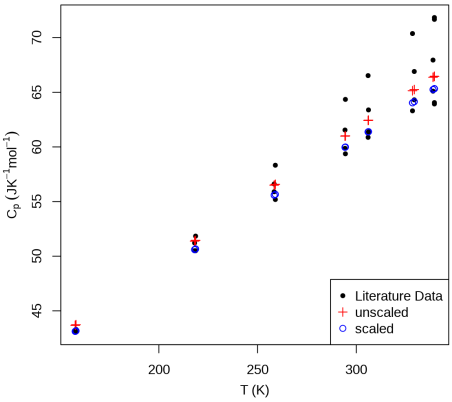

(j) propyne

- ωB97X-D3

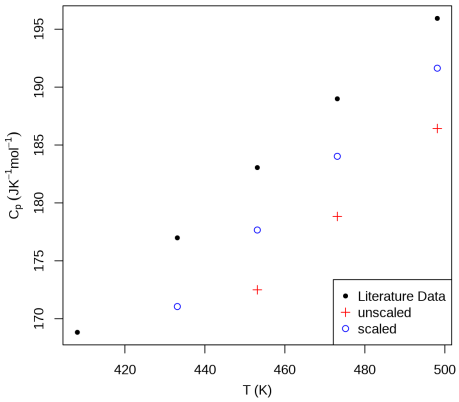

(k) anisole

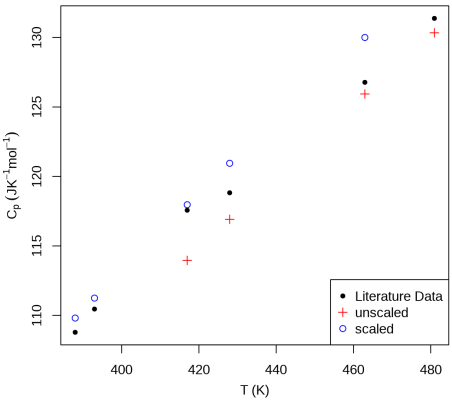

(l) benzene

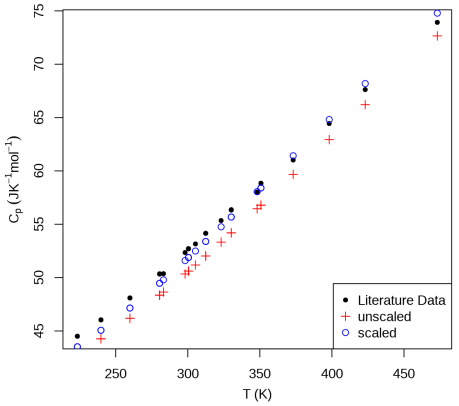

(m) ethane

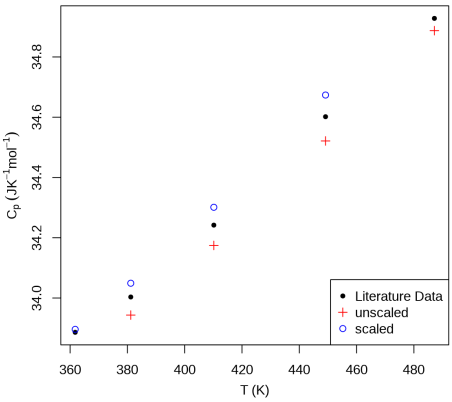

(n) H2O

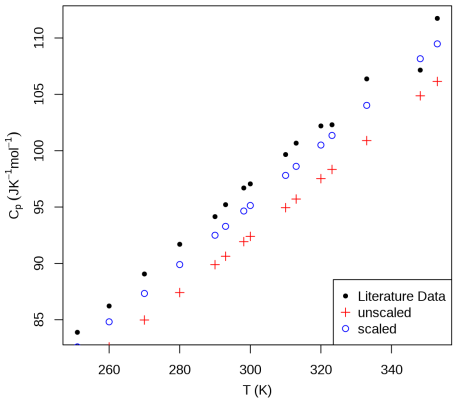

(o) iso-butane

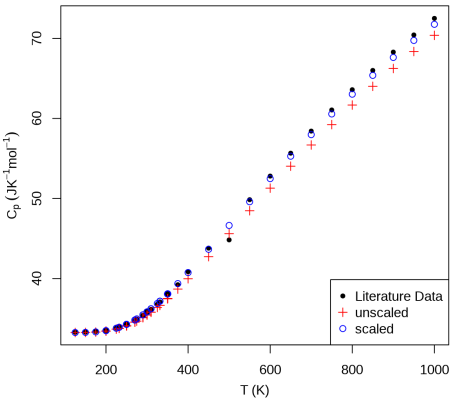

(p) methane

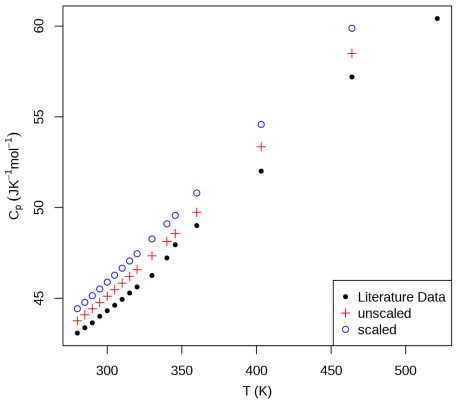

(q) methanol

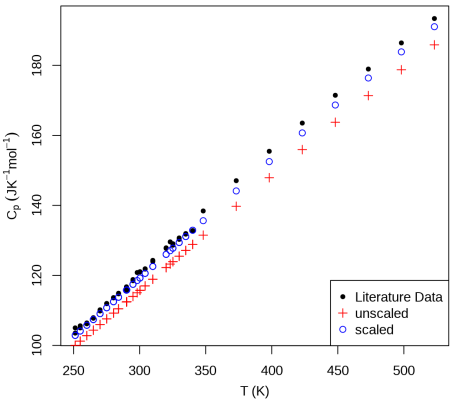

(r) neopentane

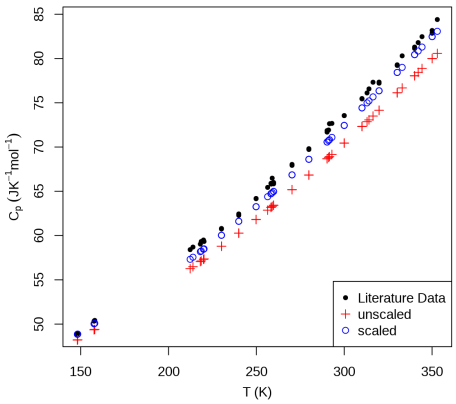

(s) propane

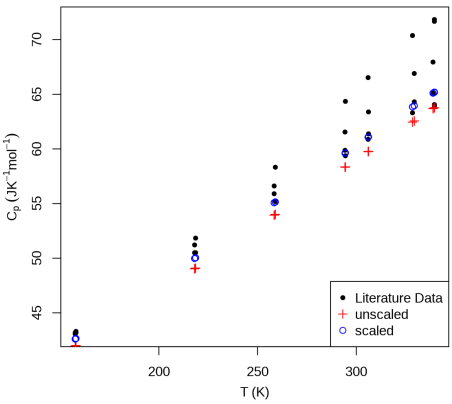

(t) propyne

Appendix C

Solvation energies and activity coefficients predictions

C.1 Abraham's model prediction of ΔG_{solv} for binary systems (kcal/mol)

Table C.1: ΔG_{solv} for binary systems (kcal/mol).

solvent		solute		T (K)	ΔG^{ref}_{solv}	$\Delta G^{calc,1}_{solv}$	$\Delta G^{calc,2}_{solv}$	$\Delta G^{calc,1}_{solv}$-ΔG^{ref}_{solv}	$\Delta G^{calc,2}_{solv}$-ΔG^{ref}_{solv}
111-87-5	1-octanol	592-41-6	1-hexene	293.44	-3.38	-3.19	-3.62	0.19	0.24
111-87-5	1-octanol	592-41-6	1-hexene	303.45	-3.25	-3.29	-3.51	0.04	0.26
111-87-5	1-octanol	592-41-6	1-hexene	313.55	-3.16	-3.4	-3.4	0.24	0.24
111-87-5	1-octanol	592-41-6	1-hexene	323.45	-3.05	-3.51	-3.29	0.46	0.24
111-87-5	1-octanol	592-41-6	1-hexene	298.15	-3.29	-3.24	-3.56	0.05	0.27
111-87-5	1-octanol	124-11-8	1-nonene	298.15	-5.19	-5.16	-5.5	0.03	0.31
111-87-5	1-octanol	111-66-0	1-octene	298.15	-4.58	-4.51	-4.85	0.07	0.27
111-87-5	1-octanol	109-67-1	1-pentene	293.44	-2.67	-2.52	-2.94	0.15	0.27
111-87-5	1-octanol	109-67-1	1-pentene	303.45	-2.56	-2.61	-2.85	0.05	0.29
111-87-5	1-octanol	109-67-1	1-pentene	313.55	-2.47	-2.69	-2.75	0.22	0.28
111-87-5	1-octanol	109-67-1	1-pentene	323.45	-2.4	-2.78	-2.66	0.38	0.26
111-87-5	1-octanol	107-83-5	2-methylpentane	298.15	-3.2	-3.04	-3.41	0.16	0.21
111-87-5	1-octanol	107-83-5	2-methylpentane	298.15	-3.17	-3.04	-3.41	0.13	0.24
111-87-5	1-octanol	75-28-5	2-methylpropane	278.17	-1.88	-1.53	-2.25	0.35	0.37
111-87-5	1-octanol	75-28-5	2-methylpropane	298.16	-1.72	-1.64	-2.09	0.08	0.37
111-87-5	1-octanol	75-28-5	2-methylpropane	323.19	-1.52	-1.78	-1.89	0.26	0.37
111-87-5	1-octanol	75-28-5	2-methylpropane	343.16	-1.38	-1.89	-1.74	0.51	0.36
111-87-5	1-octanol	75-07-0	acetaldehyde	298.15	-3.65	-2.3	-2.63	1.35	1.02
111-87-5	1-octanol	75-07-0	acetaldehyde	333.15	-2.88	-2.57	-2.35	0.31	0.53
111-87-5	1-octanol	110-82-7	cyclohexane	293.44	-3.8	-3.57	-3.97	0.23	0.17
111-87-5	1-octanol	110-82-7	cyclohexane	303.45	-3.68	-3.69	-3.86	0.01	0.18
111-87-5	1-octanol	110-82-7	cyclohexane	313.55	-3.6	-3.81	-3.74	0.21	0.14
111-87-5	1-octanol	110-82-7	cyclohexane	323.45	-3.5	-3.93	-3.64	0.43	0.14
111-87-5	1-octanol	110-82-7	cyclohexane	298.15	-3.7	-3.62	-3.92	0.08	0.22
111-87-5	1-octanol	110-82-7	cyclohexane	298.15	-3.79	-3.62	-3.92	0.17	0.13
111-87-5	1-octanol	110-82-7	cyclohexane	298.15	-3.73	-3.62	-3.92	0.11	0.19
111-87-5	1-octanol	110-83-8	cyclohexene	293.44	-3.92	-3.78	-4.12	0.14	0.2
111-87-5	1-octanol	110-83-8	cyclohexene	303.45	-3.8	-3.91	-4.01	0.11	0.21
111-87-5	1-octanol	110-83-8	cyclohexene	313.55	-3.71	-4.04	-3.9	0.33	0.19
111-87-5	1-octanol	110-83-8	cyclohexene	323.45	-3.61	-4.17	-3.79	0.56	0.18
111-87-5	1-octanol	120-92-3	cyclopentanone	298.15	-5.03	-5.01	-5.46	0.02	0.43
111-87-5	1-octanol	74-84-0	ethane	278.15	-0.68	-0.44	-1.03	0.25	0.35
111-87-5	1-octanol	74-84-0	ethane	298.15	-0.57	-0.47	-0.92	0.1	0.35
111-87-5	1-octanol	74-84-0	ethane	323.15	-0.44	-0.51	-0.79	0.07	0.35
111-87-5	1-octanol	74-84-0	ethane	343.15	-0.35	-0.54	-0.69	0.19	0.34

Table C.1: ΔG_{solv} for binary systems (kcal/mol).

solvent		solute		T (K)	ΔG^{ref}_{solv}	$\Delta G^{calc,1}_{solv}$	$\Delta G^{calc,2}_{solv}$	$\Delta G^{calc,1}_{solv}$-ΔG^{ref}_{solv}	$\Delta G^{calc,2}_{solv}$-ΔG^{ref}_{solv}
111-87-5	1-octanol	64-17-5	ethanol	298.15	-4.55	-4.25	-4.5	0.3	0.05
111-87-5	1-octanol	64-17-5	ethanol	452.19	-1.8	-6.44	-2.18	4.64	0.38
111-87-5	1-octanol	64-17-5	ethanol	298.15	-4.42	-4.25	-4.5	0.17	0.08
111-87-5	1-octanol	64-17-5	ethanol	298.15	-4.36	-4.25	-4.5	0.11	0.14
111-87-5	1-octanol	64-17-5	ethanol	293.44	-4.49	-4.18	-4.58	0.31	0.09
111-87-5	1-octanol	64-17-5	ethanol	303.45	-4.3	-4.32	-4.41	0.02	0.11
111-87-5	1-octanol	64-17-5	ethanol	313.55	-4.12	-4.47	-4.23	0.35	0.11
111-87-5	1-octanol	64-17-5	ethanol	323.45	-3.98	-4.61	-4.07	0.63	0.09
111-87-5	1-octanol	74-85-1	ethene	278.15	-0.46	-0.3	-0.8	0.16	0.35
111-87-5	1-octanol	74-85-1	ethene	298.15	-0.36	-0.32	-0.72	0.04	0.36
111-87-5	1-octanol	74-85-1	ethene	323.15	-0.25	-0.35	-0.61	0.09	0.36
111-87-5	1-octanol	74-85-1	ethene	343.15	-0.18	-0.37	-0.54	0.18	0.36
111-87-5	1-octanol	66-25-1	hexanal	298.15	-5.95	-5.02	-5.31	0.93	0.64
111-87-5	1-octanol	74-82-8	methane	278.15	0.45	0.54	-0.65	0.09	1.1
111-87-5	1-octanol	74-82-8	methane	298.15	0.52	0.58	-0.93	0.06	1.45
111-87-5	1-octanol	74-82-8	methane	323.15	0.61	0.63	-1.65	0.01	2.26
111-87-5	1-octanol	74-82-8	methane	343.15	0.69	0.66	-2.76	0.02	3.45
111-87-5	1-octanol	67-56-1	methanol	298.55	-3.97	-3.88	-3.98	0.09	0.01
111-87-5	1-octanol	67-56-1	methanol	444.51	-1.66	-5.78	-1.93	4.12	0.27
111-87-5	1-octanol	67-56-1	methanol	383.64	-2.62	-4.99	-2.73	2.37	0.11
111-87-5	1-octanol	67-56-1	methanol	298.15	-3.88	-3.88	-3.98	0	0.1
111-87-5	1-octanol	67-56-1	methanol	293.44	-4	-3.81	-4.06	0.19	0.06
111-87-5	1-octanol	67-56-1	methanol	303.45	-3.83	-3.94	-3.9	0.11	0.07
111-87-5	1-octanol	67-56-1	methanol	313.55	-3.67	-4.08	-3.74	0.41	0.07
111-87-5	1-octanol	67-56-1	methanol	323.45	-3.55	-4.2	-3.59	0.65	0.04
111-87-5	1-octanol	108-87-2	methylcyclohexane	293.44	-4.22	-4.04	-4.35	0.18	0.13
111-87-5	1-octanol	108-87-2	methylcyclohexane	303.45	-4.09	-4.17	-4.23	0.08	0.14
111-87-5	1-octanol	108-87-2	methylcyclohexane	313.55	-3.99	-4.31	-4.11	0.32	0.12
111-87-5	1-octanol	108-87-2	methylcyclohexane	323.45	-3.89	-4.45	-4	0.56	0.11
111-87-5	1-octanol	124-13-0	octanal	298.15	-7.26	-6.3	-6.6	0.96	0.66
111-87-5	1-octanol	74-98-6	propane	278.14	-1.41	-1.1	-1.75	0.31	0.34
111-87-5	1-octanol	74-98-6	propane	298.15	-1.25	-1.18	-1.59	0.07	0.34
111-87-5	1-octanol	74-98-6	propane	323.05	-1.07	-1.28	-1.42	0.21	0.35
111-87-5	1-octanol	74-98-6	propane	343.15	-0.94	-1.36	-1.28	0.42	0.35
111-87-5	1-octanol	109-99-9	tetrahydrofuran	298.15	-3.9	-3.99	-4.22	0.09	0.32
111-87-5	1-octanol	7732-18-5	water	313.15	-3.71	-5.07	-3.95	1.36	0.24
111-87-5	1-octanol	7732-18-5	water	363.15	-2.9	-5.88	-3.01	2.98	0.11
111-87-5	1-octanol	7732-18-5	water	363.15	-2.89	-5.88	-3.01	2.99	0.12
111-87-5	1-octanol	7732-18-5	water	322.94	-3.27	-5.23	-3.75	1.96	0.48
111-87-5	1-octanol	7732-18-5	water	332.8	-3.03	-5.39	-3.56	2.36	0.53
111-87-5	1-octanol	7732-18-5	water	343.55	-3.1	-5.56	-3.36	2.46	0.26
111-87-5	1-octanol	7732-18-5	water	353.1	-3.18	-5.72	-3.19	2.54	0.01
111-87-5	1-octanol	7732-18-5	water	298.15	-4.15	-4.83	-4.25	0.68	0.1
111-87-5	1-octanol	7732-18-5	water	333.15	-3.5	-5.4	-3.56	1.9	0.06
111-87-5	1-octanol	7732-18-5	water	373.15	-2.82	-6.04	-2.83	3.22	0.01
75-05-8	acetonitrile	106-98-9	1-butene	278.15	-2.01	-1.6	-2.14	0.41	0.13
75-05-8	acetonitrile	106-98-9	1-butene	278.15	-1.98	-1.6	-2.14	0.38	0.16
75-05-8	acetonitrile	106-98-9	1-butene	283.15	-1.97	-1.63	-2.1	0.34	0.13
75-05-8	acetonitrile	106-98-9	1-butene	288.15	-1.95	-1.66	-2.06	0.29	0.11
75-05-8	acetonitrile	106-98-9	1-butene	288.15	-1.93	-1.66	-2.06	0.27	0.13
75-05-8	acetonitrile	106-98-9	1-butene	293.15	-1.9	-1.69	-2.02	0.21	0.12
75-05-8	acetonitrile	106-98-9	1-butene	298.15	-1.86	-1.72	-1.98	0.14	0.12
75-05-8	acetonitrile	106-98-9	1-butene	303.15	-1.85	-1.75	-1.94	0.1	0.09
75-05-8	acetonitrile	106-98-9	1-butene	308.15	-1.79	-1.78	-1.9	0.01	0.11
75-05-8	acetonitrile	106-98-9	1-butene	313.15	-1.78	-1.8	-1.86	0.02	0.08
75-05-8	acetonitrile	106-98-9	1-butene	318.15	-1.72	-1.83	-1.83	0.11	0.11
75-05-8	acetonitrile	106-98-9	1-butene	323.15	-1.72	-1.86	-1.79	0.14	0.07
75-05-8	acetonitrile	106-98-9	1-butene	328.15	-1.65	-1.89	-1.76	0.24	0.11
75-05-8	acetonitrile	106-98-9	1-butene	333.15	-1.66	-1.92	-1.72	0.26	0.06
75-05-8	acetonitrile	106-98-9	1-butene	333.15	-1.59	-1.92	-1.72	0.33	0.13
75-05-8	acetonitrile	592-76-7	1-heptene	298.15	-3.4	-3.31	-3.47	0.09	0.07
75-05-8	acetonitrile	592-76-7	1-heptene	298.15	-3.35	-3.31	-3.47	0.04	0.12
75-05-8	acetonitrile	592-76-7	1-heptene	298.15	-3.56	-3.31	-3.47	0.25	0.09
75-05-8	acetonitrile	592-76-7	1-heptene	293.15	-3.5	-3.25	-3.53	0.25	0.03
75-05-8	acetonitrile	592-41-6	1-hexene	298.15	-3	-2.82	-2.98	0.18	0.02
75-05-8	acetonitrile	592-41-6	1-hexene	298.15	-2.91	-2.82	-2.98	0.09	0.07
75-05-8	acetonitrile	592-41-6	1-hexene	298.15	-2.98	-2.82	-2.98	0.16	0

Table C.1: ΔG_{solv} for binary systems (kcal/mol).

solvent		solute		T (K)	ΔG^{ref}_{solv}	$\Delta G^{calc,1}_{solv}$	$\Delta G^{calc,2}_{solv}$	$\Delta G^{calc,1}_{solv}$-ΔG^{ref}_{solv}	$\Delta G^{calc,2}_{solv}$-ΔG^{ref}_{solv}
75-05-8	acetonitrile	111-66-0	1-octene	298.15	-4.08	-3.81	-3.95	0.27	0.13
75-05-8	acetonitrile	111-66-0	1-octene	298.15	-3.89	-3.81	-3.95	0.08	0.06
75-05-8	acetonitrile	109-67-1	1-pentene	293.15	-2.25	-2.25	-2.52	0	0.27
75-05-8	acetonitrile	109-67-1	1-pentene	313.15	-2.13	-2.4	-2.34	0.27	0.21
75-05-8	acetonitrile	109-67-1	1-pentene	273.15	-2.57	-2.09	-2.72	0.48	0.15
75-05-8	acetonitrile	109-67-1	1-pentene	298.15	-2.42	-2.28	-2.48	0.14	0.06
75-05-8	acetonitrile	109-67-1	1-pentene	298.15	-2.68	-2.28	-2.48	0.4	0.2
75-05-8	acetonitrile	109-67-1	1-pentene	298.15	-2.41	-2.28	-2.48	0.13	0.07
75-05-8	acetonitrile	78-78-4	2-methylbutane	293.15	-1.83	-1.98	-1.9	0.15	0.07
75-05-8	acetonitrile	78-78-4	2-methylbutane	313.15	-1.7	-2.12	-1.72	0.42	0.02
75-05-8	acetonitrile	78-78-4	2-methylbutane	333.15	-1.63	-2.25	-1.56	0.62	0.07
75-05-8	acetonitrile	78-78-4	2-methylbutane	298.15	-1.9	-2.02	-1.85	0.12	0.05
75-05-8	acetonitrile	591-76-4	2-methylhexane	298.15	-2.9	-3.01	-2.82	0.11	0.08
75-05-8	acetonitrile	591-76-4	2-methylhexane	298.15	-3.08	-3.01	-2.82	0.07	0.26
75-05-8	acetonitrile	107-83-5	2-methylpentane	298.15	-2.57	-2.51	-2.36	0.06	0.21
75-05-8	acetonitrile	107-83-5	2-methylpentane	298.15	-2.55	-2.51	-2.36	0.04	0.19
75-05-8	acetonitrile	107-83-5	2-methylpentane	298.15	-2.48	-2.51	-2.36	0.03	0.12
75-05-8	acetonitrile	107-83-5	2-methylpentane	298.15	-2.4	-2.51	-2.36	0.11	0.04
75-05-8	acetonitrile	96-14-0	3-methylpentane	298.15	-2.49	-2.59	-2.44	0.1	0.05
75-05-8	acetonitrile	96-14-0	3-methylpentane	298.15	-2.67	-2.59	-2.44	0.08	0.23
75-05-8	acetonitrile	110-82-7	cyclohexane	298.15	-2.96	-3.06	-2.91	0.1	0.05
75-05-8	acetonitrile	110-82-7	cyclohexane	298.15	-3.1	-3.06	-2.91	0.04	0.19
75-05-8	acetonitrile	110-82-7	cyclohexane	298.15	-3.01	-3.06	-2.91	0.05	0.1
75-05-8	acetonitrile	110-82-7	cyclohexane	298.15	-2.94	-3.06	-2.91	0.12	0.03
75-05-8	acetonitrile	110-82-7	cyclohexane	298.15	-3.04	-3.06	-2.91	0.02	0.13
75-05-8	acetonitrile	110-82-7	cyclohexane	298.15	-3.11	-3.06	-2.91	0.05	0.2
75-05-8	acetonitrile	110-83-8	cyclohexene	298.15	-3.43	-3.44	-3.51	0.01	0.08
75-05-8	acetonitrile	110-83-8	cyclohexene	298.15	-3.43	-3.44	-3.51	0.01	0.08
75-05-8	acetonitrile	110-83-8	cyclohexene	303.15	-3.39	-3.5	-3.46	0.11	0.07
75-05-8	acetonitrile	287-92-3	cyclopentane	298.15	-2.52	-2.61	-2.45	0.09	0.07
75-05-8	acetonitrile	64-17-5	ethanol	333.15	-4.11	-4.49	-3.78	0.38	0.33
75-05-8	acetonitrile	64-17-5	ethanol	351.55	-3.8	-4.74	-3.52	0.94	0.28
75-05-8	acetonitrile	64-17-5	ethanol	330	-3.98	-4.45	-3.82	0.47	0.16
75-05-8	acetonitrile	64-17-5	ethanol	328.91	-4.1	-4.44	-3.84	0.34	0.26
75-05-8	acetonitrile	64-17-5	ethanol	335.47	-4	-4.52	-3.75	0.52	0.25
75-05-8	acetonitrile	64-17-5	ethanol	334.53	-4.02	-4.51	-3.76	0.49	0.26
75-05-8	acetonitrile	64-17-5	ethanol	340.81	-3.93	-4.6	-3.67	0.67	0.26
75-05-8	acetonitrile	64-17-5	ethanol	347.26	-3.83	-4.68	-3.58	0.85	0.25
75-05-8	acetonitrile	64-17-5	ethanol	293.2	-4.38	-3.95	-4.37	0.43	0.01
75-05-8	acetonitrile	64-17-5	ethanol	298.15	-4.34	-4.02	-4.29	0.32	0.05
75-05-8	acetonitrile	64-17-5	ethanol	298.15	-4.36	-4.02	-4.29	0.34	0.07
75-05-8	acetonitrile	64-17-5	ethanol	298.15	-4.43	-4.02	-4.29	0.41	0.14
75-05-8	acetonitrile	74-85-1	ethene	298.15	-0.62	-0.57	-0.88	0.04	0.27
75-05-8	acetonitrile	67-56-1	methanol	319.33	-3.91	-3.97	-3.61	0.06	0.3
75-05-8	acetonitrile	67-56-1	methanol	348.35	-3.59	-4.33	-3.24	0.74	0.35
75-05-8	acetonitrile	67-56-1	methanol	348.27	-3.61	-4.33	-3.24	0.72	0.37
75-05-8	acetonitrile	67-56-1	methanol	326.04	-3.73	-4.06	-3.52	0.33	0.21
75-05-8	acetonitrile	67-56-1	methanol	326.04	-3.8	-4.06	-3.52	0.26	0.28
75-05-8	acetonitrile	67-56-1	methanol	323.79	-3.75	-4.03	-3.55	0.28	0.2
75-05-8	acetonitrile	67-56-1	methanol	322.14	-3.84	-4.01	-3.57	0.17	0.27
75-05-8	acetonitrile	67-56-1	methanol	334.4	-3.66	-4.16	-3.41	0.5	0.25
75-05-8	acetonitrile	67-56-1	methanol	346.01	-3.58	-4.3	-3.27	0.72	0.31
75-05-8	acetonitrile	67-56-1	methanol	349.15	-3.55	-4.34	-3.23	0.79	0.32
75-05-8	acetonitrile	67-56-1	methanol	352.35	-3.43	-4.38	-3.19	0.95	0.24
75-05-8	acetonitrile	67-56-1	methanol	350.19	-3.46	-4.36	-3.22	0.9	0.24
75-05-8	acetonitrile	67-56-1	methanol	298.15	-4.03	-3.71	-3.89	0.32	0.14
75-05-8	acetonitrile	108-87-2	methylcyclohexane	348.15	-3.24	-4.05	-2.65	0.81	0.59
75-05-8	acetonitrile	108-87-2	methylcyclohexane	352.85	-3.15	-4.11	-2.61	0.96	0.54
75-05-8	acetonitrile	108-87-2	methylcyclohexane	298.15	-3.24	-3.47	-3.16	0.23	0.08
75-05-8	acetonitrile	108-87-2	methylcyclohexane	298.15	-3.32	-3.47	-3.16	0.15	0.16
75-05-8	acetonitrile	96-37-7	methylcyclopentane	298.15	-2.8	-2.98	-2.72	0.18	0.08
75-05-8	acetonitrile	7732-18-5	water	352.55	-3.67	-5.08	-3	1.41	0.67
75-05-8	acetonitrile	7732-18-5	water	351.75	-3.95	-5.07	-3.01	1.12	0.94
75-05-8	acetonitrile	7732-18-5	water	351.1	-3.7	-5.06	-3.02	1.36	0.68
75-05-8	acetonitrile	7732-18-5	water	352.25	-3.75	-5.07	-3	1.32	0.75
75-05-8	acetonitrile	7732-18-5	water	353.04	-3.79	-5.08	-2.99	1.29	0.8
75-05-8	acetonitrile	7732-18-5	water	353.64	-3.75	-5.09	-2.98	1.34	0.77

Table C.1: ΔG_{solv} for binary systems (kcal/mol).

solvent		solute		T (K)	ΔG^{ref}_{solv}	$\Delta G^{calc,1}_{solv}$	$\Delta G^{calc,2}_{solv}$	$\Delta G^{calc,1}_{solv}$-ΔG^{ref}_{solv}	$\Delta G^{calc,2}_{solv}$-ΔG^{ref}_{solv}
75-05-8	acetonitrile	7732-18-5	water	309.15	-4.36	-4.45	-3.66	0.09	0.7
75-05-8	acetonitrile	7732-18-5	water	325.45	-3.66	-4.69	-3.41	1.03	0.25
75-05-8	acetonitrile	7732-18-5	water	326.35	-3.61	-4.7	-3.39	1.09	0.22
75-05-8	acetonitrile	7732-18-5	water	351.88	-3.76	-5.07	-3.01	1.31	0.75
75-05-8	acetonitrile	7732-18-5	water	352.29	-3.79	-5.07	-3	1.28	0.79
75-05-8	acetonitrile	7732-18-5	water	353.25	-3.8	-5.09	-2.99	1.29	0.81
75-05-8	acetonitrile	7732-18-5	water	353.91	-3.89	-5.1	-2.98	1.21	0.91
75-05-8	acetonitrile	7732-18-5	water	350.55	-3.84	-5.05	-3.03	1.21	0.81
75-05-8	acetonitrile	7732-18-5	water	351.75	-3.74	-5.07	-3.01	1.33	0.73
75-05-8	acetonitrile	7732-18-5	water	353.15	-3.6	-5.09	-2.99	1.49	0.61
75-05-8	acetonitrile	7732-18-5	water	353.55	-3.42	-5.09	-2.98	1.67	0.44
75-05-8	acetonitrile	7732-18-5	water	297.15	-4.46	-4.28	-3.86	0.18	0.6
71-43-2	benzene	106-98-9	1-butene	298.15	-2.91	-2.31	-2.6	0.6	0.31
71-43-2	benzene	106-98-9	1-butene	279.99	-2.54	-2.17	-2.74	0.37	0.2
71-43-2	benzene	106-98-9	1-butene	289.99	-2.48	-2.25	-2.66	0.23	0.18
71-43-2	benzene	106-98-9	1-butene	309.99	-2.36	-2.4	-2.52	0.04	0.16
71-43-2	benzene	106-98-9	1-butene	329.99	-2.24	-2.55	-2.38	0.31	0.14
71-43-2	benzene	106-98-9	1-butene	298.15	-2.42	-2.31	-2.6	0.11	0.18
71-43-2	benzene	592-76-7	1-heptene	328.15	-4.34	-4.95	-4.34	0.61	0
71-43-2	benzene	592-76-7	1-heptene	328.15	-4.31	-4.95	-4.34	0.64	0.03
71-43-2	benzene	592-41-6	1-hexene	348.8	-3.47	-4.47	-3.53	1	0.06
71-43-2	benzene	592-41-6	1-hexene	347.69	-3.51	-4.46	-3.54	0.95	0.03
71-43-2	benzene	592-41-6	1-hexene	346.2	-3.56	-4.44	-3.55	0.88	0.01
71-43-2	benzene	109-67-1	1-pentene	293.15	-3.16	-3.03	-3.32	0.13	0.16
71-43-2	benzene	107-83-5	2-methylpentane	313.14	-3.59	-3.81	-3.49	0.22	0.1
71-43-2	benzene	107-83-5	2-methylpentane	313.14	-3.58	-3.81	-3.49	0.23	0.09
71-43-2	benzene	107-83-5	2-methylpentane	313.14	-3.69	-3.81	-3.49	0.12	0.2
71-43-2	benzene	107-83-5	2-methylpentane	313.14	-3.73	-3.81	-3.49	0.08	0.24
71-43-2	benzene	107-83-5	2-methylpentane	323.14	-3.48	-3.93	-3.41	0.45	0.07
71-43-2	benzene	107-83-5	2-methylpentane	323.14	-3.68	-3.93	-3.41	0.25	0.27
71-43-2	benzene	107-83-5	2-methylpentane	333.13	-3.63	-4.05	-3.33	0.42	0.3
71-43-2	benzene	107-83-5	2-methylpentane	298.15	-3.6	-3.63	-3.61	0.03	0.01
71-43-2	benzene	107-83-5	2-methylpentane	298.15	-3.62	-3.63	-3.61	0.01	0.01
71-43-2	benzene	75-28-5	2-methylpropane	279.99	-2.19	-1.98	-2.36	0.21	0.17
71-43-2	benzene	75-28-5	2-methylpropane	289.99	-2.14	-2.05	-2.3	0.09	0.16
71-43-2	benzene	75-28-5	2-methylpropane	309.99	-2.04	-2.19	-2.17	0.15	0.13
71-43-2	benzene	75-28-5	2-methylpropane	329.99	-1.96	-2.33	-2.05	0.37	0.09
71-43-2	benzene	75-28-5	2-methylpropane	298.15	-2.08	-2.11	-2.24	0.03	0.16
71-43-2	benzene	75-07-0	acetaldehyde	319.35	-3.14	-3.04	-3.02	0.1	0.12
71-43-2	benzene	110-82-7	cyclohexane	373.15	-3.75	-5.36	-3.44	1.61	0.31
71-43-2	benzene	110-82-7	cyclohexane	328.2	-4.07	-4.71	-3.8	0.64	0.27
71-43-2	benzene	110-82-7	cyclohexane	352.85	-3.91	-5.07	-3.6	1.16	0.31
71-43-2	benzene	110-82-7	cyclohexane	361.35	-3.7	-5.19	-3.53	1.49	0.17
71-43-2	benzene	110-82-7	cyclohexane	335.15	-3.91	-4.81	-3.74	0.9	0.17
71-43-2	benzene	110-82-7	cyclohexane	350.55	-3.79	-5.03	-3.62	1.24	0.17
71-43-2	benzene	110-82-7	cyclohexane	328.15	-4.01	-4.71	-3.8	0.7	0.21
71-43-2	benzene	110-82-7	cyclohexane	343.15	-3.88	-4.93	-3.67	1.05	0.21
71-43-2	benzene	110-82-7	cyclohexane	343.13	-3.91	-4.93	-3.68	1.02	0.23
71-43-2	benzene	110-82-7	cyclohexane	343.13	-3.93	-4.93	-3.68	1	0.25
71-43-2	benzene	110-82-7	cyclohexane	313.1	-4.15	-4.5	-3.92	0.35	0.23
71-43-2	benzene	110-82-7	cyclohexane	328.2	-4.01	-4.71	-3.8	0.7	0.21
71-43-2	benzene	110-82-7	cyclohexane	323.15	-4.06	-4.64	-3.84	0.58	0.22
71-43-2	benzene	110-82-7	cyclohexane	323.15	-4.05	-4.64	-3.84	0.59	0.21
71-43-2	benzene	110-82-7	cyclohexane	323.15	-4.03	-4.64	-3.84	0.61	0.19
71-43-2	benzene	110-82-7	cyclohexane	333.15	-4.01	-4.79	-3.76	0.78	0.25
71-43-2	benzene	110-82-7	cyclohexane	333.15	-3.99	-4.79	-3.76	0.8	0.23
71-43-2	benzene	110-82-7	cyclohexane	333.15	-3.98	-4.79	-3.76	0.81	0.22
71-43-2	benzene	110-82-7	cyclohexane	333.15	-3.96	-4.79	-3.76	0.83	0.2
71-43-2	benzene	110-82-7	cyclohexane	343.15	-3.86	-4.93	-3.67	1.07	0.19
71-43-2	benzene	110-82-7	cyclohexane	283.15	-4.41	-4.07	-4.19	0.34	0.22
71-43-2	benzene	110-82-7	cyclohexane	333.15	-4	-4.79	-3.76	0.79	0.24
71-43-2	benzene	110-82-7	cyclohexane	333.15	-3.99	-4.79	-3.76	0.8	0.23
71-43-2	benzene	110-82-7	cyclohexane	298.15	-4.25	-4.28	-4.06	0.03	0.19
71-43-2	benzene	110-82-7	cyclohexane	352.1	-3.82	-5.06	-3.6	1.24	0.22
71-43-2	benzene	110-82-7	cyclohexane	352.17	-3.83	-5.06	-3.6	1.23	0.23
71-43-2	benzene	110-82-7	cyclohexane	352.45	-3.79	-5.06	-3.6	1.27	0.19
71-43-2	benzene	110-82-7	cyclohexane	352.05	-3.83	-5.06	-3.6	1.23	0.23

Table C.1: ΔG_{solv} for binary systems (kcal/mol).

solvent		solute		T (K)	ΔG^{ref}_{solv}	$\Delta G^{calc,1}_{solv}$	$\Delta G^{calc,2}_{solv}$	$\Delta G^{calc,1}_{solv}$-ΔG^{ref}_{solv}	$\Delta G^{calc,2}_{solv}$-ΔG^{ref}_{solv}
71-43-2	benzene	110-82-7	cyclohexane	352.65	-3.81	-5.07	-3.6	1.26	0.21
71-43-2	benzene	110-82-7	cyclohexane	352.05	-3.85	-5.06	-3.6	1.21	0.25
71-43-2	benzene	110-82-7	cyclohexane	351.95	-3.86	-5.06	-3.6	1.2	0.26
71-43-2	benzene	110-82-7	cyclohexane	352.2	-3.84	-5.06	-3.6	1.22	0.24
71-43-2	benzene	110-82-7	cyclohexane	352.4	-3.82	-5.06	-3.6	1.24	0.22
71-43-2	benzene	110-82-7	cyclohexane	352.7	-3.82	-5.07	-3.6	1.25	0.22
71-43-2	benzene	110-82-7	cyclohexane	351.79	-3.86	-5.05	-3.61	1.19	0.25
71-43-2	benzene	110-82-7	cyclohexane	352.45	-3.82	-5.06	-3.6	1.24	0.22
71-43-2	benzene	110-82-7	cyclohexane	352.13	-3.84	-5.06	-3.6	1.22	0.24
71-43-2	benzene	110-82-7	cyclohexane	352.3	-3.83	-5.06	-3.6	1.23	0.23
71-43-2	benzene	110-82-7	cyclohexane	352.79	-3.8	-5.07	-3.6	1.27	0.2
71-43-2	benzene	110-82-7	cyclohexane	352.1	-3.82	-5.06	-3.6	1.24	0.22
71-43-2	benzene	110-82-7	cyclohexane	352.17	-3.83	-5.06	-3.6	1.23	0.23
71-43-2	benzene	110-82-7	cyclohexane	352.25	-3.86	-5.06	-3.6	1.2	0.26
71-43-2	benzene	110-82-7	cyclohexane	351.35	-3.86	-5.05	-3.61	1.19	0.25
71-43-2	benzene	110-82-7	cyclohexane	351.85	-3.83	-5.05	-3.61	1.22	0.22
71-43-2	benzene	110-82-7	cyclohexane	352.05	-3.83	-5.06	-3.6	1.23	0.23
71-43-2	benzene	110-82-7	cyclohexane	352.15	-3.82	-5.06	-3.6	1.24	0.22
71-43-2	benzene	110-82-7	cyclohexane	352.35	-3.82	-5.06	-3.6	1.24	0.22
71-43-2	benzene	110-82-7	cyclohexane	352.45	-3.82	-5.06	-3.6	1.24	0.22
71-43-2	benzene	110-82-7	cyclohexane	352.65	-3.82	-5.07	-3.6	1.25	0.22
71-43-2	benzene	110-82-7	cyclohexane	351.75	-3.84	-5.05	-3.61	1.21	0.23
71-43-2	benzene	110-82-7	cyclohexane	352.35	-3.8	-5.06	-3.6	1.26	0.2
71-43-2	benzene	110-82-7	cyclohexane	298.15	-4.21	-4.28	-4.06	0.07	0.15
71-43-2	benzene	110-82-7	cyclohexane	293.15	-4.27	-4.21	-4.1	0.06	0.17
71-43-2	benzene	110-82-7	cyclohexane	298.15	-4.23	-4.28	-4.06	0.05	0.17
71-43-2	benzene	110-82-7	cyclohexane	293.15	-4.27	-4.21	-4.1	0.06	0.17
71-43-2	benzene	110-82-7	cyclohexane	293.15	-4.28	-4.21	-4.1	0.07	0.18
71-43-2	benzene	110-82-7	cyclohexane	314.55	-4.08	-4.52	-3.91	0.44	0.17
71-43-2	benzene	110-83-8	cyclohexene	298.15	-4.49	-4.49	-4.4	0	0.09
71-43-2	benzene	110-83-8	cyclohexene	298.15	-4.47	-4.49	-4.4	0.02	0.07
71-43-2	benzene	110-83-8	cyclohexene	298.15	-4.46	-4.49	-4.4	0.03	0.06
71-43-2	benzene	110-83-8	cyclohexene	323.15	-4.24	-4.87	-4.16	0.63	0.08
71-43-2	benzene	110-83-8	cyclohexene	323.15	-4.21	-4.87	-4.16	0.66	0.05
71-43-2	benzene	110-83-8	cyclohexene	348.15	-4.04	-5.24	-3.94	1.2	0.1
71-43-2	benzene	110-83-8	cyclohexene	348.15	-4.02	-5.24	-3.94	1.22	0.08
71-43-2	benzene	110-83-8	cyclohexene	348.15	-4.02	-5.24	-3.94	1.22	0.08
71-43-2	benzene	110-83-8	cyclohexene	348.15	-4.02	-5.24	-3.94	1.22	0.08
71-43-2	benzene	110-83-8	cyclohexene	348.15	-3.99	-5.24	-3.94	1.25	0.05
71-43-2	benzene	110-83-8	cyclohexene	293.15	-4.54	-4.41	-4.45	0.13	0.09
71-43-2	benzene	110-83-8	cyclohexene	333.15	-4.14	-5.02	-4.07	0.88	0.07
71-43-2	benzene	110-83-8	cyclohexene	333.15	-4.14	-5.02	-4.07	0.88	0.07
71-43-2	benzene	110-83-8	cyclohexene	353.15	-3.97	-5.32	-3.9	1.35	0.07
71-43-2	benzene	287-92-3	cyclopentane	351.95	-3.16	-4.28	-3.01	1.12	0.15
71-43-2	benzene	287-92-3	cyclopentane	351.05	-3.19	-4.27	-3.02	1.08	0.17
71-43-2	benzene	287-92-3	cyclopentane	349.8	-3.22	-4.25	-3.03	1.03	0.19
71-43-2	benzene	287-92-3	cyclopentane	348.2	-3.22	-4.23	-3.04	1.01	0.18
71-43-2	benzene	287-92-3	cyclopentane	346.7	-3.25	-4.21	-3.05	0.96	0.2
71-43-2	benzene	120-92-3	cyclopentanone	313.15	-5.52	-6.11	-5.76	0.59	0.24
71-43-2	benzene	120-92-3	cyclopentanone	313.15	-5.44	-6.11	-5.76	0.67	0.32
71-43-2	benzene	120-92-3	cyclopentanone	313.15	-5.38	-6.11	-5.76	0.73	0.38
71-43-2	benzene	74-84-0	ethane	298.15	-0.84	-0.83	-1.01	0.01	0.17
71-43-2	benzene	64-17-5	ethanol	313.15	-3.08	-3.2	-2.95	0.12	0.13
71-43-2	benzene	64-17-5	ethanol	323.15	-2.99	-3.31	-2.81	0.32	0.18
71-43-2	benzene	64-17-5	ethanol	333.15	-2.9	-3.41	-2.67	0.51	0.23
71-43-2	benzene	64-17-5	ethanol	333.15	-3.12	-3.41	-2.67	0.29	0.45
71-43-2	benzene	64-17-5	ethanol	333.15	-2.88	-3.41	-2.67	0.53	0.21
71-43-2	benzene	64-17-5	ethanol	313.15	-3.25	-3.2	-2.95	0.05	0.3
71-43-2	benzene	64-17-5	ethanol	349.25	-2.83	-3.57	-2.46	0.74	0.37
71-43-2	benzene	64-17-5	ethanol	347.45	-2.95	-3.56	-2.48	0.61	0.47
71-43-2	benzene	64-17-5	ethanol	350.25	-2.98	-3.58	-2.44	0.6	0.54
71-43-2	benzene	64-17-5	ethanol	347.75	-3	-3.56	-2.48	0.56	0.52
71-43-2	benzene	64-17-5	ethanol	344.35	-2.94	-3.52	-2.52	0.58	0.42
71-43-2	benzene	64-17-5	ethanol	343.45	-3.07	-3.51	-2.53	0.44	0.54
71-43-2	benzene	64-17-5	ethanol	351.15	-2.75	-3.59	-2.43	0.84	0.32
71-43-2	benzene	64-17-5	ethanol	351.15	-2.85	-3.59	-2.43	0.74	0.42
71-43-2	benzene	64-17-5	ethanol	349.15	-2.9	-3.57	-2.46	0.67	0.44

Table C.1: ΔG_{solv} for binary systems (kcal/mol).

solvent		solute		T (K)	ΔG^{ref}_{solv}	$\Delta G^{calc,1}_{solv}$	$\Delta G^{calc,2}_{solv}$	$\Delta G^{calc,1}_{solv}$-ΔG^{ref}_{solv}	$\Delta G^{calc,2}_{solv}$-ΔG^{ref}_{solv}
71-43-2	benzene	64-17-5	ethanol	351.15	-2.84	-3.59	-2.43	0.75	0.41
71-43-2	benzene	64-17-5	ethanol	344.95	-2.63	-3.53	-2.51	0.9	0.12
71-43-2	benzene	64-17-5	ethanol	349.95	-2.54	-3.58	-2.45	1.04	0.09
71-43-2	benzene	64-17-5	ethanol	348.4	-2.65	-3.57	-2.47	0.92	0.18
71-43-2	benzene	64-17-5	ethanol	346	-2.95	-3.54	-2.5	0.59	0.45
71-43-2	benzene	64-17-5	ethanol	348.5	-2.96	-3.57	-2.47	0.61	0.49
71-43-2	benzene	64-17-5	ethanol	298.15	-3.41	-3.05	-3.16	0.36	0.25
71-43-2	benzene	64-17-5	ethanol	298.15	-3.22	-3.05	-3.16	0.17	0.06
71-43-2	benzene	64-17-5	ethanol	298.15	-3.17	-3.05	-3.16	0.12	0.01
71-43-2	benzene	64-17-5	ethanol	298.15	-3.16	-3.05	-3.16	0.11	0
71-43-2	benzene	64-17-5	ethanol	313.15	-3	-3.2	-2.95	0.2	0.05
71-43-2	benzene	64-17-5	ethanol	342.35	-2.72	-3.5	-2.55	0.78	0.17
71-43-2	benzene	64-17-5	ethanol	348.95	-2.62	-3.57	-2.46	0.95	0.16
71-43-2	benzene	64-17-5	ethanol	307.25	-3.06	-3.14	-3.03	0.08	0.03
71-43-2	benzene	64-17-5	ethanol	307.25	-3.05	-3.14	-3.03	0.09	0.02
71-43-2	benzene	64-17-5	ethanol	317.35	-2.96	-3.25	-2.89	0.29	0.07
71-43-2	benzene	64-17-5	ethanol	317.65	-3.01	-3.25	-2.88	0.24	0.13
71-43-2	benzene	64-17-5	ethanol	320.95	-2.99	-3.28	-2.84	0.29	0.15
71-43-2	benzene	64-17-5	ethanol	320.95	-2.94	-3.28	-2.84	0.34	0.1
71-43-2	benzene	64-17-5	ethanol	337.25	-2.83	-3.45	-2.62	0.62	0.21
71-43-2	benzene	64-17-5	ethanol	338.15	-2.74	-3.46	-2.6	0.72	0.14
71-43-2	benzene	64-17-5	ethanol	352.15	-2.75	-3.6	-2.42	0.85	0.33
71-43-2	benzene	64-17-5	ethanol	354.15	-2.72	-3.62	-2.39	0.9	0.33
71-43-2	benzene	64-17-5	ethanol	298.15	-3.42	-3.05	-3.16	0.37	0.26
71-43-2	benzene	74-85-1	ethene	298.15	-0.66	-0.66	-1.05	0	0.39
71-43-2	benzene	67-56-1	methanol	318.15	-2.52	-2.54	-2.01	0.02	0.51
71-43-2	benzene	67-56-1	methanol	345.9	-2.32	-2.77	-1.67	0.45	0.65
71-43-2	benzene	67-56-1	methanol	318.15	-2.49	-2.54	-2.01	0.05	0.48
71-43-2	benzene	67-56-1	methanol	336.89	-2.37	-2.69	-1.78	0.32	0.59
71-43-2	benzene	67-56-1	methanol	332.89	-2.44	-2.66	-1.83	0.22	0.61
71-43-2	benzene	67-56-1	methanol	308.15	-2.7	-2.46	-2.13	0.24	0.57
71-43-2	benzene	67-56-1	methanol	350.18	-2.3	-2.8	-1.62	0.5	0.68
71-43-2	benzene	67-56-1	methanol	346.92	-2.09	-2.77	-1.66	0.68	0.43
71-43-2	benzene	67-56-1	methanol	340.49	-2	-2.72	-1.74	0.72	0.26
71-43-2	benzene	67-56-1	methanol	339.5	-2.45	-2.72	-1.75	0.27	0.7
71-43-2	benzene	67-56-1	methanol	341.65	-2.56	-2.73	-1.72	0.17	0.84
71-43-2	benzene	67-56-1	methanol	342.55	-2.24	-2.74	-1.71	0.5	0.53
71-43-2	benzene	67-56-1	methanol	332.15	-2.71	-2.66	-1.83	0.05	0.88
71-43-2	benzene	67-56-1	methanol	332.35	-2.73	-2.66	-1.83	0.07	0.9
71-43-2	benzene	67-56-1	methanol	344.72	-2.25	-2.76	-1.69	0.51	0.56
71-43-2	benzene	67-56-1	methanol	337.69	-2.54	-2.7	-1.77	0.16	0.77
71-43-2	benzene	67-56-1	methanol	336.49	-2.62	-2.69	-1.78	0.07	0.84
71-43-2	benzene	67-56-1	methanol	347.19	-1.96	-2.78	-1.66	0.82	0.3
71-43-2	benzene	67-56-1	methanol	323.19	-2.51	-2.59	-1.94	0.08	0.57
71-43-2	benzene	67-56-1	methanol	336.39	-2.36	-2.69	-1.78	0.33	0.58
71-43-2	benzene	67-56-1	methanol	335.43	-2.37	-2.68	-1.8	0.31	0.57
71-43-2	benzene	67-56-1	methanol	293.15	-2.93	-2.34	-2.32	0.59	0.61
71-43-2	benzene	67-56-1	methanol	298.15	-2.63	-2.38	-2.26	0.25	0.37
71-43-2	benzene	67-56-1	methanol	298.15	-2.48	-2.38	-2.26	0.1	0.22
71-43-2	benzene	108-87-2	methylcyclohexane	348.15	-4.3	-5.61	-4.02	1.31	0.28
71-43-2	benzene	108-87-2	methylcyclohexane	348.15	-4.28	-5.61	-4.02	1.33	0.26
71-43-2	benzene	108-87-2	methylcyclohexane	348.15	-4.27	-5.61	-4.02	1.34	0.25
71-43-2	benzene	108-87-2	methylcyclohexane	354.63	-4.23	-5.72	-3.97	1.49	0.26
71-43-2	benzene	108-87-2	methylcyclohexane	353.85	-4.19	-5.71	-3.97	1.52	0.22
71-43-2	benzene	108-87-2	methylcyclohexane	353.86	-4.2	-5.71	-3.97	1.51	0.23
71-43-2	benzene	108-87-2	methylcyclohexane	354.8	-4.24	-5.72	-3.97	1.48	0.27
71-43-2	benzene	108-87-2	methylcyclohexane	354.35	-4.23	-5.71	-3.97	1.48	0.26
71-43-2	benzene	108-87-2	methylcyclohexane	354.05	-4.2	-5.71	-3.97	1.51	0.23
71-43-2	benzene	108-87-2	methylcyclohexane	353.75	-4.19	-5.7	-3.97	1.51	0.22
71-43-2	benzene	108-87-2	methylcyclohexane	353.5	-4.2	-5.7	-3.98	1.5	0.22
71-43-2	benzene	96-37-7	methylcyclopentane	349.77	-3.71	-4.82	-3.45	1.11	0.26
71-43-2	benzene	96-37-7	methylcyclopentane	333.15	-3.72	-4.59	-3.58	0.87	0.14
71-43-2	benzene	96-37-7	methylcyclopentane	313.14	-3.94	-4.32	-3.75	0.38	0.19
71-43-2	benzene	96-37-7	methylcyclopentane	328.15	-3.83	-4.52	-3.62	0.69	0.21
71-43-2	benzene	96-37-7	methylcyclopentane	353	-3.61	-4.87	-3.43	1.26	0.18
71-43-2	benzene	96-37-7	methylcyclopentane	352.6	-3.59	-4.86	-3.43	1.27	0.16
71-43-2	benzene	96-37-7	methylcyclopentane	352.15	-3.63	-4.86	-3.43	1.23	0.2

Table C.1: ΔG_{solv} for binary systems (kcal/mol).

solvent			solute	T (K)	ΔG^{ref}_{solv}	$\Delta G^{calc,1}_{solv}$	$\Delta G^{calc,2}_{solv}$	$\Delta G^{calc,1}_{solv}$-ΔG^{ref}_{solv}	$\Delta G^{calc,2}_{solv}$-ΔG^{ref}_{solv}
71-43-2	benzene	96-37-7	methylcyclopentane	351.5	-3.65	-4.85	-3.44	1.2	0.21
71-43-2	benzene	96-37-7	methylcyclopentane	350.95	-3.65	-4.84	-3.44	1.19	0.21
71-43-2	benzene	96-37-7	methylcyclopentane	350.3	-3.68	-4.83	-3.45	1.15	0.23
71-43-2	benzene	96-37-7	methylcyclopentane	352.79	-3.6	-4.86	-3.43	1.26	0.17
71-43-2	benzene	96-37-7	methylcyclopentane	350.77	-3.68	-4.84	-3.44	1.16	0.24
71-43-2	benzene	110-62-3	pentanal	313.15	-4.95	-5.33	-5.07	0.38	0.12
71-43-2	benzene	110-62-3	pentanal	313.15	-4.95	-5.33	-5.07	0.38	0.12
71-43-2	benzene	110-62-3	pentanal	313.15	-4.94	-5.33	-5.07	0.39	0.13
71-43-2	benzene	110-62-3	pentanal	313.15	-4.87	-5.33	-5.07	0.46	0.2
71-43-2	benzene	110-62-3	pentanal	313.15	-4.85	-5.33	-5.07	0.48	0.22
71-43-2	benzene	74-98-6	propane	298.15	-1.61	-1.61	-1.72	0	0.11
71-43-2	benzene	74-98-6	propane	279.99	-1.68	-1.51	-1.82	0.17	0.14
71-43-2	benzene	74-98-6	propane	289.99	-1.63	-1.56	-1.76	0.07	0.13
71-43-2	benzene	74-98-6	propane	309.99	-1.54	-1.67	-1.65	0.13	0.11
71-43-2	benzene	74-98-6	propane	329.99	-1.46	-1.78	-1.54	0.32	0.08
71-43-2	benzene	109-99-9	tetrahydrofuran	333.15	-4.01	-5.08	-4.01	1.07	0
71-43-2	benzene	109-99-9	tetrahydrofuran	303.15	-4.27	-4.62	-4.32	0.35	0.05
71-43-2	benzene	109-99-9	tetrahydrofuran	303.15	-4.26	-4.62	-4.32	0.36	0.06
71-43-2	benzene	109-99-9	tetrahydrofuran	313.15	-4.19	-4.78	-4.21	0.59	0.02
71-43-2	benzene	109-99-9	tetrahydrofuran	313.15	-4.16	-4.78	-4.21	0.62	0.05
71-43-2	benzene	109-99-9	tetrahydrofuran	313.15	-4.16	-4.78	-4.21	0.62	0.05
71-43-2	benzene	109-99-9	tetrahydrofuran	313.15	-4.14	-4.78	-4.21	0.64	0.07
71-43-2	benzene	109-99-9	tetrahydrofuran	323.15	-4.08	-4.93	-4.11	0.85	0.03
71-43-2	benzene	109-99-9	tetrahydrofuran	323.15	-4.07	-4.93	-4.11	0.86	0.04
71-43-2	benzene	109-99-9	tetrahydrofuran	323.15	-4.06	-4.93	-4.11	0.87	0.05
71-43-2	benzene	109-99-9	tetrahydrofuran	323.15	-4.06	-4.93	-4.11	0.87	0.05
71-43-2	benzene	109-99-9	tetrahydrofuran	323.15	-4.05	-4.93	-4.11	0.88	0.06
71-43-2	benzene	109-99-9	tetrahydrofuran	323.15	-4.04	-4.93	-4.11	0.89	0.07
71-43-2	benzene	109-99-9	tetrahydrofuran	323.15	-4.04	-4.93	-4.11	0.89	0.07
71-43-2	benzene	109-99-9	tetrahydrofuran	333.15	-3.97	-5.08	-4.01	1.11	0.04
71-43-2	benzene	109-99-9	tetrahydrofuran	333.15	-3.96	-5.08	-4.01	1.12	0.05
71-43-2	benzene	109-99-9	tetrahydrofuran	333.15	-3.95	-5.08	-4.01	1.13	0.06
71-43-2	benzene	109-99-9	tetrahydrofuran	333.15	-3.94	-5.08	-4.01	1.14	0.07
71-43-2	benzene	109-99-9	tetrahydrofuran	333.15	-3.94	-5.08	-4.01	1.14	0.07
71-43-2	benzene	109-99-9	tetrahydrofuran	333.15	-3.94	-5.08	-4.01	1.14	0.07
71-43-2	benzene	109-99-9	tetrahydrofuran	313.15	-4.21	-4.78	-4.21	0.57	0
71-43-2	benzene	7732-18-5	water	293.15	-2.25	-1.72	-0.28	0.53	1.97
71-43-2	benzene	7732-18-5	water	308.15	-2.07	-1.8	-0.07	0.27	2
71-43-2	benzene	7732-18-5	water	323.15	-1.83	-1.89	0.13	0.06	1.96
71-43-2	benzene	7732-18-5	water	293.15	-2.25	-1.72	-0.28	0.53	1.97
71-43-2	benzene	7732-18-5	water	308.15	-2.07	-1.8	-0.07	0.27	2
71-43-2	benzene	7732-18-5	water	323.15	-1.84	-1.89	0.13	0.05	1.97
110-82-7	cyclohexane	106-98-9	1-butene	298.15	-2.47	-2.27	-2.46	0.2	0.01
110-82-7	cyclohexane	107-83-5	2-methylpentane	298.15	-3.86	-3.68	-3.97	0.18	0.11
110-82-7	cyclohexane	107-83-5	2-methylpentane	298.15	-3.87	-3.68	-3.97	0.19	0.1
110-82-7	cyclohexane	108-94-1	cyclohexanone	355.31	-4.79	-6.44	-5.05	1.65	0.26
110-82-7	cyclohexane	108-94-1	cyclohexanone	353.75	-4.65	-6.41	-5.06	1.76	0.41
110-82-7	cyclohexane	110-83-8	cyclohexene	354.5	-3.91	-5.16	-3.87	1.25	0.04
110-82-7	cyclohexane	110-83-8	cyclohexene	354.7	-3.91	-5.16	-3.87	1.25	0.04
110-82-7	cyclohexane	110-83-8	cyclohexene	354.4	-3.91	-5.15	-3.87	1.24	0.04
110-82-7	cyclohexane	110-83-8	cyclohexene	354.6	-3.92	-5.16	-3.87	1.24	0.05
110-82-7	cyclohexane	110-83-8	cyclohexene	354.1	-3.9	-5.15	-3.87	1.25	0.03
110-82-7	cyclohexane	110-83-8	cyclohexene	353.6	-3.91	-5.14	-3.88	1.23	0.03
110-82-7	cyclohexane	110-83-8	cyclohexene	353.5	-3.91	-5.14	-3.88	1.23	0.03
110-82-7	cyclohexane	110-83-8	cyclohexene	353.8	-3.93	-5.15	-3.87	1.22	0.06
110-82-7	cyclohexane	110-83-8	cyclohexene	353.45	-3.95	-5.14	-3.88	1.19	0.07
110-82-7	cyclohexane	110-83-8	cyclohexene	318.84	-4.26	-4.64	-4.21	0.38	0.05
110-82-7	cyclohexane	110-83-8	cyclohexene	318.7	-4.26	-4.64	-4.21	0.38	0.05
110-82-7	cyclohexane	110-83-8	cyclohexene	318.62	-4.26	-4.63	-4.21	0.37	0.05
110-82-7	cyclohexane	110-83-8	cyclohexene	318.55	-4.25	-4.63	-4.21	0.38	0.04
110-82-7	cyclohexane	110-83-8	cyclohexene	318.46	-4.25	-4.63	-4.21	0.38	0.04
110-82-7	cyclohexane	110-83-8	cyclohexene	318.38	-4.25	-4.63	-4.21	0.38	0.04
110-82-7	cyclohexane	110-83-8	cyclohexene	318.34	-4.25	-4.63	-4.21	0.38	0.04
110-82-7	cyclohexane	110-83-8	cyclohexene	318.24	-4.25	-4.63	-4.21	0.38	0.04
110-82-7	cyclohexane	110-83-8	cyclohexene	318.18	-4.24	-4.63	-4.21	0.39	0.03
110-82-7	cyclohexane	110-83-8	cyclohexene	318.14	-4.25	-4.63	-4.21	0.38	0.04
110-82-7	cyclohexane	110-83-8	cyclohexene	337.93	-4.07	-4.92	-4.02	0.85	0.05

Table C.1: ΔG_{solv} for binary systems (kcal/mol).

solvent		solute		T (K)	ΔG^{ref}_{solv}	$\Delta G^{calc,1}_{solv}$	$\Delta G^{calc,2}_{solv}$	$\Delta G^{calc,1}_{solv}$-ΔG^{ref}_{solv}	$\Delta G^{calc,2}_{solv}$-ΔG^{ref}_{solv}
110-82-7	cyclohexane	110-83-8	cyclohexene	337.7	-4.07	-4.91	-4.02	0.84	0.05
110-82-7	cyclohexane	110-83-8	cyclohexene	337.62	-4.07	-4.91	-4.02	0.84	0.05
110-82-7	cyclohexane	110-83-8	cyclohexene	337.55	-4.06	-4.91	-4.02	0.85	0.04
110-82-7	cyclohexane	110-83-8	cyclohexene	337.52	-4.06	-4.91	-4.03	0.85	0.03
110-82-7	cyclohexane	110-83-8	cyclohexene	337.44	-4.06	-4.91	-4.03	0.85	0.03
110-82-7	cyclohexane	110-83-8	cyclohexene	337.41	-4.06	-4.91	-4.03	0.85	0.03
110-82-7	cyclohexane	110-83-8	cyclohexene	337.36	-4.06	-4.91	-4.03	0.85	0.03
110-82-7	cyclohexane	110-83-8	cyclohexene	354.33	-3.91	-5.15	-3.87	1.24	0.04
110-82-7	cyclohexane	110-83-8	cyclohexene	354.23	-3.91	-5.15	-3.87	1.24	0.04
110-82-7	cyclohexane	110-83-8	cyclohexene	354.15	-3.91	-5.15	-3.87	1.24	0.04
110-82-7	cyclohexane	110-83-8	cyclohexene	354.05	-3.91	-5.15	-3.87	1.24	0.04
110-82-7	cyclohexane	110-83-8	cyclohexene	354.02	-3.91	-5.15	-3.87	1.24	0.04
110-82-7	cyclohexane	110-83-8	cyclohexene	353.95	-3.9	-5.15	-3.87	1.25	0.03
110-82-7	cyclohexane	110-83-8	cyclohexene	353.9	-3.9	-5.15	-3.87	1.25	0.03
110-82-7	cyclohexane	110-83-8	cyclohexene	353.84	-3.9	-5.15	-3.87	1.25	0.03
110-82-7	cyclohexane	110-83-8	cyclohexene	353.81	-3.88	-5.15	-3.87	1.27	0.01
110-82-7	cyclohexane	110-83-8	cyclohexene	353.78	-3.88	-5.15	-3.87	1.27	0.01
110-82-7	cyclohexane	110-83-8	cyclohexene	354.82	-3.91	-5.16	-3.86	1.25	0.05
110-82-7	cyclohexane	110-83-8	cyclohexene	354.67	-3.9	-5.16	-3.87	1.26	0.03
110-82-7	cyclohexane	110-83-8	cyclohexene	354.61	-3.91	-5.16	-3.87	1.25	0.04
110-82-7	cyclohexane	110-83-8	cyclohexene	354.5	-3.91	-5.16	-3.87	1.25	0.04
110-82-7	cyclohexane	110-83-8	cyclohexene	354.27	-3.9	-5.15	-3.87	1.25	0.03
110-82-7	cyclohexane	120-92-3	cyclopentanone	313.15	-4.56	-4.85	-4.81	0.29	0.25
110-82-7	cyclohexane	64-17-5	ethanol	293.2	-2.36	-2.2	-2.21	0.16	0.15
110-82-7	cyclohexane	64-17-5	ethanol	313.2	-2.24	-2.35	-1.94	0.11	0.3
110-82-7	cyclohexane	64-17-5	ethanol	333.2	-2.25	-2.5	-1.69	0.25	0.56
110-82-7	cyclohexane	64-17-5	ethanol	279.85	-2.29	-2.1	-2.39	0.19	0.1
110-82-7	cyclohexane	64-17-5	ethanol	298.15	-2.12	-2.24	-2.14	0.12	0.02
110-82-7	cyclohexane	64-17-5	ethanol	318.15	-1.95	-2.39	-1.88	0.44	0.07
110-82-7	cyclohexane	64-17-5	ethanol	302.95	-2.15	-2.27	-2.08	0.12	0.07
110-82-7	cyclohexane	64-17-5	ethanol	323.45	-2.01	-2.43	-1.81	0.42	0.2
110-82-7	cyclohexane	64-17-5	ethanol	323.45	-2	-2.43	-1.81	0.43	0.19
110-82-7	cyclohexane	64-17-5	ethanol	342.75	-1.9	-2.57	-1.57	0.67	0.33
110-82-7	cyclohexane	64-17-5	ethanol	342.75	-1.89	-2.57	-1.57	0.68	0.32
110-82-7	cyclohexane	64-17-5	ethanol	361.15	-1.83	-2.71	-1.35	0.88	0.48
110-82-7	cyclohexane	64-17-5	ethanol	361.15	-1.78	-2.71	-1.35	0.93	0.43
110-82-7	cyclohexane	64-17-5	ethanol	323.15	-1.99	-2.42	-1.81	0.43	0.18
110-82-7	cyclohexane	64-17-5	ethanol	312.8	-2.36	-2.35	-1.95	0.01	0.41
110-82-7	cyclohexane	64-17-5	ethanol	322.9	-2.26	-2.42	-1.82	0.16	0.44
110-82-7	cyclohexane	64-17-5	ethanol	333	-2.19	-2.5	-1.69	0.31	0.5
110-82-7	cyclohexane	64-17-5	ethanol	343	-2.13	-2.57	-1.56	0.44	0.57
110-82-7	cyclohexane	64-17-5	ethanol	352.9	-2.1	-2.65	-1.44	0.55	0.66
110-82-7	cyclohexane	64-17-5	ethanol	298.15	-2.26	-2.24	-2.14	0.02	0.12
110-82-7	cyclohexane	64-17-5	ethanol	298.15	-2.59	-2.24	-2.14	0.35	0.45
110-82-7	cyclohexane	67-56-1	methanol	328.15	-1.48	-1.67	-0.73	0.19	0.75
110-82-7	cyclohexane	67-56-1	methanol	328.15	-2.03	-1.67	-0.73	0.36	1.3
110-82-7	cyclohexane	67-56-1	methanol	334.35	-2.13	-1.71	-0.67	0.42	1.46
110-82-7	cyclohexane	67-56-1	methanol	293.15	-1.4	-1.5	-1.12	0.1	0.28
110-82-7	cyclohexane	67-56-1	methanol	293.15	-1.38	-1.5	-1.12	0.12	0.26
110-82-7	cyclohexane	67-56-1	methanol	283.15	-1.82	-1.44	-1.24	0.38	0.58
110-82-7	cyclohexane	67-56-1	methanol	293.15	-1.81	-1.5	-1.12	0.31	0.69
110-82-7	cyclohexane	67-56-1	methanol	313.15	-1.46	-1.6	-0.9	0.14	0.56
110-82-7	cyclohexane	67-56-1	methanol	318.15	-2.54	-1.62	-0.84	0.92	1.7
110-82-7	cyclohexane	67-56-1	methanol	328.15	-2.42	-1.67	-0.73	0.75	1.69
110-82-7	cyclohexane	67-56-1	methanol	308.15	-1.67	-1.57	-0.95	0.1	0.72
110-82-7	cyclohexane	67-56-1	methanol	318.15	-1.67	-1.62	-0.84	0.05	0.83
110-82-7	cyclohexane	67-56-1	methanol	333.15	-1.56	-1.7	-0.68	0.14	0.88
110-82-7	cyclohexane	67-56-1	methanol	293.15	-1.36	-1.5	-1.12	0.14	0.24
110-82-7	cyclohexane	67-56-1	methanol	313.15	-1.29	-1.6	-0.9	0.31	0.39
110-82-7	cyclohexane	108-87-2	methylcyclohexane	357.35	-4.4	-5.72	-4.27	1.32	0.13
110-82-7	cyclohexane	108-87-2	methylcyclohexane	360.8	-4.22	-5.78	-4.24	1.56	0.02
110-82-7	cyclohexane	108-87-2	methylcyclohexane	359.6	-4.24	-5.76	-4.25	1.52	0.01
110-82-7	cyclohexane	108-87-2	methylcyclohexane	358.4	-4.24	-5.74	-4.26	1.5	0.02
110-82-7	cyclohexane	108-87-2	methylcyclohexane	357.9	-4.24	-5.73	-4.27	1.49	0.03
110-82-7	cyclohexane	108-87-2	methylcyclohexane	357.3	-4.26	-5.72	-4.27	1.46	0.01
110-82-7	cyclohexane	108-87-2	methylcyclohexane	356.8	-4.25	-5.72	-4.28	1.47	0.03
110-82-7	cyclohexane	108-87-2	methylcyclohexane	356.3	-4.27	-5.71	-4.28	1.44	0.01

Table C.1: ΔG_{solv} for binary systems (kcal/mol).

solvent		solute		T (K)	ΔG^{ref}_{solv}	$\Delta G^{calc,1}_{solv}$	$\Delta G^{calc,2}_{solv}$	$\Delta G^{calc,1}_{solv}$-ΔG^{ref}_{solv}	$\Delta G^{calc,2}_{solv}$-ΔG^{ref}_{solv}
110-82-7	cyclohexane	108-87-2	methylcyclohexane	355.8	-4.27	-5.7	-4.29	1.43	0.02
110-82-7	cyclohexane	108-87-2	methylcyclohexane	355.5	-4.25	-5.7	-4.29	1.45	0.04
110-82-7	cyclohexane	108-87-2	methylcyclohexane	355.1	-4.26	-5.69	-4.29	1.43	0.03
110-82-7	cyclohexane	108-87-2	methylcyclohexane	354.8	-4.29	-5.68	-4.3	1.39	0.01
110-82-7	cyclohexane	108-87-2	methylcyclohexane	354.5	-4.28	-5.68	-4.3	1.4	0.02
110-82-7	cyclohexane	108-87-2	methylcyclohexane	354.4	-4.3	-5.68	-4.3	1.38	0
110-82-7	cyclohexane	96-37-7	methylcyclopentane	352.83	-3.69	-4.83	-3.7	1.14	0.01
110-82-7	cyclohexane	96-37-7	methylcyclopentane	352.62	-3.69	-4.82	-3.7	1.13	0.01
110-82-7	cyclohexane	96-37-7	methylcyclopentane	351.36	-3.7	-4.81	-3.71	1.11	0.01
110-82-7	cyclohexane	109-99-9	tetrahydrofuran	303.15	-3.87	-3.88	-3.8	0.01	0.07
110-82-7	cyclohexane	109-99-9	tetrahydrofuran	303.15	-3.86	-3.88	-3.8	0.02	0.06
110-82-7	cyclohexane	109-99-9	tetrahydrofuran	303.15	-3.85	-3.88	-3.8	0.03	0.05
110-82-7	cyclohexane	109-99-9	tetrahydrofuran	303.15	-3.85	-3.88	-3.8	0.03	0.05
110-82-7	cyclohexane	109-99-9	tetrahydrofuran	313.15	-3.74	-4.01	-3.7	0.27	0.04
110-82-7	cyclohexane	109-99-9	tetrahydrofuran	313.15	-3.73	-4.01	-3.7	0.28	0.03
110-82-7	cyclohexane	109-99-9	tetrahydrofuran	323.15	-3.6	-4.14	-3.6	0.54	0
110-82-7	cyclohexane	109-99-9	tetrahydrofuran	323.15	-3.6	-4.14	-3.6	0.54	0
110-82-7	cyclohexane	109-99-9	tetrahydrofuran	313.15	-3.66	-4.01	-3.7	0.35	0.04
110-82-7	cyclohexane	109-99-9	tetrahydrofuran	313.15	-3.67	-4.01	-3.7	0.34	0.03
110-82-7	cyclohexane	109-99-9	tetrahydrofuran	313.15	-3.65	-4.01	-3.7	0.36	0.05
110-82-7	cyclohexane	109-99-9	tetrahydrofuran	333.15	-3.44	-4.27	-3.5	0.83	0.06
110-82-7	cyclohexane	109-99-9	tetrahydrofuran	351.31	-3.29	-4.5	-3.33	1.21	0.04
110-82-7	cyclohexane	109-99-9	tetrahydrofuran	313.15	-3.63	-4.01	-3.7	0.38	0.07
110-82-7	cyclohexane	109-99-9	tetrahydrofuran	333.15	-3.44	-4.27	-3.5	0.83	0.06
110-82-7	cyclohexane	7732-18-5	water	303.25	-0.78	-0.59	1.73	0.19	2.51
110-82-7	cyclohexane	7732-18-5	water	293.15	-0.88	-0.57	1.61	0.3	2.49
110-82-7	cyclohexane	7732-18-5	water	298.15	-0.58	-0.58	1.67	0	2.25
110-82-7	cyclohexane	7732-18-5	water	313.15	-0.65	-0.61	1.84	0.03	2.48
110-82-7	cyclohexane	7732-18-5	water	313.15	-0.67	-0.61	1.84	0.06	2.51
110-82-7	cyclohexane	7732-18-5	water	283.15	-0.97	-0.55	1.5	0.42	2.47
110-82-7	cyclohexane	7732-18-5	water	293.15	-0.99	-0.57	1.61	0.42	2.6
110-82-7	cyclohexane	7732-18-5	water	303.15	-0.96	-0.59	1.73	0.37	2.68
110-82-7	cyclohexane	7732-18-5	water	298.15	-0.81	-0.58	1.67	0.23	2.48
110-82-7	cyclohexane	7732-18-5	water	298.15	-0.37	-0.58	1.67	0.21	2.04
110-82-7	cyclohexane	7732-18-5	water	293.15	-0.88	-0.57	1.61	0.31	2.49
110-82-7	cyclohexane	7732-18-5	water	298.15	-0.49	-0.58	1.67	0.09	2.16
110-82-7	cyclohexane	7732-18-5	water	293.15	-0.86	-0.57	1.61	0.29	2.48
110-82-7	cyclohexane	7732-18-5	water	298.15	-0.47	-0.58	1.67	0.11	2.14
110-82-7	cyclohexane	7732-18-5	water	283.15	-0.58	-0.55	1.5	0.03	2.08
110-82-7	cyclohexane	7732-18-5	water	288.15	-0.55	-0.56	1.55	0.01	2.1
110-82-7	cyclohexane	7732-18-5	water	293.15	-0.57	-0.57	1.61	0	2.18
110-82-7	cyclohexane	7732-18-5	water	298.15	-0.51	-0.58	1.67	0.07	2.18
110-82-7	cyclohexane	7732-18-5	water	303.15	-0.54	-0.59	1.73	0.06	2.26
110-82-7	cyclohexane	7732-18-5	water	308.15	-0.48	-0.6	1.78	0.12	2.27
110-82-7	cyclohexane	7732-18-5	water	313.15	-0.41	-0.61	1.84	0.2	2.25
110-82-7	cyclohexane	7732-18-5	water	287.15	-0.67	-0.56	1.54	0.11	2.22
110-82-7	cyclohexane	7732-18-5	water	292.15	-0.91	-0.57	1.6	0.34	2.51
110-82-7	cyclohexane	7732-18-5	water	301.65	-0.85	-0.59	1.71	0.26	2.56
110-82-7	cyclohexane	7732-18-5	water	305.65	-0.9	-0.6	1.75	0.31	2.66
110-82-7	cyclohexane	7732-18-5	water	288.15	-0.74	-0.56	1.55	0.18	2.3
110-82-7	cyclohexane	7732-18-5	water	298.15	-0.54	-0.58	1.67	0.04	2.21
110-82-7	cyclohexane	7732-18-5	water	303.15	-0.47	-0.59	1.73	0.13	2.19
124-18-5	decane	106-98-9	1-butene	298.15	-2.42	-2.2	-2.26	0.22	0.16
124-18-5	decane	78-78-4	2-methylbutane	303.15	-2.89	-2.98	-2.97	0.09	0.08
124-18-5	decane	78-78-4	2-methylbutane	333.15	-2.64	-3.27	-2.7	0.63	0.06
124-18-5	decane	78-78-4	2-methylbutane	303.15	-2.89	-2.98	-2.97	0.09	0.08
124-18-5	decane	107-83-5	2-methylpentane	298.15	-3.66	-3.59	-3.67	0.07	0.01
124-18-5	decane	107-83-5	2-methylpentane	303.15	-3.57	-3.65	-3.62	0.08	0.05
124-18-5	decane	107-83-5	2-methylpentane	333.15	-3.26	-4.01	-3.31	0.75	0.05
124-18-5	decane	107-83-5	2-methylpentane	303.65	-3.59	-3.65	-3.61	0.06	0.02
124-18-5	decane	107-83-5	2-methylpentane	298.15	-3.62	-3.59	-3.67	0.03	0.05
124-18-5	decane	75-28-5	2-methylpropane	298.15	-2.23	-2.11	-2.26	0.12	0.03
124-18-5	decane	96-14-0	3-methylpentane	303.15	-3.64	-3.76	-3.69	0.12	0.05
124-18-5	decane	96-14-0	3-methylpentane	333.15	-3.34	-4.13	-3.38	0.79	0.04
124-18-5	decane	96-14-0	3-methylpentane	303.65	-3.67	-3.76	-3.68	0.09	0.01
124-18-5	decane	110-82-7	cyclohexane	303.15	-4.06	-4.22	-4.1	0.16	0.04
124-18-5	decane	110-82-7	cyclohexane	298.15	-4.11	-4.15	-4.16	0.04	0.05

Table C.1: ΔG_{solv} for binary systems (kcal/mol).

solvent		solute		T (K)	ΔG^{ref}_{solv}	$\Delta G^{calc,1}_{solv}$	$\Delta G^{calc,2}_{solv}$	$\Delta G^{calc,1}_{solv}$-ΔG^{ref}_{solv}	$\Delta G^{calc,2}_{solv}$-ΔG^{ref}_{solv}
124-18-5	decane	110-82-7	cyclohexane	298.15	-4.14	-4.15	-4.16	0.01	0.02
124-18-5	decane	110-82-7	cyclohexane	303.15	-4.06	-4.22	-4.1	0.16	0.04
124-18-5	decane	287-92-3	cyclopentane	303.15	-3.41	-3.56	-3.45	0.15	0.04
124-18-5	decane	287-92-3	cyclopentane	303.15	-3.41	-3.56	-3.45	0.15	0.04
124-18-5	decane	74-84-0	ethane	278.15	-1.01	-0.82	-1.14	0.19	0.13
124-18-5	decane	74-84-0	ethane	293.15	-0.9	-0.86	-1.06	0.03	0.16
124-18-5	decane	74-84-0	ethane	303.15	-0.85	-0.89	-1.02	0.04	0.17
124-18-5	decane	74-84-0	ethane	323.15	-0.74	-0.95	-0.9	0.21	0.16
124-18-5	decane	74-84-0	ethane	298.15	-0.89	-0.88	-1.03	0.01	0.15
124-18-5	decane	64-17-5	ethanol	433.15	-1.5	-3.15	-0.36	1.65	1.14
124-18-5	decane	64-17-5	ethanol	333.15	-1.94	-2.42	-1.54	0.48	0.4
124-18-5	decane	64-17-5	ethanol	343.15	-1.71	-2.49	-1.41	0.78	0.3
124-18-5	decane	64-17-5	ethanol	306.35	-2.02	-2.23	-1.89	0.21	0.13
124-18-5	decane	64-17-5	ethanol	321.35	-1.89	-2.34	-1.69	0.45	0.2
124-18-5	decane	64-17-5	ethanol	338.65	-1.8	-2.46	-1.47	0.66	0.33
124-18-5	decane	64-17-5	ethanol	357.45	-1.65	-2.6	-1.23	0.95	0.42
124-18-5	decane	64-17-5	ethanol	293.15	-2.09	-2.13	-2.08	0.04	0.01
124-18-5	decane	64-17-5	ethanol	298.15	-2.16	-2.17	-2.01	0.01	0.15
124-18-5	decane	64-17-5	ethanol	298.15	-2.45	-2.17	-2.01	0.28	0.44
124-18-5	decane	74-85-1	ethene	298.15	-0.58	-0.58	-0.61	0.01	0.03
124-18-5	decane	74-85-1	ethene	283.65	-0.44	-0.55	-0.67	0.12	0.24
124-18-5	decane	74-85-1	ethene	292.65	-0.4	-0.57	-0.63	0.18	0.24
124-18-5	decane	74-82-8	methane	298.15	0.24	0.22	-0.99	0.02	1.23
124-18-5	decane	67-56-1	methanol	293.15	-1.49	-1.44	-1.03	0.05	0.46
124-18-5	decane	67-56-1	methanol	293.15	-1.43	-1.44	-1.03	0.01	0.4
124-18-5	decane	108-87-2	methylcyclohexane	303.15	-4.51	-4.73	-4.51	0.22	0
124-18-5	decane	108-87-2	methylcyclohexane	303.15	-4.52	-4.73	-4.51	0.21	0.01
124-18-5	decane	96-37-7	methylcyclopentane	303.15	-3.86	-4.03	-3.9	0.17	0.04
124-18-5	decane	96-37-7	methylcyclopentane	303.15	-3.87	-4.03	-3.9	0.16	0.03
124-18-5	decane	74-98-6	propane	298.15	-1.63	-1.63	-1.74	0	0.11
124-18-5	decane	74-98-6	propane	298.15	-1.7	-1.63	-1.74	0.07	0.04
124-18-5	decane	74-98-6	propane	298.15	-1.65	-1.63	-1.74	0.02	0.09
124-18-5	decane	7732-18-5	water	298.15	-0.49	-0.56	1.7	0.08	2.19
124-18-5	decane	7732-18-5	water	310.93	-0.35	-0.59	1.85	0.23	2.2
112-40-3	dodecane	109-67-1	1-pentene	293.15	-2.97	-2.78	-2.97	0.19	0
112-40-3	dodecane	78-78-4	2-methylbutane	293.15	-2.93	-2.73	-3.01	0.2	0.08
112-40-3	dodecane	107-83-5	2-methylpentane	298.15	-3.52	-3.44	-3.62	0.08	0.1
112-40-3	dodecane	110-82-7	cyclohexane	280.15	-4.25	-3.81	-4.32	0.44	0.07
112-40-3	dodecane	110-82-7	cyclohexane	280.15	-4.24	-3.81	-4.32	0.43	0.08
112-40-3	dodecane	110-82-7	cyclohexane	280.15	-4.24	-3.81	-4.32	0.43	0.08
112-40-3	dodecane	110-82-7	cyclohexane	298.15	-4.04	-4.06	-4.11	0.02	0.07
112-40-3	dodecane	110-82-7	cyclohexane	298.15	-4.04	-4.06	-4.11	0.02	0.07
112-40-3	dodecane	110-82-7	cyclohexane	298.15	-4.02	-4.06	-4.11	0.04	0.09
112-40-3	dodecane	287-92-3	cyclopentane	280.15	-3.55	-3.2	-3.65	0.35	0.1
112-40-3	dodecane	287-92-3	cyclopentane	280.15	-3.54	-3.2	-3.65	0.34	0.11
112-40-3	dodecane	287-92-3	cyclopentane	280.15	-3.54	-3.2	-3.65	0.34	0.11
112-40-3	dodecane	287-92-3	cyclopentane	298.15	-3.37	-3.4	-3.46	0.03	0.09
112-40-3	dodecane	287-92-3	cyclopentane	298.15	-3.37	-3.4	-3.46	0.03	0.09
112-40-3	dodecane	287-92-3	cyclopentane	298.15	-3.37	-3.4	-3.46	0.03	0.09
112-40-3	dodecane	74-84-0	ethane	278.15	-0.94	-0.68	-1.12	0.26	0.18
112-40-3	dodecane	74-84-0	ethane	298.15	-0.84	-0.73	-1.01	0.11	0.17
112-40-3	dodecane	74-84-0	ethane	323.15	-0.73	-0.8	-0.87	0.07	0.15
112-40-3	dodecane	64-17-5	ethanol	293.15	-2.03	-2.03	-2.04	0	0.01
112-40-3	dodecane	74-82-8	methane	298.15	0.32	0.36	-0.97	0.05	1.29
112-40-3	dodecane	67-56-1	methanol	293.15	-1.37	-1.35	-1	0.02	0.37
112-40-3	dodecane	74-98-6	propane	298.15	-1.53	-1.48	-1.71	0.05	0.18
112-40-3	dodecane	74-98-6	propane	308.15	-1.48	-1.53	-1.64	0.05	0.16
112-40-3	dodecane	74-98-6	propane	318.15	-1.44	-1.58	-1.57	0.14	0.13
112-40-3	dodecane	74-98-6	propane	298.15	-1.55	-1.48	-1.71	0.07	0.16
112-40-3	dodecane	74-98-6	propane	323.15	-1.44	-1.61	-1.53	0.17	0.09
112-40-3	dodecane	7732-18-5	water	298.15	-0.44	-0.42	1.72	0.02	2.16
64-17-5	ethanol	107-83-5	2-methylpentane	347.6	-2.5	-3.41	-2.89	0.91	0.39
64-17-5	ethanol	107-83-5	2-methylpentane	345.3	-2.58	-3.39	-2.91	0.81	0.33
64-17-5	ethanol	107-83-5	2-methylpentane	343.1	-2.61	-3.37	-2.93	0.76	0.32
64-17-5	ethanol	107-83-5	2-methylpentane	341.3	-2.67	-3.35	-2.95	0.68	0.28
64-17-5	ethanol	107-83-5	2-methylpentane	338.3	-2.76	-3.32	-2.97	0.56	0.21
64-17-5	ethanol	107-83-5	2-methylpentane	336.8	-2.81	-3.31	-2.99	0.5	0.18

Table C.1: ΔG_{solv} for binary systems (kcal/mol).

solvent		solute		T (K)	ΔG^{ref}_{solv}	$\Delta G^{calc,1}_{solv}$	$\Delta G^{calc,2}_{solv}$	$\Delta G^{calc,1}_{solv}$-ΔG^{ref}_{solv}	$\Delta G^{calc,2}_{solv}$-ΔG^{ref}_{solv}
64-17-5	ethanol	107-83-5	2-methylpentane	334.7	-2.88	-3.29	-3.01	0.41	0.13
64-17-5	ethanol	107-83-5	2-methylpentane	333.3	-2.94	-3.27	-3.02	0.33	0.08
64-17-5	ethanol	107-83-5	2-methylpentane	298.15	-2.96	-2.93	-3.37	0.03	0.41
64-17-5	ethanol	107-83-5	2-methylpentane	298.15	-3.02	-2.93	-3.37	0.09	0.35
64-17-5	ethanol	96-14-0	3-methylpentane	341	-2.68	-3.45	-3.02	0.77	0.34
64-17-5	ethanol	96-14-0	3-methylpentane	337.9	-2.8	-3.42	-3.04	0.62	0.24
64-17-5	ethanol	96-14-0	3-methylpentane	334.9	-2.93	-3.39	-3.07	0.46	0.14
64-17-5	ethanol	75-07-0	acetaldehyde	303.25	-4.13	-2.96	-3.16	1.17	0.97
64-17-5	ethanol	75-07-0	acetaldehyde	333.15	-3.65	-3.26	-2.94	0.39	0.71
64-17-5	ethanol	75-07-0	acetaldehyde	353.15	-3.27	-3.45	-2.8	0.18	0.47
64-17-5	ethanol	110-82-7	cyclohexane	313.55	-3.34	-3.67	-3.69	0.33	0.35
64-17-5	ethanol	110-82-7	cyclohexane	283.15	-3.81	-3.31	-4.02	0.5	0.21
64-17-5	ethanol	110-82-7	cyclohexane	293.15	-3.68	-3.43	-3.9	0.25	0.22
64-17-5	ethanol	110-82-7	cyclohexane	303.15	-3.71	-3.54	-3.79	0.17	0.08
64-17-5	ethanol	110-82-7	cyclohexane	298.15	-3.75	-3.49	-3.85	0.26	0.1
64-17-5	ethanol	110-82-7	cyclohexane	327.21	-3.18	-3.83	-3.55	0.65	0.37
64-17-5	ethanol	110-82-7	cyclohexane	335.05	-3.27	-3.92	-3.47	0.65	0.2
64-17-5	ethanol	110-82-7	cyclohexane	340.04	-3.11	-3.98	-3.42	0.87	0.31
64-17-5	ethanol	110-82-7	cyclohexane	343.25	-3.21	-4.01	-3.39	0.8	0.18
64-17-5	ethanol	110-82-7	cyclohexane	346.05	-3.05	-4.05	-3.36	1	0.31
64-17-5	ethanol	110-82-7	cyclohexane	344.26	-3.17	-4.03	-3.38	0.86	0.21
64-17-5	ethanol	110-82-7	cyclohexane	345.48	-3.11	-4.04	-3.37	0.93	0.26
64-17-5	ethanol	110-82-7	cyclohexane	348.56	-3.05	-4.08	-3.34	1.03	0.29
64-17-5	ethanol	110-82-7	cyclohexane	350.5	-3.11	-4.1	-3.32	0.99	0.21
64-17-5	ethanol	110-82-7	cyclohexane	297.45	-3.41	-3.48	-3.86	0.07	0.45
64-17-5	ethanol	110-82-7	cyclohexane	297.45	-3.36	-3.48	-3.86	0.12	0.5
64-17-5	ethanol	110-82-7	cyclohexane	318.55	-3.19	-3.72	-3.63	0.53	0.44
64-17-5	ethanol	110-82-7	cyclohexane	318.65	-3.21	-3.73	-3.63	0.52	0.42
64-17-5	ethanol	110-82-7	cyclohexane	336.35	-3.05	-3.93	-3.46	0.88	0.41
64-17-5	ethanol	110-82-7	cyclohexane	353.15	-2.9	-4.13	-3.3	1.23	0.4
64-17-5	ethanol	110-82-7	cyclohexane	298.15	-3.52	-3.49	-3.85	0.03	0.33
64-17-5	ethanol	110-82-7	cyclohexane	313.15	-3.31	-3.66	-3.69	0.35	0.38
64-17-5	ethanol	110-82-7	cyclohexane	298.15	-3.45	-3.49	-3.85	0.04	0.4
64-17-5	ethanol	110-82-7	cyclohexane	351.31	-3	-4.11	-3.31	1.11	0.31
64-17-5	ethanol	110-82-7	cyclohexane	412.86	-2.44	-4.83	-2.76	2.39	0.32
64-17-5	ethanol	110-82-7	cyclohexane	423.19	-2.37	-4.95	-2.66	2.58	0.29
64-17-5	ethanol	110-82-7	cyclohexane	318.15	-3.25	-3.72	-3.64	0.47	0.39
64-17-5	ethanol	110-82-7	cyclohexane	323.15	-3.22	-3.78	-3.59	0.56	0.37
64-17-5	ethanol	110-82-7	cyclohexane	298.15	-3.47	-3.49	-3.85	0.02	0.38
64-17-5	ethanol	110-82-7	cyclohexane	298.15	-3.41	-3.49	-3.85	0.08	0.44
64-17-5	ethanol	110-82-7	cyclohexane	298.15	-3.46	-3.49	-3.85	0.03	0.39
64-17-5	ethanol	110-82-7	cyclohexane	323.15	-3.34	-3.78	-3.59	0.44	0.25
64-17-5	ethanol	110-82-7	cyclohexane	343.15	-3.09	-4.01	-3.39	0.92	0.3
64-17-5	ethanol	110-82-7	cyclohexane	363.15	-2.9	-4.25	-3.2	1.35	0.3
64-17-5	ethanol	110-82-7	cyclohexane	383.15	-2.74	-4.48	-3.02	1.74	0.28
64-17-5	ethanol	110-82-7	cyclohexane	403.15	-2.59	-4.71	-2.84	2.12	0.25
64-17-5	ethanol	110-82-7	cyclohexane	351.8	-2.93	-4.11	-3.31	1.18	0.38
64-17-5	ethanol	287-92-3	cyclopentane	313.15	-2.78	-3.08	-3.12	0.3	0.34
64-17-5	ethanol	74-82-8	methane	293.15	0.36	0.35	-0.86	0	1.22
64-17-5	ethanol	67-56-1	methanol	349.35	-3.89	-5.29	-3.92	1.4	0.03
64-17-5	ethanol	67-56-1	methanol	347.75	-3.93	-5.26	-3.94	1.33	0.01
64-17-5	ethanol	67-56-1	methanol	313.05	-4.44	-4.74	-4.4	0.3	0.04
64-17-5	ethanol	67-56-1	methanol	350.86	-3.83	-5.31	-3.9	1.48	0.07
64-17-5	ethanol	67-56-1	methanol	349.23	-3.87	-5.29	-3.92	1.42	0.05
64-17-5	ethanol	67-56-1	methanol	347.8	-3.9	-5.26	-3.94	1.36	0.04
64-17-5	ethanol	67-56-1	methanol	347.64	-3.9	-5.26	-3.94	1.36	0.04
64-17-5	ethanol	67-56-1	methanol	347.59	-3.9	-5.26	-3.94	1.36	0.04
64-17-5	ethanol	67-56-1	methanol	351.35	-3.74	-5.32	-3.89	1.58	0.15
64-17-5	ethanol	67-56-1	methanol	350.25	-4.01	-5.3	-3.91	1.29	0.1
64-17-5	ethanol	67-56-1	methanol	349.75	-4.04	-5.29	-3.92	1.25	0.12
64-17-5	ethanol	67-56-1	methanol	373.15	-3.68	-5.65	-3.62	1.97	0.06
64-17-5	ethanol	67-56-1	methanol	373.15	-3.65	-5.65	-3.62	2	0.03
64-17-5	ethanol	67-56-1	methanol	350.15	-3.92	-5.3	-3.91	1.38	0.01
64-17-5	ethanol	67-56-1	methanol	348.95	-3.94	-5.28	-3.93	1.34	0.01
64-17-5	ethanol	67-56-1	methanol	347.15	-3.96	-5.25	-3.95	1.29	0.01
64-17-5	ethanol	67-56-1	methanol	345.45	-4	-5.23	-3.97	1.23	0.03
64-17-5	ethanol	67-56-1	methanol	350.71	-3.94	-5.31	-3.9	1.37	0.04

Table C.1: ΔG_{solv} for binary systems (kcal/mol).

solvent		solute		T (K)	ΔG^{ref}_{solv}	$\Delta G^{calc,1}_{solv}$	$\Delta G^{calc,2}_{solv}$	$\Delta G^{calc,1}_{solv}$-ΔG^{ref}_{solv}	$\Delta G^{calc,2}_{solv}$-ΔG^{ref}_{solv}
64-17-5	ethanol	67-56-1	methanol	349.88	-3.95	-5.29	-3.91	1.34	0.04
64-17-5	ethanol	67-56-1	methanol	348.98	-3.97	-5.28	-3.92	1.31	0.05
64-17-5	ethanol	67-56-1	methanol	347.57	-3.99	-5.26	-3.94	1.27	0.05
64-17-5	ethanol	67-56-1	methanol	350.26	-3.94	-5.3	-3.91	1.36	0.03
64-17-5	ethanol	67-56-1	methanol	349.63	-3.95	-5.29	-3.92	1.34	0.03
64-17-5	ethanol	67-56-1	methanol	348.36	-3.96	-5.27	-3.93	1.31	0.03
64-17-5	ethanol	67-56-1	methanol	347.68	-3.97	-5.26	-3.94	1.29	0.03
64-17-5	ethanol	67-56-1	methanol	350.45	-3.95	-5.3	-3.91	1.35	0.04
64-17-5	ethanol	67-56-1	methanol	346.15	-3.97	-5.24	-3.96	1.27	0.01
64-17-5	ethanol	67-56-1	methanol	348.03	-4	-5.27	-3.94	1.27	0.06
64-17-5	ethanol	67-56-1	methanol	346.73	-4.01	-5.25	-3.95	1.24	0.06
64-17-5	ethanol	67-56-1	methanol	345.87	-4.01	-5.23	-3.97	1.22	0.04
64-17-5	ethanol	67-56-1	methanol	345.38	-4.02	-5.23	-3.97	1.21	0.05
64-17-5	ethanol	67-56-1	methanol	345.05	-4.02	-5.22	-3.98	1.2	0.04
64-17-5	ethanol	67-56-1	methanol	345.45	-4.01	-5.23	-3.97	1.22	0.04
64-17-5	ethanol	67-56-1	methanol	344.85	-4.01	-5.22	-3.98	1.21	0.03
64-17-5	ethanol	67-56-1	methanol	350.55	-3.95	-5.31	-3.9	1.36	0.05
64-17-5	ethanol	67-56-1	methanol	349.85	-3.96	-5.29	-3.91	1.33	0.05
64-17-5	ethanol	67-56-1	methanol	349.05	-3.98	-5.28	-3.92	1.3	0.06
64-17-5	ethanol	67-56-1	methanol	381.05	-3.58	-5.77	-3.52	2.19	0.06
64-17-5	ethanol	67-56-1	methanol	380.35	-3.58	-5.76	-3.52	2.18	0.06
64-17-5	ethanol	67-56-1	methanol	379.65	-3.59	-5.75	-3.53	2.16	0.06
64-17-5	ethanol	67-56-1	methanol	378.95	-3.6	-5.73	-3.54	2.13	0.06
64-17-5	ethanol	67-56-1	methanol	378.25	-3.61	-5.72	-3.55	2.11	0.06
64-17-5	ethanol	67-56-1	methanol	377.45	-3.61	-5.71	-3.56	2.1	0.05
64-17-5	ethanol	67-56-1	methanol	376.75	-3.62	-5.7	-3.57	2.08	0.05
64-17-5	ethanol	67-56-1	methanol	376.05	-3.63	-5.69	-3.58	2.06	0.05
64-17-5	ethanol	67-56-1	methanol	375.35	-3.63	-5.68	-3.59	2.05	0.04
64-17-5	ethanol	67-56-1	methanol	349.1	-3.96	-5.28	-3.92	1.32	0.04
64-17-5	ethanol	67-56-1	methanol	348.7	-3.96	-5.28	-3.93	1.32	0.03
64-17-5	ethanol	67-56-1	methanol	347.8	-3.97	-5.26	-3.94	1.29	0.03
64-17-5	ethanol	67-56-1	methanol	346.2	-3.99	-5.24	-3.96	1.25	0.03
64-17-5	ethanol	67-56-1	methanol	345.6	-4	-5.23	-3.97	1.23	0.03
64-17-5	ethanol	67-56-1	methanol	344.4	-4.01	-5.21	-3.98	1.2	0.03
64-17-5	ethanol	67-56-1	methanol	351.32	-3.92	-5.32	-3.89	1.4	0.03
64-17-5	ethanol	67-56-1	methanol	381.74	-3.58	-5.78	-3.51	2.2	0.07
64-17-5	ethanol	67-56-1	methanol	381.89	-3.58	-5.78	-3.5	2.2	0.08
64-17-5	ethanol	67-56-1	methanol	382.13	-3.58	-5.78	-3.5	2.2	0.08
64-17-5	ethanol	67-56-1	methanol	423.97	-3.12	-6.42	-2.97	3.3	0.15
64-17-5	ethanol	108-87-2	methylcyclohexane	303.15	-3.89	-3.99	-4.15	0.1	0.26
64-17-5	ethanol	108-87-2	methylcyclohexane	308.15	-3.85	-4.05	-4.1	0.2	0.25
64-17-5	ethanol	108-87-2	methylcyclohexane	348.35	-3.46	-4.58	-3.67	1.12	0.21
64-17-5	ethanol	108-87-2	methylcyclohexane	349.75	-3.33	-4.6	-3.66	1.27	0.33
64-17-5	ethanol	108-87-2	methylcyclohexane	351.55	-3.24	-4.62	-3.64	1.38	0.4
64-17-5	ethanol	108-87-2	methylcyclohexane	386.6	-2.84	-5.08	-3.31	2.24	0.47
64-17-5	ethanol	108-87-2	methylcyclohexane	401.66	-2.78	-5.28	-3.18	2.5	0.4
64-17-5	ethanol	108-87-2	methylcyclohexane	412.86	-2.78	-5.43	-3.07	2.65	0.29
64-17-5	ethanol	108-87-2	methylcyclohexane	423.97	-2.72	-5.58	-2.97	2.86	0.25
64-17-5	ethanol	108-87-2	methylcyclohexane	423.97	-2.72	-5.58	-2.97	2.86	0.25
64-17-5	ethanol	108-87-2	methylcyclohexane	313.15	-3.61	-4.12	-4.04	0.51	0.43
64-17-5	ethanol	108-87-2	methylcyclohexane	333.15	-3.4	-4.38	-3.83	0.98	0.43
64-17-5	ethanol	96-37-7	methylcyclopentane	349.25	-2.99	-3.91	-3.16	0.92	0.17
64-17-5	ethanol	96-37-7	methylcyclopentane	313.15	-3.16	-3.5	-3.51	0.34	0.35
64-17-5	ethanol	109-99-9	tetrahydrofuran	346.35	-3.84	-5.13	-4.13	1.29	0.29
64-17-5	ethanol	109-99-9	tetrahydrofuran	318.85	-3.83	-4.73	-4.4	0.9	0.57
64-17-5	ethanol	109-99-9	tetrahydrofuran	350.85	-3.82	-5.2	-4.09	1.38	0.27
64-17-5	ethanol	109-99-9	tetrahydrofuran	347.75	-3.79	-5.15	-4.12	1.36	0.33
64-17-5	ethanol	109-99-9	tetrahydrofuran	317.45	-3.95	-4.71	-4.41	0.76	0.46
64-17-5	ethanol	109-99-9	tetrahydrofuran	314.75	-4	-4.67	-4.44	0.67	0.44
64-17-5	ethanol	109-99-9	tetrahydrofuran	333.55	-3.83	-4.94	-4.26	1.11	0.43
64-17-5	ethanol	109-99-9	tetrahydrofuran	332.25	-3.87	-4.92	-4.27	1.05	0.4
64-17-5	ethanol	109-99-9	tetrahydrofuran	329.95	-3.91	-4.89	-4.29	0.98	0.38
64-17-5	ethanol	109-99-9	tetrahydrofuran	350.55	-3.75	-5.2	-4.1	1.45	0.35
64-17-5	ethanol	109-99-9	tetrahydrofuran	349.35	-3.73	-5.18	-4.11	1.45	0.38
64-17-5	ethanol	109-99-9	tetrahydrofuran	348.5	-3.74	-5.17	-4.11	1.43	0.37
64-17-5	ethanol	109-99-9	tetrahydrofuran	346.3	-3.81	-5.13	-4.13	1.32	0.32
64-17-5	ethanol	109-99-9	tetrahydrofuran	348.85	-3.75	-5.17	-4.11	1.42	0.36

Table C.1: ΔG_{solv} for binary systems (kcal/mol).

solvent		solute		T (K)	ΔG^{ref}_{solv}	$\Delta G^{calc,1}_{solv}$	$\Delta G^{calc,2}_{solv}$	$\Delta G^{calc,1}_{solv}$-ΔG^{ref}_{solv}	$\Delta G^{calc,2}_{solv}$-ΔG^{ref}_{solv}
64-17-5	ethanol	109-99-9	tetrahydrofuran	349.85	-3.77	-5.19	-4.1	1.42	0.33
64-17-5	ethanol	109-99-9	tetrahydrofuran	348.35	-3.74	-5.16	-4.12	1.42	0.38
64-17-5	ethanol	109-99-9	tetrahydrofuran	347.05	-3.76	-5.14	-4.13	1.38	0.37
64-17-5	ethanol	109-99-9	tetrahydrofuran	345.85	-3.8	-5.13	-4.14	1.33	0.34
64-17-5	ethanol	109-99-9	tetrahydrofuran	344.85	-3.83	-5.11	-4.15	1.28	0.32
64-17-5	ethanol	109-99-9	tetrahydrofuran	298.15	-4.09	-4.42	-4.61	0.33	0.52
64-17-5	ethanol	7732-18-5	water	349.25	-4.33	-6.44	-4.3	2.11	0.03
64-17-5	ethanol	7732-18-5	water	323.65	-4.79	-5.96	-4.72	1.17	0.07
64-17-5	ethanol	7732-18-5	water	323.65	-4.71	-5.96	-4.72	1.25	0.01
64-17-5	ethanol	7732-18-5	water	333.75	-4.54	-6.15	-4.55	1.61	0.01
64-17-5	ethanol	7732-18-5	water	313.15	-4.9	-5.77	-4.89	0.87	0.01
64-17-5	ethanol	7732-18-5	water	323.15	-4.72	-5.95	-4.72	1.23	0
64-17-5	ethanol	7732-18-5	water	323.15	-4.67	-5.95	-4.72	1.28	0.05
64-17-5	ethanol	7732-18-5	water	333.15	-4.54	-6.14	-4.56	1.6	0.02
64-17-5	ethanol	7732-18-5	water	333.15	-4.54	-6.14	-4.56	1.6	0.02
64-17-5	ethanol	7732-18-5	water	333.15	-4.54	-6.14	-4.56	1.6	0.02
64-17-5	ethanol	7732-18-5	water	298.15	-5.05	-5.49	-5.15	0.44	0.1
64-17-5	ethanol	7732-18-5	water	327.96	-4.63	-6.04	-4.64	1.41	0.01
64-17-5	ethanol	7732-18-5	water	347.94	-4.34	-6.41	-4.32	2.07	0.02
64-17-5	ethanol	7732-18-5	water	338.15	-4.57	-6.23	-4.48	1.66	0.09
64-17-5	ethanol	7732-18-5	water	348.15	-4.39	-6.42	-4.31	2.03	0.08
64-17-5	ethanol	7732-18-5	water	323.15	-4.77	-5.95	-4.72	1.18	0.05
64-17-5	ethanol	7732-18-5	water	323.15	-4.72	-5.95	-4.72	1.23	0
64-17-5	ethanol	7732-18-5	water	323.15	-4.73	-5.95	-4.72	1.22	0.01
64-17-5	ethanol	7732-18-5	water	323.15	-4.7	-5.95	-4.72	1.25	0.02
64-17-5	ethanol	7732-18-5	water	298.14	-5.14	-5.49	-5.15	0.35	0.01
64-17-5	ethanol	7732-18-5	water	313.15	-4.93	-5.77	-4.89	0.84	0.04
64-17-5	ethanol	7732-18-5	water	313.15	-4.88	-5.77	-4.89	0.89	0.01
64-17-5	ethanol	7732-18-5	water	313.15	-4.84	-5.77	-4.89	0.93	0.05
64-17-5	ethanol	7732-18-5	water	328.15	-4.65	-6.05	-4.64	1.4	0.01
64-17-5	ethanol	7732-18-5	water	328.15	-4.6	-6.05	-4.64	1.45	0.04
64-17-5	ethanol	7732-18-5	water	343.15	-4.38	-6.32	-4.39	1.94	0.01
64-17-5	ethanol	7732-18-5	water	343.15	-4.37	-6.32	-4.39	1.95	0.02
64-17-5	ethanol	7732-18-5	water	323.15	-4.75	-5.95	-4.72	1.2	0.03
64-17-5	ethanol	7732-18-5	water	323.15	-4.74	-5.95	-4.72	1.21	0.02
64-17-5	ethanol	7732-18-5	water	323.15	-4.74	-5.95	-4.72	1.21	0.02
64-17-5	ethanol	7732-18-5	water	323.15	-4.73	-5.95	-4.72	1.22	0.01
64-17-5	ethanol	7732-18-5	water	323.15	-4.73	-5.95	-4.72	1.22	0.01
64-17-5	ethanol	7732-18-5	water	323.15	-4.73	-5.95	-4.72	1.22	0.01
64-17-5	ethanol	7732-18-5	water	323.15	-4.72	-5.95	-4.72	1.23	0
64-17-5	ethanol	7732-18-5	water	323.15	-4.72	-5.95	-4.72	1.23	0
64-17-5	ethanol	7732-18-5	water	323.15	-4.71	-5.95	-4.72	1.24	0.01
64-17-5	ethanol	7732-18-5	water	323.15	-4.71	-5.95	-4.72	1.24	0.01
64-17-5	ethanol	7732-18-5	water	323.15	-4.69	-5.95	-4.72	1.26	0.03
64-17-5	ethanol	7732-18-5	water	323.15	-4.69	-5.95	-4.72	1.26	0.03
64-17-5	ethanol	7732-18-5	water	323.15	-4.68	-5.95	-4.72	1.27	0.04
64-17-5	ethanol	7732-18-5	water	328.15	-4.67	-6.05	-4.64	1.38	0.03
64-17-5	ethanol	7732-18-5	water	328.15	-4.66	-6.05	-4.64	1.39	0.02
64-17-5	ethanol	7732-18-5	water	328.15	-4.66	-6.05	-4.64	1.39	0.02
64-17-5	ethanol	7732-18-5	water	328.15	-4.65	-6.05	-4.64	1.4	0.01
64-17-5	ethanol	7732-18-5	water	328.15	-4.64	-6.05	-4.64	1.41	0
64-17-5	ethanol	7732-18-5	water	328.15	-4.64	-6.05	-4.64	1.41	0
64-17-5	ethanol	7732-18-5	water	328.15	-4.63	-6.05	-4.64	1.42	0.01
64-17-5	ethanol	7732-18-5	water	328.15	-4.62	-6.05	-4.64	1.43	0.02
64-17-5	ethanol	7732-18-5	water	328.15	-4.61	-6.05	-4.64	1.44	0.03
64-17-5	ethanol	7732-18-5	water	328.15	-4.6	-6.05	-4.64	1.45	0.04
64-17-5	ethanol	7732-18-5	water	333.15	-4.59	-6.14	-4.56	1.55	0.03
64-17-5	ethanol	7732-18-5	water	333.15	-4.58	-6.14	-4.56	1.56	0.02
64-17-5	ethanol	7732-18-5	water	333.15	-4.57	-6.14	-4.56	1.57	0.01
64-17-5	ethanol	7732-18-5	water	333.15	-4.57	-6.14	-4.56	1.57	0.01
64-17-5	ethanol	7732-18-5	water	333.15	-4.56	-6.14	-4.56	1.58	0
64-17-5	ethanol	7732-18-5	water	333.15	-4.55	-6.14	-4.56	1.59	0.01
64-17-5	ethanol	7732-18-5	water	333.15	-4.55	-6.14	-4.56	1.59	0.01
64-17-5	ethanol	7732-18-5	water	333.15	-4.54	-6.14	-4.56	1.6	0.02
64-17-5	ethanol	7732-18-5	water	333.15	-4.54	-6.14	-4.56	1.6	0.02
64-17-5	ethanol	7732-18-5	water	333.15	-4.53	-6.14	-4.56	1.61	0.03
64-17-5	ethanol	7732-18-5	water	333.15	-4.53	-6.14	-4.56	1.61	0.03

Table C.1: ΔG_{solv} for binary systems (kcal/mol).

solvent		solute		T (K)	ΔG^{ref}_{solv}	$\Delta G^{calc,1}_{solv}$	$\Delta G^{calc,2}_{solv}$	$\Delta G^{calc,1}_{solv}$-ΔG^{ref}_{solv}	$\Delta G^{calc,2}_{solv}$-ΔG^{ref}_{solv}
64-17-5	ethanol	7732-18-5	water	333.15	-4.52	-6.14	-4.56	1.62	0.04
64-17-5	ethanol	7732-18-5	water	351.33	-4.27	-6.47	-4.26	2.2	0.01
64-17-5	ethanol	7732-18-5	water	351.37	-4.24	-6.47	-4.26	2.23	0.02
64-17-5	ethanol	7732-18-5	water	315.35	-4.88	-5.81	-4.86	0.93	0.02
64-17-5	ethanol	7732-18-5	water	315.25	-4.8	-5.81	-4.86	1.01	0.06
64-17-5	ethanol	7732-18-5	water	329.25	-4.49	-6.07	-4.62	1.58	0.13
64-17-5	ethanol	7732-18-5	water	329.3	-4.52	-6.07	-4.62	1.55	0.1
64-17-5	ethanol	7732-18-5	water	329.35	-4.41	-6.07	-4.62	1.66	0.21
64-17-5	ethanol	7732-18-5	water	335.7	-4.42	-6.19	-4.52	1.77	0.1
64-17-5	ethanol	7732-18-5	water	351.2	-4.11	-6.47	-4.26	2.36	0.15
64-17-5	ethanol	7732-18-5	water	355.6	-3.72	-6.55	-4.19	2.83	0.47
64-17-5	ethanol	7732-18-5	water	351.95	-4.35	-6.49	-4.25	2.14	0.1
64-17-5	ethanol	7732-18-5	water	351.45	-4.31	-6.48	-4.26	2.17	0.05
64-17-5	ethanol	7732-18-5	water	351.35	-4.3	-6.47	-4.26	2.17	0.04
64-17-5	ethanol	7732-18-5	water	351.32	-4.28	-6.47	-4.26	2.19	0.02
64-17-5	ethanol	7732-18-5	water	351.31	-4.28	-6.47	-4.26	2.19	0.02
64-17-5	ethanol	7732-18-5	water	351.34	-4.28	-6.47	-4.26	2.19	0.02
64-17-5	ethanol	7732-18-5	water	351.35	-4.25	-6.47	-4.26	2.22	0.01
64-17-5	ethanol	7732-18-5	water	351.39	-4.25	-6.47	-4.26	2.22	0.01
64-17-5	ethanol	7732-18-5	water	350.85	-4.27	-6.46	-4.27	2.19	0
64-17-5	ethanol	7732-18-5	water	341.25	-4.46	-6.29	-4.42	1.83	0.04
64-17-5	ethanol	7732-18-5	water	341.19	-4.45	-6.29	-4.43	1.84	0.02
64-17-5	ethanol	7732-18-5	water	341.2	-4.41	-6.29	-4.43	1.88	0.02
64-17-5	ethanol	7732-18-5	water	341.25	-4.41	-6.29	-4.42	1.88	0.01
64-17-5	ethanol	7732-18-5	water	351.49	-4.31	-6.48	-4.26	2.17	0.05
64-17-5	ethanol	7732-18-5	water	351.42	-4.28	-6.48	-4.26	2.2	0.02
64-17-5	ethanol	7732-18-5	water	351.45	-4.21	-6.48	-4.26	2.27	0.05
64-17-5	ethanol	7732-18-5	water	351.47	-4.18	-6.48	-4.26	2.3	0.08
64-17-5	ethanol	7732-18-5	water	351.66	-4.33	-6.48	-4.26	2.15	0.07
64-17-5	ethanol	7732-18-5	water	351.31	-4.29	-6.47	-4.26	2.18	0.03
64-17-5	ethanol	7732-18-5	water	351.39	-4.25	-6.47	-4.26	2.22	0.01
64-17-5	ethanol	7732-18-5	water	351.41	-4.25	-6.48	-4.26	2.23	0.01
64-17-5	ethanol	7732-18-5	water	351.4	-4.3	-6.47	-4.26	2.17	0.04
64-17-5	ethanol	7732-18-5	water	350.15	-4.41	-6.45	-4.28	2.04	0.13
64-17-5	ethanol	7732-18-5	water	350.15	-4.39	-6.45	-4.28	2.06	0.11
64-17-5	ethanol	7732-18-5	water	350.15	-4.4	-6.45	-4.28	2.05	0.12
64-17-5	ethanol	7732-18-5	water	350.15	-4.39	-6.45	-4.28	2.06	0.11
64-17-5	ethanol	7732-18-5	water	350.15	-4.39	-6.45	-4.28	2.06	0.11
64-17-5	ethanol	7732-18-5	water	351.27	-4.28	-6.47	-4.26	2.19	0.02
64-17-5	ethanol	7732-18-5	water	351.31	-4.25	-6.47	-4.26	2.22	0.01
64-17-5	ethanol	7732-18-5	water	351.45	-4.26	-6.48	-4.26	2.22	0
64-17-5	ethanol	7732-18-5	water	351.55	-4.28	-6.48	-4.26	2.2	0.02
64-17-5	ethanol	7732-18-5	water	351.45	-4.31	-6.48	-4.26	2.17	0.05
64-17-5	ethanol	7732-18-5	water	351.45	-4.27	-6.48	-4.26	2.21	0.01
64-17-5	ethanol	7732-18-5	water	351.99	-4.32	-6.49	-4.25	2.17	0.07
64-17-5	ethanol	7732-18-5	water	351.99	-4.33	-6.49	-4.25	2.16	0.08
64-17-5	ethanol	7732-18-5	water	351.45	-4.2	-6.48	-4.26	2.28	0.06
64-17-5	ethanol	7732-18-5	water	351.35	-4.18	-6.47	-4.26	2.29	0.08
64-17-5	ethanol	7732-18-5	water	307.54	-5.01	-5.67	-4.99	0.66	0.02
64-17-5	ethanol	7732-18-5	water	307.56	-4.99	-5.67	-4.99	0.68	0
64-17-5	ethanol	7732-18-5	water	307.51	-4.99	-5.67	-4.99	0.68	0
64-17-5	ethanol	7732-18-5	water	315.19	-4.88	-5.81	-4.86	0.93	0.02
64-17-5	ethanol	7732-18-5	water	315.15	-4.85	-5.81	-4.86	0.96	0.01
64-17-5	ethanol	7732-18-5	water	315.16	-4.84	-5.81	-4.86	0.97	0.02
64-17-5	ethanol	7732-18-5	water	315.13	-4.84	-5.81	-4.86	0.97	0.02
64-17-5	ethanol	7732-18-5	water	325.53	-4.71	-6	-4.68	1.29	0.03
64-17-5	ethanol	7732-18-5	water	325.51	-4.73	-6	-4.68	1.27	0.05
64-17-5	ethanol	7732-18-5	water	325.46	-4.67	-6	-4.68	1.33	0.01
64-17-5	ethanol	7732-18-5	water	325.43	-4.67	-6	-4.69	1.33	0.02
64-17-5	ethanol	7732-18-5	water	325.42	-4.69	-6	-4.69	1.31	0
64-17-5	ethanol	7732-18-5	water	325.45	-4.63	-6	-4.69	1.37	0.06
64-17-5	ethanol	7732-18-5	water	351.67	-4.28	-6.48	-4.26	2.2	0.02
64-17-5	ethanol	7732-18-5	water	351.66	-4.33	-6.48	-4.26	2.15	0.07
64-17-5	ethanol	7732-18-5	water	351.31	-4.29	-6.47	-4.26	2.18	0.03
64-17-5	ethanol	7732-18-5	water	351.35	-4.28	-6.47	-4.26	2.19	0.02
64-17-5	ethanol	7732-18-5	water	351.35	-4.29	-6.47	-4.26	2.18	0.03
64-17-5	ethanol	7732-18-5	water	351.35	-4.25	-6.47	-4.26	2.22	0.01

Table C.1: ΔG_{solv} for binary systems (kcal/mol).

solvent		solute		T (K)	ΔG^{ref}_{solv}	$\Delta G^{calc,1}_{solv}$	$\Delta G^{calc,2}_{solv}$	$\Delta G^{calc,1}_{solv}$-ΔG^{ref}_{solv}	$\Delta G^{calc,2}_{solv}$-ΔG^{ref}_{solv}
64-17-5	ethanol	7732-18-5	water	351.35	-4.21	-6.47	-4.26	2.26	0.05
64-17-5	ethanol	7732-18-5	water	351.35	-4.22	-6.47	-4.26	2.25	0.04
64-17-5	ethanol	7732-18-5	water	351.92	-4.34	-6.48	-4.25	2.14	0.09
64-17-5	ethanol	7732-18-5	water	334.7	-4.54	-6.17	-4.53	1.63	0.01
64-17-5	ethanol	7732-18-5	water	351.45	-4.25	-6.48	-4.26	2.23	0.01
64-17-5	ethanol	7732-18-5	water	340.85	-4.38	-6.28	-4.43	1.9	0.05
64-17-5	ethanol	7732-18-5	water	340.75	-4.39	-6.28	-4.43	1.89	0.04
64-17-5	ethanol	7732-18-5	water	351.04	-4.29	-6.47	-4.27	2.18	0.02
64-17-5	ethanol	7732-18-5	water	351.04	-4.26	-6.47	-4.27	2.21	0.01
64-17-5	ethanol	7732-18-5	water	351.06	-4.26	-6.47	-4.27	2.21	0.01
64-17-5	ethanol	7732-18-5	water	351.1	-4.25	-6.47	-4.27	2.22	0.02
64-17-5	ethanol	7732-18-5	water	351.14	-4.26	-6.47	-4.27	2.21	0.01
64-17-5	ethanol	7732-18-5	water	351.34	-4.29	-6.47	-4.26	2.18	0.03
64-17-5	ethanol	7732-18-5	water	351.33	-4.27	-6.47	-4.26	2.2	0.01
64-17-5	ethanol	7732-18-5	water	351.33	-4.26	-6.47	-4.26	2.21	0
64-17-5	ethanol	7732-18-5	water	345.45	-4.32	-6.37	-4.36	2.05	0.04
64-17-5	ethanol	7732-18-5	water	373.15	-3.78	-6.88	-3.92	3.1	0.14
64-17-5	ethanol	7732-18-5	water	298.15	-4.92	-5.49	-5.15	0.57	0.23
142-82-5	heptane	106-98-9	1-butene	298.15	-2.48	-2.35	-2.35	0.13	0.13
142-82-5	heptane	592-76-7	1-heptene	328.15	-4.18	-4.91	-4.17	0.73	0.01
142-82-5	heptane	592-76-7	1-heptene	328.15	-4.18	-4.91	-4.17	0.73	0.01
142-82-5	heptane	592-76-7	1-heptene	328.15	-4.19	-4.91	-4.17	0.72	0.02
142-82-5	heptane	592-41-6	1-hexene	365.72	-3.18	-4.67	-3.13	1.49	0.05
142-82-5	heptane	592-41-6	1-hexene	363.49	-3.2	-4.64	-3.15	1.44	0.05
142-82-5	heptane	592-41-6	1-hexene	361.06	-3.24	-4.61	-3.17	1.37	0.07
142-82-5	heptane	592-41-6	1-hexene	359.12	-3.25	-4.58	-3.19	1.33	0.06
142-82-5	heptane	592-41-6	1-hexene	357.32	-3.27	-4.56	-3.21	1.29	0.06
142-82-5	heptane	592-41-6	1-hexene	355.67	-3.29	-4.54	-3.22	1.25	0.07
142-82-5	heptane	592-41-6	1-hexene	353.64	-3.31	-4.51	-3.24	1.2	0.07
142-82-5	heptane	592-41-6	1-hexene	351.24	-3.33	-4.48	-3.27	1.15	0.06
142-82-5	heptane	592-41-6	1-hexene	349.88	-3.34	-4.47	-3.28	1.13	0.06
142-82-5	heptane	592-41-6	1-hexene	347.9	-3.36	-4.44	-3.3	1.08	0.06
142-82-5	heptane	109-67-1	1-pentene	293.15	-3.2	-3.05	-3.12	0.15	0.08
142-82-5	heptane	591-76-4	2-methylhexane	330.95	-4.11	-4.88	-4.1	0.77	0.01
142-82-5	heptane	591-76-4	2-methylhexane	330.1	-4.11	-4.87	-4.11	0.76	0
142-82-5	heptane	591-76-4	2-methylhexane	329.25	-4.12	-4.86	-4.12	0.74	0
142-82-5	heptane	591-76-4	2-methylhexane	328.45	-4.14	-4.85	-4.13	0.71	0.01
142-82-5	heptane	591-76-4	2-methylhexane	350.35	-3.89	-5.17	-3.9	1.28	0.01
142-82-5	heptane	591-76-4	2-methylhexane	349.5	-3.91	-5.16	-3.91	1.25	0
142-82-5	heptane	591-76-4	2-methylhexane	348.65	-3.92	-5.14	-3.91	1.22	0.01
142-82-5	heptane	107-83-5	2-methylpentane	328.15	-3.48	-4.11	-3.49	0.63	0.01
142-82-5	heptane	107-83-5	2-methylpentane	328.15	-3.5	-4.11	-3.49	0.61	0.01
142-82-5	heptane	107-83-5	2-methylpentane	328.15	-3.49	-4.11	-3.49	0.62	0
142-82-5	heptane	107-83-5	2-methylpentane	328.15	-3.49	-4.11	-3.49	0.62	0
142-82-5	heptane	107-83-5	2-methylpentane	298.15	-3.81	-3.73	-3.79	0.08	0.02
142-82-5	heptane	107-83-5	2-methylpentane	298.15	-3.77	-3.73	-3.79	0.04	0.02
142-82-5	heptane	75-28-5	2-methylpropane	298.15	-2.31	-2.26	-2.35	0.05	0.04
142-82-5	heptane	96-14-0	3-methylpentane	308.15	-3.77	-3.96	-3.75	0.19	0.02
142-82-5	heptane	96-14-0	3-methylpentane	308.15	-3.76	-3.96	-3.75	0.2	0.01
142-82-5	heptane	96-14-0	3-methylpentane	308.15	-3.76	-3.96	-3.75	0.2	0.01
142-82-5	heptane	96-14-0	3-methylpentane	308.15	-3.76	-3.96	-3.75	0.2	0.01
142-82-5	heptane	96-14-0	3-methylpentane	308.15	-3.75	-3.96	-3.75	0.21	0
142-82-5	heptane	96-14-0	3-methylpentane	308.15	-3.75	-3.96	-3.75	0.21	0
142-82-5	heptane	96-14-0	3-methylpentane	318.15	-3.67	-4.09	-3.65	0.42	0.02
142-82-5	heptane	96-14-0	3-methylpentane	328.15	-3.58	-4.22	-3.55	0.64	0.03
142-82-5	heptane	96-14-0	3-methylpentane	328.15	-3.58	-4.22	-3.55	0.64	0.03
142-82-5	heptane	110-82-7	cyclohexane	371.05	-3.26	-5.33	-3.52	2.07	0.26
142-82-5	heptane	110-82-7	cyclohexane	403.15	-3.22	-5.79	-3.22	2.57	0
142-82-5	heptane	110-82-7	cyclohexane	313.15	-4.08	-4.5	-4.1	0.42	0.02
142-82-5	heptane	110-82-7	cyclohexane	333.15	-3.87	-4.78	-3.89	0.91	0.02
142-82-5	heptane	110-82-7	cyclohexane	370.33	-3.5	-5.32	-3.53	1.82	0.03
142-82-5	heptane	110-82-7	cyclohexane	369.29	-3.5	-5.3	-3.54	1.8	0.04
142-82-5	heptane	110-82-7	cyclohexane	368.3	-3.51	-5.29	-3.55	1.78	0.04
142-82-5	heptane	110-82-7	cyclohexane	367.42	-3.49	-5.28	-3.56	1.79	0.07
142-82-5	heptane	110-82-7	cyclohexane	364.37	-3.53	-5.23	-3.58	1.7	0.05
142-82-5	heptane	110-82-7	cyclohexane	369.25	-3.51	-5.3	-3.54	1.79	0.03
142-82-5	heptane	110-82-7	cyclohexane	368.3	-3.51	-5.29	-3.55	1.78	0.04

Table C.1: ΔG_{solv} for binary systems (kcal/mol).

solvent		solute		T (K)	ΔG^{ref}_{solv}	$\Delta G^{calc,1}_{solv}$	$\Delta G^{calc,2}_{solv}$	$\Delta G^{calc,1}_{solv}$-ΔG^{ref}_{solv}	$\Delta G^{calc,2}_{solv}$-ΔG^{ref}_{solv}
142-82-5	heptane	110-82-7	cyclohexane	366.45	-3.54	-5.26	-3.56	1.72	0.02
142-82-5	heptane	110-82-7	cyclohexane	365.65	-3.54	-5.25	-3.57	1.71	0.03
142-82-5	heptane	110-82-7	cyclohexane	363.9	-3.57	-5.23	-3.59	1.66	0.02
142-82-5	heptane	110-82-7	cyclohexane	370.87	-3.46	-5.33	-3.52	1.87	0.06
142-82-5	heptane	110-82-7	cyclohexane	370.32	-3.46	-5.32	-3.53	1.86	0.07
142-82-5	heptane	110-82-7	cyclohexane	369.66	-3.47	-5.31	-3.53	1.84	0.06
142-82-5	heptane	110-82-7	cyclohexane	368.66	-3.49	-5.29	-3.54	1.8	0.05
142-82-5	heptane	110-82-7	cyclohexane	367.06	-3.51	-5.27	-3.56	1.76	0.05
142-82-5	heptane	110-82-7	cyclohexane	366.56	-3.51	-5.26	-3.56	1.75	0.05
142-82-5	heptane	110-82-7	cyclohexane	365.62	-3.53	-5.25	-3.57	1.72	0.04
142-82-5	heptane	110-82-7	cyclohexane	364.41	-3.54	-5.23	-3.58	1.69	0.04
142-82-5	heptane	110-82-7	cyclohexane	363.6	-3.55	-5.22	-3.59	1.67	0.04
142-82-5	heptane	110-82-7	cyclohexane	369.45	-3.49	-5.3	-3.54	1.81	0.05
142-82-5	heptane	110-82-7	cyclohexane	368.4	-3.51	-5.29	-3.55	1.78	0.04
142-82-5	heptane	110-82-7	cyclohexane	365.95	-3.53	-5.25	-3.57	1.72	0.04
142-82-5	heptane	110-82-7	cyclohexane	364.34	-3.55	-5.23	-3.58	1.68	0.03
142-82-5	heptane	110-82-7	cyclohexane	362.77	-3.57	-5.21	-3.6	1.64	0.03
142-82-5	heptane	110-82-7	cyclohexane	362.06	-3.58	-5.2	-3.61	1.62	0.03
142-82-5	heptane	110-82-7	cyclohexane	370.25	-3.5	-5.32	-3.53	1.82	0.03
142-82-5	heptane	110-82-7	cyclohexane	367.75	-3.51	-5.28	-3.55	1.77	0.04
142-82-5	heptane	110-82-7	cyclohexane	370.48	-3.5	-5.32	-3.53	1.82	0.03
142-82-5	heptane	110-82-7	cyclohexane	369.41	-3.51	-5.3	-3.54	1.79	0.03
142-82-5	heptane	110-82-7	cyclohexane	368.37	-3.52	-5.29	-3.55	1.77	0.03
142-82-5	heptane	110-82-7	cyclohexane	367.35	-3.53	-5.27	-3.56	1.74	0.03
142-82-5	heptane	110-82-7	cyclohexane	366.36	-3.54	-5.26	-3.57	1.72	0.03
142-82-5	heptane	110-82-7	cyclohexane	365.39	-3.55	-5.25	-3.57	1.7	0.02
142-82-5	heptane	110-82-7	cyclohexane	364.45	-3.56	-5.23	-3.58	1.67	0.02
142-82-5	heptane	110-82-7	cyclohexane	363.52	-3.57	-5.22	-3.59	1.65	0.02
142-82-5	heptane	110-82-7	cyclohexane	362.62	-3.58	-5.21	-3.6	1.63	0.02
142-82-5	heptane	110-82-7	cyclohexane	298.15	-4.17	-4.28	-4.26	0.11	0.09
142-82-5	heptane	110-82-7	cyclohexane	343.15	-3.72	-4.93	-3.79	1.21	0.07
142-82-5	heptane	110-82-7	cyclohexane	293.15	-4.31	-4.21	-4.32	0.1	0.01
142-82-5	heptane	110-82-7	cyclohexane	303.95	-4.15	-4.36	-4.2	0.21	0.05
142-82-5	heptane	110-82-7	cyclohexane	298.15	-4.24	-4.28	-4.26	0.04	0.02
142-82-5	heptane	110-82-7	cyclohexane	298.15	-4.19	-4.28	-4.26	0.09	0.07
142-82-5	heptane	74-84-0	ethane	298.15	-0.99	-1.03	-1.09	0.04	0.1
142-82-5	heptane	64-17-5	ethanol	303.15	-2.33	-2.35	-2.02	0.02	0.31
142-82-5	heptane	64-17-5	ethanol	313.15	-2.6	-2.43	-1.88	0.17	0.72
142-82-5	heptane	64-17-5	ethanol	298.15	-2.23	-2.31	-2.09	0.08	0.14
142-82-5	heptane	64-17-5	ethanol	314.45	-2.01	-2.44	-1.86	0.43	0.15
142-82-5	heptane	64-17-5	ethanol	314.55	-2.04	-2.44	-1.86	0.4	0.18
142-82-5	heptane	64-17-5	ethanol	332.15	-1.88	-2.58	-1.63	0.7	0.25
142-82-5	heptane	64-17-5	ethanol	349.55	-1.81	-2.71	-1.41	0.9	0.4
142-82-5	heptane	64-17-5	ethanol	349.55	-1.78	-2.71	-1.41	0.93	0.37
142-82-5	heptane	64-17-5	ethanol	366.75	-1.73	-2.84	-1.19	1.11	0.54
142-82-5	heptane	64-17-5	ethanol	293.15	-2.34	-2.27	-2.16	0.07	0.18
142-82-5	heptane	64-17-5	ethanol	298.15	-2.23	-2.31	-2.09	0.08	0.14
142-82-5	heptane	64-17-5	ethanol	333.15	-2.08	-2.58	-1.62	0.5	0.46
142-82-5	heptane	64-17-5	ethanol	298.15	-2.25	-2.31	-2.09	0.06	0.16
142-82-5	heptane	64-17-5	ethanol	313.15	-1.93	-2.43	-1.88	0.5	0.05
142-82-5	heptane	64-17-5	ethanol	323.15	-1.87	-2.51	-1.75	0.64	0.12
142-82-5	heptane	64-17-5	ethanol	333.15	-1.84	-2.58	-1.62	0.74	0.22
142-82-5	heptane	64-17-5	ethanol	293.5	-2.36	-2.28	-2.15	0.08	0.21
142-82-5	heptane	64-17-5	ethanol	303.3	-2.18	-2.35	-2.01	0.17	0.17
142-82-5	heptane	64-17-5	ethanol	313.1	-2.13	-2.43	-1.88	0.3	0.25
142-82-5	heptane	64-17-5	ethanol	322.8	-2.13	-2.5	-1.75	0.37	0.38
142-82-5	heptane	64-17-5	ethanol	323.15	-2.28	-2.51	-1.75	0.23	0.53
142-82-5	heptane	64-17-5	ethanol	333.15	-2.1	-2.58	-1.62	0.48	0.48
142-82-5	heptane	64-17-5	ethanol	343.15	-1.94	-2.66	-1.49	0.72	0.45
142-82-5	heptane	64-17-5	ethanol	353.15	-1.79	-2.74	-1.36	0.95	0.43
142-82-5	heptane	64-17-5	ethanol	363.15	-1.64	-2.82	-1.24	1.18	0.4
142-82-5	heptane	64-17-5	ethanol	373.15	-1.5	-2.89	-1.12	1.39	0.38
142-82-5	heptane	64-17-5	ethanol	298.15	-2.09	-2.31	-2.09	0.22	0
142-82-5	heptane	64-17-5	ethanol	303.25	-2.06	-2.35	-2.01	0.29	0.05
142-82-5	heptane	64-17-5	ethanol	308.15	-2.04	-2.39	-1.95	0.35	0.09
142-82-5	heptane	64-17-5	ethanol	313.15	-2	-2.43	-1.88	0.43	0.12
142-82-5	heptane	64-17-5	ethanol	318.25	-1.96	-2.47	-1.81	0.51	0.15

Table C.1: ΔG_{solv} for binary systems (kcal/mol).

solvent		solute		T (K)	ΔG^{ref}_{solv}	$\Delta G^{calc,1}_{solv}$	$\Delta G^{calc,2}_{solv}$	$\Delta G^{calc,1}_{solv}$-ΔG^{ref}_{solv}	$\Delta G^{calc,2}_{solv}$-ΔG^{ref}_{solv}
142-82-5	heptane	64-17-5	ethanol	288.15	-2.19	-2.23	-2.23	0.04	0.04
142-82-5	heptane	64-17-5	ethanol	293.15	-2.17	-2.27	-2.16	0.1	0.01
142-82-5	heptane	64-17-5	ethanol	298.15	-2.13	-2.31	-2.09	0.18	0.04
142-82-5	heptane	64-17-5	ethanol	303.15	-2.1	-2.35	-2.02	0.25	0.08
142-82-5	heptane	64-17-5	ethanol	308.15	-2.07	-2.39	-1.95	0.32	0.12
142-82-5	heptane	64-17-5	ethanol	313.15	-2.02	-2.43	-1.88	0.41	0.14
142-82-5	heptane	64-17-5	ethanol	318.15	-2	-2.47	-1.81	0.47	0.19
142-82-5	heptane	64-17-5	ethanol	323.15	-1.96	-2.51	-1.75	0.55	0.21
142-82-5	heptane	64-17-5	ethanol	313.15	-1.98	-2.43	-1.88	0.45	0.1
142-82-5	heptane	64-17-5	ethanol	333.15	-2.09	-2.58	-1.62	0.49	0.47
142-82-5	heptane	64-17-5	ethanol	309.15	-2.14	-2.4	-1.93	0.26	0.21
142-82-5	heptane	74-85-1	ethene	298.15	-0.63	-0.74	-0.66	0.11	0.04
142-82-5	heptane	74-82-8	methane	298.15	0.1	0.06	-1.02	0.04	1.12
142-82-5	heptane	67-56-1	methanol	297.05	-1.76	-1.61	-1.05	0.15	0.71
142-82-5	heptane	67-56-1	methanol	313.15	-1.62	-1.7	-0.86	0.08	0.76
142-82-5	heptane	67-56-1	methanol	313.15	-1.71	-1.7	-0.86	0.01	0.85
142-82-5	heptane	67-56-1	methanol	313.15	-2.25	-1.7	-0.86	0.55	1.39
142-82-5	heptane	67-56-1	methanol	363.15	-1.23	-1.97	-0.31	0.74	0.92
142-82-5	heptane	67-56-1	methanol	363.15	-1.26	-1.97	-0.31	0.71	0.95
142-82-5	heptane	67-56-1	methanol	363.15	-1.25	-1.97	-0.31	0.72	0.94
142-82-5	heptane	67-56-1	methanol	363.15	-1.25	-1.97	-0.31	0.72	0.94
142-82-5	heptane	67-56-1	methanol	339.15	-1.75	-1.84	-0.57	0.09	1.18
142-82-5	heptane	67-56-1	methanol	293.15	-1.62	-1.59	-1.09	0.03	0.53
142-82-5	heptane	67-56-1	methanol	313.57	-1.4	-1.7	-0.86	0.3	0.54
142-82-5	heptane	67-56-1	methanol	322.45	-1.37	-1.75	-0.76	0.38	0.61
142-82-5	heptane	67-56-1	methanol	333.55	-1.33	-1.81	-0.63	0.48	0.7
142-82-5	heptane	67-56-1	methanol	283.15	-1.51	-1.53	-1.22	0.02	0.29
142-82-5	heptane	67-56-1	methanol	293.15	-1.41	-1.59	-1.09	0.18	0.32
142-82-5	heptane	67-56-1	methanol	293.15	-1.41	-1.59	-1.09	0.18	0.32
142-82-5	heptane	67-56-1	methanol	303.15	-1.34	-1.64	-0.98	0.3	0.36
142-82-5	heptane	67-56-1	methanol	323.15	-1.84	-1.75	-0.75	0.09	1.09
142-82-5	heptane	67-56-1	methanol	333.15	-1.73	-1.8	-0.64	0.07	1.09
142-82-5	heptane	67-56-1	methanol	343.15	-1.64	-1.86	-0.53	0.22	1.11
142-82-5	heptane	67-56-1	methanol	353.15	-1.57	-1.91	-0.42	0.34	1.15
142-82-5	heptane	67-56-1	methanol	363.15	-1.5	-1.97	-0.31	0.47	1.19
142-82-5	heptane	67-56-1	methanol	373.15	-1.44	-2.02	-0.21	0.58	1.23
142-82-5	heptane	67-56-1	methanol	308.15	-1.35	-1.67	-0.92	0.32	0.43
142-82-5	heptane	67-56-1	methanol	313.25	-1.29	-1.7	-0.86	0.41	0.43
142-82-5	heptane	67-56-1	methanol	288.15	-1.54	-1.56	-1.15	0.02	0.39
142-82-5	heptane	67-56-1	methanol	293.15	-1.51	-1.59	-1.09	0.08	0.42
142-82-5	heptane	67-56-1	methanol	298.15	-1.48	-1.61	-1.04	0.13	0.44
142-82-5	heptane	67-56-1	methanol	303.15	-1.44	-1.64	-0.98	0.2	0.46
142-82-5	heptane	67-56-1	methanol	308.15	-1.42	-1.67	-0.92	0.25	0.5
142-82-5	heptane	67-56-1	methanol	313.15	-1.38	-1.7	-0.86	0.32	0.52
142-82-5	heptane	67-56-1	methanol	318.15	-1.35	-1.72	-0.8	0.37	0.55
142-82-5	heptane	67-56-1	methanol	323.15	-1.32	-1.75	-0.75	0.43	0.57
142-82-5	heptane	67-56-1	methanol	298.15	-1.9	-1.61	-1.04	0.29	0.86
142-82-5	heptane	67-56-1	methanol	313.15	-1.4	-1.7	-0.86	0.3	0.54
142-82-5	heptane	67-56-1	methanol	323.15	-1.36	-1.75	-0.75	0.39	0.61
142-82-5	heptane	67-56-1	methanol	333.15	-1.34	-1.8	-0.64	0.46	0.7
142-82-5	heptane	67-56-1	methanol	298.15	-1.41	-1.61	-1.04	0.2	0.37
142-82-5	heptane	67-56-1	methanol	333.15	-1.31	-1.8	-0.64	0.49	0.67
142-82-5	heptane	67-56-1	methanol	373.15	-1.12	-2.02	-0.21	0.9	0.91
142-82-5	heptane	67-56-1	methanol	309.15	-1.45	-1.67	-0.91	0.22	0.54
142-82-5	heptane	67-56-1	methanol	263.15	-1.83	-1.42	-1.47	0.41	0.36
142-82-5	heptane	67-56-1	methanol	273.15	-1.71	-1.48	-1.34	0.23	0.37
142-82-5	heptane	67-56-1	methanol	293.15	-1.42	-1.59	-1.09	0.17	0.33
142-82-5	heptane	67-56-1	methanol	313.15	-1.23	-1.7	-0.86	0.47	0.37
142-82-5	heptane	108-87-2	methylcyclohexane	371.57	-4.02	-5.95	-3.91	1.93	0.11
142-82-5	heptane	108-87-2	methylcyclohexane	323.15	-4.41	-5.18	-4.4	0.77	0.01
142-82-5	heptane	108-87-2	methylcyclohexane	323.15	-4.4	-5.18	-4.4	0.78	0
142-82-5	heptane	108-87-2	methylcyclohexane	323.15	-4.41	-5.18	-4.4	0.77	0.01
142-82-5	heptane	108-87-2	methylcyclohexane	320.65	-4.43	-5.14	-4.43	0.71	0
142-82-5	heptane	108-87-2	methylcyclohexane	320.65	-4.43	-5.14	-4.43	0.71	0
142-82-5	heptane	108-87-2	methylcyclohexane	320.65	-4.43	-5.14	-4.43	0.71	0
142-82-5	heptane	108-87-2	methylcyclohexane	372.6	-3.9	-5.97	-3.9	2.07	0
142-82-5	heptane	108-87-2	methylcyclohexane	372.38	-3.9	-5.96	-3.9	2.06	0

Table C.1: ΔG_{solv} for binary systems (kcal/mol).

solvent		solute		T (K)	ΔG^{ref}_{solv}	$\Delta G^{calc,1}_{solv}$	$\Delta G^{calc,2}_{solv}$	$\Delta G^{calc,1}_{solv}$-ΔG^{ref}_{solv}	$\Delta G^{calc,2}_{solv}$-ΔG^{ref}_{solv}
142-82-5	heptane	108-87-2	methylcyclohexane	372.21	-3.91	-5.96	-3.9	2.05	0.01
142-82-5	heptane	108-87-2	methylcyclohexane	371.94	-3.91	-5.96	-3.9	2.05	0.01
142-82-5	heptane	108-87-2	methylcyclohexane	371.77	-3.92	-5.96	-3.9	2.04	0.02
142-82-5	heptane	108-87-2	methylcyclohexane	372.3	-3.9	-5.96	-3.9	2.06	0
142-82-5	heptane	108-87-2	methylcyclohexane	372	-3.9	-5.96	-3.9	2.06	0
142-82-5	heptane	108-87-2	methylcyclohexane	371.8	-3.9	-5.96	-3.9	2.06	0
142-82-5	heptane	108-87-2	methylcyclohexane	371.75	-3.91	-5.95	-3.9	2.04	0.01
142-82-5	heptane	108-87-2	methylcyclohexane	371.65	-3.91	-5.95	-3.91	2.04	0
142-82-5	heptane	108-87-2	methylcyclohexane	372.18	-3.89	-5.96	-3.9	2.07	0.01
142-82-5	heptane	108-87-2	methylcyclohexane	371.98	-3.89	-5.96	-3.9	2.07	0.01
142-82-5	heptane	108-87-2	methylcyclohexane	371.79	-3.88	-5.96	-3.9	2.08	0.02
142-82-5	heptane	108-87-2	methylcyclohexane	371.67	-3.88	-5.95	-3.91	2.07	0.03
142-82-5	heptane	108-87-2	methylcyclohexane	372.58	-3.9	-5.97	-3.9	2.07	0
142-82-5	heptane	108-87-2	methylcyclohexane	372.58	-3.9	-5.97	-3.9	2.07	0
142-82-5	heptane	108-87-2	methylcyclohexane	372.32	-3.91	-5.96	-3.9	2.05	0.01
142-82-5	heptane	108-87-2	methylcyclohexane	372.05	-3.91	-5.96	-3.9	2.05	0.01
142-82-5	heptane	108-87-2	methylcyclohexane	371.91	-3.92	-5.96	-3.9	2.04	0.02
142-82-5	heptane	108-87-2	methylcyclohexane	371.77	-3.93	-5.96	-3.9	2.03	0.03
142-82-5	heptane	108-87-2	methylcyclohexane	371.65	-3.93	-5.95	-3.91	2.02	0.02
142-82-5	heptane	108-87-2	methylcyclohexane	371.69	-3.91	-5.95	-3.9	2.04	0.01
142-82-5	heptane	108-87-2	methylcyclohexane	371.81	-3.91	-5.96	-3.9	2.05	0.01
142-82-5	heptane	108-87-2	methylcyclohexane	371.92	-3.91	-5.96	-3.9	2.05	0.01
142-82-5	heptane	108-87-2	methylcyclohexane	372.04	-3.91	-5.96	-3.9	2.05	0.01
142-82-5	heptane	108-87-2	methylcyclohexane	372.16	-3.91	-5.96	-3.9	2.05	0.01
142-82-5	heptane	108-87-2	methylcyclohexane	372.28	-3.91	-5.96	-3.9	2.05	0.01
142-82-5	heptane	108-87-2	methylcyclohexane	372.39	-3.91	-5.97	-3.9	2.06	0.01
142-82-5	heptane	108-87-2	methylcyclohexane	372.51	-3.9	-5.97	-3.9	2.07	0
142-82-5	heptane	108-87-2	methylcyclohexane	372.64	-3.9	-5.97	-3.9	2.07	0
142-82-5	heptane	108-87-2	methylcyclohexane	372.65	-3.91	-5.97	-3.9	2.06	0.01
142-82-5	heptane	108-87-2	methylcyclohexane	372.25	-3.92	-5.96	-3.9	2.04	0.02
142-82-5	heptane	108-87-2	methylcyclohexane	372.05	-3.91	-5.96	-3.9	2.05	0.01
142-82-5	heptane	110-62-3	pentanal	348.15	-3.52	-4.86	-3.77	1.34	0.25
142-82-5	heptane	110-62-3	pentanal	363.15	-3.45	-5.07	-3.61	1.62	0.16
142-82-5	heptane	110-62-3	pentanal	363.15	-3.4	-5.07	-3.61	1.67	0.21
142-82-5	heptane	74-98-6	propane	298.15	-1.78	-1.78	-1.82	0	0.04
142-82-5	heptane	109-99-9	tetrahydrofuran	313.15	-3.42	-4.04	-3.59	0.62	0.17
142-82-5	heptane	109-99-9	tetrahydrofuran	298.15	-3.7	-3.84	-3.75	0.14	0.05
142-82-5	heptane	109-99-9	tetrahydrofuran	370.16	-2.89	-4.77	-3.02	1.88	0.13
142-82-5	heptane	109-99-9	tetrahydrofuran	368.46	-2.93	-4.75	-3.03	1.82	0.1
142-82-5	heptane	109-99-9	tetrahydrofuran	365.56	-2.99	-4.71	-3.06	1.72	0.07
142-82-5	heptane	109-99-9	tetrahydrofuran	363.73	-3.02	-4.69	-3.08	1.67	0.06
142-82-5	heptane	109-99-9	tetrahydrofuran	361.95	-3.04	-4.67	-3.1	1.63	0.06
142-82-5	heptane	109-99-9	tetrahydrofuran	365.55	-2.95	-4.71	-3.06	1.76	0.11
142-82-5	heptane	109-99-9	tetrahydrofuran	333.15	-3.32	-4.3	-3.38	0.98	0.06
142-82-5	heptane	109-99-9	tetrahydrofuran	303.15	-3.62	-3.91	-3.7	0.29	0.08
142-82-5	heptane	109-99-9	tetrahydrofuran	343.15	-3.23	-4.43	-3.28	1.2	0.05
142-82-5	heptane	7732-18-5	water	298.15	-0.78	-0.72	1.66	0.06	2.44
142-82-5	heptane	7732-18-5	water	296.15	-0.9	-0.72	1.64	0.18	2.54
142-82-5	heptane	7732-18-5	water	283.15	-0.98	-0.69	1.48	0.29	2.46
142-82-5	heptane	7732-18-5	water	293.15	-0.94	-0.71	1.6	0.23	2.54
142-82-5	heptane	7732-18-5	water	293.15	-0.98	-0.71	1.6	0.27	2.58
142-82-5	heptane	7732-18-5	water	298.15	-0.89	-0.72	1.66	0.16	2.54
142-82-5	heptane	7732-18-5	water	298.15	-0.53	-0.72	1.66	0.2	2.18
142-82-5	heptane	7732-18-5	water	283.15	-0.78	-0.69	1.48	0.09	2.26
142-82-5	heptane	7732-18-5	water	293.15	-0.78	-0.71	1.6	0.07	2.38
142-82-5	heptane	7732-18-5	water	303.15	-0.81	-0.74	1.72	0.07	2.53
142-82-5	heptane	7732-18-5	water	298.15	-0.59	-0.72	1.66	0.14	2.25
142-82-5	heptane	7732-18-5	water	298.15	-0.76	-0.72	1.66	0.03	2.41
142-82-5	heptane	7732-18-5	water	313.15	-0.44	-0.76	1.83	0.32	2.27
142-82-5	heptane	7732-18-5	water	298.15	-0.89	-0.72	1.66	0.16	2.55
142-82-5	heptane	7732-18-5	water	295.65	-0.4	-0.72	1.63	0.32	2.02
142-82-5	heptane	7732-18-5	water	293.15	-0.74	-0.71	1.6	0.03	2.34
142-82-5	heptane	7732-18-5	water	313.15	-0.31	-0.76	1.83	0.45	2.14
544-76-3	hexadecane	106-98-9	1-butene	293.15	-2.14	-2	-2.21	0.14	0.07
544-76-3	hexadecane	592-76-7	1-heptene	323.15	-3.91	-4.53	-3.91	0.62	0
544-76-3	hexadecane	592-76-7	1-heptene	333.15	-3.79	-4.67	-3.8	0.88	0.01
544-76-3	hexadecane	592-76-7	1-heptene	343.15	-3.7	-4.81	-3.69	1.11	0.01

Table C.1: ΔG_{solv} for binary systems (kcal/mol).

solvent		solute		T (K)	ΔG^{ref}_{solv}	$\Delta G^{calc,1}_{solv}$	$\Delta G^{calc,2}_{solv}$	$\Delta G^{calc,1}_{solv}$-ΔG^{ref}_{solv}	$\Delta G^{calc,2}_{solv}$-ΔG^{ref}_{solv}
544-76-3	hexadecane	592-76-7	1-heptene	353.15	-3.59	-4.95	-3.58	1.36	0.01
544-76-3	hexadecane	592-76-7	1-heptene	373.15	-3.41	-5.23	-3.37	1.82	0.04
544-76-3	hexadecane	592-76-7	1-heptene	304.85	-4.1	-4.27	-4.13	0.17	0.03
544-76-3	hexadecane	592-76-7	1-heptene	315.35	-3.96	-4.42	-4.01	0.46	0.05
544-76-3	hexadecane	592-76-7	1-heptene	324.45	-3.86	-4.55	-3.9	0.69	0.04
544-76-3	hexadecane	592-41-6	1-hexene	293.15	-3.6	-3.45	-3.6	0.15	0
544-76-3	hexadecane	592-41-6	1-hexene	323.15	-3.27	-3.8	-3.27	0.53	0
544-76-3	hexadecane	592-41-6	1-hexene	333.15	-3.14	-3.92	-3.17	0.78	0.03
544-76-3	hexadecane	592-41-6	1-hexene	343.15	-3.08	-4.04	-3.07	0.96	0.01
544-76-3	hexadecane	592-41-6	1-hexene	353.15	-3.02	-4.15	-2.97	1.13	0.05
544-76-3	hexadecane	592-41-6	1-hexene	373.15	-2.86	-4.39	-2.77	1.53	0.09
544-76-3	hexadecane	592-41-6	1-hexene	304.85	-3.42	-3.59	-3.47	0.17	0.05
544-76-3	hexadecane	592-41-6	1-hexene	315.35	-3.31	-3.71	-3.36	0.4	0.05
544-76-3	hexadecane	592-41-6	1-hexene	324.45	-3.21	-3.82	-3.26	0.61	0.05
544-76-3	hexadecane	592-41-6	1-hexene	298.15	-3.51	-3.51	-3.55	0	0.04
544-76-3	hexadecane	109-67-1	1-pentene	315.35	-2.6	-2.95	-2.69	0.35	0.09
544-76-3	hexadecane	109-67-1	1-pentene	293.15	-2.86	-2.74	-2.9	0.12	0.04
544-76-3	hexadecane	109-67-1	1-pentene	323.15	-2.62	-3.03	-2.62	0.41	0
544-76-3	hexadecane	109-67-1	1-pentene	333.15	-2.53	-3.12	-2.53	0.59	0
544-76-3	hexadecane	109-67-1	1-pentene	343.15	-2.51	-3.21	-2.44	0.7	0.07
544-76-3	hexadecane	109-67-1	1-pentene	353.15	-2.46	-3.31	-2.36	0.85	0.1
544-76-3	hexadecane	109-67-1	1-pentene	373.15	-2.34	-3.49	-2.19	1.15	0.15
544-76-3	hexadecane	78-78-4	2-methylbutane	333.15	-2.43	-3.07	-2.59	0.64	0.16
544-76-3	hexadecane	78-78-4	2-methylbutane	298.15	-2.76	-2.75	-2.91	0.01	0.15
544-76-3	hexadecane	78-78-4	2-methylbutane	303.15	-2.68	-2.79	-2.86	0.11	0.18
544-76-3	hexadecane	78-78-4	2-methylbutane	297.5	-2.73	-2.74	-2.92	0.01	0.19
544-76-3	hexadecane	78-78-4	2-methylbutane	323.15	-2.58	-2.98	-2.68	0.4	0.1
544-76-3	hexadecane	78-78-4	2-methylbutane	333.15	-2.48	-3.07	-2.59	0.59	0.11
544-76-3	hexadecane	78-78-4	2-methylbutane	343.15	-2.45	-3.16	-2.5	0.71	0.05
544-76-3	hexadecane	78-78-4	2-methylbutane	353.15	-2.4	-3.25	-2.41	0.85	0.01
544-76-3	hexadecane	78-78-4	2-methylbutane	373.15	-2.28	-3.44	-2.25	1.16	0.03
544-76-3	hexadecane	107-83-5	2-methylpentane	298.15	-3.45	-3.41	-3.55	0.04	0.1
544-76-3	hexadecane	107-83-5	2-methylpentane	298.15	-3.48	-3.41	-3.55	0.07	0.07
544-76-3	hexadecane	107-83-5	2-methylpentane	298.15	-3.47	-3.41	-3.55	0.06	0.08
544-76-3	hexadecane	107-83-5	2-methylpentane	303.15	-3.38	-3.47	-3.5	0.09	0.12
544-76-3	hexadecane	107-83-5	2-methylpentane	313.15	-3.29	-3.59	-3.39	0.3	0.1
544-76-3	hexadecane	107-83-5	2-methylpentane	298.15	-3.43	-3.41	-3.55	0.02	0.12
544-76-3	hexadecane	107-83-5	2-methylpentane	298.15	-3.43	-3.41	-3.55	0.02	0.12
544-76-3	hexadecane	107-83-5	2-methylpentane	298.15	-3.41	-3.41	-3.55	0	0.14
544-76-3	hexadecane	75-28-5	2-methylpropane	298.15	-1.89	-1.92	-2.17	0.03	0.28
544-76-3	hexadecane	75-28-5	2-methylpropane	298.15	-1.92	-1.92	-2.17	0	0.25
544-76-3	hexadecane	96-14-0	3-methylpentane	298.15	-3.55	-3.52	-3.62	0.03	0.07
544-76-3	hexadecane	96-14-0	3-methylpentane	293.15	-3.56	-3.46	-3.68	0.1	0.12
544-76-3	hexadecane	96-14-0	3-methylpentane	303.15	-3.45	-3.58	-3.57	0.13	0.12
544-76-3	hexadecane	96-14-0	3-methylpentane	313.15	-3.35	-3.7	-3.46	0.35	0.11
544-76-3	hexadecane	96-14-0	3-methylpentane	323.15	-3.24	-3.82	-3.35	0.58	0.11
544-76-3	hexadecane	96-14-0	3-methylpentane	333.15	-3.14	-3.93	-3.25	0.79	0.11
544-76-3	hexadecane	96-14-0	3-methylpentane	343.15	-3.04	-4.05	-3.15	1.01	0.11
544-76-3	hexadecane	96-14-0	3-methylpentane	353.15	-2.97	-4.17	-3.05	1.2	0.08
544-76-3	hexadecane	75-07-0	acetaldehyde	298.15	-1.35	-1.68	-1.92	0.33	0.57
544-76-3	hexadecane	75-07-0	acetaldehyde	313.15	-1.23	-1.76	-1.81	0.53	0.58
544-76-3	hexadecane	75-07-0	acetaldehyde	303.15	-1.64	-1.71	-1.88	0.07	0.24
544-76-3	hexadecane	75-07-0	acetaldehyde	298.15	-1.68	-1.68	-1.92	0	0.24
544-76-3	hexadecane	110-82-7	cyclohexane	323.15	-3.65	-4.38	-3.78	0.73	0.13
544-76-3	hexadecane	110-82-7	cyclohexane	323.15	-3.65	-4.38	-3.78	0.73	0.13
544-76-3	hexadecane	110-82-7	cyclohexane	298.15	-4.01	-4.04	-4.06	0.03	0.05
544-76-3	hexadecane	110-82-7	cyclohexane	298.07	-3.97	-4.04	-4.06	0.07	0.09
544-76-3	hexadecane	110-82-7	cyclohexane	298.15	-3.97	-4.04	-4.06	0.07	0.09
544-76-3	hexadecane	110-82-7	cyclohexane	293.15	-4.02	-3.97	-4.11	0.05	0.09
544-76-3	hexadecane	110-82-7	cyclohexane	303.15	-3.92	-4.11	-4	0.19	0.08
544-76-3	hexadecane	110-82-7	cyclohexane	313.15	-3.81	-4.25	-3.89	0.44	0.08
544-76-3	hexadecane	110-82-7	cyclohexane	323.15	-3.73	-4.38	-3.78	0.65	0.05
544-76-3	hexadecane	110-82-7	cyclohexane	333.15	-3.61	-4.52	-3.67	0.91	0.06
544-76-3	hexadecane	110-82-7	cyclohexane	343.15	-3.55	-4.65	-3.57	1.1	0.02
544-76-3	hexadecane	110-82-7	cyclohexane	353.15	-3.46	-4.79	-3.47	1.33	0.01
544-76-3	hexadecane	110-82-7	cyclohexane	373.15	-3.29	-5.06	-3.27	1.77	0.02
544-76-3	hexadecane	110-82-7	cyclohexane	298.15	-3.97	-4.04	-4.06	0.07	0.09

Table C.1: ΔG_{solv} for binary systems (kcal/mol).

solvent		solute		T (K)	ΔG^{ref}_{solv}	$\Delta G^{calc,1}_{solv}$	$\Delta G^{calc,2}_{solv}$	$\Delta G^{calc,1}_{solv}$-ΔG^{ref}_{solv}	$\Delta G^{calc,2}_{solv}$-ΔG^{ref}_{solv}
544-76-3	hexadecane	110-82-7	cyclohexane	313.15	-3.83	-4.25	-3.89	0.42	0.06
544-76-3	hexadecane	110-82-7	cyclohexane	323.15	-3.71	-4.38	-3.78	0.67	0.07
544-76-3	hexadecane	110-82-7	cyclohexane	333.15	-3.62	-4.52	-3.67	0.9	0.05
544-76-3	hexadecane	110-82-7	cyclohexane	313	-3.81	-4.24	-3.89	0.43	0.08
544-76-3	hexadecane	110-82-7	cyclohexane	293.15	-4	-3.97	-4.11	0.03	0.11
544-76-3	hexadecane	110-82-7	cyclohexane	312.85	-3.82	-4.24	-3.89	0.42	0.07
544-76-3	hexadecane	110-82-7	cyclohexane	293.15	-4.02	-3.97	-4.11	0.05	0.09
544-76-3	hexadecane	110-82-7	cyclohexane	303.15	-3.91	-4.11	-4	0.2	0.09
544-76-3	hexadecane	110-82-7	cyclohexane	313.15	-3.81	-4.25	-3.89	0.44	0.08
544-76-3	hexadecane	110-82-7	cyclohexane	323.15	-3.71	-4.38	-3.78	0.67	0.07
544-76-3	hexadecane	110-82-7	cyclohexane	333.15	-3.61	-4.52	-3.67	0.91	0.06
544-76-3	hexadecane	110-82-7	cyclohexane	343.15	-3.52	-4.65	-3.57	1.13	0.05
544-76-3	hexadecane	110-82-7	cyclohexane	353.15	-3.43	-4.79	-3.47	1.36	0.04
544-76-3	hexadecane	110-82-7	cyclohexane	298.15	-3.98	-4.04	-4.06	0.06	0.08
544-76-3	hexadecane	110-82-7	cyclohexane	298.15	-3.96	-4.04	-4.06	0.08	0.1
544-76-3	hexadecane	110-82-7	cyclohexane	298.15	-3.95	-4.04	-4.06	0.09	0.11
544-76-3	hexadecane	110-82-7	cyclohexane	303.15	-3.93	-4.11	-4	0.18	0.07
544-76-3	hexadecane	110-82-7	cyclohexane	333.15	-3.62	-4.52	-3.67	0.9	0.05
544-76-3	hexadecane	110-82-7	cyclohexane	303.15	-3.88	-4.11	-4	0.23	0.12
544-76-3	hexadecane	110-82-7	cyclohexane	293.15	-4.01	-3.97	-4.11	0.04	0.1
544-76-3	hexadecane	110-82-7	cyclohexane	298.15	-3.96	-4.04	-4.06	0.08	0.1
544-76-3	hexadecane	110-82-7	cyclohexane	303.15	-3.9	-4.11	-4	0.21	0.1
544-76-3	hexadecane	110-82-7	cyclohexane	313.15	-3.8	-4.25	-3.89	0.45	0.09
544-76-3	hexadecane	110-82-7	cyclohexane	323.15	-3.69	-4.38	-3.78	0.69	0.09
544-76-3	hexadecane	110-82-7	cyclohexane	333.15	-3.59	-4.52	-3.67	0.93	0.08
544-76-3	hexadecane	110-82-7	cyclohexane	298.15	-3.97	-4.04	-4.06	0.07	0.09
544-76-3	hexadecane	108-94-1	cyclohexanone	298.15	-4.97	-5.17	-5.36	0.2	0.39
544-76-3	hexadecane	287-92-3	cyclopentane	333.15	-2.98	-3.77	-3.06	0.79	0.08
544-76-3	hexadecane	287-92-3	cyclopentane	323.15	-3.11	-3.66	-3.16	0.55	0.05
544-76-3	hexadecane	287-92-3	cyclopentane	333.15	-2.99	-3.77	-3.06	0.78	0.07
544-76-3	hexadecane	287-92-3	cyclopentane	343.15	-2.94	-3.89	-2.97	0.95	0.03
544-76-3	hexadecane	287-92-3	cyclopentane	353.15	-2.88	-4	-2.88	1.12	0
544-76-3	hexadecane	287-92-3	cyclopentane	373.15	-2.75	-4.23	-2.7	1.48	0.05
544-76-3	hexadecane	287-92-3	cyclopentane	293.15	-3.35	-3.32	-3.46	0.03	0.11
544-76-3	hexadecane	287-92-3	cyclopentane	298.15	-3.3	-3.38	-3.41	0.08	0.11
544-76-3	hexadecane	287-92-3	cyclopentane	298.15	-3.34	-3.38	-3.41	0.04	0.07
544-76-3	hexadecane	287-92-3	cyclopentane	303.15	-3.26	-3.43	-3.36	0.17	0.1
544-76-3	hexadecane	287-92-3	cyclopentane	313.15	-3.18	-3.55	-3.26	0.37	0.08
544-76-3	hexadecane	287-92-3	cyclopentane	293.09	-3.35	-3.32	-3.46	0.03	0.11
544-76-3	hexadecane	287-92-3	cyclopentane	298.08	-3.31	-3.38	-3.41	0.07	0.1
544-76-3	hexadecane	287-92-3	cyclopentane	303.07	-3.25	-3.43	-3.36	0.18	0.11
544-76-3	hexadecane	120-92-3	cyclopentanone	298.15	-4.23	-4.39	-4.66	0.16	0.43
544-76-3	hexadecane	120-92-3	cyclopentanone	298.15	-4.2	-4.39	-4.66	0.19	0.46
544-76-3	hexadecane	142-29-0	cyclopentene	323.15	-2.99	-3.55	-3	0.56	0.01
544-76-3	hexadecane	142-29-0	cyclopentene	333.15	-2.87	-3.66	-2.91	0.79	0.04
544-76-3	hexadecane	142-29-0	cyclopentene	343.15	-2.81	-3.77	-2.82	0.96	0.01
544-76-3	hexadecane	142-29-0	cyclopentene	353.15	-2.77	-3.88	-2.72	1.11	0.05
544-76-3	hexadecane	142-29-0	cyclopentene	373.15	-2.61	-4.1	-2.55	1.49	0.06
544-76-3	hexadecane	74-84-0	ethane	498	0.05	-1.12	-1.11	1.17	1.16
544-76-3	hexadecane	74-84-0	ethane	298.15	-0.68	-0.67	-0.98	0.01	0.3
544-76-3	hexadecane	74-84-0	ethane	300	-0.67	-0.68	-0.97	0	0.3
544-76-3	hexadecane	74-84-0	ethane	325	-0.57	-0.73	-0.83	0.16	0.26
544-76-3	hexadecane	74-84-0	ethane	350	-0.46	-0.79	-0.7	0.33	0.24
544-76-3	hexadecane	74-84-0	ethane	375	-0.36	-0.84	-0.6	0.48	0.24
544-76-3	hexadecane	74-84-0	ethane	400	-0.26	-0.9	-0.52	0.64	0.26
544-76-3	hexadecane	74-84-0	ethane	425	-0.18	-0.96	-0.5	0.77	0.31
544-76-3	hexadecane	74-84-0	ethane	450	-0.12	-1.01	-0.56	0.89	0.44
544-76-3	hexadecane	74-84-0	ethane	475	-0.08	-1.07	-0.75	0.99	0.67
544-76-3	hexadecane	74-84-0	ethane	298.15	-0.66	-0.67	-0.98	0.01	0.32
544-76-3	hexadecane	74-84-0	ethane	298.15	-0.61	-0.67	-0.98	0.06	0.36
544-76-3	hexadecane	74-84-0	ethane	298.15	-0.67	-0.67	-0.98	0	0.3
544-76-3	hexadecane	74-84-0	ethane	298.15	-0.65	-0.67	-0.98	0.02	0.33
544-76-3	hexadecane	74-84-0	ethane	313.15	-0.58	-0.7	-0.9	0.12	0.31
544-76-3	hexadecane	74-84-0	ethane	328.15	-0.54	-0.74	-0.81	0.2	0.27
544-76-3	hexadecane	64-17-5	ethanol	293.15	-1.89	-1.99	-1.99	0.1	0.1
544-76-3	hexadecane	64-17-5	ethanol	323.2	-1.89	-2.2	-1.58	0.31	0.31
544-76-3	hexadecane	64-17-5	ethanol	298.15	-1.94	-2.03	-1.92	0.09	0.02

Table C.1: ΔG_{solv} for binary systems (kcal/mol).

solvent		solute		T (K)	ΔG^{ref}_{solv}	$\Delta G^{calc,1}_{solv}$	$\Delta G^{calc,2}_{solv}$	$\Delta G^{calc,1}_{solv}$-ΔG^{ref}_{solv}	$\Delta G^{calc,2}_{solv}$-ΔG^{ref}_{solv}
544-76-3	hexadecane	64-17-5	ethanol	333.15	-1.77	-2.26	-1.45	0.49	0.32
544-76-3	hexadecane	64-17-5	ethanol	373.15	-1.52	-2.53	-0.96	1.01	0.56
544-76-3	hexadecane	64-17-5	ethanol	393.15	-1.39	-2.67	-0.72	1.28	0.67
544-76-3	hexadecane	64-17-5	ethanol	403.15	-1.32	-2.74	-0.61	1.42	0.71
544-76-3	hexadecane	64-17-5	ethanol	413.15	-1.27	-2.81	-0.5	1.54	0.77
544-76-3	hexadecane	64-17-5	ethanol	325.25	-1.69	-2.21	-1.55	0.52	0.14
544-76-3	hexadecane	64-17-5	ethanol	293.15	-1.94	-1.99	-1.99	0.05	0.05
544-76-3	hexadecane	64-17-5	ethanol	298.15	-2.11	-2.03	-1.92	0.08	0.19
544-76-3	hexadecane	64-17-5	ethanol	298.15	-1.85	-2.03	-1.92	0.18	0.07
544-76-3	hexadecane	64-17-5	ethanol	313.15	-1.72	-2.13	-1.72	0.41	0
544-76-3	hexadecane	64-17-5	ethanol	298.15	-2.03	-2.03	-1.92	0	0.11
544-76-3	hexadecane	64-17-5	ethanol	298.15	-1.94	-2.03	-1.92	0.09	0.02
544-76-3	hexadecane	64-17-5	ethanol	293.15	-2	-1.99	-1.99	0.01	0.01
544-76-3	hexadecane	64-17-5	ethanol	303.15	-1.94	-2.06	-1.85	0.12	0.09
544-76-3	hexadecane	64-17-5	ethanol	313.15	-1.86	-2.13	-1.72	0.27	0.14
544-76-3	hexadecane	64-17-5	ethanol	323.15	-1.86	-2.19	-1.58	0.33	0.28
544-76-3	hexadecane	64-17-5	ethanol	333.15	-1.81	-2.26	-1.45	0.45	0.36
544-76-3	hexadecane	64-17-5	ethanol	343.15	-1.74	-2.33	-1.32	0.59	0.42
544-76-3	hexadecane	64-17-5	ethanol	353.15	-1.68	-2.4	-1.2	0.72	0.48
544-76-3	hexadecane	64-17-5	ethanol	317.1	-1.95	-2.15	-1.66	0.2	0.29
544-76-3	hexadecane	64-17-5	ethanol	312.15	-2	-2.12	-1.73	0.12	0.27
544-76-3	hexadecane	64-17-5	ethanol	317.15	-1.78	-2.15	-1.66	0.37	0.12
544-76-3	hexadecane	64-17-5	ethanol	303.15	-1.85	-2.06	-1.85	0.21	0
544-76-3	hexadecane	64-17-5	ethanol	313.15	-1.77	-2.13	-1.72	0.36	0.05
544-76-3	hexadecane	64-17-5	ethanol	323.15	-1.69	-2.19	-1.58	0.5	0.11
544-76-3	hexadecane	74-85-1	ethene	298.15	-0.39	-0.39	-0.55	0	0.16
544-76-3	hexadecane	74-85-1	ethene	292.65	-0.14	-0.39	-0.57	0.24	0.43
544-76-3	hexadecane	111-71-7	heptanal	363.15	-4.31	-6.42	-4.51	2.11	0.2
544-76-3	hexadecane	111-71-7	heptanal	393.15	-4.01	-6.95	-4.13	2.94	0.12
544-76-3	hexadecane	111-71-7	heptanal	423.15	-3.72	-7.48	-3.78	3.76	0.06
544-76-3	hexadecane	66-25-1	hexanal	298.15	-4.52	-4.58	-4.79	0.06	0.27
544-76-3	hexadecane	66-25-1	hexanal	333.15	-4.03	-5.12	-4.3	1.09	0.27
544-76-3	hexadecane	66-25-1	hexanal	363.15	-3.71	-5.58	-3.92	1.87	0.21
544-76-3	hexadecane	66-25-1	hexanal	393.15	-3.42	-6.04	-3.57	2.62	0.15
544-76-3	hexadecane	66-25-1	hexanal	423.15	-3.18	-6.5	-3.25	3.32	0.07
544-76-3	hexadecane	74-82-8	methane	298.15	0.55	0.44	-0.95	0.11	1.5
544-76-3	hexadecane	74-82-8	methane	300	0.44	0.44	-0.98	0.01	1.42
544-76-3	hexadecane	74-82-8	methane	325	0.5	0.48	-1.75	0.02	2.24
544-76-3	hexadecane	74-82-8	methane	350	0.55	0.52	-3.32	0.03	3.87
544-76-3	hexadecane	74-82-8	methane	375	0.6	0.55	-6.46	0.04	7.06
544-76-3	hexadecane	74-82-8	methane	400	0.64	0.59	-12.7	0.05	13.34
544-76-3	hexadecane	74-82-8	methane	425	0.67	0.63	-25.18	0.04	25.85
544-76-3	hexadecane	74-82-8	methane	450	0.69	0.66	-50.54	0.03	51.23
544-76-3	hexadecane	74-82-8	methane	475	0.7	0.7	-99.21	0	99.91
544-76-3	hexadecane	74-82-8	methane	298.15	0.46	0.44	-0.95	0.01	1.4
544-76-3	hexadecane	74-82-8	methane	313.15	0.49	0.46	-1.31	0.03	1.8
544-76-3	hexadecane	74-82-8	methane	328.15	0.5	0.48	-1.89	0.02	2.39
544-76-3	hexadecane	74-82-8	methane	298.15	0.58	0.44	-0.95	0.14	1.53
544-76-3	hexadecane	74-82-8	methane	298.15	0.32	0.44	-0.95	0.12	1.27
544-76-3	hexadecane	74-82-8	methane	298.15	0.43	0.44	-0.95	0.01	1.38
544-76-3	hexadecane	74-82-8	methane	298.15	0.43	0.44	-0.95	0.01	1.38
544-76-3	hexadecane	74-82-8	methane	373.15	0.59	0.55	-6.15	0.04	6.74
544-76-3	hexadecane	74-82-8	methane	473.15	0.69	0.7	-97.87	0.01	98.56
544-76-3	hexadecane	74-82-8	methane	298.15	0.4	0.44	-0.95	0.04	1.35
544-76-3	hexadecane	67-56-1	methanol	373.15	-0.88	-1.66	-0.09	0.78	0.79
544-76-3	hexadecane	67-56-1	methanol	393.15	-0.79	-1.74	0.11	0.96	0.9
544-76-3	hexadecane	67-56-1	methanol	403.15	-0.72	-1.79	0.21	1.07	0.93
544-76-3	hexadecane	67-56-1	methanol	298.15	-1.73	-1.32	-0.91	0.41	0.82
544-76-3	hexadecane	67-56-1	methanol	298.15	-1.33	-1.32	-0.91	0.01	0.42
544-76-3	hexadecane	67-56-1	methanol	312.15	-1.54	-1.38	-0.75	0.16	0.79
544-76-3	hexadecane	67-56-1	methanol	317.15	-1.23	-1.41	-0.69	0.18	0.54
544-76-3	hexadecane	67-56-1	methanol	298.15	-1.12	-1.32	-0.91	0.2	0.21
544-76-3	hexadecane	67-56-1	methanol	333.15	-1.02	-1.48	-0.51	0.46	0.51
544-76-3	hexadecane	67-56-1	methanol	373.15	-0.82	-1.66	-0.09	0.84	0.73
544-76-3	hexadecane	67-56-1	methanol	303.15	-1.76	-1.35	-0.85	0.41	0.91
544-76-3	hexadecane	67-56-1	methanol	298.15	-1.15	-1.32	-0.91	0.17	0.24
544-76-3	hexadecane	67-56-1	methanol	313.15	-1.06	-1.39	-0.73	0.33	0.33

Table C.1: ΔG_{solv} for binary systems (kcal/mol).

solvent		solute		T (K)	ΔG^{ref}_{solv}	$\Delta G^{calc,1}_{solv}$	$\Delta G^{calc,2}_{solv}$	$\Delta G^{calc,1}_{solv}$-ΔG^{ref}_{solv}	$\Delta G^{calc,2}_{solv}$-ΔG^{ref}_{solv}
544-76-3	hexadecane	67-56-1	methanol	293.15	-1.29	-1.3	-0.97	0.01	0.32
544-76-3	hexadecane	67-56-1	methanol	323.2	-1.41	-1.43	-0.62	0.02	0.79
544-76-3	hexadecane	67-56-1	methanol	303.15	-1.18	-1.35	-0.85	0.17	0.33
544-76-3	hexadecane	67-56-1	methanol	313.15	-1.13	-1.39	-0.73	0.26	0.4
544-76-3	hexadecane	67-56-1	methanol	323.15	-1.06	-1.43	-0.62	0.37	0.44
544-76-3	hexadecane	67-56-1	methanol	293.15	-1.4	-1.3	-0.97	0.1	0.43
544-76-3	hexadecane	67-56-1	methanol	303.15	-1.23	-1.35	-0.85	0.12	0.38
544-76-3	hexadecane	67-56-1	methanol	313.15	-1.16	-1.39	-0.73	0.23	0.43
544-76-3	hexadecane	67-56-1	methanol	323.15	-1.11	-1.43	-0.62	0.32	0.49
544-76-3	hexadecane	67-56-1	methanol	333.15	-1.12	-1.48	-0.51	0.36	0.61
544-76-3	hexadecane	67-56-1	methanol	343.15	-0.96	-1.52	-0.4	0.56	0.56
544-76-3	hexadecane	67-56-1	methanol	293.15	-1.19	-1.3	-0.97	0.11	0.22
544-76-3	hexadecane	67-56-1	methanol	317.1	-1.46	-1.41	-0.69	0.05	0.77
544-76-3	hexadecane	108-87-2	methylcyclohexane	333.15	-4.02	-5.06	-4.05	1.04	0.03
544-76-3	hexadecane	108-87-2	methylcyclohexane	323.15	-4.07	-4.91	-4.16	0.84	0.09
544-76-3	hexadecane	108-87-2	methylcyclohexane	323.15	-4.07	-4.91	-4.16	0.84	0.09
544-76-3	hexadecane	96-37-7	methylcyclopentane	303.15	-3.72	-3.9	-3.79	0.18	0.07
544-76-3	hexadecane	96-37-7	methylcyclopentane	333.15	-3.41	-4.29	-3.47	0.88	0.06
544-76-3	hexadecane	124-13-0	octanal	298.15	-5.82	-5.95	-6.14	0.13	0.32
544-76-3	hexadecane	110-62-3	pentanal	333.15	-3.39	-4.34	-3.67	0.95	0.28
544-76-3	hexadecane	110-62-3	pentanal	363.15	-3.09	-4.74	-3.33	1.65	0.24
544-76-3	hexadecane	110-62-3	pentanal	393.15	-2.8	-5.13	-3.02	2.33	0.22
544-76-3	hexadecane	110-62-3	pentanal	423.15	-2.58	-5.52	-2.72	2.94	0.14
544-76-3	hexadecane	74-98-6	propane	293.15	-1.53	-1.41	-1.71	0.12	0.18
544-76-3	hexadecane	74-98-6	propane	425	-0.78	-2.04	-0.8	1.26	0.02
544-76-3	hexadecane	74-98-6	propane	450	-0.69	-2.16	-0.65	1.47	0.04
544-76-3	hexadecane	74-98-6	propane	475	-0.61	-2.28	-0.51	1.68	0.1
544-76-3	hexadecane	74-98-6	propane	298.15	-1.41	-1.43	-1.67	0.02	0.26
544-76-3	hexadecane	74-98-6	propane	303.15	-1.39	-1.46	-1.63	0.07	0.24
544-76-3	hexadecane	74-98-6	propane	323.15	-1.27	-1.55	-1.49	0.28	0.22
544-76-3	hexadecane	74-98-6	propane	343.15	-1.15	-1.65	-1.35	0.5	0.2
544-76-3	hexadecane	74-98-6	propane	498	-0.33	-2.39	-0.39	2.06	0.06
544-76-3	hexadecane	74-98-6	propane	298.15	-1.41	-1.43	-1.67	0.02	0.26
544-76-3	hexadecane	74-98-6	propane	308.15	-1.37	-1.48	-1.59	0.11	0.22
544-76-3	hexadecane	74-98-6	propane	318.15	-1.32	-1.53	-1.52	0.21	0.2
544-76-3	hexadecane	74-98-6	propane	298.15	-1.43	-1.43	-1.67	0	0.24
544-76-3	hexadecane	74-98-6	propane	300	-1.37	-1.44	-1.65	0.07	0.28
544-76-3	hexadecane	74-98-6	propane	325	-1.24	-1.56	-1.47	0.32	0.23
544-76-3	hexadecane	74-98-6	propane	350	-1.12	-1.68	-1.31	0.56	0.19
544-76-3	hexadecane	74-98-6	propane	375	-1	-1.8	-1.13	0.8	0.13
544-76-3	hexadecane	74-98-6	propane	400	-0.89	-1.92	-0.96	1.03	0.07
544-76-3	hexadecane	74-98-6	propane	298.15	-1.39	-1.43	-1.67	0.04	0.28
544-76-3	hexadecane	74-98-6	propane	313.15	-1.33	-1.5	-1.56	0.17	0.23
544-76-3	hexadecane	74-98-6	propane	328.15	-1.24	-1.58	-1.45	0.34	0.21
544-76-3	hexadecane	74-98-6	propane	298.15	-1.43	-1.43	-1.67	0	0.24
544-76-3	hexadecane	74-98-6	propane	298.15	-1.42	-1.43	-1.67	0.01	0.25
544-76-3	hexadecane	74-98-6	propane	298.15	-1.44	-1.43	-1.67	0.01	0.23
544-76-3	hexadecane	109-99-9	tetrahydrofuran	293.15	-3.49	-3.53	-3.62	0.04	0.13
544-76-3	hexadecane	109-99-9	tetrahydrofuran	303.15	-3.38	-3.66	-3.5	0.28	0.12
544-76-3	hexadecane	109-99-9	tetrahydrofuran	313.15	-3.29	-3.78	-3.39	0.49	0.1
544-76-3	hexadecane	109-99-9	tetrahydrofuran	298.15	-3.43	-3.59	-3.56	0.16	0.13
544-76-3	hexadecane	109-99-9	tetrahydrofuran	298.15	-3.43	-3.59	-3.56	0.16	0.13
544-76-3	hexadecane	7732-18-5	water	298.15	-0.48	-0.35	1.75	0.13	2.23
544-76-3	hexadecane	7732-18-5	water	293.15	-0.66	-0.35	1.69	0.31	2.35
544-76-3	hexadecane	7732-18-5	water	298.15	-0.35	-0.35	1.75	0.01	2.1
110-54-3	hexane	106-98-9	1-butene	298.15	-2.49	-2.37	-2.4	0.12	0.09
110-54-3	hexane	592-41-6	1-hexene	353.15	-3.43	-4.52	-3.31	1.09	0.12
110-54-3	hexane	592-41-6	1-hexene	333.15	-3.56	-4.26	-3.51	0.7	0.05
110-54-3	hexane	592-41-6	1-hexene	333.15	-3.57	-4.26	-3.51	0.69	0.06
110-54-3	hexane	592-41-6	1-hexene	333.15	-3.56	-4.26	-3.51	0.7	0.05
110-54-3	hexane	592-41-6	1-hexene	333.15	-3.56	-4.26	-3.51	0.7	0.05
110-54-3	hexane	592-41-6	1-hexene	333.15	-3.57	-4.26	-3.51	0.69	0.06
110-54-3	hexane	592-41-6	1-hexene	333.15	-3.57	-4.26	-3.51	0.69	0.06
110-54-3	hexane	592-41-6	1-hexene	328.15	-3.61	-4.2	-3.56	0.59	0.05
110-54-3	hexane	592-41-6	1-hexene	328.15	-3.62	-4.2	-3.56	0.58	0.06
110-54-3	hexane	592-41-6	1-hexene	328.15	-3.62	-4.2	-3.56	0.58	0.06
110-54-3	hexane	592-41-6	1-hexene	328.15	-3.63	-4.2	-3.56	0.57	0.07

Table C.1: ΔG_{solv} for binary systems (kcal/mol).

solvent		solute		T (K)	ΔG^{ref}_{solv}	$\Delta G^{calc,1}_{solv}$	$\Delta G^{calc,2}_{solv}$	$\Delta G^{calc,1}_{solv}$-ΔG^{ref}_{solv}	$\Delta G^{calc,2}_{solv}$-ΔG^{ref}_{solv}
110-54-3	hexane	592-41-6	1-hexene	328.15	-3.62	-4.2	-3.56	0.58	0.06
110-54-3	hexane	592-41-6	1-hexene	328.15	-3.62	-4.2	-3.56	0.58	0.06
110-54-3	hexane	592-41-6	1-hexene	353.15	-3.41	-4.52	-3.31	1.11	0.1
110-54-3	hexane	592-41-6	1-hexene	353.15	-3.42	-4.52	-3.31	1.1	0.11
110-54-3	hexane	592-41-6	1-hexene	320.95	-3.69	-4.11	-3.63	0.42	0.06
110-54-3	hexane	592-41-6	1-hexene	341.05	-3.49	-4.36	-3.43	0.87	0.06
110-54-3	hexane	592-41-6	1-hexene	340.95	-3.48	-4.36	-3.43	0.88	0.05
110-54-3	hexane	592-41-6	1-hexene	307.4	-3.82	-3.93	-3.77	0.11	0.05
110-54-3	hexane	592-41-6	1-hexene	307.24	-3.82	-3.93	-3.77	0.11	0.05
110-54-3	hexane	592-41-6	1-hexene	307	-3.83	-3.93	-3.77	0.1	0.06
110-54-3	hexane	592-41-6	1-hexene	306.82	-3.83	-3.93	-3.77	0.1	0.06
110-54-3	hexane	592-41-6	1-hexene	306.59	-3.83	-3.92	-3.78	0.09	0.05
110-54-3	hexane	592-41-6	1-hexene	306.29	-3.84	-3.92	-3.78	0.08	0.06
110-54-3	hexane	592-41-6	1-hexene	306.02	-3.84	-3.91	-3.78	0.07	0.06
110-54-3	hexane	592-41-6	1-hexene	305.84	-3.84	-3.91	-3.78	0.07	0.06
110-54-3	hexane	592-41-6	1-hexene	305.61	-3.84	-3.91	-3.79	0.07	0.05
110-54-3	hexane	592-41-6	1-hexene	305.43	-3.85	-3.91	-3.79	0.06	0.06
110-54-3	hexane	592-41-6	1-hexene	325.88	-3.63	-4.17	-3.58	0.54	0.05
110-54-3	hexane	592-41-6	1-hexene	325.6	-3.63	-4.17	-3.58	0.54	0.05
110-54-3	hexane	592-41-6	1-hexene	325.32	-3.64	-4.16	-3.59	0.52	0.05
110-54-3	hexane	592-41-6	1-hexene	325.23	-3.65	-4.16	-3.59	0.51	0.06
110-54-3	hexane	592-41-6	1-hexene	324.97	-3.65	-4.16	-3.59	0.51	0.06
110-54-3	hexane	592-41-6	1-hexene	324.76	-3.65	-4.15	-3.59	0.5	0.06
110-54-3	hexane	592-41-6	1-hexene	324.42	-3.65	-4.15	-3.6	0.5	0.05
110-54-3	hexane	592-41-6	1-hexene	324.21	-3.66	-4.15	-3.6	0.49	0.06
110-54-3	hexane	592-41-6	1-hexene	323.91	-3.66	-4.14	-3.6	0.48	0.06
110-54-3	hexane	592-41-6	1-hexene	323.62	-3.66	-4.14	-3.6	0.48	0.06
110-54-3	hexane	592-41-6	1-hexene	323.22	-3.67	-4.13	-3.61	0.46	0.06
110-54-3	hexane	592-41-6	1-hexene	341.73	-3.49	-4.37	-3.42	0.88	0.07
110-54-3	hexane	592-41-6	1-hexene	341.57	-3.49	-4.37	-3.43	0.88	0.06
110-54-3	hexane	592-41-6	1-hexene	341.4	-3.47	-4.37	-3.43	0.9	0.04
110-54-3	hexane	592-41-6	1-hexene	341.14	-3.48	-4.36	-3.43	0.88	0.05
110-54-3	hexane	592-41-6	1-hexene	340.83	-3.49	-4.36	-3.43	0.87	0.06
110-54-3	hexane	592-41-6	1-hexene	340.54	-3.5	-4.36	-3.44	0.86	0.06
110-54-3	hexane	592-41-6	1-hexene	340.24	-3.5	-4.35	-3.44	0.85	0.06
110-54-3	hexane	592-41-6	1-hexene	339.76	-3.5	-4.35	-3.44	0.85	0.06
110-54-3	hexane	592-41-6	1-hexene	339.57	-3.5	-4.34	-3.45	0.84	0.05
110-54-3	hexane	107-83-5	2-methylpentane	298.15	-3.9	-3.74	-3.85	0.16	0.05
110-54-3	hexane	107-83-5	2-methylpentane	298.15	-3.86	-3.74	-3.85	0.12	0.01
110-54-3	hexane	75-28-5	2-methylpropane	298.15	-2.34	-2.28	-2.4	0.06	0.06
110-54-3	hexane	110-82-7	cyclohexane	343.15	-3.83	-4.93	-3.84	1.1	0.01
110-54-3	hexane	110-82-7	cyclohexane	346.05	-3.8	-4.97	-3.81	1.17	0.01
110-54-3	hexane	110-82-7	cyclohexane	345.2	-3.8	-4.96	-3.82	1.16	0.02
110-54-3	hexane	110-82-7	cyclohexane	343.55	-3.8	-4.94	-3.84	1.14	0.04
110-54-3	hexane	110-82-7	cyclohexane	346.75	-3.79	-4.98	-3.81	1.19	0.02
110-54-3	hexane	110-82-7	cyclohexane	346.55	-3.79	-4.98	-3.81	1.19	0.02
110-54-3	hexane	110-82-7	cyclohexane	346.4	-3.79	-4.98	-3.81	1.19	0.02
110-54-3	hexane	110-82-7	cyclohexane	345.9	-3.79	-4.97	-3.82	1.18	0.03
110-54-3	hexane	110-82-7	cyclohexane	345.25	-3.79	-4.96	-3.82	1.17	0.03
110-54-3	hexane	110-82-7	cyclohexane	344.85	-3.8	-4.96	-3.83	1.16	0.03
110-54-3	hexane	110-82-7	cyclohexane	344.55	-3.8	-4.95	-3.83	1.15	0.03
110-54-3	hexane	110-82-7	cyclohexane	344.1	-3.79	-4.95	-3.83	1.16	0.04
110-54-3	hexane	110-82-7	cyclohexane	344.05	-3.79	-4.94	-3.83	1.15	0.04
110-54-3	hexane	110-82-7	cyclohexane	343.95	-3.81	-4.94	-3.84	1.13	0.03
110-54-3	hexane	110-82-7	cyclohexane	343.7	-3.8	-4.94	-3.84	1.14	0.04
110-54-3	hexane	110-82-7	cyclohexane	343.5	-3.81	-4.94	-3.84	1.13	0.03
110-54-3	hexane	110-82-7	cyclohexane	343.3	-3.79	-4.93	-3.84	1.14	0.05
110-54-3	hexane	110-82-7	cyclohexane	343.1	-3.79	-4.93	-3.84	1.14	0.05
110-54-3	hexane	110-82-7	cyclohexane	342.9	-3.82	-4.93	-3.85	1.11	0.03
110-54-3	hexane	110-82-7	cyclohexane	342.5	-3.79	-4.92	-3.85	1.13	0.06
110-54-3	hexane	110-82-7	cyclohexane	342.2	-3.78	-4.92	-3.85	1.14	0.07
110-54-3	hexane	110-82-7	cyclohexane	342.2	-3.78	-4.92	-3.85	1.14	0.07
110-54-3	hexane	110-82-7	cyclohexane	342.5	-3.79	-4.92	-3.85	1.13	0.06
110-54-3	hexane	110-82-7	cyclohexane	342.9	-3.82	-4.93	-3.85	1.11	0.03
110-54-3	hexane	110-82-7	cyclohexane	343.1	-3.79	-4.93	-3.84	1.14	0.05
110-54-3	hexane	110-82-7	cyclohexane	343.3	-3.79	-4.93	-3.84	1.14	0.05
110-54-3	hexane	110-82-7	cyclohexane	343.5	-3.81	-4.94	-3.84	1.13	0.03

Table C.1: ΔG_{solv} for binary systems (kcal/mol).

solvent		solute		T (K)	ΔG^{ref}_{solv}	$\Delta G^{calc,1}_{solv}$	$\Delta G^{calc,2}_{solv}$	$\Delta G^{calc,1}_{solv}$-ΔG^{ref}_{solv}	$\Delta G^{calc,2}_{solv}$-ΔG^{ref}_{solv}
110-54-3	hexane	110-82-7	cyclohexane	343.7	-3.8	-4.94	-3.84	1.14	0.04
110-54-3	hexane	110-82-7	cyclohexane	343.95	-3.81	-4.94	-3.84	1.13	0.03
110-54-3	hexane	110-82-7	cyclohexane	344.05	-3.79	-4.94	-3.83	1.15	0.04
110-54-3	hexane	110-82-7	cyclohexane	344.1	-3.79	-4.95	-3.83	1.16	0.04
110-54-3	hexane	110-82-7	cyclohexane	344.55	-3.8	-4.95	-3.83	1.15	0.03
110-54-3	hexane	110-82-7	cyclohexane	344.85	-3.8	-4.96	-3.83	1.16	0.03
110-54-3	hexane	110-82-7	cyclohexane	345.25	-3.79	-4.96	-3.82	1.17	0.03
110-54-3	hexane	110-82-7	cyclohexane	345.9	-3.79	-4.97	-3.82	1.18	0.03
110-54-3	hexane	110-82-7	cyclohexane	346.4	-3.79	-4.98	-3.81	1.19	0.02
110-54-3	hexane	110-82-7	cyclohexane	346.55	-3.79	-4.98	-3.81	1.19	0.02
110-54-3	hexane	110-82-7	cyclohexane	346.75	-3.79	-4.98	-3.81	1.19	0.02
110-54-3	hexane	110-82-7	cyclohexane	343.6	-3.79	-4.94	-3.84	1.15	0.05
110-54-3	hexane	110-82-7	cyclohexane	300.95	-4.23	-4.33	-4.28	0.1	0.05
110-54-3	hexane	110-82-7	cyclohexane	315.25	-4.07	-4.53	-4.13	0.46	0.06
110-54-3	hexane	110-82-7	cyclohexane	331.95	-3.91	-4.77	-3.96	0.86	0.05
110-54-3	hexane	110-82-7	cyclohexane	340.25	-3.83	-4.89	-3.87	1.06	0.04
110-54-3	hexane	110-82-7	cyclohexane	298.15	-4.26	-4.29	-4.31	0.03	0.05
110-54-3	hexane	110-82-7	cyclohexane	341	-3.83	-4.9	-3.86	1.07	0.03
110-54-3	hexane	110-82-7	cyclohexane	298.15	-4.23	-4.29	-4.31	0.06	0.08
110-54-3	hexane	108-94-1	cyclohexanone	297.95	-5.03	-5.36	-5.67	0.33	0.64
110-54-3	hexane	108-94-1	cyclohexanone	315.05	-4.9	-5.67	-5.44	0.77	0.54
110-54-3	hexane	108-94-1	cyclohexanone	331.95	-4.7	-5.98	-5.22	1.28	0.52
110-54-3	hexane	74-84-0	ethane	338.71	-1.24	-1.2	-0.9	0.04	0.34
110-54-3	hexane	74-84-0	ethane	298.15	-1.03	-1.06	-1.12	0.03	0.09
110-54-3	hexane	64-17-5	ethanol	323.15	-2.6	-2.52	-1.79	0.08	0.81
110-54-3	hexane	64-17-5	ethanol	323.15	-2.53	-2.52	-1.79	0.01	0.74
110-54-3	hexane	64-17-5	ethanol	323.15	-2.53	-2.52	-1.79	0.01	0.74
110-54-3	hexane	64-17-5	ethanol	313.15	-2.31	-2.44	-1.92	0.13	0.39
110-54-3	hexane	64-17-5	ethanol	336.65	-1.69	-2.62	-1.61	0.93	0.08
110-54-3	hexane	64-17-5	ethanol	304.75	-2.29	-2.38	-2.03	0.09	0.26
110-54-3	hexane	64-17-5	ethanol	322.55	-2.18	-2.51	-1.79	0.33	0.39
110-54-3	hexane	64-17-5	ethanol	298.15	-2.23	-2.32	-2.12	0.09	0.11
110-54-3	hexane	64-17-5	ethanol	313.15	-2.18	-2.44	-1.92	0.26	0.26
110-54-3	hexane	64-17-5	ethanol	333.25	-1.93	-2.6	-1.65	0.67	0.28
110-54-3	hexane	64-17-5	ethanol	298.15	-2.17	-2.32	-2.12	0.15	0.05
110-54-3	hexane	64-17-5	ethanol	308.15	-2.11	-2.4	-1.99	0.29	0.12
110-54-3	hexane	64-17-5	ethanol	313.15	-2.07	-2.44	-1.92	0.37	0.15
110-54-3	hexane	64-17-5	ethanol	318.15	-2.05	-2.48	-1.85	0.43	0.2
110-54-3	hexane	64-17-5	ethanol	288.15	-2.25	-2.25	-2.27	0	0.02
110-54-3	hexane	64-17-5	ethanol	293.15	-2.22	-2.29	-2.19	0.07	0.03
110-54-3	hexane	64-17-5	ethanol	298.15	-2.18	-2.32	-2.12	0.14	0.06
110-54-3	hexane	64-17-5	ethanol	303.15	-2.14	-2.36	-2.06	0.22	0.08
110-54-3	hexane	64-17-5	ethanol	308.15	-2.12	-2.4	-1.99	0.28	0.13
110-54-3	hexane	64-17-5	ethanol	313.15	-2.08	-2.44	-1.92	0.36	0.16
110-54-3	hexane	64-17-5	ethanol	318.15	-2.03	-2.48	-1.85	0.45	0.18
110-54-3	hexane	64-17-5	ethanol	297.15	-2.18	-2.32	-2.14	0.14	0.04
110-54-3	hexane	64-17-5	ethanol	297.35	-2.22	-2.32	-2.14	0.1	0.08
110-54-3	hexane	64-17-5	ethanol	297.65	-2.2	-2.32	-2.13	0.12	0.07
110-54-3	hexane	64-17-5	ethanol	316.55	-2.01	-2.47	-1.87	0.46	0.14
110-54-3	hexane	64-17-5	ethanol	316.65	-2.04	-2.47	-1.87	0.43	0.17
110-54-3	hexane	64-17-5	ethanol	333.95	-1.95	-2.6	-1.64	0.65	0.31
110-54-3	hexane	64-17-5	ethanol	333.95	-1.93	-2.6	-1.64	0.67	0.29
110-54-3	hexane	64-17-5	ethanol	351.45	-1.83	-2.74	-1.42	0.91	0.41
110-54-3	hexane	64-17-5	ethanol	351.55	-1.82	-2.74	-1.42	0.92	0.4
110-54-3	hexane	64-17-5	ethanol	298.15	-2.61	-2.32	-2.12	0.29	0.49
110-54-3	hexane	74-85-1	ethene	298.15	-0.64	-0.76	-0.69	0.12	0.04
110-54-3	hexane	74-82-8	methane	298.15	0.03	0.03	-1.04	0	1.07
110-54-3	hexane	67-56-1	methanol	340.21	-1.3	-1.86	-0.59	0.56	0.71
110-54-3	hexane	67-56-1	methanol	337.17	-1.46	-1.84	-0.62	0.38	0.84
110-54-3	hexane	67-56-1	methanol	335.8	-1.54	-1.83	-0.64	0.29	0.9
110-54-3	hexane	67-56-1	methanol	326.25	-2.02	-1.78	-0.74	0.24	1.28
110-54-3	hexane	67-56-1	methanol	298.15	-1.47	-1.63	-1.07	0.16	0.4
110-54-3	hexane	67-56-1	methanol	303.15	-1.43	-1.66	-1.01	0.23	0.42
110-54-3	hexane	67-56-1	methanol	313.15	-1.36	-1.71	-0.89	0.35	0.47
110-54-3	hexane	67-56-1	methanol	318.15	-1.32	-1.74	-0.83	0.42	0.49
110-54-3	hexane	67-56-1	methanol	288.15	-1.55	-1.57	-1.19	0.02	0.36
110-54-3	hexane	67-56-1	methanol	293.15	-1.54	-1.6	-1.12	0.06	0.42

Table C.1: ΔG_{solv} for binary systems (kcal/mol).

solvent		solute		T (K)	ΔG^{ref}_{solv}	$\Delta G^{calc,1}_{solv}$	$\Delta G^{calc,2}_{solv}$	$\Delta G^{calc,1}_{solv}$-ΔG^{ref}_{solv}	$\Delta G^{calc,2}_{solv}$-ΔG^{ref}_{solv}
110-54-3	hexane	67-56-1	methanol	298.15	-1.49	-1.63	-1.07	0.14	0.42
110-54-3	hexane	67-56-1	methanol	303.15	-1.46	-1.66	-1.01	0.2	0.45
110-54-3	hexane	67-56-1	methanol	308.15	-1.42	-1.68	-0.95	0.26	0.47
110-54-3	hexane	67-56-1	methanol	313.15	-1.4	-1.71	-0.89	0.31	0.51
110-54-3	hexane	67-56-1	methanol	318.15	-1.37	-1.74	-0.83	0.37	0.54
110-54-3	hexane	67-56-1	methanol	263.15	-1.62	-1.44	-1.5	0.18	0.12
110-54-3	hexane	67-56-1	methanol	273.15	-1.59	-1.49	-1.37	0.1	0.22
110-54-3	hexane	67-56-1	methanol	293.15	-1.38	-1.6	-1.12	0.22	0.26
110-54-3	hexane	67-56-1	methanol	313.15	-1.22	-1.71	-0.89	0.49	0.33
110-54-3	hexane	67-56-1	methanol	313.15	-1.42	-1.71	-0.89	0.29	0.53
110-54-3	hexane	67-56-1	methanol	333.25	-1.19	-1.82	-0.66	0.63	0.53
110-54-3	hexane	67-56-1	methanol	341.2	-1.1	-1.86	-0.58	0.76	0.52
110-54-3	hexane	67-56-1	methanol	293.15	-1.42	-1.6	-1.12	0.18	0.3
110-54-3	hexane	67-56-1	methanol	293.15	-1.38	-1.6	-1.12	0.22	0.26
110-54-3	hexane	108-87-2	methylcyclohexane	353.75	-4.15	-5.67	-4.14	1.52	0.01
110-54-3	hexane	108-87-2	methylcyclohexane	353.51	-4.14	-5.67	-4.14	1.53	0
110-54-3	hexane	108-87-2	methylcyclohexane	353	-4.15	-5.66	-4.15	1.51	0
110-54-3	hexane	108-87-2	methylcyclohexane	352.6	-4.16	-5.65	-4.15	1.49	0.01
110-54-3	hexane	108-87-2	methylcyclohexane	351.85	-4.15	-5.64	-4.16	1.49	0.01
110-54-3	hexane	108-87-2	methylcyclohexane	351.55	-4.16	-5.63	-4.16	1.47	0
110-54-3	hexane	108-87-2	methylcyclohexane	350.8	-4.16	-5.62	-4.17	1.46	0.01
110-54-3	hexane	108-87-2	methylcyclohexane	345.25	-4.2	-5.53	-4.23	1.33	0.03
110-54-3	hexane	108-87-2	methylcyclohexane	345.2	-4.23	-5.53	-4.23	1.3	0
110-54-3	hexane	108-87-2	methylcyclohexane	344.65	-4.23	-5.52	-4.23	1.29	0
110-54-3	hexane	108-87-2	methylcyclohexane	343.7	-4.24	-5.51	-4.24	1.27	0
110-54-3	hexane	96-37-7	methylcyclopentane	333.15	-3.75	-4.59	-3.75	0.84	0
110-54-3	hexane	96-37-7	methylcyclopentane	333.15	-3.74	-4.59	-3.75	0.85	0.01
110-54-3	hexane	96-37-7	methylcyclopentane	333.15	-3.74	-4.59	-3.75	0.85	0.01
110-54-3	hexane	96-37-7	methylcyclopentane	333.15	-3.73	-4.59	-3.75	0.86	0.02
110-54-3	hexane	74-98-6	propane	298.15	-1.8	-1.8	-1.85	0	0.05
110-54-3	hexane	109-99-9	tetrahydrofuran	313.15	-3.53	-4.04	-3.64	0.51	0.11
110-54-3	hexane	109-99-9	tetrahydrofuran	313.15	-3.53	-4.04	-3.64	0.51	0.11
110-54-3	hexane	109-99-9	tetrahydrofuran	313.15	-3.56	-4.04	-3.64	0.48	0.08
110-54-3	hexane	109-99-9	tetrahydrofuran	333.15	-3.34	-4.3	-3.43	0.96	0.09
110-54-3	hexane	109-99-9	tetrahydrofuran	333.15	-3.37	-4.3	-3.43	0.93	0.06
110-54-3	hexane	109-99-9	tetrahydrofuran	333.15	-3.34	-4.3	-3.43	0.96	0.09
110-54-3	hexane	109-99-9	tetrahydrofuran	340.36	-3.32	-4.4	-3.36	1.08	0.04
110-54-3	hexane	109-99-9	tetrahydrofuran	304.75	-3.64	-3.94	-3.73	0.3	0.09
110-54-3	hexane	109-99-9	tetrahydrofuran	322.35	-3.45	-4.16	-3.54	0.71	0.09
110-54-3	hexane	109-99-9	tetrahydrofuran	340.15	-3.28	-4.39	-3.36	1.11	0.08
110-54-3	hexane	109-99-9	tetrahydrofuran	313.15	-3.51	-4.04	-3.64	0.53	0.13
110-54-3	hexane	109-99-9	tetrahydrofuran	333.15	-3.33	-4.3	-3.43	0.97	0.1
110-54-3	hexane	7732-18-5	water	298.15	-0.75	-0.75	1.64	0.01	2.39
110-54-3	hexane	7732-18-5	water	283.15	-0.86	-0.71	1.46	0.15	2.32
110-54-3	hexane	7732-18-5	water	303.15	-0.75	-0.76	1.7	0	2.45
110-54-3	hexane	7732-18-5	water	293.15	-0.63	-0.73	1.58	0.1	2.21
110-54-3	hexane	7732-18-5	water	293.15	-1.08	-0.73	1.58	0.35	2.66
110-54-3	hexane	7732-18-5	water	293.15	-1.04	-0.73	1.58	0.31	2.62
110-54-3	hexane	7732-18-5	water	298.15	-0.66	-0.75	1.64	0.09	2.3
110-54-3	hexane	7732-18-5	water	298.15	-0.82	-0.75	1.64	0.07	2.45
110-54-3	hexane	7732-18-5	water	303.15	-0.77	-0.76	1.7	0.01	2.47
110-54-3	hexane	7732-18-5	water	293.15	-0.84	-0.73	1.58	0.11	2.42
110-54-3	hexane	7732-18-5	water	298.15	-0.49	-0.75	1.64	0.25	2.13
110-54-3	hexane	7732-18-5	water	298.15	-0.56	-0.75	1.64	0.19	2.19
110-54-3	hexane	7732-18-5	water	293.15	-0.79	-0.73	1.58	0.05	2.36
110-54-3	hexane	7732-18-5	water	303.15	-0.81	-0.76	1.7	0.05	2.51
111-84-2	nonane	106-98-9	1-butene	298.15	-2.43	-2.25	-2.28	0.18	0.15
111-84-2	nonane	107-83-5	2-methylpentane	298.15	-3.66	-3.62	-3.71	0.04	0.05
111-84-2	nonane	107-83-5	2-methylpentane	298.15	-3.67	-3.62	-3.71	0.05	0.04
111-84-2	nonane	75-28-5	2-methylpropane	298.15	-2.27	-2.16	-2.29	0.11	0.02
111-84-2	nonane	75-28-5	2-methylpropane	278.15	-2.27	-2.01	-2.45	0.26	0.18
111-84-2	nonane	75-28-5	2-methylpropane	298.15	-2.14	-2.16	-2.29	0.02	0.15
111-84-2	nonane	75-28-5	2-methylpropane	323.15	-2	-2.34	-2.09	0.34	0.09
111-84-2	nonane	75-28-5	2-methylpropane	343.15	-1.88	-2.48	-1.95	0.6	0.07
111-84-2	nonane	110-82-7	cyclohexane	420.8	-2.94	-5.89	-2.99	2.95	0.05
111-84-2	nonane	110-82-7	cyclohexane	298.15	-4.13	-4.17	-4.19	0.04	0.06
111-84-2	nonane	110-82-7	cyclohexane	298.15	-4.13	-4.17	-4.19	0.04	0.06

Table C.1: ΔG_{solv} for binary systems (kcal/mol).

solvent		solute		T (K)	ΔG_{solv}^{ref}	$\Delta G_{solv}^{calc,1}$	$\Delta G_{solv}^{calc,2}$	$\Delta G_{solv}^{calc,1}$-ΔG_{solv}^{ref}	$\Delta G_{solv}^{calc,2}$-ΔG_{solv}^{ref}
111-84-2	nonane	74-84-0	ethane	278.15	-1.01	-0.87	-1.16	0.14	0.15
111-84-2	nonane	74-84-0	ethane	298.15	-0.91	-0.93	-1.05	0.02	0.14
111-84-2	nonane	74-84-0	ethane	323.15	-0.8	-1.01	-0.92	0.21	0.12
111-84-2	nonane	74-84-0	ethane	343.15	-0.72	-1.07	-0.81	0.36	0.1
111-84-2	nonane	74-84-0	ethane	298.15	-0.93	-0.93	-1.05	0	0.12
111-84-2	nonane	64-17-5	ethanol	333.15	-1.96	-2.47	-1.56	0.51	0.4
111-84-2	nonane	64-17-5	ethanol	296.05	-2.15	-2.19	-2.06	0.04	0.09
111-84-2	nonane	64-17-5	ethanol	296.05	-2.14	-2.19	-2.06	0.05	0.08
111-84-2	nonane	64-17-5	ethanol	302.35	-2.1	-2.24	-1.97	0.14	0.13
111-84-2	nonane	64-17-5	ethanol	312.25	-2.01	-2.31	-1.83	0.3	0.18
111-84-2	nonane	64-17-5	ethanol	312.35	-2.01	-2.31	-1.83	0.3	0.18
111-84-2	nonane	64-17-5	ethanol	314.95	-1.99	-2.33	-1.8	0.34	0.19
111-84-2	nonane	64-17-5	ethanol	315.45	-1.98	-2.34	-1.79	0.36	0.19
111-84-2	nonane	64-17-5	ethanol	323.65	-1.94	-2.4	-1.68	0.46	0.26
111-84-2	nonane	64-17-5	ethanol	323.65	-1.92	-2.4	-1.68	0.48	0.24
111-84-2	nonane	64-17-5	ethanol	333.85	-1.86	-2.47	-1.55	0.61	0.31
111-84-2	nonane	64-17-5	ethanol	333.95	-1.85	-2.47	-1.55	0.62	0.3
111-84-2	nonane	64-17-5	ethanol	355.45	-1.72	-2.63	-1.28	0.91	0.44
111-84-2	nonane	64-17-5	ethanol	355.45	-1.72	-2.63	-1.28	0.91	0.44
111-84-2	nonane	74-85-1	ethene	298.15	-0.59	-0.64	-0.62	0.05	0.04
111-84-2	nonane	74-85-1	ethene	278.09	-0.7	-0.59	-0.7	0.11	0
111-84-2	nonane	74-85-1	ethene	298.14	-0.61	-0.64	-0.62	0.03	0.01
111-84-2	nonane	74-85-1	ethene	323.18	-0.52	-0.69	-0.52	0.18	0
111-84-2	nonane	74-85-1	ethene	343.15	-0.45	-0.73	-0.46	0.29	0.01
111-84-2	nonane	74-82-8	methane	278.15	0.14	0.15	-0.72	0	0.86
111-84-2	nonane	74-82-8	methane	298.15	0.2	0.16	-0.99	0.04	1.19
111-84-2	nonane	74-82-8	methane	323.15	0.25	0.17	-1.71	0.08	1.97
111-84-2	nonane	74-82-8	methane	343.15	0.29	0.18	-2.82	0.11	3.11
111-84-2	nonane	74-82-8	methane	298.15	0.2	0.16	-0.99	0.04	1.19
111-84-2	nonane	67-56-1	methanol	293.15	-1.45	-1.49	-1.05	0.04	0.4
111-84-2	nonane	74-98-6	propane	298.15	-1.72	-1.68	-1.76	0.04	0.04
111-84-2	nonane	74-98-6	propane	298.15	-1.7	-1.68	-1.76	0.02	0.06
111-84-2	nonane	7732-18-5	water	298.15	-0.53	-0.62	1.69	0.09	2.22
111-65-9	octane	106-98-9	1-butene	298.15	-2.45	-2.25	-2.31	0.2	0.14
111-65-9	octane	592-76-7	1-heptene	328.15	-4.07	-4.76	-4.1	0.69	0.03
111-65-9	octane	592-41-6	1-hexene	328.15	-3.54	-4.05	-3.44	0.51	0.1
111-65-9	octane	592-41-6	1-hexene	328.15	-3.54	-4.05	-3.44	0.51	0.1
111-65-9	octane	592-41-6	1-hexene	328.15	-3.52	-4.05	-3.44	0.53	0.08
111-65-9	octane	592-41-6	1-hexene	328.15	-3.52	-4.05	-3.44	0.53	0.08
111-65-9	octane	592-41-6	1-hexene	328.15	-3.51	-4.05	-3.44	0.54	0.07
111-65-9	octane	109-67-1	1-pentene	293.15	-3.15	-2.94	-3.08	0.21	0.07
111-65-9	octane	107-83-5	2-methylpentane	298.15	-3.71	-3.59	-3.74	0.12	0.03
111-65-9	octane	75-28-5	2-methylpropane	298.15	-2.3	-2.15	-2.32	0.15	0.02
111-65-9	octane	110-82-7	cyclohexane	298.15	-4.18	-4.18	-4.22	0	0.04
111-65-9	octane	110-82-7	cyclohexane	298.15	-4.18	-4.18	-4.22	0	0.04
111-65-9	octane	110-82-7	cyclohexane	298.15	-4.18	-4.18	-4.22	0	0.04
111-65-9	octane	110-82-7	cyclohexane	298.15	-4.18	-4.18	-4.22	0	0.04
111-65-9	octane	110-82-7	cyclohexane	298.15	-4.18	-4.18	-4.22	0	0.04
111-65-9	octane	110-82-7	cyclohexane	298.15	-4.18	-4.18	-4.22	0	0.04
111-65-9	octane	110-82-7	cyclohexane	298.15	-4.18	-4.18	-4.22	0	0.04
111-65-9	octane	110-82-7	cyclohexane	298.15	-4.18	-4.18	-4.22	0	0.04
111-65-9	octane	110-82-7	cyclohexane	298.15	-4.18	-4.18	-4.22	0	0.04
111-65-9	octane	110-82-7	cyclohexane	298.15	-4.18	-4.18	-4.22	0	0.04
111-65-9	octane	110-82-7	cyclohexane	396.25	-3.28	-5.56	-3.24	2.28	0.04
111-65-9	octane	110-82-7	cyclohexane	393.84	-3.29	-5.52	-3.26	2.23	0.03
111-65-9	octane	110-82-7	cyclohexane	391.95	-3.31	-5.5	-3.28	2.19	0.03
111-65-9	octane	110-82-7	cyclohexane	391.8	-3.31	-5.5	-3.28	2.19	0.03
111-65-9	octane	110-82-7	cyclohexane	298.15	-4.16	-4.18	-4.22	0.02	0.06
111-65-9	octane	287-92-3	cyclopentane	293.2	-3.52	-3.48	-3.61	0.04	0.09
111-65-9	octane	120-92-3	cyclopentanone	293.2	-4.45	-4.44	-4.9	0.01	0.45
111-65-9	octane	74-84-0	ethane	298.15	-0.96	-0.94	-1.07	0.02	0.11
111-65-9	octane	64-17-5	ethanol	328.15	-2.18	-2.46	-1.65	0.28	0.53
111-65-9	octane	64-17-5	ethanol	288.15	-2.17	-2.16	-2.19	0.01	0.02
111-65-9	octane	64-17-5	ethanol	293.15	-2.15	-2.2	-2.12	0.05	0.03
111-65-9	octane	64-17-5	ethanol	298.15	-2.1	-2.24	-2.05	0.14	0.05
111-65-9	octane	64-17-5	ethanol	303.15	-2.06	-2.27	-1.98	0.21	0.08
111-65-9	octane	64-17-5	ethanol	308.15	-2.03	-2.31	-1.92	0.28	0.11

Table C.1: ΔG_{solv} for binary systems (kcal/mol).

solvent		solute		T (K)	ΔG^{ref}_{solv}	$\Delta G^{calc,1}_{solv}$	$\Delta G^{calc,2}_{solv}$	$\Delta G^{calc,1}_{solv}$-ΔG^{ref}_{solv}	$\Delta G^{calc,2}_{solv}$-ΔG^{ref}_{solv}
111-65-9	octane	64-17-5	ethanol	313.15	-1.99	-2.35	-1.85	0.36	0.14
111-65-9	octane	64-17-5	ethanol	318.15	-1.96	-2.39	-1.78	0.43	0.18
111-65-9	octane	64-17-5	ethanol	323.15	-1.92	-2.42	-1.71	0.5	0.21
111-65-9	octane	64-17-5	ethanol	313.15	-1.98	-2.35	-1.85	0.37	0.13
111-65-9	octane	64-17-5	ethanol	333.15	-1.67	-2.5	-1.58	0.83	0.09
111-65-9	octane	64-17-5	ethanol	293.15	-2.29	-2.2	-2.12	0.09	0.17
111-65-9	octane	64-17-5	ethanol	333.15	-1.94	-2.5	-1.58	0.56	0.36
111-65-9	octane	64-17-5	ethanol	293.2	-3.66	-2.2	-2.12	1.46	1.54
111-65-9	octane	74-85-1	ethene	298.15	-0.6	-0.67	-0.64	0.06	0.04
111-65-9	octane	66-25-1	hexanal	328.15	-4.4	-5.18	-4.61	0.78	0.21
111-65-9	octane	66-25-1	hexanal	348.15	-4.18	-5.5	-4.35	1.32	0.17
111-65-9	octane	66-25-1	hexanal	388.15	-3.76	-6.13	-3.89	2.37	0.13
111-65-9	octane	74-82-8	methane	298.15	0.15	0.13	-1.01	0.02	1.16
111-65-9	octane	67-56-1	methanol	293.15	-1.43	-1.53	-1.07	0.1	0.36
111-65-9	octane	67-56-1	methanol	313.15	-1.2	-1.63	-0.84	0.43	0.36
111-65-9	octane	67-56-1	methanol	333.15	-0.87	-1.74	-0.61	0.87	0.26
111-65-9	octane	67-56-1	methanol	293.15	-1.43	-1.53	-1.07	0.1	0.36
111-65-9	octane	67-56-1	methanol	288.15	-1.49	-1.5	-1.13	0.01	0.36
111-65-9	octane	67-56-1	methanol	293.15	-1.46	-1.53	-1.07	0.07	0.39
111-65-9	octane	67-56-1	methanol	298.15	-1.41	-1.55	-1.01	0.14	0.4
111-65-9	octane	67-56-1	methanol	303.15	-1.38	-1.58	-0.95	0.2	0.43
111-65-9	octane	67-56-1	methanol	308.15	-1.37	-1.61	-0.89	0.24	0.48
111-65-9	octane	67-56-1	methanol	313.15	-1.31	-1.63	-0.84	0.32	0.47
111-65-9	octane	67-56-1	methanol	318.15	-1.29	-1.66	-0.78	0.37	0.51
111-65-9	octane	67-56-1	methanol	323.15	-1.26	-1.68	-0.72	0.42	0.54
111-65-9	octane	67-56-1	methanol	293.15	-1.56	-1.53	-1.07	0.03	0.49
111-65-9	octane	110-62-3	pentanal	328.15	-3.67	-4.45	-3.94	0.78	0.27
111-65-9	octane	110-62-3	pentanal	348.15	-3.48	-4.72	-3.72	1.24	0.24
111-65-9	octane	110-62-3	pentanal	388.15	-3.09	-5.26	-3.29	2.17	0.2
111-65-9	octane	74-98-6	propane	298.15	-1.75	-1.68	-1.79	0.07	0.04
111-65-9	octane	74-98-6	propane	298.15	-1.71	-1.68	-1.78	0.03	0.07
111-65-9	octane	74-98-6	propane	323.15	-1.59	-1.82	-1.61	0.23	0.02
111-65-9	octane	109-99-9	tetrahydrofuran	391.4	-2.72	-4.92	-2.78	2.2	0.06
111-65-9	octane	109-99-9	tetrahydrofuran	388.27	-2.75	-4.88	-2.81	2.13	0.06
111-65-9	octane	109-99-9	tetrahydrofuran	293.15	-3.71	-3.69	-3.77	0.02	0.06
111-65-9	octane	109-99-9	tetrahydrofuran	293.2	-3.69	-3.69	-3.77	0	0.08
111-65-9	octane	7732-18-5	water	368.45	-1.33	-0.79	2.43	0.54	3.76
111-65-9	octane	7732-18-5	water	366.97	-1.42	-0.78	2.41	0.64	3.83
111-65-9	octane	7732-18-5	water	365.29	-1.44	-0.78	2.4	0.66	3.84
111-65-9	octane	7732-18-5	water	310.9	-0.54	-0.66	1.82	0.12	2.36
111-65-9	octane	7732-18-5	water	293.15	-0.59	-0.63	1.62	0.03	2.21
111-65-9	octane	7732-18-5	water	298.15	-0.87	-0.64	1.68	0.23	2.54
111-65-9	octane	7732-18-5	water	283.15	-0.76	-0.6	1.5	0.16	2.26
111-65-9	octane	7732-18-5	water	293.15	-0.79	-0.63	1.62	0.16	2.41
111-65-9	octane	7732-18-5	water	293.15	-1.02	-0.63	1.62	0.39	2.64
111-65-9	octane	7732-18-5	water	278.15	-0.77	-0.59	1.44	0.17	2.2
111-65-9	octane	7732-18-5	water	283.15	-0.76	-0.6	1.5	0.16	2.26
111-65-9	octane	7732-18-5	water	288.15	-0.81	-0.61	1.56	0.2	2.37
111-65-9	octane	7732-18-5	water	293.15	-0.84	-0.63	1.62	0.22	2.46
111-65-9	octane	7732-18-5	water	298.15	-0.86	-0.64	1.68	0.22	2.53
111-65-9	octane	7732-18-5	water	298.15	-0.52	-0.64	1.68	0.12	2.2
109-66-0	pentane	106-98-9	1-butene	298.15	-2.53	-2.39	-2.45	0.14	0.08
109-66-0	pentane	78-78-4	2-methylbutane	307.95	-3.08	-3.22	-3.14	0.14	0.06
109-66-0	pentane	78-78-4	2-methylbutane	307.65	-3.1	-3.21	-3.14	0.11	0.04
109-66-0	pentane	78-78-4	2-methylbutane	307.15	-3.12	-3.21	-3.15	0.09	0.03
109-66-0	pentane	107-83-5	2-methylpentane	298.15	-3.94	-3.76	-3.93	0.18	0.01
109-66-0	pentane	107-83-5	2-methylpentane	298.15	-3.92	-3.76	-3.93	0.16	0.01
109-66-0	pentane	75-28-5	2-methylpropane	298.15	-2.38	-2.32	-2.45	0.06	0.07
109-66-0	pentane	110-82-7	cyclohexane	321.45	-4.07	-4.59	-4.13	0.52	0.06
109-66-0	pentane	110-82-7	cyclohexane	318.85	-4.09	-4.55	-4.15	0.46	0.06
109-66-0	pentane	110-82-7	cyclohexane	317.85	-4.1	-4.54	-4.16	0.44	0.06
109-66-0	pentane	110-82-7	cyclohexane	316.05	-4.12	-4.51	-4.18	0.39	0.06
109-66-0	pentane	110-82-7	cyclohexane	314.65	-4.12	-4.49	-4.2	0.37	0.08
109-66-0	pentane	110-82-7	cyclohexane	313.1	-4.11	-4.47	-4.21	0.36	0.1
109-66-0	pentane	110-82-7	cyclohexane	312.15	-4.09	-4.45	-4.22	0.36	0.13
109-66-0	pentane	110-82-7	cyclohexane	312.15	-4.09	-4.45	-4.22	0.36	0.13
109-66-0	pentane	110-82-7	cyclohexane	313.1	-4.11	-4.47	-4.21	0.36	0.1

Table C.1: ΔG_{solv} for binary systems (kcal/mol).

solvent		solute		T (K)	ΔG^{ref}_{solv}	$\Delta G^{calc,1}_{solv}$	$\Delta G^{calc,2}_{solv}$	$\Delta G^{calc,1}_{solv}$-ΔG^{ref}_{solv}	$\Delta G^{calc,2}_{solv}$-ΔG^{ref}_{solv}
109-66-0	pentane	110-82-7	cyclohexane	314.65	-4.12	-4.49	-4.2	0.37	0.08
109-66-0	pentane	110-82-7	cyclohexane	316.05	-4.12	-4.51	-4.18	0.39	0.06
109-66-0	pentane	110-82-7	cyclohexane	317.85	-4.1	-4.54	-4.16	0.44	0.06
109-66-0	pentane	110-82-7	cyclohexane	318.85	-4.09	-4.55	-4.15	0.46	0.06
109-66-0	pentane	110-82-7	cyclohexane	321.45	-4.07	-4.59	-4.13	0.52	0.06
109-66-0	pentane	110-82-7	cyclohexane	298.15	-4.26	-4.25	-4.37	0.01	0.11
109-66-0	pentane	110-82-7	cyclohexane	298.15	-4.23	-4.25	-4.37	0.02	0.14
109-66-0	pentane	74-84-0	ethane	298.15	-1.01	-1.11	-1.15	0.1	0.14
109-66-0	pentane	64-17-5	ethanol	309.65	-2.11	-2.41	-2.01	0.3	0.1
109-66-0	pentane	64-17-5	ethanol	310.15	-2.07	-2.42	-2.01	0.35	0.06
109-66-0	pentane	64-17-5	ethanol	323.65	-1.99	-2.52	-1.82	0.53	0.17
109-66-0	pentane	64-17-5	ethanol	338.65	-1.94	-2.64	-1.63	0.7	0.31
109-66-0	pentane	64-17-5	ethanol	339.15	-1.87	-2.64	-1.62	0.77	0.25
109-66-0	pentane	74-85-1	ethene	298.15	-0.69	-0.8	-0.72	0.11	0.03
109-66-0	pentane	67-56-1	methanol	303.4	-2.34	-1.66	-1.04	0.68	1.3
109-66-0	pentane	108-87-2	methylcyclohexane	325.5	-4.49	-5.19	-4.51	0.7	0.02
109-66-0	pentane	108-87-2	methylcyclohexane	321.35	-4.51	-5.12	-4.55	0.61	0.04
109-66-0	pentane	108-87-2	methylcyclohexane	319.75	-4.54	-5.1	-4.57	0.56	0.03
109-66-0	pentane	108-87-2	methylcyclohexane	318.45	-4.55	-5.08	-4.58	0.53	0.03
109-66-0	pentane	96-37-7	methylcyclopentane	320.85	-3.91	-4.4	-3.94	0.49	0.03
109-66-0	pentane	96-37-7	methylcyclopentane	320.75	-3.91	-4.4	-3.94	0.49	0.03
109-66-0	pentane	96-37-7	methylcyclopentane	320.35	-3.91	-4.39	-3.95	0.48	0.04
109-66-0	pentane	96-37-7	methylcyclopentane	319.25	-3.93	-4.38	-3.96	0.45	0.03
109-66-0	pentane	96-37-7	methylcyclopentane	317.9	-3.93	-4.36	-3.97	0.43	0.04
109-66-0	pentane	96-37-7	methylcyclopentane	317.05	-3.92	-4.35	-3.98	0.43	0.06
109-66-0	pentane	96-37-7	methylcyclopentane	316.25	-3.92	-4.34	-3.99	0.42	0.07
109-66-0	pentane	96-37-7	methylcyclopentane	314.65	-3.94	-4.32	-4.01	0.38	0.07
109-66-0	pentane	96-37-7	methylcyclopentane	313.55	-3.96	-4.3	-4.02	0.34	0.06
109-66-0	pentane	96-37-7	methylcyclopentane	312.7	-3.93	-4.29	-4.02	0.36	0.09
109-66-0	pentane	96-37-7	methylcyclopentane	311.9	-3.95	-4.28	-4.03	0.33	0.08
109-66-0	pentane	96-37-7	methylcyclopentane	311.45	-3.96	-4.27	-4.04	0.31	0.08
109-66-0	pentane	96-37-7	methylcyclopentane	311.05	-3.98	-4.27	-4.04	0.29	0.06
109-66-0	pentane	74-98-6	propane	298.15	-1.81	-1.84	-1.9	0.03	0.09
109-66-0	pentane	109-99-9	tetrahydrofuran	313.15	-3.43	-4.02	-3.69	0.59	0.26
109-66-0	pentane	7732-18-5	water	278.65	-0.66	-0.75	1.37	0.09	2.03
109-66-0	pentane	7732-18-5	water	288.15	-0.63	-0.77	1.49	0.14	2.12
109-66-0	pentane	7732-18-5	water	297.95	-0.7	-0.8	1.61	0.1	2.31
109-66-0	pentane	7732-18-5	water	297.95	-0.7	-0.8	1.61	0.1	2.31
109-66-0	pentane	7732-18-5	water	311.48	-0.16	-0.84	1.77	0.67	1.93
109-66-0	pentane	7732-18-5	water	298.15	-0.59	-0.8	1.61	0.21	2.21
109-66-0	pentane	7732-18-5	water	298.15	-0.7	-0.8	1.61	0.11	2.31
1120-21-4	undecane	74-82-8	methane	298.15	0.27	0.27	-0.98	0	1.25
1120-21-4	undecane	7732-18-5	water	298.15	-0.47	-0.5	1.72	0.03	2.18
7732-18-5	water	106-98-9	1-butene	344.26	2.06	1.5	2.05	0.56	0.01
7732-18-5	water	106-98-9	1-butene	310.93	1.56	1.35	0.52	0.21	1.04
7732-18-5	water	106-98-9	1-butene	293.15	1.19	1.27	0.3	0.08	0.89
7732-18-5	water	106-98-9	1-butene	295.15	1.24	1.28	0.33	0.04	0.91
7732-18-5	water	106-98-9	1-butene	298.15	1.3	1.3	0.37	0	0.93
7732-18-5	water	106-98-9	1-butene	300.15	1.35	1.3	0.39	0.05	0.96
7732-18-5	water	106-98-9	1-butene	303.15	1.42	1.32	0.43	0.1	0.99
7732-18-5	water	106-98-9	1-butene	305.15	1.45	1.33	0.45	0.12	1
7732-18-5	water	106-98-9	1-butene	308.15	1.51	1.34	0.49	0.17	1.02
7732-18-5	water	106-98-9	1-butene	310.15	1.56	1.35	0.51	0.21	1.05
7732-18-5	water	106-98-9	1-butene	313.15	1.61	1.36	0.55	0.25	1.06
7732-18-5	water	106-98-9	1-butene	315.15	1.65	1.37	0.57	0.28	1.08
7732-18-5	water	106-98-9	1-butene	318.15	1.7	1.38	0.6	0.32	1.1
7732-18-5	water	106-98-9	1-butene	320.15	1.74	1.39	0.63	0.35	1.11
7732-18-5	water	106-98-9	1-butene	323.15	1.79	1.4	0.66	0.39	1.13
7732-18-5	water	592-41-6	1-hexene	298.15	1.66	1.63	0.3	0.03	1.36
7732-18-5	water	592-41-6	1-hexene	310.93	1.96	1.7	0.51	0.26	1.45
7732-18-5	water	592-41-6	1-hexene	366.48	2.97	2.01	2.53	0.96	0.44
7732-18-5	water	592-41-6	1-hexene	422.04	3.23	2.31	3.35	0.92	0.12
7732-18-5	water	592-41-6	1-hexene	477.59	2.78	2.62	4.06	0.16	1.28
7732-18-5	water	592-41-6	1-hexene	494.26	2.56	2.71	4.25	0.15	1.69
7732-18-5	water	592-41-6	1-hexene	298.15	1.6	1.63	0.3	0.03	1.3
7732-18-5	water	111-66-0	1-octene	298.15	2.17	1.91	0.27	0.26	1.9
7732-18-5	water	111-66-0	1-octene	310.93	2.52	1.99	0.54	0.53	1.98

Table C.1: ΔG_{solv} for binary systems (kcal/mol).

solvent		solute		T (K)	ΔG^{ref}_{solv}	$\Delta G^{calc,1}_{solv}$	$\Delta G^{calc,2}_{solv}$	$\Delta G^{calc,1}_{solv}$-ΔG^{ref}_{solv}	$\Delta G^{calc,2}_{solv}$-ΔG^{ref}_{solv}
7732-18-5	water	111-66-0	1-octene	366.48	3.63	2.34	2.77	1.29	0.86
7732-18-5	water	111-66-0	1-octene	422.04	3.66	2.7	3.73	0.96	0.07
7732-18-5	water	109-67-1	1-pentene	298.15	1.65	1.46	0.33	0.19	1.32
7732-18-5	water	78-78-4	2-methylbutane	293.2	2.23	2.28	1.13	0.05	1.1
7732-18-5	water	78-78-4	2-methylbutane	293.15	2.26	2.28	1.13	0.02	1.13
7732-18-5	water	78-78-4	2-methylbutane	313.15	2.67	2.43	1.4	0.24	1.27
7732-18-5	water	78-78-4	2-methylbutane	323.15	2.79	2.51	1.53	0.28	1.26
7732-18-5	water	78-78-4	2-methylbutane	333.15	2.95	2.59	1.66	0.36	1.29
7732-18-5	water	78-78-4	2-methylbutane	293.15	2.26	2.28	1.13	0.02	1.13
7732-18-5	water	78-78-4	2-methylbutane	313.15	2.67	2.43	1.4	0.24	1.27
7732-18-5	water	78-78-4	2-methylbutane	323.15	2.79	2.51	1.53	0.28	1.26
7732-18-5	water	78-78-4	2-methylbutane	333.15	2.95	2.59	1.66	0.36	1.29
7732-18-5	water	78-78-4	2-methylbutane	298.15	2.38	2.32	1.2	0.06	1.18
7732-18-5	water	78-78-4	2-methylbutane	298.15	2.38	2.32	1.2	0.06	1.18
7732-18-5	water	78-78-4	2-methylbutane	298.15	2.38	2.32	1.2	0.06	1.18
7732-18-5	water	78-78-4	2-methylbutane	298.15	2.36	2.32	1.2	0.04	1.16
7732-18-5	water	591-76-4	2-methylhexane	298.15	2.93	2.61	1.17	0.32	1.76
7732-18-5	water	107-83-5	2-methylpentane	298.15	2.53	2.46	1.16	0.07	1.37
7732-18-5	water	107-83-5	2-methylpentane	298.15	2.45	2.46	1.16	0.01	1.29
7732-18-5	water	107-83-5	2-methylpentane	298.15	2.51	2.46	1.16	0.05	1.35
7732-18-5	water	107-83-5	2-methylpentane	298.15	2.56	2.46	1.16	0.1	1.4
7732-18-5	water	107-83-5	2-methylpentane	313.25	3	2.59	1.4	0.41	1.6
7732-18-5	water	107-83-5	2-methylpentane	328.85	3.39	2.71	1.63	0.68	1.76
7732-18-5	water	107-83-5	2-methylpentane	372.25	4.23	3.07	3.45	1.16	0.78
7732-18-5	water	107-83-5	2-methylpentane	391.15	4.34	3.23	3.73	1.11	0.61
7732-18-5	water	107-83-5	2-methylpentane	410.45	4.28	3.39	4	0.89	0.28
7732-18-5	water	107-83-5	2-methylpentane	422.65	4.34	3.49	4.16	0.85	0.18
7732-18-5	water	107-83-5	2-methylpentane	298.15	2.53	2.46	1.16	0.07	1.37
7732-18-5	water	75-28-5	2-methylpropane	298.23	1.91	2.14	1.28	0.23	0.63
7732-18-5	water	75-28-5	2-methylpropane	303.33	2.01	2.18	1.34	0.17	0.67
7732-18-5	water	75-28-5	2-methylpropane	313.3	2.19	2.25	1.46	0.06	0.73
7732-18-5	water	75-28-5	2-methylpropane	323.21	2.38	2.32	1.57	0.06	0.81
7732-18-5	water	75-28-5	2-methylpropane	333.24	2.56	2.39	2.8	0.17	0.24
7732-18-5	water	75-28-5	2-methylpropane	283.15	1.8	2.03	1.1	0.23	0.7
7732-18-5	water	75-28-5	2-methylpropane	293.15	2.08	2.11	1.23	0.03	0.85
7732-18-5	water	75-28-5	2-methylpropane	303.15	2.37	2.18	1.35	0.19	1.02
7732-18-5	water	75-28-5	2-methylpropane	313.15	2.64	2.25	1.47	0.39	1.17
7732-18-5	water	589-81-1	3-methylheptane	298.15	2.98	2.75	1.08	0.23	1.9
7732-18-5	water	589-34-4	3-methylhexane	298.15	2.49	2.62	1.06	0.13	1.43
7732-18-5	water	589-34-4	3-methylhexane	298.15	2.87	2.62	1.06	0.25	1.81
7732-18-5	water	96-14-0	3-methylpentane	298.15	2.49	2.48	1.03	0.01	1.46
7732-18-5	water	96-14-0	3-methylpentane	298.3	2.53	2.48	1.03	0.05	1.5
7732-18-5	water	96-14-0	3-methylpentane	324.5	3.23	2.7	1.44	0.53	1.79
7732-18-5	water	96-14-0	3-methylpentane	351.2	3.72	2.92	2.99	0.8	0.73
7732-18-5	water	96-14-0	3-methylpentane	377.2	4.07	3.14	3.39	0.93	0.68
7732-18-5	water	96-14-0	3-methylpentane	401.2	4.21	3.34	3.74	0.87	0.47
7732-18-5	water	96-14-0	3-methylpentane	432.2	4.41	3.6	4.15	0.81	0.26
7732-18-5	water	96-14-0	3-methylpentane	462.1	4.32	3.85	4.52	0.47	0.2
7732-18-5	water	96-14-0	3-methylpentane	491.9	3.68	4.1	4.88	0.42	1.2
7732-18-5	water	96-14-0	3-methylpentane	298.15	2.51	2.48	1.03	0.03	1.48
7732-18-5	water	96-14-0	3-methylpentane	298.15	2.31	2.48	1.03	0.17	1.28
7732-18-5	water	75-07-0	acetaldehyde	355.15	-2.43	-4.29	-1.55	1.86	0.88
7732-18-5	water	75-07-0	acetaldehyde	350.65	-2.56	-4.24	-1.6	1.68	0.96
7732-18-5	water	75-07-0	acetaldehyde	298.13	-3.34	-3.6	-3.29	0.26	0.05
7732-18-5	water	75-07-0	acetaldehyde	293.15	-3.47	-3.54	-3.34	0.07	0.13
7732-18-5	water	75-07-0	acetaldehyde	303.15	-3.26	-3.66	-3.24	0.4	0.02
7732-18-5	water	75-07-0	acetaldehyde	313.15	-3.27	-3.78	-3.13	0.51	0.14
7732-18-5	water	75-07-0	acetaldehyde	303.15	-3.25	-3.66	-3.24	0.41	0.01
7732-18-5	water	75-07-0	acetaldehyde	283.15	-3.33	-3.42	-3.45	0.09	0.12
7732-18-5	water	75-07-0	acetaldehyde	288.15	-3.42	-3.48	-3.4	0.06	0.02
7732-18-5	water	75-07-0	acetaldehyde	293.15	-3.47	-3.54	-3.34	0.07	0.13
7732-18-5	water	75-07-0	acetaldehyde	298.15	-3.43	-3.6	-3.29	0.17	0.14
7732-18-5	water	75-07-0	acetaldehyde	303.15	-3.39	-3.66	-3.24	0.27	0.15
7732-18-5	water	75-07-0	acetaldehyde	297.45	-3.32	-3.59	-3.3	0.27	0.02
7732-18-5	water	75-07-0	acetaldehyde	298.15	-3.33	-3.6	-3.29	0.27	0.04
7732-18-5	water	75-07-0	acetaldehyde	333.15	-2.75	-4.03	-2.94	1.28	0.19
7732-18-5	water	75-07-0	acetaldehyde	373.15	-2.21	-4.51	-1.33	2.3	0.88

Table C.1: ΔG_{solv} for binary systems (kcal/mol).

solvent		solute		T (K)	ΔG^{ref}_{solv}	$\Delta G^{calc,1}_{solv}$	$\Delta G^{calc,2}_{solv}$	$\Delta G^{calc,1}_{solv}$-ΔG^{ref}_{solv}	$\Delta G^{calc,2}_{solv}$-ΔG^{ref}_{solv}
7732-18-5	water	75-07-0	acetaldehyde	298.15	-3.37	-3.6	-3.29	0.23	0.08
7732-18-5	water	75-07-0	acetaldehyde	283.15	-3.8	-3.42	-3.45	0.38	0.35
7732-18-5	water	75-07-0	acetaldehyde	288.15	-3.67	-3.48	-3.4	0.19	0.27
7732-18-5	water	75-07-0	acetaldehyde	293.15	-3.55	-3.54	-3.34	0.01	0.21
7732-18-5	water	75-07-0	acetaldehyde	303.15	-3.31	-3.66	-3.24	0.35	0.07
7732-18-5	water	75-07-0	acetaldehyde	313.15	-3.06	-3.78	-3.13	0.72	0.07
7732-18-5	water	75-07-0	acetaldehyde	298.15	-3.33	-3.6	-3.29	0.27	0.04
7732-18-5	water	75-07-0	acetaldehyde	323.15	-2.9	-3.91	-3.04	1.01	0.14
7732-18-5	water	75-07-0	acetaldehyde	298	-3.4	-3.6	-3.29	0.2	0.11
7732-18-5	water	75-07-0	acetaldehyde	298.13	-3.34	-3.6	-3.29	0.26	0.05
7732-18-5	water	75-07-0	acetaldehyde	298.13	-3.33	-3.6	-3.29	0.27	0.04
7732-18-5	water	75-07-0	acetaldehyde	298.15	-3.33	-3.6	-3.29	0.27	0.04
7732-18-5	water	75-07-0	acetaldehyde	298.13	-3.33	-3.6	-3.29	0.27	0.04
7732-18-5	water	75-07-0	acetaldehyde	298.13	-3.32	-3.6	-3.29	0.28	0.03
7732-18-5	water	110-82-7	cyclohexane	343.15	2.16	2.16	2	0	0.16
7732-18-5	water	110-82-7	cyclohexane	373.25	2.53	2.35	2.48	0.18	0.05
7732-18-5	water	110-82-7	cyclohexane	403.65	2.8	2.54	2.91	0.26	0.11
7732-18-5	water	110-82-7	cyclohexane	424.15	2.61	2.67	3.18	0.06	0.57
7732-18-5	water	110-82-7	cyclohexane	298.15	1.24	1.88	0.18	0.64	1.06
7732-18-5	water	110-82-7	cyclohexane	298.1	1.2	1.88	0.18	0.68	1.02
7732-18-5	water	110-82-7	cyclohexane	313.15	1.59	1.97	0.42	0.38	1.17
7732-18-5	water	110-82-7	cyclohexane	333.14	2	2.1	0.71	0.1	1.29
7732-18-5	water	110-82-7	cyclohexane	353.16	2.28	2.22	2.16	0.06	0.12
7732-18-5	water	110-82-7	cyclohexane	298.15	1.22	1.88	0.18	0.66	1.04
7732-18-5	water	110-82-7	cyclohexane	298.15	0.87	1.88	0.18	1.01	0.68
7732-18-5	water	110-82-7	cyclohexane	293.15	0.95	1.85	0.1	0.89	0.85
7732-18-5	water	110-82-7	cyclohexane	313.15	1.49	1.97	0.42	0.48	1.07
7732-18-5	water	110-82-7	cyclohexane	423.15	2.59	2.67	3.17	0.08	0.58
7732-18-5	water	110-82-7	cyclohexane	473.15	2.55	2.98	3.78	0.43	1.23
7732-18-5	water	110-82-7	cyclohexane	373.15	2.47	2.35	2.47	0.12	0
7732-18-5	water	110-82-7	cyclohexane	422.04	2.77	2.66	3.15	0.11	0.38
7732-18-5	water	110-82-7	cyclohexane	482.21	2.5	3.04	3.88	0.54	1.38
7732-18-5	water	110-82-7	cyclohexane	298.15	1.26	1.88	0.18	0.62	1.08
7732-18-5	water	110-82-7	cyclohexane	289.15	0.91	1.82	0.04	0.92	0.87
7732-18-5	water	110-82-7	cyclohexane	288.36	0.68	1.82	0.02	1.14	0.66
7732-18-5	water	110-82-7	cyclohexane	298.26	0.96	1.88	0.19	0.92	0.77
7732-18-5	water	110-82-7	cyclohexane	308.36	1.24	1.94	0.34	0.7	0.9
7732-18-5	water	110-82-7	cyclohexane	318.36	1.5	2.01	0.5	0.51	1
7732-18-5	water	110-82-7	cyclohexane	298.15	1.02	1.88	0.18	0.86	0.84
7732-18-5	water	110-82-7	cyclohexane	329.15	1.38	2.07	0.65	0.69	0.73
7732-18-5	water	110-82-7	cyclohexane	367.15	1.98	2.31	2.38	0.33	0.4
7732-18-5	water	110-82-7	cyclohexane	400.15	2.24	2.52	2.86	0.28	0.62
7732-18-5	water	110-82-7	cyclohexane	435.15	2.08	2.74	3.32	0.66	1.24
7732-18-5	water	110-82-7	cyclohexane	289.25	0.92	1.82	0.04	0.9	0.88
7732-18-5	water	110-82-7	cyclohexane	294.25	1.09	1.85	0.12	0.76	0.97
7732-18-5	water	110-82-7	cyclohexane	298.75	1.21	1.88	0.19	0.67	1.02
7732-18-5	water	110-82-7	cyclohexane	302.25	1.3	1.9	0.25	0.6	1.05
7732-18-5	water	110-82-7	cyclohexane	308.15	1.42	1.94	0.34	0.52	1.08
7732-18-5	water	110-82-7	cyclohexane	313.35	1.57	1.97	0.42	0.4	1.15
7732-18-5	water	110-82-7	cyclohexane	323.15	1.78	2.04	0.57	0.26	1.21
7732-18-5	water	110-82-7	cyclohexane	298.15	1.13	1.88	0.18	0.75	0.95
7732-18-5	water	110-82-7	cyclohexane	313.15	1.66	1.97	0.42	0.31	1.24
7732-18-5	water	110-82-7	cyclohexane	333.15	1.99	2.1	0.71	0.11	1.28
7732-18-5	water	110-82-7	cyclohexane	343.15	2.39	2.16	2	0.23	0.39
7732-18-5	water	110-82-7	cyclohexane	353.15	2.75	2.22	2.16	0.53	0.59
7732-18-5	water	108-94-1	cyclohexanone	323.15	-4.42	-4.89	-4.98	0.47	0.56
7732-18-5	water	108-94-1	cyclohexanone	333.15	-3.94	-5.04	-4.81	1.1	0.87
7732-18-5	water	108-94-1	cyclohexanone	293.15	-5.08	-4.43	-5.54	0.65	0.46
7732-18-5	water	108-94-1	cyclohexanone	308.15	-4.75	-4.66	-5.25	0.09	0.5
7732-18-5	water	108-94-1	cyclohexanone	343.15	-3.78	-5.19	-3.49	1.41	0.29
7732-18-5	water	108-94-1	cyclohexanone	353.15	-3.61	-5.34	-3.31	1.73	0.3
7732-18-5	water	110-83-8	cyclohexene	278.26	-0.32	0.71	-1.11	1.03	0.79
7732-18-5	water	110-83-8	cyclohexene	288.36	-0.09	0.74	-0.94	0.83	0.85
7732-18-5	water	110-83-8	cyclohexene	298.26	0.17	0.76	-0.77	0.59	0.94
7732-18-5	water	110-83-8	cyclohexene	308.36	0.42	0.79	-0.61	0.37	1.03
7732-18-5	water	110-83-8	cyclohexene	318.36	0.66	0.82	-0.46	0.16	1.12
7732-18-5	water	110-83-8	cyclohexene	296.15	0.29	0.76	-0.81	0.47	1.09

Table C.1: ΔG_{solv} for binary systems (kcal/mol).

solvent		solute		T (K)	ΔG^{ref}_{solv}	$\Delta G^{calc,1}_{solv}$	$\Delta G^{calc,2}_{solv}$	$\Delta G^{calc,1}_{solv}$-ΔG^{ref}_{solv}	$\Delta G^{calc,2}_{solv}$-ΔG^{ref}_{solv}
7732-18-5	water	110-83-8	cyclohexene	293.15	0.2	0.75	-0.86	0.55	1.05
7732-18-5	water	110-83-8	cyclohexene	298.15	0.37	0.76	-0.77	0.39	1.14
7732-18-5	water	110-83-8	cyclohexene	283.15	-0.07	0.73	-1.03	0.8	0.95
7732-18-5	water	110-83-8	cyclohexene	288.15	0.02	0.74	-0.94	0.72	0.96
7732-18-5	water	110-83-8	cyclohexene	293.15	0.04	0.75	-0.86	0.71	0.9
7732-18-5	water	110-83-8	cyclohexene	298.15	0.11	0.76	-0.77	0.66	0.88
7732-18-5	water	287-92-3	cyclopentane	298.15	1.21	1.78	0.28	0.57	0.93
7732-18-5	water	287-92-3	cyclopentane	276.5	0.57	1.65	-0.04	1.08	0.61
7732-18-5	water	287-92-3	cyclopentane	282.2	0.76	1.69	0.05	0.93	0.71
7732-18-5	water	287-92-3	cyclopentane	296.2	1.14	1.77	0.25	0.63	0.89
7732-18-5	water	287-92-3	cyclopentane	278.26	0.27	1.66	-0.01	1.4	0.28
7732-18-5	water	287-92-3	cyclopentane	288.36	0.51	1.73	0.14	1.22	0.37
7732-18-5	water	287-92-3	cyclopentane	298.26	0.75	1.78	0.28	1.04	0.46
7732-18-5	water	287-92-3	cyclopentane	308.36	0.94	1.85	0.42	0.9	0.52
7732-18-5	water	287-92-3	cyclopentane	318.36	1.23	1.9	0.56	0.67	0.67
7732-18-5	water	287-92-3	cyclopentane	298.15	1.19	1.78	0.28	0.59	0.91
7732-18-5	water	287-92-3	cyclopentane	313.25	1.57	1.87	0.49	0.3	1.08
7732-18-5	water	287-92-3	cyclopentane	328.85	1.89	1.97	0.7	0.08	1.19
7732-18-5	water	287-92-3	cyclopentane	372.25	2.53	2.23	2.45	0.3	0.08
7732-18-5	water	287-92-3	cyclopentane	391.15	2.76	2.34	2.7	0.42	0.06
7732-18-5	water	287-92-3	cyclopentane	410.45	2.75	2.46	2.95	0.29	0.2
7732-18-5	water	287-92-3	cyclopentane	426.25	2.83	2.55	3.14	0.28	0.31
7732-18-5	water	287-92-3	cyclopentane	326.15	1.26	1.95	0.66	0.69	0.6
7732-18-5	water	287-92-3	cyclopentane	390.15	1.66	2.33	2.69	0.67	1.03
7732-18-5	water	287-92-3	cyclopentane	298.15	1.21	1.78	0.28	0.57	0.93
7732-18-5	water	120-92-3	cyclopentanone	298.15	-4.76	-4.38	-5.32	0.38	0.56
7732-18-5	water	120-92-3	cyclopentanone	333.15	-3.96	-4.89	-4.75	0.93	0.79
7732-18-5	water	120-92-3	cyclopentanone	353.15	-3.65	-5.19	-3.27	1.54	0.38
7732-18-5	water	120-92-3	cyclopentanone	293.2	-5.14	-4.31	-5.41	0.83	0.27
7732-18-5	water	142-29-0	cyclopentene	298.26	-0.1	0.65	-0.42	0.75	0.32
7732-18-5	water	142-29-0	cyclopentene	308.36	0.07	0.67	-0.28	0.6	0.35
7732-18-5	water	142-29-0	cyclopentene	298.15	0.57	0.65	-0.42	0.08	0.98
7732-18-5	water	142-29-0	cyclopentene	293.15	0.26	0.64	-0.49	0.38	0.75
7732-18-5	water	142-29-0	cyclopentene	283.15	0.13	0.62	-0.64	0.49	0.77
7732-18-5	water	142-29-0	cyclopentene	288.15	0.2	0.63	-0.56	0.43	0.76
7732-18-5	water	142-29-0	cyclopentene	293.15	0.27	0.64	-0.49	0.37	0.76
7732-18-5	water	142-29-0	cyclopentene	298.15	0.34	0.65	-0.42	0.31	0.76
7732-18-5	water	74-84-0	ethane	344.15	2.51	2.17	2.81	0.34	0.3
7732-18-5	water	74-84-0	ethane	298.15	1.83	1.88	1.33	0.05	0.5
7732-18-5	water	74-84-0	ethane	298.15	1.82	1.88	1.32	0.06	0.5
7732-18-5	water	74-84-0	ethane	344.15	2.51	2.17	2.81	0.34	0.3
7732-18-5	water	74-84-0	ethane	283.15	1.46	1.78	1.21	0.32	0.25
7732-18-5	water	74-84-0	ethane	288.15	1.56	1.81	1.25	0.25	0.31
7732-18-5	water	74-84-0	ethane	293.15	1.75	1.84	1.29	0.09	0.46
7732-18-5	water	74-84-0	ethane	295.4	1.78	1.86	1.31	0.08	0.47
7732-18-5	water	74-84-0	ethane	300.5	1.89	1.89	1.34	0	0.55
7732-18-5	water	74-84-0	ethane	300.9	1.89	1.89	1.34	0	0.55
7732-18-5	water	74-84-0	ethane	300.9	1.86	1.89	1.34	0.03	0.52
7732-18-5	water	74-84-0	ethane	313.9	2.14	1.98	1.44	0.16	0.7
7732-18-5	water	74-84-0	ethane	314.8	2.13	1.98	1.45	0.15	0.68
7732-18-5	water	74-84-0	ethane	314.8	2.13	1.98	1.45	0.15	0.68
7732-18-5	water	74-84-0	ethane	318.4	2.2	2	1.48	0.2	0.72
7732-18-5	water	74-84-0	ethane	321.5	2.22	2.02	1.5	0.2	0.72
7732-18-5	water	74-84-0	ethane	330	2.33	2.08	1.56	0.25	0.77
7732-18-5	water	74-84-0	ethane	336.3	2.45	2.12	2.73	0.33	0.28
7732-18-5	water	74-84-0	ethane	341.5	2.48	2.15	2.78	0.33	0.3
7732-18-5	water	74-84-0	ethane	348.8	2.56	2.19	2.85	0.37	0.29
7732-18-5	water	74-84-0	ethane	351.3	2.61	2.21	2.87	0.4	0.26
7732-18-5	water	74-84-0	ethane	351.6	2.6	2.21	2.88	0.39	0.28
7732-18-5	water	74-84-0	ethane	364.3	2.7	2.29	2.99	0.41	0.29
7732-18-5	water	74-84-0	ethane	368.6	2.72	2.32	3.02	0.4	0.3
7732-18-5	water	74-84-0	ethane	395.8	2.86	2.49	3.21	0.37	0.35
7732-18-5	water	74-84-0	ethane	404.3	2.87	2.54	3.26	0.33	0.39
7732-18-5	water	74-84-0	ethane	429	2.87	2.7	3.35	0.17	0.48
7732-18-5	water	74-84-0	ethane	441.5	2.81	2.78	3.36	0.03	0.55
7732-18-5	water	74-84-0	ethane	473.5	2.63	2.98	3.24	0.35	0.61
7732-18-5	water	74-84-0	ethane	275.45	1.32	1.73	1.15	0.41	0.17

Table C.1: ΔG_{solv} for binary systems (kcal/mol).

solvent		solute		T (K)	ΔG^{ref}_{solv}	$\Delta G^{calc,1}_{solv}$	$\Delta G^{calc,2}_{solv}$	$\Delta G^{calc,1}_{solv}$-ΔG^{ref}_{solv}	$\Delta G^{calc,2}_{solv}$-ΔG^{ref}_{solv}
7732-18-5	water	74-84-0	ethane	275.44	1.32	1.73	1.15	0.41	0.17
7732-18-5	water	74-84-0	ethane	278.15	1.39	1.75	1.17	0.36	0.22
7732-18-5	water	74-84-0	ethane	283.16	1.51	1.78	1.21	0.27	0.3
7732-18-5	water	74-84-0	ethane	283.14	1.51	1.78	1.21	0.27	0.3
7732-18-5	water	74-84-0	ethane	283.77	1.52	1.79	1.22	0.27	0.3
7732-18-5	water	74-84-0	ethane	288.15	1.62	1.81	1.25	0.19	0.37
7732-18-5	water	74-84-0	ethane	293.15	1.73	1.84	1.29	0.11	0.44
7732-18-5	water	74-84-0	ethane	298.15	1.83	1.88	1.33	0.05	0.5
7732-18-5	water	74-84-0	ethane	298.15	1.83	1.88	1.33	0.05	0.5
7732-18-5	water	74-84-0	ethane	298.14	1.83	1.88	1.33	0.05	0.5
7732-18-5	water	74-84-0	ethane	298.16	1.83	1.88	1.33	0.05	0.5
7732-18-5	water	74-84-0	ethane	303.15	1.93	1.91	1.35	0.02	0.58
7732-18-5	water	74-84-0	ethane	308.16	2.02	1.94	1.4	0.08	0.62
7732-18-5	water	74-84-0	ethane	313.14	2.11	1.97	1.44	0.14	0.67
7732-18-5	water	74-84-0	ethane	318.14	2.19	2	1.48	0.19	0.71
7732-18-5	water	74-84-0	ethane	318.16	2.19	2	1.48	0.19	0.71
7732-18-5	water	74-84-0	ethane	318.16	2.19	2	1.48	0.19	0.71
7732-18-5	water	74-84-0	ethane	318.16	2.18	2	1.48	0.18	0.7
7732-18-5	water	74-84-0	ethane	318.16	2.19	2	1.48	0.19	0.71
7732-18-5	water	74-84-0	ethane	318.16	2.18	2	1.47	0.18	0.71
7732-18-5	water	74-84-0	ethane	323.14	2.26	2.03	1.51	0.23	0.75
7732-18-5	water	74-84-0	ethane	323.15	2.26	2.03	1.51	0.23	0.75
7732-18-5	water	64-17-5	ethanol	368.05	-3.7	-5.93	-2.26	2.23	1.44
7732-18-5	water	64-17-5	ethanol	366.55	-3.76	-5.91	-2.29	2.15	1.47
7732-18-5	water	64-17-5	ethanol	364.25	-3.83	-5.87	-2.32	2.04	1.51
7732-18-5	water	64-17-5	ethanol	364.35	-3.81	-5.87	-2.32	2.06	1.49
7732-18-5	water	64-17-5	ethanol	361.85	-3.96	-5.83	-2.36	1.87	1.6
7732-18-5	water	64-17-5	ethanol	361.45	-3.98	-5.82	-2.37	1.84	1.61
7732-18-5	water	64-17-5	ethanol	361.45	-3.98	-5.82	-2.37	1.84	1.61
7732-18-5	water	64-17-5	ethanol	359.65	-4.05	-5.79	-2.4	1.74	1.65
7732-18-5	water	64-17-5	ethanol	359.75	-4.04	-5.8	-2.4	1.76	1.64
7732-18-5	water	64-17-5	ethanol	359.15	-4.07	-5.79	-2.41	1.72	1.66
7732-18-5	water	64-17-5	ethanol	364.95	-3.81	-5.88	-2.31	2.07	1.5
7732-18-5	water	64-17-5	ethanol	364.75	-3.87	-5.88	-2.32	2.01	1.55
7732-18-5	water	64-17-5	ethanol	368.05	-3.71	-5.93	-2.26	2.22	1.45
7732-18-5	water	64-17-5	ethanol	366.55	-3.77	-5.91	-2.29	2.14	1.48
7732-18-5	water	64-17-5	ethanol	364.25	-3.83	-5.87	-2.32	2.04	1.51
7732-18-5	water	64-17-5	ethanol	361.65	-3.95	-5.83	-2.37	1.88	1.58
7732-18-5	water	64-17-5	ethanol	361.85	-3.96	-5.83	-2.36	1.87	1.6
7732-18-5	water	64-17-5	ethanol	361.45	-3.98	-5.82	-2.37	1.84	1.61
7732-18-5	water	64-17-5	ethanol	361.45	-3.99	-5.82	-2.37	1.83	1.62
7732-18-5	water	64-17-5	ethanol	359.65	-4.05	-5.79	-2.4	1.74	1.65
7732-18-5	water	64-17-5	ethanol	359.75	-4.04	-5.8	-2.4	1.76	1.64
7732-18-5	water	64-17-5	ethanol	292.25	-5.16	-4.71	-4.64	0.45	0.52
7732-18-5	water	64-17-5	ethanol	370	-3.71	-5.96	-2.23	2.25	1.48
7732-18-5	water	64-17-5	ethanol	368.06	-3.84	-5.93	-2.26	2.09	1.58
7732-18-5	water	64-17-5	ethanol	357.15	-4.61	-5.75	-2.44	1.14	2.17
7732-18-5	water	64-17-5	ethanol	313.15	-4.8	-5.05	-4.3	0.25	0.5
7732-18-5	water	64-17-5	ethanol	298.15	-5.07	-4.8	-4.54	0.27	0.53
7732-18-5	water	64-17-5	ethanol	393.15	-3.59	-6.33	-1.86	2.74	1.73
7732-18-5	water	64-17-5	ethanol	298.15	-5.14	-4.8	-4.54	0.34	0.6
7732-18-5	water	64-17-5	ethanol	312.91	-5.03	-5.04	-4.3	0.01	0.73
7732-18-5	water	64-17-5	ethanol	347.94	-4.42	-5.61	-2.6	1.19	1.82
7732-18-5	water	64-17-5	ethanol	347.94	-4.45	-5.61	-2.6	1.16	1.85
7732-18-5	water	64-17-5	ethanol	348.15	-4.25	-5.61	-2.6	1.36	1.65
7732-18-5	water	64-17-5	ethanol	353.15	-4.09	-5.69	-2.51	1.6	1.58
7732-18-5	water	64-17-5	ethanol	361.65	-4.09	-5.83	-2.37	1.74	1.72
7732-18-5	water	64-17-5	ethanol	313.15	-4.67	-5.05	-4.3	0.38	0.37
7732-18-5	water	64-17-5	ethanol	323.15	-4.6	-5.21	-4.14	0.61	0.46
7732-18-5	water	64-17-5	ethanol	318.9	-4.9	-5.14	-4.21	0.24	0.69
7732-18-5	water	64-17-5	ethanol	356.5	-4.24	-5.74	-2.46	1.5	1.78
7732-18-5	water	64-17-5	ethanol	356.2	-3.88	-5.74	-2.46	1.86	1.42
7732-18-5	water	64-17-5	ethanol	351.9	-4.1	-5.67	-2.53	1.57	1.57
7732-18-5	water	64-17-5	ethanol	351	-4.35	-5.65	-2.55	1.3	1.8
7732-18-5	water	64-17-5	ethanol	348.5	-4.3	-5.61	-2.59	1.31	1.71
7732-18-5	water	64-17-5	ethanol	298.14	-5.09	-4.8	-4.54	0.29	0.55
7732-18-5	water	64-17-5	ethanol	381.4	-3.65	-6.14	-2.04	2.49	1.61

Table C.1: ΔG_{solv} for binary systems (kcal/mol).

solvent		solute		T (K)	ΔG^{ref}_{solv}	$\Delta G^{calc,1}_{solv}$	$\Delta G^{calc,2}_{solv}$	$\Delta G^{calc,1}_{solv}$-ΔG^{ref}_{solv}	$\Delta G^{calc,2}_{solv}$-ΔG^{ref}_{solv}
7732-18-5	water	64-17-5	ethanol	333.15	-4.47	-5.37	-3.99	0.9	0.48
7732-18-5	water	64-17-5	ethanol	369.27	-3.79	-5.95	-2.24	2.16	1.55
7732-18-5	water	64-17-5	ethanol	365.61	-3.9	-5.89	-2.3	1.99	1.6
7732-18-5	water	64-17-5	ethanol	341.8	-4.4	-5.51	-2.71	1.11	1.69
7732-18-5	water	64-17-5	ethanol	363.6	-3.94	-5.86	-2.33	1.92	1.61
7732-18-5	water	64-17-5	ethanol	368.8	-3.87	-5.94	-2.25	2.07	1.62
7732-18-5	water	64-17-5	ethanol	364.8	-4.05	-5.88	-2.31	1.83	1.74
7732-18-5	water	64-17-5	ethanol	366.95	-3.82	-5.91	-2.28	2.09	1.54
7732-18-5	water	64-17-5	ethanol	364.75	-3.88	-5.88	-2.32	2	1.56
7732-18-5	water	64-17-5	ethanol	389.95	-3.83	-6.28	-1.91	2.45	1.92
7732-18-5	water	64-17-5	ethanol	362.95	-4.08	-5.85	-2.35	1.77	1.73
7732-18-5	water	64-17-5	ethanol	364.5	-3.91	-5.87	-2.32	1.96	1.59
7732-18-5	water	64-17-5	ethanol	363.15	-3.94	-5.85	-2.34	1.91	1.6
7732-18-5	water	64-17-5	ethanol	368.35	-3.61	-5.93	-2.26	2.32	1.35
7732-18-5	water	64-17-5	ethanol	367.45	-3.68	-5.92	-2.27	2.24	1.41
7732-18-5	water	64-17-5	ethanol	364.45	-3.9	-5.87	-2.32	1.97	1.58
7732-18-5	water	64-17-5	ethanol	368.18	-3.72	-5.93	-2.26	2.21	1.46
7732-18-5	water	64-17-5	ethanol	368.05	-3.68	-5.93	-2.26	2.25	1.42
7732-18-5	water	64-17-5	ethanol	367.55	-3.65	-5.92	-2.27	2.27	1.38
7732-18-5	water	64-17-5	ethanol	362.45	-3.92	-5.84	-2.35	1.92	1.57
7732-18-5	water	64-17-5	ethanol	360.25	-4.09	-5.8	-2.39	1.71	1.7
7732-18-5	water	64-17-5	ethanol	340.35	-4.32	-5.48	-2.74	1.16	1.58
7732-18-5	water	64-17-5	ethanol	368.9	-3.73	-5.94	-2.25	2.21	1.48
7732-18-5	water	64-17-5	ethanol	364.95	-3.88	-5.88	-2.31	2	1.57
7732-18-5	water	64-17-5	ethanol	368.08	-3.81	-5.93	-2.26	2.12	1.55
7732-18-5	water	64-17-5	ethanol	367.61	-3.82	-5.92	-2.27	2.1	1.55
7732-18-5	water	64-17-5	ethanol	367.09	-3.83	-5.91	-2.28	2.08	1.55
7732-18-5	water	64-17-5	ethanol	366.57	-3.83	-5.91	-2.29	2.08	1.54
7732-18-5	water	64-17-5	ethanol	370.05	-3.77	-5.96	-2.23	2.19	1.54
7732-18-5	water	64-17-5	ethanol	368.75	-3.81	-5.94	-2.25	2.13	1.56
7732-18-5	water	64-17-5	ethanol	367.95	-3.84	-5.93	-2.26	2.09	1.58
7732-18-5	water	64-17-5	ethanol	366.65	-3.9	-5.91	-2.28	2.01	1.62
7732-18-5	water	64-17-5	ethanol	366.05	-3.9	-5.9	-2.29	2	1.61
7732-18-5	water	64-17-5	ethanol	369.75	-3.77	-5.96	-2.23	2.19	1.54
7732-18-5	water	64-17-5	ethanol	369.15	-3.78	-5.95	-2.24	2.17	1.54
7732-18-5	water	64-17-5	ethanol	365.35	-3.92	-5.89	-2.31	1.97	1.61
7732-18-5	water	64-17-5	ethanol	369.25	-3.77	-5.95	-2.24	2.18	1.53
7732-18-5	water	64-17-5	ethanol	362.15	-3.78	-5.83	-2.36	2.05	1.42
7732-18-5	water	64-17-5	ethanol	353.95	-4.24	-5.7	-2.5	1.46	1.74
7732-18-5	water	64-17-5	ethanol	359.55	-4.16	-5.79	-2.4	1.63	1.76
7732-18-5	water	64-17-5	ethanol	393.75	-3.53	-6.34	-1.85	2.81	1.68
7732-18-5	water	64-17-5	ethanol	370.05	-3.69	-5.96	-2.23	2.27	1.46
7732-18-5	water	64-17-5	ethanol	369	-3.77	-5.94	-2.25	2.17	1.52
7732-18-5	water	64-17-5	ethanol	369.15	-3.73	-5.95	-2.24	2.22	1.49
7732-18-5	water	64-17-5	ethanol	366.45	-3.88	-5.9	-2.29	2.02	1.59
7732-18-5	water	64-17-5	ethanol	305.25	-4.94	-4.92	-4.43	0.02	0.51
7732-18-5	water	64-17-5	ethanol	367.45	-3.75	-5.92	-2.27	2.17	1.48
7732-18-5	water	64-17-5	ethanol	323.53	-4.65	-5.21	-4.13	0.56	0.52
7732-18-5	water	64-17-5	ethanol	369.8	-3.71	-5.96	-2.23	2.25	1.48
7732-18-5	water	64-17-5	ethanol	360.33	-4.13	-5.81	-2.39	1.68	1.74
7732-18-5	water	64-17-5	ethanol	366.1	-3.94	-5.9	-2.29	1.96	1.65
7732-18-5	water	64-17-5	ethanol	360.87	-4.09	-5.81	-2.38	1.72	1.71
7732-18-5	water	64-17-5	ethanol	369.9	-3.72	-5.96	-2.23	2.24	1.49
7732-18-5	water	64-17-5	ethanol	370	-3.71	-5.96	-2.23	2.25	1.48
7732-18-5	water	64-17-5	ethanol	368.06	-3.84	-5.93	-2.26	2.09	1.58
7732-18-5	water	64-17-5	ethanol	346.15	-4.2	-5.58	-2.63	1.38	1.57
7732-18-5	water	64-17-5	ethanol	366.65	-3.83	-5.91	-2.28	2.08	1.55
7732-18-5	water	64-17-5	ethanol	368.88	-3.69	-5.94	-2.25	2.25	1.44
7732-18-5	water	64-17-5	ethanol	360.95	-4.01	-5.82	-2.38	1.81	1.63
7732-18-5	water	64-17-5	ethanol	358.62	-4.18	-5.78	-2.42	1.6	1.76
7732-18-5	water	64-17-5	ethanol	369.12	-3.81	-5.95	-2.24	2.14	1.57
7732-18-5	water	64-17-5	ethanol	362.19	-3.95	-5.84	-2.36	1.89	1.59
7732-18-5	water	64-17-5	ethanol	358.15	-3.79	-5.77	-2.43	1.98	1.36
7732-18-5	water	64-17-5	ethanol	363.15	-3.71	-5.85	-2.34	2.14	1.37
7732-18-5	water	64-17-5	ethanol	368.15	-3.63	-5.93	-2.26	2.3	1.37
7732-18-5	water	64-17-5	ethanol	372.15	-3.56	-6	-2.19	2.44	1.37
7732-18-5	water	64-17-5	ethanol	303.15	-4.73	-4.88	-4.46	0.15	0.27

Table C.1: ΔG_{solv} for binary systems (kcal/mol).

solvent		solute		T (K)	ΔG^{ref}_{solv}	$\Delta G^{calc,1}_{solv}$	$\Delta G^{calc,2}_{solv}$	$\Delta G^{calc,1}_{solv}$-ΔG^{ref}_{solv}	$\Delta G^{calc,2}_{solv}$-ΔG^{ref}_{solv}
7732-18-5	water	64-17-5	ethanol	313.15	-4.54	-5.05	-4.3	0.51	0.24
7732-18-5	water	64-17-5	ethanol	323.15	-4.34	-5.21	-4.14	0.87	0.2
7732-18-5	water	64-17-5	ethanol	333.15	-4.16	-5.37	-3.99	1.21	0.17
7732-18-5	water	64-17-5	ethanol	298.65	-4.91	-4.81	-4.53	0.1	0.38
7732-18-5	water	64-17-5	ethanol	298.15	-5	-4.8	-4.54	0.2	0.46
7732-18-5	water	64-17-5	ethanol	328.15	-4.31	-5.29	-4.06	0.98	0.25
7732-18-5	water	64-17-5	ethanol	303.15	-4.8	-4.88	-4.46	0.08	0.34
7732-18-5	water	64-17-5	ethanol	313.15	-4.59	-5.05	-4.3	0.46	0.29
7732-18-5	water	64-17-5	ethanol	323.15	-4.35	-5.21	-4.14	0.86	0.21
7732-18-5	water	64-17-5	ethanol	333.15	-4.19	-5.37	-3.99	1.18	0.2
7732-18-5	water	64-17-5	ethanol	298.15	-5	-4.8	-4.54	0.2	0.46
7732-18-5	water	64-17-5	ethanol	298.15	-5.03	-4.8	-4.54	0.23	0.49
7732-18-5	water	64-17-5	ethanol	283.15	-5.33	-4.56	-4.8	0.77	0.53
7732-18-5	water	64-17-5	ethanol	273.35	-5.61	-4.4	-4.97	1.21	0.64
7732-18-5	water	64-17-5	ethanol	283.15	-5.34	-4.56	-4.8	0.78	0.54
7732-18-5	water	64-17-5	ethanol	303.15	-4.86	-4.88	-4.46	0.02	0.4
7732-18-5	water	64-17-5	ethanol	308.15	-4.74	-4.96	-4.38	0.22	0.36
7732-18-5	water	64-17-5	ethanol	313.15	-4.63	-5.05	-4.3	0.42	0.33
7732-18-5	water	64-17-5	ethanol	318.15	-4.53	-5.13	-4.22	0.6	0.31
7732-18-5	water	64-17-5	ethanol	323.15	-4.43	-5.21	-4.14	0.78	0.29
7732-18-5	water	64-17-5	ethanol	328.15	-4.33	-5.29	-4.06	0.96	0.27
7732-18-5	water	64-17-5	ethanol	333.15	-4.24	-5.37	-3.99	1.13	0.25
7732-18-5	water	64-17-5	ethanol	298.15	-4.99	-4.8	-4.54	0.19	0.45
7732-18-5	water	64-17-5	ethanol	298.15	-5.08	-4.8	-4.54	0.28	0.54
7732-18-5	water	64-17-5	ethanol	283.15	-5.33	-4.56	-4.8	0.77	0.53
7732-18-5	water	64-17-5	ethanol	293.15	-5.07	-4.72	-4.63	0.35	0.44
7732-18-5	water	64-17-5	ethanol	298.15	-4.94	-4.8	-4.54	0.14	0.4
7732-18-5	water	64-17-5	ethanol	303.15	-4.82	-4.88	-4.46	0.06	0.36
7732-18-5	water	64-17-5	ethanol	313.15	-4.62	-5.05	-4.3	0.43	0.32
7732-18-5	water	64-17-5	ethanol	298.15	-5.04	-4.8	-4.54	0.24	0.5
7732-18-5	water	64-17-5	ethanol	333.15	-4.35	-5.37	-3.99	1.02	0.36
7732-18-5	water	64-17-5	ethanol	373.15	-3.67	-6.01	-2.18	2.34	1.49
7732-18-5	water	64-17-5	ethanol	298.15	-4.96	-4.8	-4.54	0.16	0.42
7732-18-5	water	64-17-5	ethanol	303.25	-4.74	-4.89	-4.46	0.15	0.28
7732-18-5	water	64-17-5	ethanol	313.25	-4.55	-5.05	-4.3	0.5	0.25
7732-18-5	water	64-17-5	ethanol	323.25	-4.36	-5.21	-4.14	0.85	0.22
7732-18-5	water	64-17-5	ethanol	333.25	-4.18	-5.37	-2.86	1.19	1.32
7732-18-5	water	64-17-5	ethanol	343.25	-4.01	-5.53	-2.68	1.52	1.33
7732-18-5	water	64-17-5	ethanol	298.15	-5	-4.8	-4.54	0.2	0.46
7732-18-5	water	64-17-5	ethanol	297.45	-4.87	-4.79	-4.55	0.08	0.32
7732-18-5	water	64-17-5	ethanol	283.15	-5.15	-4.56	-4.8	0.59	0.35
7732-18-5	water	64-17-5	ethanol	293.15	-4.93	-4.72	-4.63	0.21	0.3
7732-18-5	water	64-17-5	ethanol	313.15	-4.57	-5.05	-4.3	0.48	0.27
7732-18-5	water	64-17-5	ethanol	333.15	-4.21	-5.37	-3.99	1.16	0.22
7732-18-5	water	64-17-5	ethanol	293.15	-4.76	-4.72	-4.63	0.04	0.13
7732-18-5	water	64-17-5	ethanol	303.15	-4.62	-4.88	-4.46	0.26	0.16
7732-18-5	water	64-17-5	ethanol	313.15	-4.53	-5.05	-4.3	0.52	0.23
7732-18-5	water	64-17-5	ethanol	373.3	-3.56	-6.01	-2.18	2.45	1.38
7732-18-5	water	64-17-5	ethanol	351.35	-3.91	-5.66	-2.54	1.75	1.37
7732-18-5	water	64-17-5	ethanol	322.05	-4.42	-5.19	-4.16	0.77	0.26
7732-18-5	water	64-17-5	ethanol	333.25	-4.18	-5.37	-2.86	1.19	1.32
7732-18-5	water	64-17-5	ethanol	343.15	-3.99	-5.53	-2.69	1.54	1.3
7732-18-5	water	64-17-5	ethanol	353.05	-3.84	-5.69	-2.51	1.85	1.33
7732-18-5	water	64-17-5	ethanol	362.85	-3.63	-5.85	-2.35	2.22	1.28
7732-18-5	water	64-17-5	ethanol	372.25	-3.54	-6	-2.19	2.46	1.35
7732-18-5	water	64-17-5	ethanol	298.15	-4.97	-4.8	-4.54	0.17	0.43
7732-18-5	water	64-17-5	ethanol	298.15	-4.97	-4.8	-4.54	0.17	0.43
7732-18-5	water	64-17-5	ethanol	278.2	-5.47	-4.48	-4.88	0.99	0.59
7732-18-5	water	64-17-5	ethanol	283.2	-5.33	-4.56	-4.8	0.77	0.53
7732-18-5	water	64-17-5	ethanol	288.2	-5.29	-4.64	-4.71	0.65	0.58
7732-18-5	water	64-17-5	ethanol	293.2	-5.14	-4.72	-4.63	0.42	0.51
7732-18-5	water	64-17-5	ethanol	298.2	-5.08	-4.8	-4.54	0.28	0.54
7732-18-5	water	64-17-5	ethanol	303.2	-5.03	-4.88	-4.46	0.15	0.57
7732-18-5	water	64-17-5	ethanol	288.15	-5.14	-4.64	-4.71	0.5	0.43
7732-18-5	water	64-17-5	ethanol	293.15	-5.16	-4.72	-4.63	0.44	0.53
7732-18-5	water	64-17-5	ethanol	298.15	-5.07	-4.8	-4.54	0.27	0.53
7732-18-5	water	64-17-5	ethanol	298.15	-4.8	-4.8	-4.54	0	0.26

Table C.1: ΔG_{solv} for binary systems (kcal/mol).

solvent		solute		T (K)	ΔG^{ref}_{solv}	$\Delta G^{calc,1}_{solv}$	$\Delta G^{calc,2}_{solv}$	$\Delta G^{calc,1}_{solv}$-ΔG^{ref}_{solv}	$\Delta G^{calc,2}_{solv}$-ΔG^{ref}_{solv}
7732-18-5	water	64-17-5	ethanol	298	-5.01	-4.8	-4.55	0.21	0.46
7732-18-5	water	64-17-5	ethanol	313	-4.76	-5.04	-4.3	0.28	0.46
7732-18-5	water	64-17-5	ethanol	323	-4.45	-5.2	-4.14	0.75	0.31
7732-18-5	water	64-17-5	ethanol	333	-4.23	-5.36	-3.99	1.13	0.24
7732-18-5	water	64-17-5	ethanol	343	-4.09	-5.53	-2.69	1.44	1.4
7732-18-5	water	64-17-5	ethanol	353	-3.89	-5.69	-2.52	1.8	1.37
7732-18-5	water	64-17-5	ethanol	363	-3.7	-5.85	-2.35	2.15	1.35
7732-18-5	water	64-17-5	ethanol	298.15	-5.12	-4.8	-4.54	0.32	0.58
7732-18-5	water	64-17-5	ethanol	298.15	-5	-4.8	-4.54	0.2	0.46
7732-18-5	water	74-85-1	ethene	278.15	0.9	0.81	0.37	0.09	0.52
7732-18-5	water	74-85-1	ethene	298.15	1.26	0.86	0.51	0.4	0.75
7732-18-5	water	74-85-1	ethene	298.15	1.25	0.86	0.51	0.39	0.74
7732-18-5	water	74-85-1	ethene	323.15	1.6	0.94	0.67	0.66	0.93
7732-18-5	water	74-85-1	ethene	343.15	1.81	0.99	1.92	0.82	0.11
7732-18-5	water	74-85-1	ethene	298.15	1.27	0.86	0.51	0.41	0.76
7732-18-5	water	111-71-7	heptanal	303.15	-2.23	-2.73	-3.16	0.5	0.93
7732-18-5	water	111-71-7	heptanal	293.15	-2.75	-2.64	-3.38	0.11	0.63
7732-18-5	water	111-71-7	heptanal	313.15	-2.09	-2.82	-2.95	0.73	0.86
7732-18-5	water	111-71-7	heptanal	283.15	-2.85	-2.55	-3.61	0.3	0.76
7732-18-5	water	111-71-7	heptanal	293.15	-2.52	-2.64	-3.38	0.12	0.86
7732-18-5	water	111-71-7	heptanal	303.15	-2.19	-2.73	-3.16	0.54	0.97
7732-18-5	water	111-71-7	heptanal	313.15	-1.83	-2.82	-2.95	0.99	1.12
7732-18-5	water	111-71-7	heptanal	323.15	-1.63	-2.91	-2.74	1.28	1.11
7732-18-5	water	111-71-7	heptanal	333.15	-1.38	-3	-2.55	1.62	1.17
7732-18-5	water	111-71-7	heptanal	343.15	-1.13	-3.09	-1.21	1.96	0.08
7732-18-5	water	111-71-7	heptanal	353.15	-0.93	-3.18	-0.99	2.25	0.06
7732-18-5	water	111-71-7	heptanal	363.15	-0.79	-3.27	-0.79	2.49	0
7732-18-5	water	66-25-1	hexanal	363.15	-0.93	-3.46	-0.9	2.53	0.02
7732-18-5	water	66-25-1	hexanal	353.15	-1.04	-3.37	-1.09	2.33	0.05
7732-18-5	water	66-25-1	hexanal	298.15	-2.58	-2.84	-3.3	0.26	0.72
7732-18-5	water	66-25-1	hexanal	313.15	-2.57	-2.98	-3	0.41	0.43
7732-18-5	water	66-25-1	hexanal	318.15	-2.45	-3.03	-2.9	0.58	0.45
7732-18-5	water	66-25-1	hexanal	323.15	-2.39	-3.08	-2.81	0.69	0.42
7732-18-5	water	66-25-1	hexanal	298.15	-2.74	-2.84	-3.3	0.1	0.56
7732-18-5	water	66-25-1	hexanal	298.15	-2.56	-2.84	-3.3	0.28	0.74
7732-18-5	water	66-25-1	hexanal	371.7	-2.58	-3.54	-0.74	0.96	1.84
7732-18-5	water	66-25-1	hexanal	293.15	-2.7	-2.79	-3.41	0.09	0.71
7732-18-5	water	66-25-1	hexanal	303.15	-2.36	-2.89	-3.2	0.53	0.84
7732-18-5	water	66-25-1	hexanal	313.15	-2.1	-2.98	-3	0.88	0.9
7732-18-5	water	66-25-1	hexanal	323.15	-1.76	-3.08	-2.81	1.32	1.05
7732-18-5	water	66-25-1	hexanal	333.15	-1.39	-3.17	-2.62	1.78	1.23
7732-18-5	water	66-25-1	hexanal	343.15	-1.23	-3.27	-1.29	2.04	0.06
7732-18-5	water	66-25-1	hexanal	353.15	-1.07	-3.37	-1.09	2.3	0.02
7732-18-5	water	66-25-1	hexanal	363.15	-0.97	-3.46	-0.9	2.49	0.06
7732-18-5	water	67-56-1	methanol	283.15	-5.38	-5.05	-4.99	0.33	0.39
7732-18-5	water	67-56-1	methanol	293.15	-5.14	-5.23	-4.85	0.09	0.29
7732-18-5	water	67-56-1	methanol	313.95	-4.82	-5.6	-4.57	0.78	0.25
7732-18-5	water	67-56-1	methanol	331.65	-4.6	-5.91	-4.34	1.31	0.26
7732-18-5	water	67-56-1	methanol	353.05	-4.32	-6.3	-2.9	1.98	1.42
7732-18-5	water	67-56-1	methanol	364.35	-4.18	-6.5	-2.73	2.32	1.45
7732-18-5	water	67-56-1	methanol	368.25	-4.13	-6.57	-2.68	2.44	1.45
7732-18-5	water	67-56-1	methanol	368.85	-4.1	-6.58	-2.67	2.48	1.43
7732-18-5	water	67-56-1	methanol	370.65	-3.99	-6.61	-2.64	2.62	1.35
7732-18-5	water	67-56-1	methanol	371.45	-4.03	-6.62	-2.63	2.59	1.4
7732-18-5	water	67-56-1	methanol	298.15	-5.04	-5.32	-4.78	0.28	0.26
7732-18-5	water	67-56-1	methanol	308.15	-4.91	-5.5	-4.64	0.59	0.27
7732-18-5	water	67-56-1	methanol	318.15	-4.78	-5.67	-4.51	0.89	0.27
7732-18-5	water	67-56-1	methanol	328.15	-4.65	-5.85	-4.38	1.2	0.27
7732-18-5	water	67-56-1	methanol	353.1	-4.18	-6.3	-2.9	2.12	1.28
7732-18-5	water	67-56-1	methanol	353.2	-4.31	-6.3	-2.9	1.99	1.41
7732-18-5	water	67-56-1	methanol	393.9	-3.7	-7.03	-2.32	3.33	1.38
7732-18-5	water	67-56-1	methanol	368.59	-4	-6.57	-2.67	2.57	1.33
7732-18-5	water	67-56-1	methanol	353.37	-4.21	-6.3	-2.89	2.09	1.32
7732-18-5	water	67-56-1	methanol	329.18	-4.55	-5.87	-4.37	1.32	0.18
7732-18-5	water	67-56-1	methanol	298.15	-5	-5.32	-4.78	0.32	0.22
7732-18-5	water	67-56-1	methanol	388.15	-4	-6.92	-2.4	2.92	1.6
7732-18-5	water	67-56-1	methanol	298.15	-5.12	-5.32	-4.78	0.2	0.34

Table C.1: ΔG_{solv} for binary systems (kcal/mol).

solvent		solute		T (K)	ΔG^{ref}_{solv}	$\Delta G^{calc,1}_{solv}$	$\Delta G^{calc,2}_{solv}$	$\Delta G^{calc,1}_{solv}$-ΔG^{ref}_{solv}	$\Delta G^{calc,2}_{solv}$-ΔG^{ref}_{solv}
7732-18-5	water	67-56-1	methanol	373.15	-3.89	-6.66	-2.61	2.77	1.28
7732-18-5	water	67-56-1	methanol	333.15	-4.64	-5.94	-4.32	1.3	0.32
7732-18-5	water	67-56-1	methanol	333.15	-4.63	-5.94	-4.32	1.31	0.31
7732-18-5	water	67-56-1	methanol	338.15	-4.49	-6.03	-3.12	1.54	1.37
7732-18-5	water	67-56-1	methanol	338.15	-4.54	-6.03	-3.12	1.49	1.42
7732-18-5	water	67-56-1	methanol	338.15	-4.55	-6.03	-3.12	1.48	1.43
7732-18-5	water	67-56-1	methanol	338.15	-4.55	-6.03	-3.12	1.48	1.43
7732-18-5	water	67-56-1	methanol	343.15	-4.43	-6.12	-3.05	1.69	1.38
7732-18-5	water	67-56-1	methanol	343.15	-4.42	-6.12	-3.05	1.7	1.37
7732-18-5	water	67-56-1	methanol	343.15	-4.45	-6.12	-3.05	1.67	1.4
7732-18-5	water	67-56-1	methanol	343.15	-4.46	-6.12	-3.05	1.66	1.41
7732-18-5	water	67-56-1	methanol	343.15	-4.5	-6.12	-3.05	1.62	1.45
7732-18-5	water	67-56-1	methanol	333.15	-4.57	-5.94	-4.32	1.37	0.25
7732-18-5	water	67-56-1	methanol	333.15	-4.54	-5.94	-4.32	1.4	0.22
7732-18-5	water	67-56-1	methanol	333.15	-4.54	-5.94	-4.32	1.4	0.22
7732-18-5	water	67-56-1	methanol	333.15	-4.57	-5.94	-4.32	1.37	0.25
7732-18-5	water	67-56-1	methanol	333.15	-4.64	-5.94	-4.32	1.3	0.32
7732-18-5	water	67-56-1	methanol	373.1	-4.03	-6.65	-2.61	2.62	1.42
7732-18-5	water	67-56-1	methanol	308.15	-4.63	-5.5	-4.64	0.87	0.01
7732-18-5	water	67-56-1	methanol	373.15	-3.89	-6.66	-2.61	2.77	1.28
7732-18-5	water	67-56-1	methanol	313.05	-5.05	-5.58	-4.58	0.53	0.47
7732-18-5	water	67-56-1	methanol	332.59	-4.78	-5.93	-4.33	1.15	0.45
7732-18-5	water	67-56-1	methanol	328.15	-4.7	-5.85	-4.38	1.15	0.32
7732-18-5	water	67-56-1	methanol	322.91	-4.75	-5.76	-4.45	1.01	0.3
7732-18-5	water	67-56-1	methanol	322.91	-4.84	-5.76	-4.45	0.92	0.39
7732-18-5	water	67-56-1	methanol	356.35	-4.36	-6.36	-2.85	2	1.51
7732-18-5	water	67-56-1	methanol	355.45	-4.38	-6.34	-2.86	1.96	1.52
7732-18-5	water	67-56-1	methanol	318.15	-4.76	-5.67	-4.51	0.91	0.25
7732-18-5	water	67-56-1	methanol	368.6	-4.31	-6.57	-2.67	2.26	1.64
7732-18-5	water	67-56-1	methanol	364.17	-4.3	-6.49	-2.73	2.19	1.57
7732-18-5	water	67-56-1	methanol	363.85	-4.44	-6.49	-2.74	2.05	1.7
7732-18-5	water	67-56-1	methanol	360.65	-4.05	-6.43	-2.79	2.38	1.26
7732-18-5	water	67-56-1	methanol	359.6	-4.29	-6.41	-2.8	2.12	1.49
7732-18-5	water	67-56-1	methanol	365.55	-4.11	-6.52	-2.71	2.41	1.4
7732-18-5	water	67-56-1	methanol	360.85	-4.25	-6.44	-2.78	2.19	1.47
7732-18-5	water	67-56-1	methanol	354.85	-4.41	-6.33	-2.87	1.92	1.54
7732-18-5	water	67-56-1	methanol	363.43	-4.21	-6.48	-2.75	2.27	1.46
7732-18-5	water	67-56-1	methanol	345.73	-4.32	-6.17	-3.01	1.85	1.31
7732-18-5	water	67-56-1	methanol	343.76	-4.38	-6.13	-3.04	1.75	1.34
7732-18-5	water	67-56-1	methanol	338.48	-4.5	-6.04	-3.12	1.54	1.38
7732-18-5	water	67-56-1	methanol	355.88	-4.23	-6.35	-2.86	2.12	1.37
7732-18-5	water	67-56-1	methanol	352.16	-4.33	-6.28	-2.91	1.95	1.42
7732-18-5	water	67-56-1	methanol	370	-3.78	-6.6	-2.65	2.82	1.13
7732-18-5	water	67-56-1	methanol	357.9	-4.31	-6.38	-2.83	2.07	1.48
7732-18-5	water	67-56-1	methanol	368.32	-3.98	-6.57	-2.68	2.59	1.3
7732-18-5	water	67-56-1	methanol	367.4	-4.07	-6.55	-2.69	2.48	1.38
7732-18-5	water	67-56-1	methanol	366.95	-4.05	-6.54	-2.69	2.49	1.36
7732-18-5	water	67-56-1	methanol	366.21	-4.06	-6.53	-2.71	2.47	1.35
7732-18-5	water	67-56-1	methanol	365.35	-4.11	-6.52	-2.72	2.41	1.39
7732-18-5	water	67-56-1	methanol	364.25	-4.14	-6.5	-2.73	2.36	1.41
7732-18-5	water	67-56-1	methanol	363.25	-4.2	-6.48	-2.75	2.28	1.45
7732-18-5	water	67-56-1	methanol	361.48	-4.22	-6.45	-2.77	2.23	1.45
7732-18-5	water	67-56-1	methanol	380.35	-3.77	-6.78	-2.5	3.01	1.27
7732-18-5	water	67-56-1	methanol	378.58	-3.87	-6.75	-2.53	2.88	1.34
7732-18-5	water	67-56-1	methanol	369.55	-4.03	-6.59	-2.66	2.56	1.37
7732-18-5	water	67-56-1	methanol	370.95	-3.99	-6.62	-2.64	2.63	1.35
7732-18-5	water	67-56-1	methanol	370.5	-4.02	-6.61	-2.64	2.59	1.38
7732-18-5	water	67-56-1	methanol	370.07	-4.1	-6.6	-2.65	2.5	1.45
7732-18-5	water	67-56-1	methanol	368.97	-4.08	-6.58	-2.67	2.5	1.41
7732-18-5	water	67-56-1	methanol	368.21	-4.13	-6.57	-2.68	2.44	1.45
7732-18-5	water	67-56-1	methanol	367.28	-4.08	-6.55	-2.69	2.47	1.39
7732-18-5	water	67-56-1	methanol	363.15	-4.19	-6.48	-2.75	2.29	1.44
7732-18-5	water	67-56-1	methanol	368.67	-4	-6.58	-2.67	2.58	1.33
7732-18-5	water	67-56-1	methanol	368.35	-4.06	-6.57	-2.67	2.51	1.39
7732-18-5	water	67-56-1	methanol	367.65	-4.07	-6.56	-2.68	2.49	1.39
7732-18-5	water	67-56-1	methanol	366.85	-4.1	-6.54	-2.7	2.44	1.4
7732-18-5	water	67-56-1	methanol	365.95	-4.03	-6.53	-2.71	2.5	1.32

Table C.1: ΔG_{solv} for binary systems (kcal/mol).

solvent		solute		T (K)	ΔG^{ref}_{solv}	$\Delta G^{calc,1}_{solv}$	$\Delta G^{calc,2}_{solv}$	$\Delta G^{calc,1}_{solv}$-ΔG^{ref}_{solv}	$\Delta G^{calc,2}_{solv}$-ΔG^{ref}_{solv}
7732-18-5	water	67-56-1	methanol	364.95	-4.13	-6.51	-2.72	2.38	1.41
7732-18-5	water	67-56-1	methanol	364.05	-4.16	-6.49	-2.74	2.33	1.42
7732-18-5	water	67-56-1	methanol	363.15	-4.17	-6.48	-2.75	2.31	1.42
7732-18-5	water	67-56-1	methanol	362.25	-4.21	-6.46	-2.76	2.25	1.45
7732-18-5	water	67-56-1	methanol	347.85	-4.33	-6.2	-2.97	1.87	1.36
7732-18-5	water	67-56-1	methanol	358.15	-4.2	-6.39	-2.82	2.19	1.38
7732-18-5	water	67-56-1	methanol	348.55	-4.37	-6.22	-2.96	1.85	1.41
7732-18-5	water	67-56-1	methanol	365.85	-4.09	-6.52	-2.71	2.43	1.38
7732-18-5	water	67-56-1	methanol	353	-4.49	-6.3	-2.9	1.81	1.59
7732-18-5	water	67-56-1	methanol	368.45	-4.1	-6.57	-2.67	2.47	1.43
7732-18-5	water	67-56-1	methanol	367.15	-4.08	-6.55	-2.69	2.47	1.39
7732-18-5	water	67-56-1	methanol	364.65	-4.15	-6.5	-2.73	2.35	1.42
7732-18-5	water	67-56-1	methanol	338.85	-4.59	-6.04	-3.11	1.45	1.48
7732-18-5	water	67-56-1	methanol	366.15	-4.12	-6.53	-2.71	2.41	1.41
7732-18-5	water	67-56-1	methanol	363.65	-4.23	-6.49	-2.74	2.26	1.49
7732-18-5	water	67-56-1	methanol	362.15	-4.17	-6.46	-2.76	2.29	1.41
7732-18-5	water	67-56-1	methanol	369.15	-3.9	-6.58	-2.66	2.68	1.24
7732-18-5	water	67-56-1	methanol	367.15	-3.99	-6.55	-2.69	2.56	1.3
7732-18-5	water	67-56-1	methanol	362.45	-4.15	-6.46	-2.76	2.31	1.39
7732-18-5	water	67-56-1	methanol	358.25	-4.28	-6.39	-2.82	2.11	1.46
7732-18-5	water	67-56-1	methanol	366.04	-4.16	-6.53	-2.71	2.37	1.45
7732-18-5	water	67-56-1	methanol	368.55	-4.08	-6.57	-2.67	2.49	1.41
7732-18-5	water	67-56-1	methanol	366.95	-4.14	-6.54	-2.69	2.4	1.45
7732-18-5	water	67-56-1	methanol	362.15	-4.04	-6.46	-2.76	2.42	1.28
7732-18-5	water	67-56-1	methanol	369.56	-3.97	-6.59	-2.66	2.62	1.31
7732-18-5	water	67-56-1	methanol	362.72	-4.19	-6.47	-2.76	2.28	1.43
7732-18-5	water	67-56-1	methanol	365.54	-4.11	-6.52	-2.71	2.41	1.4
7732-18-5	water	67-56-1	methanol	283.15	-5.32	-5.05	-4.99	0.27	0.33
7732-18-5	water	67-56-1	methanol	293.15	-5.14	-5.23	-4.85	0.09	0.29
7732-18-5	water	67-56-1	methanol	298.15	-4.98	-5.32	-4.78	0.34	0.2
7732-18-5	water	67-56-1	methanol	303.15	-4.83	-5.41	-4.71	0.58	0.12
7732-18-5	water	67-56-1	methanol	313.15	-4.64	-5.58	-4.58	0.94	0.06
7732-18-5	water	67-56-1	methanol	313.15	-4.8	-5.58	-4.58	0.78	0.22
7732-18-5	water	67-56-1	methanol	333.15	-4.46	-5.94	-4.32	1.48	0.14
7732-18-5	water	67-56-1	methanol	303.25	-4.8	-5.41	-4.71	0.61	0.09
7732-18-5	water	67-56-1	methanol	313.65	-4.65	-5.59	-4.57	0.94	0.08
7732-18-5	water	67-56-1	methanol	323.25	-4.53	-5.77	-4.45	1.24	0.08
7732-18-5	water	67-56-1	methanol	333.25	-4.38	-5.94	-3.2	1.56	1.18
7732-18-5	water	67-56-1	methanol	328.15	-4.52	-5.85	-4.38	1.33	0.14
7732-18-5	water	67-56-1	methanol	298.15	-5.04	-5.32	-4.78	0.28	0.26
7732-18-5	water	67-56-1	methanol	303.15	-4.96	-5.41	-4.71	0.45	0.25
7732-18-5	water	67-56-1	methanol	313.15	-4.77	-5.58	-4.58	0.81	0.19
7732-18-5	water	67-56-1	methanol	323.15	-4.59	-5.76	-4.45	1.17	0.14
7732-18-5	water	67-56-1	methanol	333.15	-4.45	-5.94	-4.32	1.49	0.13
7732-18-5	water	67-56-1	methanol	313.15	-4.8	-5.58	-4.58	0.78	0.22
7732-18-5	water	67-56-1	methanol	373.3	-3.95	-6.66	-2.6	2.71	1.35
7732-18-5	water	67-56-1	methanol	298.15	-5.03	-5.32	-4.78	0.29	0.25
7732-18-5	water	67-56-1	methanol	298.65	-4.99	-5.33	-4.77	0.34	0.22
7732-18-5	water	67-56-1	methanol	333.05	-4.45	-5.94	-4.32	1.49	0.13
7732-18-5	water	67-56-1	methanol	342.35	-4.3	-6.11	-3.06	1.81	1.24
7732-18-5	water	67-56-1	methanol	353.05	-4.13	-6.3	-2.9	2.17	1.23
7732-18-5	water	67-56-1	methanol	362.95	-4.01	-6.47	-2.75	2.46	1.26
7732-18-5	water	67-56-1	methanol	372.55	-3.87	-6.64	-2.61	2.77	1.26
7732-18-5	water	67-56-1	methanol	358.15	-4.11	-6.39	-2.82	2.28	1.29
7732-18-5	water	67-56-1	methanol	363.15	-4.03	-6.48	-2.75	2.45	1.28
7732-18-5	water	67-56-1	methanol	368.15	-3.97	-6.57	-2.68	2.6	1.29
7732-18-5	water	67-56-1	methanol	372.15	-3.92	-6.64	-2.62	2.72	1.3
7732-18-5	water	67-56-1	methanol	297.45	-4.9	-5.3	-4.79	0.4	0.11
7732-18-5	water	67-56-1	methanol	298.15	-5.02	-5.32	-4.78	0.3	0.24
7732-18-5	water	67-56-1	methanol	298.2	-5.01	-5.32	-4.78	0.31	0.23
7732-18-5	water	67-56-1	methanol	323.2	-4.59	-5.76	-4.45	1.17	0.14
7732-18-5	water	67-56-1	methanol	333.2	-4.42	-5.94	-3.2	1.52	1.22
7732-18-5	water	67-56-1	methanol	298.15	-5.08	-5.32	-4.78	0.24	0.3
7732-18-5	water	67-56-1	methanol	333.15	-4.53	-5.94	-4.32	1.41	0.21
7732-18-5	water	67-56-1	methanol	373.15	-3.97	-6.66	-2.61	2.69	1.36
7732-18-5	water	67-56-1	methanol	298.15	-5.04	-5.32	-4.78	0.28	0.26
7732-18-5	water	67-56-1	methanol	293.15	-5.09	-5.23	-4.85	0.14	0.24

Table C.1: ΔG_{solv} for binary systems (kcal/mol).

solvent		solute		T (K)	ΔG^{ref}_{solv}	$\Delta G^{calc,1}_{solv}$	$\Delta G^{calc,2}_{solv}$	$\Delta G^{calc,1}_{solv}$-ΔG^{ref}_{solv}	$\Delta G^{calc,2}_{solv}$-ΔG^{ref}_{solv}
7732-18-5	water	67-56-1	methanol	303.15	-4.93	-5.41	-4.71	0.48	0.22
7732-18-5	water	67-56-1	methanol	313.15	-4.76	-5.58	-4.58	0.82	0.18
7732-18-5	water	67-56-1	methanol	293.15	-4.82	-5.23	-4.85	0.41	0.03
7732-18-5	water	67-56-1	methanol	303.15	-4.72	-5.41	-4.71	0.69	0.01
7732-18-5	water	67-56-1	methanol	313.15	-4.65	-5.58	-4.58	0.93	0.07
7732-18-5	water	67-56-1	methanol	298.15	-5.08	-5.32	-4.78	0.24	0.3
7732-18-5	water	67-56-1	methanol	298.15	-5.01	-5.32	-4.78	0.31	0.23
7732-18-5	water	67-56-1	methanol	298.15	-5.06	-5.32	-4.78	0.26	0.28
7732-18-5	water	67-56-1	methanol	298.15	-5.04	-5.32	-4.78	0.28	0.26
7732-18-5	water	67-56-1	methanol	273.35	-5.52	-4.88	-5.13	0.64	0.39
7732-18-5	water	67-56-1	methanol	283.15	-5.32	-5.05	-4.99	0.27	0.33
7732-18-5	water	67-56-1	methanol	293.15	-5.14	-5.23	-4.85	0.09	0.29
7732-18-5	water	67-56-1	methanol	303.15	-4.96	-5.41	-4.71	0.45	0.25
7732-18-5	water	67-56-1	methanol	308.15	-4.86	-5.5	-4.64	0.64	0.22
7732-18-5	water	67-56-1	methanol	313.15	-4.78	-5.58	-4.58	0.8	0.2
7732-18-5	water	67-56-1	methanol	318.15	-4.69	-5.67	-4.51	0.98	0.18
7732-18-5	water	67-56-1	methanol	323.15	-4.61	-5.76	-4.45	1.15	0.16
7732-18-5	water	67-56-1	methanol	328.15	-4.53	-5.85	-4.38	1.32	0.15
7732-18-5	water	67-56-1	methanol	333.15	-4.45	-5.94	-4.32	1.49	0.13
7732-18-5	water	67-56-1	methanol	300.45	-4.84	-5.36	-4.75	0.52	0.09
7732-18-5	water	67-56-1	methanol	313.15	-4.76	-5.58	-4.58	0.82	0.18
7732-18-5	water	67-56-1	methanol	323.15	-4.6	-5.76	-4.45	1.16	0.15
7732-18-5	water	67-56-1	methanol	333.15	-4.39	-5.94	-4.32	1.55	0.07
7732-18-5	water	67-56-1	methanol	338.15	-4.32	-6.03	-3.12	1.71	1.2
7732-18-5	water	67-56-1	methanol	278.2	-5.39	-4.96	-5.06	0.43	0.33
7732-18-5	water	67-56-1	methanol	283.2	-5.41	-5.05	-4.99	0.36	0.42
7732-18-5	water	67-56-1	methanol	288.2	-5.29	-5.14	-4.91	0.15	0.38
7732-18-5	water	67-56-1	methanol	293.2	-5.14	-5.23	-4.84	0.09	0.3
7732-18-5	water	67-56-1	methanol	298.2	-5.08	-5.32	-4.78	0.24	0.3
7732-18-5	water	67-56-1	methanol	303.2	-5.05	-5.41	-4.71	0.36	0.34
7732-18-5	water	67-56-1	methanol	298	-5.1	-5.31	-4.78	0.21	0.32
7732-18-5	water	67-56-1	methanol	298.15	-4.91	-5.32	-4.78	0.41	0.13
7732-18-5	water	108-87-2	methylcyclohexane	299.25	1.65	2.06	0.33	0.41	1.32
7732-18-5	water	108-87-2	methylcyclohexane	343.65	2.68	2.36	2.2	0.32	0.48
7732-18-5	water	108-87-2	methylcyclohexane	373.65	3.05	2.57	2.7	0.48	0.35
7732-18-5	water	108-87-2	methylcyclohexane	404.15	3.14	2.78	3.15	0.36	0.01
7732-18-5	water	108-87-2	methylcyclohexane	424.55	3.18	2.92	3.44	0.26	0.26
7732-18-5	water	108-87-2	methylcyclohexane	443.95	3.17	3.05	3.69	0.12	0.52
7732-18-5	water	108-87-2	methylcyclohexane	298.15	1.62	2.05	0.31	0.43	1.31
7732-18-5	water	108-87-2	methylcyclohexane	313.25	2.03	2.15	0.57	0.12	1.46
7732-18-5	water	108-87-2	methylcyclohexane	328.85	2.48	2.26	0.82	0.22	1.66
7732-18-5	water	108-87-2	methylcyclohexane	372.25	3.37	2.56	2.68	0.81	0.69
7732-18-5	water	108-87-2	methylcyclohexane	393.15	3.29	2.7	2.99	0.59	0.3
7732-18-5	water	108-87-2	methylcyclohexane	410.45	3.26	2.82	3.24	0.44	0.02
7732-18-5	water	108-87-2	methylcyclohexane	422.65	3.09	2.91	3.41	0.18	0.32
7732-18-5	water	108-87-2	methylcyclohexane	341.15	1.67	2.35	2.16	0.68	0.49
7732-18-5	water	108-87-2	methylcyclohexane	393.65	2.12	2.71	3	0.59	0.88
7732-18-5	water	108-87-2	methylcyclohexane	430.65	2.13	2.96	3.52	0.83	1.39
7732-18-5	water	108-87-2	methylcyclohexane	298.15	1.69	2.05	0.31	0.36	1.38
7732-18-5	water	108-87-2	methylcyclohexane	449.26	3.28	3.09	3.76	0.19	0.48
7732-18-5	water	108-87-2	methylcyclohexane	475.93	3.04	3.27	4.09	0.23	1.05
7732-18-5	water	108-87-2	methylcyclohexane	310.93	2.1	2.14	0.53	0.04	1.57
7732-18-5	water	108-87-2	methylcyclohexane	394.26	3.25	2.71	3.01	0.54	0.24
7732-18-5	water	108-87-2	methylcyclohexane	298.15	1.69	2.05	0.31	0.36	1.38
7732-18-5	water	96-37-7	methylcyclopentane	334.65	1.52	2.16	2.12	0.64	0.6
7732-18-5	water	96-37-7	methylcyclopentane	457.15	1.59	2.95	3.87	1.36	2.28
7732-18-5	water	96-37-7	methylcyclopentane	298.15	1.59	1.93	0.45	0.34	1.14
7732-18-5	water	96-37-7	methylcyclopentane	298.15	1.6	1.93	0.45	0.33	1.15
7732-18-5	water	96-37-7	methylcyclopentane	419.15	1.9	2.71	3.39	0.81	1.49
7732-18-5	water	96-37-7	methylcyclopentane	298.15	1.6	1.93	0.45	0.33	1.15
7732-18-5	water	124-19-6	nonanal	293.15	-2.82	-2.37	-3.7	0.45	0.88
7732-18-5	water	124-19-6	nonanal	303.15	-2.89	-2.45	-3.37	0.44	0.48
7732-18-5	water	124-19-6	nonanal	313.15	-2.32	-2.53	-3.06	0.21	0.74
7732-18-5	water	124-19-6	nonanal	323.15	-2.35	-2.61	-2.77	0.26	0.42
7732-18-5	water	124-19-6	nonanal	333.15	-1.48	-2.69	-2.49	1.21	1.01
7732-18-5	water	124-19-6	nonanal	343.15	-1.64	-2.77	-1.08	1.13	0.56
7732-18-5	water	124-19-6	nonanal	353.15	-1.21	-2.85	-0.8	1.64	0.41

Table C.1: ΔG_{solv} for binary systems (kcal/mol).

solvent		solute		T (K)	ΔG^{ref}_{solv}	$\Delta G^{calc,1}_{solv}$	$\Delta G^{calc,2}_{solv}$	$\Delta G^{calc,1}_{solv}$-ΔG^{ref}_{solv}	$\Delta G^{calc,2}_{solv}$-ΔG^{ref}_{solv}
7732-18-5	water	124-19-6	nonanal	363.15	-0.9	-2.94	-0.54	2.03	0.36
7732-18-5	water	124-19-6	nonanal	298.15	-2.09	-2.41	-3.53	0.32	1.44
7732-18-5	water	124-19-6	nonanal	303.15	-1.84	-2.45	-3.37	0.61	1.53
7732-18-5	water	124-13-0	octanal	303.15	-2.03	-2.61	-3.2	0.58	1.17
7732-18-5	water	124-13-0	octanal	303.95	-2.08	-2.61	-3.18	0.53	1.1
7732-18-5	water	124-13-0	octanal	313.15	-1.83	-2.69	-2.96	0.86	1.13
7732-18-5	water	124-13-0	octanal	323.5	-1.54	-2.78	-2.72	1.24	1.18
7732-18-5	water	124-13-0	octanal	333.15	-1.27	-2.87	-2.5	1.6	1.23
7732-18-5	water	124-13-0	octanal	344.3	-0.97	-2.96	-1.1	1.99	0.13
7732-18-5	water	124-13-0	octanal	353.15	-0.75	-3.04	-0.89	2.28	0.14
7732-18-5	water	124-13-0	octanal	363.15	-0.5	-3.12	-0.66	2.63	0.17
7732-18-5	water	110-62-3	pentanal	298.15	-2.86	-3.01	-3.27	0.15	0.41
7732-18-5	water	74-98-6	propane	293.15	1.87	2	1.19	0.13	0.68
7732-18-5	water	74-98-6	propane	285.32	1.56	1.95	1.1	0.39	0.46
7732-18-5	water	74-98-6	propane	298.76	1.96	2.04	1.25	0.08	0.71
7732-18-5	water	74-98-6	propane	299.32	1.97	2.05	1.25	0.08	0.72
7732-18-5	water	74-98-6	propane	298.08	1.96	2.04	1.24	0.08	0.72
7732-18-5	water	109-99-9	tetrahydrofuran	346.35	-2.93	-3.39	-1.48	0.46	1.45
7732-18-5	water	109-99-9	tetrahydrofuran	308.15	-3.19	-3.02	-3.17	0.17	0.02
7732-18-5	water	109-99-9	tetrahydrofuran	323.15	-2.79	-3.17	-2.96	0.38	0.17
7732-18-5	water	109-99-9	tetrahydrofuran	273.35	-4.13	-2.68	-3.71	1.45	0.42
7732-18-5	water	109-99-9	tetrahydrofuran	278.15	-4	-2.73	-3.63	1.27	0.37
7732-18-5	water	109-99-9	tetrahydrofuran	298.15	-3.47	-2.92	-3.32	0.55	0.15
7732-18-5	water	109-99-9	tetrahydrofuran	293.15	-3.59	-2.87	-3.4	0.72	0.19
7732-18-5	water	109-99-9	tetrahydrofuran	288.15	-3.74	-2.82	-3.47	0.92	0.27
7732-18-5	water	109-99-9	tetrahydrofuran	298.15	-3.49	-2.92	-3.32	0.57	0.17
7732-18-5	water	109-99-9	tetrahydrofuran	308.15	-3.27	-3.02	-3.17	0.25	0.1
7732-18-5	water	109-99-9	tetrahydrofuran	318.15	-3.05	-3.12	-3.03	0.07	0.02
7732-18-5	water	109-99-9	tetrahydrofuran	323.15	-2.92	-3.17	-2.96	0.25	0.04
7732-18-5	water	109-99-9	tetrahydrofuran	328.15	-2.82	-3.22	-2.89	0.4	0.07
7732-18-5	water	109-99-9	tetrahydrofuran	298.15	-3.51	-2.92	-3.32	0.59	0.19

[1] Calculated from Abbraham contribution group method.
[2] Calculated with activity coefficient model of Lin and Sandler [11].
[ref] Taken from Moine solvation energy database [12].

C.2 Activity coefficients predictions

Table C.2: Prediction on infinite dilution activity coefficient in water $\ln \gamma^{\infty}_{i/Water}$ for binary systems at 298.15 K with COSMO-SAC models before and after optimisation. ([w] optimisation done in this work.)

Solute	CAS Number	$(\ln \gamma^{\infty}_{i/Water})^{exp}$ [11]	$\ln \gamma^{\infty}_{i/Water}$ COSMO-SAC					
			Lin 2002 [11]	Lin opt[w]	Mullins 2006 [18]	Mullins opt [w]	dsp [13]	dsp opt [w]
Alkanes								
butane	106-97-8	9.99	8.33	9.87	5.99	9.8	10.31	9.83
pentane	109-66-0	11.55	9.55	11.35	6.79	11.25	11.74	11.19
hexane	110-54-3	13.13	10.74	12.81	7.57	12.67	13.14	12.52
heptane	142-82-5	14.46	11.91	14.23	8.32	14.06	14.52	13.83
octane	111-65-9	16.08	13.08	15.67	9.08	15.47	15.9	15.14
2-methylpentane	107-83-5	12.76	10.45	12.46	7.41	12.38	12.8	12.16
cyclohexane	110-82-7	11.31	9.57	11.33	6.79	11.16	11.74	11.24
Alkenes								
1-butene	106-98-9	8.47	6.76	7.79	5.25	7.74	8.71	7.79
1-hexene	592-41-6	11.38	9.12	10.67	6.82	10.58	11.48	10.42
1-heptene	592-76-7	14.65	10.29	12.1	7.58	11.98	12.86	11.73
1-octene	111-66-0	15.65	11.44	13.49	8.31	13.35	14.21	13.01
1-hexyne	693-02-7	9.45	7.14	7.93	5.72	7.81	9.28	7.61
1-heptyne	628-71-7	10.95	8.25	9.29	6.46	9.16	10.65	8.92
Ketones								
acetone	67-64-1	1.95	1.52	2.32	1.67	2.13	2.13	2.25
2-butanone	78-93-3	3.24	2.8	3.67	2.35	3.43	1.11	2.77
2-pentanone	107-87-9	4.54	3.76	5.12	3.19	4.82	4.72	4.71

Table C.2: Prediction on infinite dilution activity coefficient in water $\ln \gamma^{\infty}_{i/Water}$ for binary systems at 298.15 K with COSMO-SAC models before and after optimisation. ([w] optimisation done in this work.)

Solute	CAS Number	$(\ln \gamma^{\infty}_{i/Water})^{exp}$ [11]	$\ln \gamma^{\infty}_{i/Water}$ COSMO-SAC					
			Lin 2002 [11]	Lin opt[w]	Mullins 2006 [18]	Mullins opt [w]	dsp [13]	dsp opt [w]
3-pentanone	96-22-0	4.68	4.24	5.53	3.55	5.28	7.49	5.79
Alcohols								
ethanol	64-17-5	1.34	2.09	2.73	1.61	2.63	2.42	2.76
1-propanol	71-23-8	2.65	2.83	3.8	2.09	3.65	3.42	3.83
1-butanol	71-36-3	3.98	3.85	5.07	2.74	4.89	4.71	5.06
2-butanol	78-92-2	3.27	4.3	5.41	3.15	5.34	5.18	5.32
tert-butyl alcohol	75-65-0	2.48	3.53	4.85	2.6	4.78	4.41	4.81
isobutanol	78-83-1	3.89	4.5	5.55	3.28	5.51	5.47	5.4
1-pentanol	71-41-0	5.42	4.94	6.4	3.45	6.19	6.05	6.35
1-hexanol	111-27-3	6.67	5.96	7.67	4.1	7.44	7.32	7.56
1-octanol	111-87-5	9.36	8.09	10.3	5.45	10.01	9.91	10.04
acetic acid	64-19-7	1.06	0.82	1.43	0.84	1.39	1.12	1.48
Other Families								
benzene	71-43-2	3.97	6.17	7.12	5.07	6.92	8.2	6.7
pyridine	110-86-1	7.82	2.62	4.33	2.31	4.23	6.87	5.02
aniline	62-53-3	2.99	3.14	3.84	2.84	3.7	5.27	3.87
phenol	108-95-2	4.99	1.78	3.73	1.46	3.63	4.23	3.4
chlorobenzene	108-90-7	6.31	7.19	8.53	5.8	8.5	9.16	7.54
chloroform	67-66-3	9.55	4.87	6.39	3.97	6.6	7.76	6.44
propanal	123-38-6	2.57	2.62	3.11	2.53	2.88	3.13	3.06
butyraldehyde	123-72-8	3.88	3.72	4.47	3.29	4.18	4.53	4.41
methylformate	107-31-3	2.74	2.73	2.69	2.61	2.59	4.13	2.33
methyl acetate	79-20-9	3.12	3.04	3.43	2.89	3.31	3.53	3.1
ethyl acetate	141-78-6	4.18	3.87	4.53	3.47	4.37	4.55	4.13
methyl propionate	554-12-1	4.47	3.7	4.58	3.29	4.42	4.43	4.13
nitromethane	75-52-5	3.45	3.08	2.56	2.83	2.39	3.61	2.63
nitroethane	79-24-3	4.48	3.94	3.71	3.55	3.48	4.56	3.69
nitropropane	108-03-2	5.7	4.98	5.04	4.33	4.77	5.64	4.76
acetonitrile	75-05-8	2.41	1.66	1.45	1.71	1.26	3.92	1.86
propionitrile	107-12-0	3.63	2.41	2.51	2.36	2.2	4.92	2.93
butyronitrile	109-74-0	4.72	3.39	3.72	3.07	3.34	6.19	4.17
diethyl ether	60-29-7	4.7	5.34	6.74	4.23	6.65	7.59	6.4
tetrahydrofuran	109-99-9	2.83	3.15	4.62	2.65	4.41	5.94	4.7
ethylamine	75-04-7	-0.99	-0.69	2.5	-0.75	2.46	2.79	2.93
butylamine	109-73-9	1.39	1.99	5.45	1.1	5.33	5.59	5.6
tetrachloro-methane	56-23-5	6.81	8.49	10.05	6.34	10.16	10.32	9.45
AAD			1.45	1.29	2.34	1.28	1.16	1.3

Table C.3: Prediction on infinite dilution activity coefficient in hexane $\ln \gamma^{\infty}_{i/Hexane}$ for binary systems at 298.15 K with COSMO-SAC models before and after optimisation. ([w] optimisation done in this work.)

Solute	CAS Number	$(\ln \gamma^{\infty}_{i/Hexane})^{exp}$ [11]	$\ln \gamma^{\infty}_{i/Hexane}$ COSMO-SAC					
			Lin 2002 [11]	Lin opt [w]	Mullins 2006 [18]	Mullins opt [w]	dsp [13]	dsp opt [w]
butane	106-97-8	0	-0.04	-0.04	-0.04	-0.04	-0.04	-0.04
pentane	109-66-0	-0.01	-0.01	-0.01	-0.01	-0.01	-0.01	-0.01
hexane	110-54-3	0	0	0	0	0	0	0
heptane	142-82-5	-0.03	-0.01	-0.01	-0.01	-0.01	-0.01	-0.01
octane	111-65-9	0.08	-0.03	-0.03	-0.03	-0.03	-0.03	-0.03
2-methylpentane	107-83-5	0	0	0	0	0	0	0
cyclohexane	110-82-7	0.13	0	0	0	0	0	0
1-butene	106-98-9		0.12	0.11	0	0.07	0.13	0.14
1-hexene	592-41-6		0.12	0.11	0.04	0.08	0.12	0.13
1-heptene	592-76-7		0.1	0.09	0.03	0.07	0.1	0.11
1-octene	111-66-0		0.06	0.06	0	0.04	0.07	0.07
1-hexyne	693-02-7		0.77	0.95	0.24	0.87	0.87	0.91
1-heptyne	628-71-7		0.67	0.85	0.21	0.77	0.75	0.78
diethyl ether	60-29-7		0.26	0.25	0.1	0.2	0.28	0.29
tetrahydrofuran	109-99-9		0.36	0.35	0.12	0.32	0.38	0.4
ethylamine	75-04-7		1.95	2.4	0.72	2.37	1.89	1.54
butylamine	109-73-9		1.74	2.11	0.66	2.06	1.63	1.29
acetone	67-64-1	1.9	1.41	1.73	0.51	1.92	1.8	1.86
2-pentanone	107-87-9		0.98	1.12	0.37	1.2	1.16	1.19
3-pentanone	96-22-0		0.85	0.94	0.31	1.01	1.02	1.05
propanal	123-38-6		1.1	1.24	0.38	1.34	1.47	1.52
butyraldehyde	123-72-8		0.96	1.05	0.35	1.12	1.2	1.24
methylformate	107-31-3		1.86	2.35	0.62	2.37	1.89	1.98
methyl acetate	79-20-9		1.46	1.76	0.51	1.76	1.8	1.87
ethyl acetate	141-78-6	1.23	1.23	1.41	0.45	1.4	1.47	1.53
methyl propionate	554-12-1		1.19	1.38	0.43	1.37	1.43	1.49
nitromethane	75-52-5	3.68	2.94	3.55	1	3.68	2.98	3.07
nitroethane	79-24-3	2.99	2.15	2.58	0.72	2.66	2.21	2.28
nitropropane	108-03-2	2.65	1.71	2.05	0.58	2.07	1.78	1.84
acetonitrile	75-05-8	3.32	3.15	3.98	1.19	4.38	4.04	4.15
propionitrile	107-12-0	2.92	2.18	2.7	0.8	2.98	2.7	2.77
butyronitrile	109-74-0		1.77	2.15	0.66	2.36	2.1	2.17
ethanol	64-17-5	4.01	4.19	3.43	2.31	3.29	5.23	2.95
1-propanol	71-23-8	3.76	4.16	3.35	2.32	3.23	5.02	2.79
1-butanol	71-36-3	3.59	4.02	3.19	2.22	3.07	4.81	2.59
2-butanol	78-92-2		3.4	2.77	1.8	2.58	4.23	2.25
tert-butyl alcohol	75-65-0		3.59	2.93	1.93	2.77	4.35	2.42
isobutanol	78-83-1		3.42	2.79	1.77	2.55	4.32	2.25
1-pentanol	71-41-0		3.91	3.05	2.17	2.93	4.64	2.43
1-hexanol	111-27-3		3.77	2.91	2.07	2.78	4.47	2.28
1-octanol	111-87-5		3.54	2.65	1.89	2.53	4.19	2.02
acetic acid	64-19-7		5.53	5.3	2.86	5.18	7.25	4.67
benzene	71-43-2		0.71	0.7	0.2	0.69	0.74	0.77
pyridine	110-86-1		1.54	1.91	0.53	1.97	1.6	1.67
aniline	62-53-3		3.02	3.73	1.1	3.74	3.08	3.13
phenol	108-95-2		3.54	3.67	1.5	3.65	4.87	3.25
chlorobenzene	108-90-7		0.63	0.58	0.19	0.53	0.67	0.69
chloroform	67-66-3	0.48	0.29	0.26	0.08	0.16	0.34	0.35
tetrachloro-methane	56-23-5	0.17	0.04	0.03	0.01	0.01	0.08	0.08
Mean abs deviation			1.15	1.11	0.85	1.1	1.38	1.04

Appendix D

Quantum chemistry geometries and frequencies

Optimized geometries of reactants and transition states of vinyl formation and condensation reaction.

Table D.1: Cartesian coordinates of optimized geometries in Angstroms with M062X method with the standard basis set 6-31G(d,p).

Compound	Atom type	Cartesian Coordinates in Angstroms		
		X	Y	Z
2-Methoxy 4-vinylphenol	C	-1.530661	-0.828910	2.641577
	H	-2.069582	-1.774941	2.610365
	C	-2.047737	0.175116	3.352288
	H	-1.568774	1.146739	3.428376
	H	-2.982957	0.050966	3.886445
	C	-0.278403	-0.810801	1.865904
	C	0.561305	0.312417	1.806334
	C	0.105198	-1.952348	1.157925
	C	1.726754	0.299270	1.060375
	H	0.321136	1.228149	2.337503
	C	1.277754	-1.979427	0.406450
	H	-0.524392	-2.836875	1.188754
	C	2.095482	-0.856035	0.346153
	H	1.555614	-2.873692	-0.144664
	O	2.499450	1.429323	0.984766
	O	3.242412	-0.796022	-0.378682
	H	3.397425	-1.646035	-0.809997
	C	3.723649	1.333913	1.710097
	H	3.524977	1.158972	2.773269
	H	4.351131	0.529623	1.316310
	H	4.232919	2.289998	1.587449
TS vinyl formation	C	-1.884640	-1.036656	0.190585
	C	-0.527110	-0.923238	-0.167074
	C	0.068795	0.323393	-0.218978
	C	-0.658149	1.486561	0.068665
	C	-1.996743	1.363479	0.434395
	C	-2.606670	0.111169	0.497068
	H	1.108326	0.387809	-0.524853
	H	-2.569453	2.247728	0.691366
	H	-3.651866	0.025901	0.781613
	C	0.006525	2.817933	0.064724
	H	0.909168	2.871416	0.673153
	C	-0.699865	4.030400	-0.194606
	H	-0.373138	4.921219	0.331455
	H	0.114457	3.763812	-1.341902
	H	-1.761892	3.962941	-0.408823
	O	0.868943	2.826624	-1.564434
	H	1.789083	3.110290	-1.440752
	O	0.188761	-2.040244	-0.510110
	C	0.518582	-2.871130	0.601640
	H	1.076226	-3.718443	0.202100
	H	1.145064	-2.323858	1.314766
	H	-0.384070	-3.229828	1.104082
	O	-2.416495	-2.284683	0.204820
	H	-3.345588	-2.237230	0.464050
$4-(1-Hydroxyethyl)-guaiacol$	C	-1.198899	-1.233307	0.586515
	C	-0.006179	-1.116466	-0.145233
	C	0.624696	0.114276	-0.254922
	C	0.088910	1.251306	0.354966
	C	-1.090175	1.127151	1.084015
	C	-1.733595	-0.104044	1.199248
	H	1.548967	0.176551	-0.820254
	H	-1.518491	1.999006	1.571411
	H	-2.654791	-0.190975	1.769279
	C	0.746369	2.600936	0.174116

	H	0.493846	3.225047	1.044980
	C	0.241022	3.291366	-1.091138
	H	-0.841689	3.433996	-1.047333
	H	0.711346	4.273013	-1.211846
	H	0.478994	2.676286	-1.963780
	O	2.150441	2.398421	0.109168
	H	2.555595	3.238192	-0.138018
	O	0.518421	-2.213577	-0.781926
	C	1.146553	-3.134762	0.106167
	H	1.532942	-3.948376	-0.508518
	H	1.975204	-2.651600	0.635759
	H	0.429248	-3.531078	0.830628
	O	-1.771220	-2.466341	0.651201
	H	-2.577948	-2.417419	1.179342
Quinone Methide	C	-0.611363	0.948126	-0.883300
	C	-0.328738	-0.142750	-1.695306
	C	-1.317922	-1.216547	-1.870104
	C	-2.560127	-1.053249	-1.141071
	C	-2.800126	0.028971	-0.351064
	C	-1.826236	1.063071	-0.203887
	H	0.156551	1.708998	-0.793501
	H	-3.290899	-1.845274	-1.265335
	H	-3.742794	0.121822	0.180319
	O	0.868790	-0.126626	-2.285477
	O	-1.115341	-2.209576	-2.599950
	C	1.351254	-1.200904	-3.097268
	H	2.363855	-0.905241	-3.368917
	H	1.363451	-2.137013	-2.538855
	H	0.736264	-1.323243	-3.988797
	C	-2.149286	2.198671	0.658091
	H	-3.126146	2.150626	1.135113
	C	-1.369076	3.259519	0.900225
	H	-0.384521	3.377046	0.458827
	H	-1.704987	4.052274	1.558756
Transition State of vinyl condensation reaction	C	-8.516785	-1.029283	-4.669433
	C	-8.814434	-1.950514	-5.618458
	C	-10.212718	-2.310773	-5.937390
	C	-11.235111	-1.643373	-5.136457
	C	-10.914576	-0.733877	-4.185013
	C	-9.546950	-0.375378	-3.903166
	H	-7.469198	-0.796798	-4.498390
	H	-12.265880	-1.905337	-5.352034
	H	-11.695952	-0.247419	-3.606547
	O	-7.814153	-2.509206	-6.358049
	O	-10.485320	-3.114532	-6.835693
	C	-7.665277	-3.918887	-6.184147
	H	-6.831842	-4.219939	-6.818957
	H	-7.426368	-4.146830	-5.139079
	H	-8.571616	-4.447338	-6.483636
	C	-9.271135	0.538690	-2.896554
	H	-10.122052	0.913897	-2.330235
	C	-7.978126	0.931815	-2.473869
	H	-7.162892	0.861549	-3.187611
	H	-7.904514	1.787623	-1.811039
	C	-7.237577	-0.520971	-1.290705
	H	-7.639991	-1.306231	-1.931547
	C	-7.851272	-0.360741	-0.048209
	H	-7.355717	0.151026	0.768526
	H	-8.883210	-0.657167	0.097256
	C	-5.772213	-0.315202	-1.445199
	C	-5.090728	0.686035	-0.741877
	C	-5.050935	-1.109127	-2.337715
	C	-3.730078	0.882204	-0.916173
	H	-5.609917	1.348464	-0.054697
	C	-3.682314	-0.922758	-2.517782
	H	-5.559671	-1.891129	-2.895262
	C	-3.011348	0.072478	-1.813783
	H	-3.131375	-1.548045	-3.214814
	O	-3.099745	1.900163	-0.251107
	O	-1.685132	0.328255	-1.951941
	H	-1.297852	-0.294797	-2.580165
	C	-2.236040	1.454035	0.793594
	H	-2.806271	0.908044	1.553193
	H	-1.441561	0.814705	0.399193
	H	-1.800078	2.348680	1.238535

Table D.2: Cartesian coordinates of optimized geometries in Angstroms at a higher level with BP86 D3BJ and def2-TZVP def2/J RIJCOSX basis set.

Compound	Atom type	Cartesian Coordinates in Angstroms		
		X	Y	Z
2-Methoxy 4-vinylphenol	C	-1.56615822904052	-0.83410791220054	2.62337819235738
	H	-2.10702546361824	-1.78526730553562	2.57430623165948
	C	-2.10908993373207	0.16582533741121	3.33620108538662
	H	-1.63432630191308	1.14386073091174	3.43089054808979
	H	-3.05975643258989	0.03363426456453	3.85167079304533
	C	-0.30550851348104	-0.81556174826342	1.87759289275925
	C	0.54943915042585	0.30277973718943	1.84420777664381
	C	0.08970379233780	-1.95886520857752	1.16372373332651
	C	1.73867871253388	0.30037119808804	1.12457300687155
	H	0.30020376834040	1.21685706148350	2.38393027724108
	C	1.27779072750453	-1.97796011388523	0.43485783862324
	H	-0.54758059404181	-2.84478627051185	1.17551846570761

	C	2.10671817913383	-0.85456687197540	0.39489051047676
	H	1.56257653616868	-2.87215095383885	-0.12679122203477
	O	2.48754489420149	1.45416045246625	1.08333976631504
	O	3.26315734289055	-0.81106216295947	-0.34199548956421
	H	3.36953612825952	-1.66772040597517	-0.79229500576375
	C	3.80038347895911	1.35394319329790	1.66179396834368
	H	3.72882130249328	1.07734574703561	2.72681139694036
	H	4.42221217426527	0.62108988180352	1.12851553031146
	H	4.24517928090245	2.35168134947135	1.57187970326376
TS vinyl formation	C	-1.77543211829688	-1.06810028205298	0.06188773936223
	C	-0.36632263348923	-0.98195757452570	-0.01528047713239
	C	0.22793751883951	0.27403499995184	-0.04682440027947
	C	-0.52750437989367	1.46149335899555	0.02055253225755
	C	-1.92677806956768	1.35353718706524	0.12491003803911
	C	-2.53628181859777	0.10680339644102	0.13962673297792
	H	1.31443396821762	0.31830851818076	-0.13809432547225
	H	-2.54173269614360	2.25114370570387	0.16631432528099
	H	-3.62553290707432	0.02961701591102	0.19835129911262
	C	0.15754759061233	2.73832357580224	0.00747841467623
	H	1.24682252681432	2.67394974685935	-0.02245880737708
	C	-0.42848872835830	4.01468588820533	0.28569170997585
	H	0.23612200337662	4.76093641752762	0.72839215483032
	H	-0.36947697669060	4.15402951643419	-0.99899316619195
	H	-1.44969531058100	4.03886754226214	0.67104316669040
	O	0.00485657726314	3.29969513812583	-2.02732778842184
	H	0.79158537173793	3.47211918686516	-2.58217088386366
	O	0.42800399034496	-2.09560027767222	-0.14714417410201
	C	0.41747691262810	-2.99821848745127	0.97337445855608
	H	1.12680766969374	-3.79486297601287	0.72205929392451
	H	0.75451733988758	-2.47936213952537	1.88585689242605
	H	-0.58064031419980	-3.42792559772410	1.13723777594246
	O	-2.34606220133281	-2.31039126531919	0.03784585262598
	H	-3.31391231519020	-2.20576159404748	0.07062163616232
$4-(1-Hydroxyethyl)-guaiacol$	C	-2.53550187420708	2.17965201829115	-0.47727685035177
	C	-1.43305395603641	1.63579170400781	0.42552104112163
	H	-2.52664804642622	3.27831176633746	-0.46755579173995
	H	-3.51673833297063	1.83174003591422	-0.12515903413604
	H	-2.39080807312283	1.83019560506434	-1.50831267124885
	C	-1.40479348270587	0.11975883866522	0.44746784243349
	O	-1.67196046434877	2.18927979747401	1.73384779316648
	H	-0.45530848124685	1.99150070851655	0.04546590362523
	C	-2.34133978439688	-0.60469574701821	1.19430487799016
	H	-1.04594847988686	1.76100879145042	2.34430782578705
	C	-2.33302834199541	-1.99894719068752	1.17142505207298
	C	-1.40161626501911	-2.69987986196100	0.39855976191715
	C	-0.43796334813287	-1.98169386540721	-0.34042213957818
	O	-1.39325478049715	-4.07190327663638	0.31625032447101
	O	0.48128564884741	-2.60324381233801	-1.15402913202788
	C	-0.45805016279941	-0.58609679257342	-0.30330829927904
	H	-2.11731041686980	-4.41273697035966	0.87054891781324
	C	1.41759634298116	-3.46553584427200	-0.48497523981502
	H	2.08568923803210	-3.84636499249211	-1.26612038649558
	H	0.91155168927304	-4.30452567100015	0.01250298869426
	H	2.00428331647322	-2.89363459418745	0.25315559733664
	H	-3.07478120690905	-0.07177022085715	1.80031219661335
	H	-3.07371014286554	-2.56096665637240	1.74812471291708
	H	0.29594940482981	-0.05617376955851	-0.88949529128744
Quinone Methide	C	-0.60652218952414	0.94622996289053	-0.87872106589411
	C	-0.32418521078133	-0.14739021525508	-1.68693142563195
	C	-1.32012984618851	-1.23013835803798	-1.86548005793989
	C	-2.56525582835587	-1.05664865472560	-1.13838596336024
	C	-2.80460486261366	0.03383324731554	-0.34971119076137
	C	-1.82994741841334	1.07053639339963	-0.19822424448303
	H	0.16293453204494	1.71353305046794	-0.78722478030260
	H	-3.30096780502579	-1.85187095400230	-1.26332747334167
	H	-3.75365049445649	0.13280696929539	0.18168104125439
	O	0.88525371228132	-0.13060519355420	-2.27922000383005
	O	-1.11373493197170	-2.22903414845444	-2.59516544665349
	C	1.36087869766367	-1.20934552613052	-3.11376429893576
	H	2.37468887373594	-0.90054175229334	-3.39366486376734
	H	1.37995957807596	-2.15633844642099	-2.56252401572236
	H	0.72982056342755	-1.32896656295891	-4.00156939428102
	C	-2.15111475290946	2.20112043463868	0.65217829638563
	H	-3.13887064214618	2.15573535365116	1.12151754529081
	C	-1.37342014928256	3.27364104158541	0.91268725687037
	H	-0.37804173235571	3.39352802362950	0.48293443325225
	H	-1.72048709320463	4.06861633495959	1.57141465185146
Transition State of vinyl condensation reaction	C	-1.83963597037357	-0.66233910527663	-1.65228315657596
	C	-2.30362409738979	-1.60439055756277	-2.52779705534751
	C	-3.76974874153637	-1.80562823254585	-2.71479093329664
	C	-4.63794528178849	-0.99958803502634	-1.85122915751536
	C	-4.14920296254316	-0.08267301409395	-0.98333954267475
	C	-2.72244805011934	0.13641743318056	-0.84119691387643
	H	-0.76040081263292	-0.52097885968701	-1.58098453096070
	H	-5.70851058732973	-1.16856786084120	-1.97547180490670
	H	-4.82048062425956	0.51741009203035	-0.36436682504698
	O	-1.38024767693493	-2.26253398532388	-3.27130479733425
	O	-4.23704798927632	-2.58006199771522	-3.56377354749097
	C	-1.66726509506657	-3.55981263505690	-3.83640621223626
	H	-0.68277510493415	-3.96930654661158	-4.09446131598369
	H	-2.16145738762705	-4.21113322592366	-3.10330390739077
	H	-2.29909337820670	-3.47681732245150	-4.72664934182638
	C	-2.27311633412452	1.05694438626015	0.07188010712057
	H	-3.03118838274021	1.58915833450464	0.65322009212012
	C	-0.84417167750101	1.33461336983274	0.37842872285103
	H	-0.23078472394529	1.29735340245966	-0.53319453641672

	H	-0.72509983255966	2.33697534831619	0.81345238532424
	C	-0.23804156519695	0.28813104192769	1.38830660069916
	H	-0.40924696469868	-0.69996421537415	0.90945795357953
	C	-0.93657448159863	0.31273334676099	2.69911348974456
	H	-0.43345368806785	-0.04793528072545	3.59518838628941
	H	-1.99911867968507	0.54586655139931	2.76188672622745
	C	1.26019285670843	0.47643522036133	1.49761789017186
	C	1.79833537038564	1.49172484885779	2.29938233924024
	C	2.13936133402696	-0.32898824957500	0.76700713192311
	C	3.17237618892055	1.71876763399295	2.37718761058676
	H	1.14503246282430	2.13738679806706	2.88965826325459
	C	3.51715254832976	-0.11520692556256	0.82995130842534
	H	1.74699762008670	-1.13342314555354	0.14176317688204
	C	4.04670847992726	0.91034127088351	1.61777707535611
	H	4.19644310817996	-0.74517491705035	0.24862994612858
	O	3.61810297611317	2.77646208291237	3.13461206524302
	O	5.39217302635851	1.18209548404763	1.67121247874397
	H	5.85297459875497	0.55212185035564	1.08939681331490
	C	4.49761936044215	2.43730078329278	4.22114449596271
	H	4.00220162864057	1.73136537109007	4.90808643246920
	H	5.43980952043090	2.00302431610559	3.85932374587668
	H	4.69917201000671	3.37772414531857	4.74676434134487

Frequencies of vinyl formation transition state, and vinyl condensation reaction transition state.

Table D.3: Frequencies from gaussian DFT calculation using M062X method with the standard basis set 6-31G(d,p).

Compound	Frequencies (cm^{-1})
TS vinyl formation	-1961.0319
	29.0139
	68.7024
	109.0809
	137.1607
	144.7327
	202.1596
	243.8527
	293.7229
	321.4097
	356.4208
	360.3547
	386.0320
	401.6753
	435.5046
	479.1759
	515.0062
	550.9259
	596.3917
	604.6821
	657.5627
	665.1817
	733.5490
	749.1795
	803.4081
	811.1706
	834.2028
	868.8233
	914.0222
	948.6532
	978.3947
	1052.1977
	1080.2115
	1145.0252
	1162.4543
	1183.8755
	1187.7739
	1192.5566
	1216.5447
	1242.1797
	1297.5906
	1310.6652
	1339.5189
	1389.7017
	1406.0105
	1458.4036
	1471.6865
	1491.3778
	1500.9462
	1513.8473
	1532.8817
	1586.2521
	1663.7486
	1682.5742
	1706.4443
	3061.8908
	3146.9387
	3163.3517
	3174.8875
	3182.1214
	3198.9223
	3225.5727
	3245.7566

	3256.2632
	3813.8795
	3870.3536
Transition state of vinyl condensation reaction	-838.4391
	16.3490
	23.6630
	38.5226
	47.6830
	63.7234
	84.6656
	90.7950
	116.2688
	147.9164
	148.6022
	157.6393
	163.1369
	193.3091
	199.3208
	228.0659
	239.0659
	276.7321
	301.4920
	317.6289
	334.0175
	343.0845
	353.6333
	387.0864
	396.9056
	410.4609
	429.5185
	470.3942
	472.5878
	486.6658
	497.0148
	511.4501
	515.0611
	539.7843
	600.6435
	607.3555
	632.1596
	674.3466
	701.0212
	721.9472
	745.9620
	751.2350
	791.4675
	801.8610
	809.6718
	831.7328
	840.7460
	847.6332
	905.6234
	917.9303
	921.7878
	930.7066
	939.5471
	970.6391
	982.4210
	1003.3712
	1045.0243
	1064.4549
	1069.4901
	1078.5481
	1105.8092
	1143.3295
	1152.1930
	1179.8932
	1183.8777
	1185.5382
	1187.6751
	1194.1360
	1214.6716
	1220.8032
	1235.3520
	1250.6950
	1262.8857
	1279.6890
	1282.9348
	1299.3329
	1346.0590
	1373.1945
	1377.9911
	1431.2432
	1435.4167
	1474.2172
	1477.2272
	1495.0325
	1498.0180
	1500.3384
	1504.7658
	1505.3289
	1516.0949
	1524.7304
	1526.2245
	1567.0946
	1590.2358

	1634.6669
	1683.7273
	1699.1497
	1701.7031
	1713.4132
	3059.2497
	3067.2153
	3141.6919
	3148.3077
	3157.0331
	3170.4766
	3181.2423
	3181.5126
	3188.9142
	3191.2914
	3199.2931
	3202.3216
	3202.8050
	3209.9995
	3216.0030
	3235.6878
	3261.1512
	3297.3349
	3881.7590
Quinone Methide	44.1002
	50.5148
	127.3700
	191.1390
	198.4239
	307.5149
	315.2738
	323.8869
	373.3251
	392.2259
	451.6144
	470.4819
	521.4811
	529.9731
	640.9433
	685.8550
	699.4956
	759.6339

Table D.4: Frequencies from gaussian DFT calculation at a higher level using BP86 D3BJ and def2-TZVP def2/J RIJCOSX basis set.

Compound	Frequencies (cm^{-1})
	-1597.32
	39.40
	58.13
	82.14
	126.28
	130.51
	150.72
	186.87
	209.34
	275.87
TS vinyl formation	311.13
	336.57
	353.76
	371.86
	403.84
	429.77
	435.95
	470.55
	550.50
	560.89
	591.39
	626.13
	707.20
	719.26
	758.73
	768.07
	780.31
	866.54
	879.51
	900.89
	916.33
	937.82
	1011.65
	1027.63
	1087.26
	1130.14
	1152.69
	1158.01
	1170.36
	1205.69
	1235.44
	1280.27
	1286.17
	1353.90
	1364.53
	1380.45

	1410.52
	1428.12
	1436.85
	1458.92
	1474.70
	1505.12
	1576.30
	1594.90
	1620.45
	2943.36
	3018.76
	3048.07
	3066.60
	3076.81
	3094.74
	3110.14
	3127.47
	3133.16
	3626.37
	3670.70
Transition state of vinyl condensation reaction	-632.57
	6.70
	23.69
	29.18
	44.03
	52.40
	58.82
	72.63
	101.90
	129.87
	138.90
	154.48
	172.02
	189.12
	197.03
	213.43
	236.06
	269.01
	282.39
	292.01
	327.25
	342.11
	358.51
	362.39
	377.79
	394.62
	405.43
	425.40
	441.38
	460.94
	466.23
	485.50
	501.63
	526.19
	588.55
	589.49
	612.27
	648.31
	665.89
	700.81
	706.93
	721.92
	723.58
	765.82
	770.82
	781.20
	806.83
	821.91
	848.61
	870.05
	879.46
	886.41
	894.65
	899.20
	936.47
	976.03
	996.20
	1002.78
	1024.19
	1047.49
	1089.08
	1097.02
	1102.32
	1121.04
	1130.12
	1134.53
	1140.17
	1155.13
	1164.49
	1171.45
	1190.88
	1197.49
	1218.02
	1227.92
	1241.39
	1250.80

	1278.64
	1320.43
	1350.52
	1370.28
	1380.32
	1407.89
	1421.70
	1426.92
	1431.10
	1432.30
	1436.27
	1438.60
	1444.62
	1451.88
	1459.92
	1497.85
	1505.87
	1531.27
	1580.78
	1583.23
	1598.19
	1599.02
	2943.71
	2976.15
	3021.18
	3024.65
	3051.70
	3054.28
	3066.63
	3069.12
	3072.59
	3076.74
	3079.76
	3083.46
	3101.71
	3107.17
	3107.88
	3116.78
	3129.98
	3174.16
	3675.75
	46.02
	63.05
	123.92
	175.49
	178.51
	219.33
	279.14
	308.48
	364.84
	377.88
Quinone Methide	426.20
	455.52
	506.11
	506.19
	616.35
	653.97
	668.07
	741.67
	773.23
	810.08
	852.95
	884.53
	892.27
	924.94
	975.37
	993.76
	1032.00
	1103.98
	1115.71
	1138.57
	1165.70
	1196.01
	1246.95
	1293.23
	1314.77
	1387.87
	1409.50
	1419.22
	1429.10
	1429.75
	1449.62
	1476.69
	1512.48
	1557.06
	1604.39
	2984.72
	3066.39
	3070.06
	3074.39
	3080.18
	3089.81
	3111.09
	3121.91
	3165.56

Appendix E

Kinetic: reactions and products structures

E.1 Initiation reactions kinetic

Table E.1: Summary of sensitive reactions involved in biomass pyrolysis first stage at 250 °C estimated with Reaction Mechanism Generator with corresponding kinetic parameters.

Reaction	**Reaction Family**	**Kinetics**	
		A (1/ sec or L/mol sec)	E (kcal/mol)
Guaiacol			
C6H5O2·+CH3·=C7H8O2	Radical combination	1.210e+13	0.000
C7H7O2· + C7H7O2·=C14H14O4	Radical combination	2.500e+13	0.000
H· + C7H7O2·=C7H8O2	H abstraction	7.000e+11	0.000
OH·+C7H8O2=H2O+C7H7O2·	H Abstraction	1.2000e+06	0.000
Creosol			
C7H7O2·+CH3·=creosl	Radical combination	1.210e+13	0.000
C8H9O2·+H·=creosol	H abstraction	7.000e+11	0.000
Vinyl $C_\alpha = C_\beta$ type			
C9H9O2·+H·=C9H10O2	Radical combination	7.000e+11	0.000
CH3·+C8H7O2·=C9H10O2	Radical combination	1.210e+13	0.000
OH·+C9H10O2 = C9H9O2·+H2O	H Abstraction	1.2000e+06	0.000
CH3·+C9H10O2 = C9H9O2·+CH4	H Abstraction	8.2000e+05	6.620
Phenolic $C_\alpha - OH$ type			
CH3·+C8H9O3·=C9H12O3	Radical combination	1.2100e+13	0.000
C9H12O3=C9H10O2+H2O	H_2O elimination	7.867E13	63.35
Propagation			
C7H7O2·Z=C7H7O2·Y	intra H migration	1.110000e+06	27.180
C7H7O2·I=C7H7O2·Z	intra H migration	9.349206e+05	17.654
C7H7O2·I=C7H7O2·Y	intra H migration	4.117867e+02	16.805
Termination reaction			
C7H7O2·Z+C7H7O2·Z=S(131)	Radical Recombination	2.500000e+13	0.000
C7H7O2·Y+C7H7O2·Z=S(1676)	Radical Recombination	5.000000e+13	0.000
C7H7O2·Y+C7H7O2·Y=S(3430)	Radical Recombination	6.030000e+12	0.000

E.2 Predicted products structures

- Guaiacol species

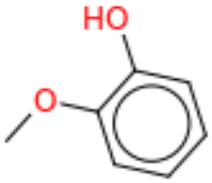

(a) Guaiacol

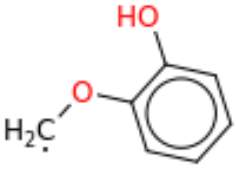

(b) Radical $C_7H_7O_2^{\#}$Y

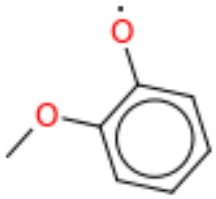

(c) Radical $C_7H_7O_2^{\#}$Z

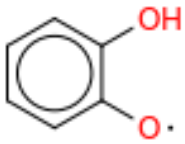

(d) radical$C_6H_5O_2$#

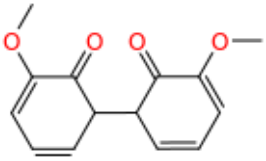

(e) Intermediate species S(383)

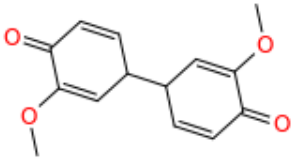

(f) Intermediate species S(387)

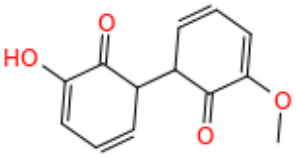

(g) Intermediate species S(371)

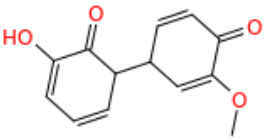

(h) Intermediate species S(373)

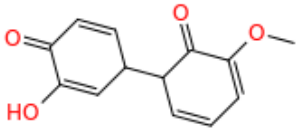

(i) Intermediate species S(375)

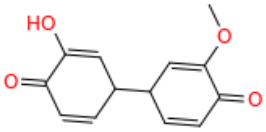

(j) Intermediate species S(377)

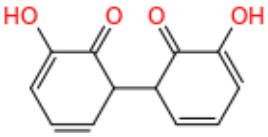

(k) Intermediate species S(278)

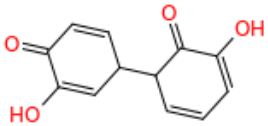

(l) Intermediate species S(280)

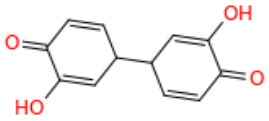

(m) Intermediate species S(283)

- Hydroxyethyl guaiacol and vinyl guaiacol species

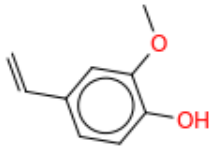

(a) $4-Vinyl$ Guaiacol $C_9H_10O_2^{\#}$

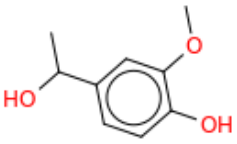

(b) $4-(1-Hydroxyethyl)$-guaiacol $C_9H_12O_3^{\#}$Y

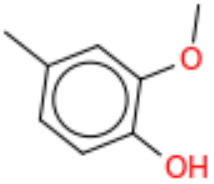

(c) Creosol $C_8H_10O_2$

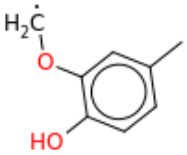

(d) Creosol radical $C_8H_9O_2\#$Y

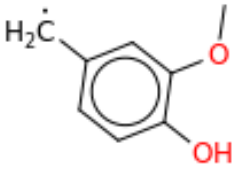

(e) Creosol radical $C_8H_9O_2\#$Z

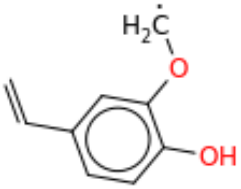

(f) $4-Vinyl$ Guaiacol radical $C_9H_9O_2^{\#}$Y

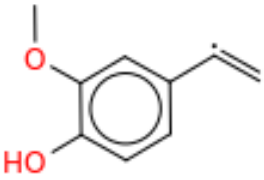

(g) $4-Vinyl$ Guaiacol radical $C_9H_9O_2^{\#}$Z

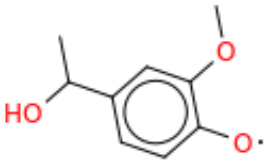

(h) $4-(1-Hydroxyethyl)$-guaiacol radical $C_9H_11O_3^{\#}$

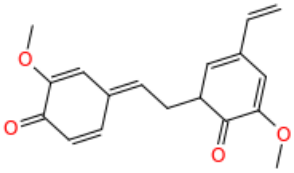

(i) Intermediate species S(972)

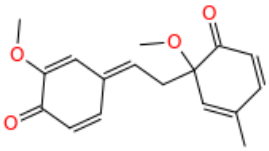

(j) Intermediate species S(930)

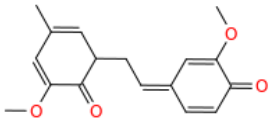

(k) Intermediate species S(920)

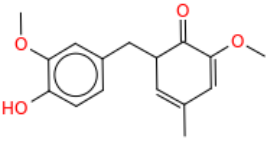

(l) Intermediate species S(847)

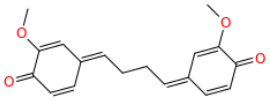

(m) Intermediate species S(978)

Bibliography

[1] International Energy Agency. *Key World Energy Statistics*. International Energy Agency Publications, 2019. doi: https://doi.org/https://doi.org/10.1787/71b3ce84-en. URL https://www.oecd-ilibrary.org/content/publication/71b3ce84-en.

[2] F. Fleming Crim. Molecular reaction dynamics across the phases: similarities and differences. *Faraday Discuss.*, 157:9–26, 2012. doi: 10.1039/C2FD20123B. URL http://dx.doi.org/10.1039/C2FD20123B.

[3] Shurong Wang, Zhongyang Luo, and China Science Publishing & Media Ltd. *Pyrolysis of Biomass*. De Gruyter, Berlin, Boston, 2017. ISBN 978-3-11-036963-2. doi: https://doi.org/10.1515/9783110369632. URL https://www.degruyter.com/view/title/497850.

[4] Bohdan Volynets, Farhad Ein-Mozaffari, and Yaser Dahman. Biomass processing into ethanol: pretreatment, enzymatic hydrolysis, fermentation, rheology, and mixing. *Green Processing and Synthesis*, 6(1):1 – 22, 2017. doi: https://doi.org/10.1515/gps-2016-0017. URL https://www.degruyter.com/view/journals/gps/6/1/article-p1.xml.

[5] X. Zhou, L.J. Broadbelt, and R. Vinu. Chapter two - mechanistic understanding of thermochemical conversion of polymers and lignocellulosic biomass. In Kevin M. [Van Geem], editor, *Thermochemical Process Engineering*, volume 49 of *Advances in Chemical Engineering*, pages 95 – 198. Academic Press, 2016. doi: https://doi.org/10.1016/bs.ache.2016.09.002. URL http://www.sciencedirect.com/science/article/pii/S0065237716300151.

[6] Eliseo Ranzi, Alberto Cuoci, Tiziano Faravelli, Alessio Frassoldati, Gabriele Migliavacca, Sauro Pierucci, and Samuele Sommariva. Chemical kinetics of biomass pyrolysis. *Energy & Fuels*, 22(6):4292–4300, 2008. doi: 10.1021/ef800551t. URL https://doi.org/10.1021/ef800551t.

[7] Eliseo Ranzi. Mathematical modeling of fast iomass pyrolyis and bio-oil formation, note i: Kinetic mechanism of biomass pyrolysis. *ACS Sustainable Chemistry & Engineering*, 5(4):2867–2881, 2017. doi: 10.1021/acssuschemeng.6b03096.

[8] Eliseo Ranzi. Mathematical modeling of fast iomass pyrolyis and biooil formation, note ii: Secondary gas-phase reactions and bio-oil formation. *ACS Sustainable Chemistry & Engineering*, 5(4):2882–2896, 2017. doi: 10.1021/acssuschemeng.6b03098.

[9] Peter Deglmann, Imke Müller, Florian Becker, Ansgar Schäfer, Klaus-Dieter Hungenberg, and Horst Weiß. Prediction of propagation rate coefficients in free radical solution polymerization based on accurate quantum chemical methods: Vinylic and related monomers, including acrylates and acrylic acid. *Macromolecular Reaction Engineering*, 3(9):496–515, 2009. doi: 10.1002/mren.200900034. URL https://onlinelibrary.wiley.com/doi/abs/10.1002/mren.200900034.

[10] Peter Deglmann, Ansgar Schäfer, and Christian Lennartz. Application of quantum calculations in the chemical industry—an overview. *International Journal of Quantum Chemistry*, 115(3):107–136, 2015. doi: 10.1002/qua.24811. URL https://onlinelibrary.wiley.com/doi/abs/10.1002/qua.24811.

[11] Shiang-Tai Lin and Stanley I.Sandler. A priori phase equilibrium prediction from a segment contribution solvation model. *Industrial & Engineering Chemistry Research*, 41(5):899–913, 2002. doi: 10.1021/ie001047w.

[12] Edouard Moine. Estimation of solvation quantities from experimental thermodynamic data: Development of the comprehensive compsol databank for pure and mixed solutes. *Journal of Physical and Chemical Reference Data*, 46(3), 2017. doi: http://dx.doi.org/10.1063/1.5000910.

[13] Chieh-Ming Hsieh, Shiang-Tai Lin, and Jadran Vrabec. Considering the dispersive interactions in the cosmo-sac model for more accurate predictions of fluid phase behavior. *Fluid Phase Equilibria*, 367:109 – 116, 2014. ISSN 0378-3812. doi: https://doi.org/10.1016/j.fluid.2014.01.032. URL http://www.sciencedirect.com/science/article/pii/S0378381214000570.

[14] Dengyu Chen, Jianbin Zhou, Qisheng Zhang, and Xifeng Zhu. Evaluation methods and research progresses in bio-oil storage stability. *Renewable and Sustainable Energy Reviews*, 40:69 – 79, 2014. ISSN 1364-0321. doi: https://doi.org/10.1016/j.rser.2014.07.159. URL http://www.sciencedirect.com/science/article/pii/S136403211400611X.

[15] Thermodataengine (tde) version 3.0 (pure compounds, eos, and binary mixtures), 2008. software.

[16] Eugene Paulechka and Andrei Kazakov. Efficient dlpno–ccsd(t)-based estimation of formation enthalpies for c-, h-, o-, and n-containing closed-shell compounds validated against critically evaluated experimental data. *The Journal of Physical Chemistry A*, 121(22):4379–4387, 2017. doi: 10.1021/acs.jpca.7b03195. URL http://dx.doi.org/10.1021/acs.jpca.7b03195. PMID: 28514153.

[17] Aurélien Demenay, Julien Glorian, Patrice Paricaud, and Laurent Catoire. Predictions of the ideal gas properties of refrigerant molecules. *International Journal of Refrigeration*, 79(Supplement C):207–216, 2017. ISSN 0140-7007. doi: 10.1016/j.ijrefrig.2017.03.023. URL http://www.sciencedirect.com/science/article/pii/S0140700717301317.

[18] Eric Mullins, Richard Oldland, Y. A. Liu, Shu Wang, Stanley I. Sandler, Chau-Chyun Chen, Michael Zwolak, and Kevin C. Seavey. Sigma-profile database for using cosmo-based thermodynamic methods. *Industrial & Engineering Chemistry Research*, 45(12):4389–4415, 2006. doi: 10.1021/ie060370h. URL https://doi.org/10.1021/ie060370h.

[19] Chieh-Ming Hsieh, Shu Wang, Shiang-Tai Lin, and Stanley I. Sandler. A predictive model for the solubility and octanol-water partition coefficient of pharmaceuticals. *Journal of Chemical & Engineering Data*, 56(4):936–945, 2011. doi: 10.1021/je1008872. URL https://doi.org/10.1021/je1008872.

[20] R. Vinu, Seth E. Levine, Lin Wang, and Linda J. Broadbelt. Detailed mechanistic modeling of poly(styrene peroxide) pyrolysis using kinetic monte carlo simulation. *Chemical Engineering Science*, 69(1):456 – 471, 2012. ISSN 0009-2509. doi: https://doi.org/10.1016/j.ces.2011.10.071. URL http://www.sciencedirect.com/science/article/pii/S0009250911007974.

[21] Andreas Klamt and Frank Eckert. Prediction of vapor liquid equilibria using cosmotherm. *Fluid Phase Equilibria*, 217(1):53 – 57, 2004. ISSN 0378-3812. doi: https://doi.org/10.1016/j.fluid.2003.08.018. URL http://www.sciencedirect.com/science/article/pii/S0378381203004989.

[22] D.W. Green and R.H. Perry. *Perry's Chemical Engineers' Handbook, Eighth Edition*. McGraw Hill professional. McGraw-Hill Education, 2007. ISBN 9780071593137. URL https://books.google.fr/books?id=tH7IVcA-MX0C.

[23] Battin-Leclerc Frédérique, M. Simmie John, and Blurock Edward. *Cleaner Combustion. Green Energy and Technology*. Springer, London, 2013. ISBN 978-1-4471-5307-8. URL https://doi.org/10.1007/978-1-4471-5307-8.

[24] Prabir Basu. *Biomass Gasification and Pyrolysis: Practical Design and Theory*. Elsevier, June 2010. ISBN 9780080961620.

[25] Belinda L. Slakman and Richard H. West. Kinetic solvent effects in organic reactions. *Journal of Physical Organic Chemistry*, 32(3):3904, 2019. doi: 10.1002/poc.3904. URL https://onlinelibrary.wiley.com/doi/abs/10.1002/poc.3904.

[26] Amrit Jalan, Ionut M. Alecu, Rubén Meana-Paneda, Jorge Aguilera-Iparraguirre, Ke R. Yang, Shamel S. Merchant, Donald G. Truhlar, and William H. Green. New pathways for formation of acids and carbonyl products in low-temperature oxidation: The korcek decomposition of γ-ketohydroperoxides. *Journal of the American Chemical Society*, 135(30):11100–11114, July 2013. doi: 10.1021/ja4034439. URL https://doi.org/10.1021/ja4034439. PMID: 23862563.

[27] Arij Ben Amara, André Nicolle, Maira Alves-Fortunato, and Nicolas Jeuland. Toward predictive modeling of petroleum and biobased fuel stability: Kinetics of methyl oleate/n-dodecane autoxidation. *Energy & Fuels*, 27(10):6125–6133, 2013. doi: 10.1021/ef401360k. URL https://doi.org/10.1021/ef401360k.

[28] Heiko Struebing, Stephan Obermeier, Eirini Siougkrou, Claire S. Adjiman, and Amparo Galindo. A qm-camd approach to solvent design for optimal reaction rates. *Chemical Engineering Science*, 159:69 – 83, 2017. ISSN 0009-2509. doi: https://doi.org/10.1016/j.ces.2016.09.032. URL http://www.sciencedirect.com/science/article/pii/S0009250916305206. iCAMD – Integrating Computer-Aided Molecular Design into Product and Process Design.

[29] Karl Chatelain. *Oxidation stability of fuels in liquid phase*. Theses, Université Paris-Saclay, December 2016. URL https://pastel.archives-ouvertes.fr/tel-01958391.

[30] David V. Avila, K. U. Ingold, J. Lusztyk, W. H. Green, and D. R. Procopio. Dramatic solvent effects on the absolute rate constants for abstraction of the hydroxylic hydrogen atom from tert-butyl hydroperoxide and phenol by the cumyloxyl radical. the role of hydrogen bonding. *Journal of the American Chemical Society*, 117(10):2929–2930, 1995. doi: 10.1021/ja00115a029. URL https://doi.org/10.1021/ja00115a029.

[31] Philip A. MacFaul, K. U. Ingold, and J. Lusztyk. Kinetic solvent effects on hydrogen atom abstraction from phenol, aniline, and diphenylamine. the importance of hydrogen bonding on their radical-trapping (antioxidant) activities1. *The Journal of Organic Chemistry*, 61(4):1316–1321, 1996. doi: 10.1021/jo951244i. URL https://doi.org/10.1021/jo951244i.

[32] Darren W. Snelgrove, Janusz Lusztyk, J. T. Banks, Peter Mulder, and K. U. Ingold. Kinetic solvent effects on hydrogen atom abstractions: Reliable, quantitative predictions via a single empirical equation1. *Journal of the American Chemical Society*, 123(3):469–477, 2001. doi: 10.1021/ja002301e. URL https://doi.org/10.1021/ja002301e.

[33] Grzegorz Litwinienko and K. U. Ingold. Solvent effects on the rates and mechanisms of reaction of phenols with free radicals. *Accounts of Chemical Research*, 40(3):222–230, 2007. doi: 10.1021/ar0682029. URL https://doi.org/10.1021/ar0682029. PMID: 17370994.

[34] D. V. Avila, C. E. Brown, K. U. Ingold, and J. Lusztyk. Solvent effects on the competitive β-scission and hydrogen atom abstraction reactions of the cumyloxyl radical. resolution of a long-standing problem. *Journal of the American Chemical Society*, 115(2):466–470, 1993. doi: 10.1021/ja00055a015. URL https://doi.org/10.1021/ja00055a015.

[35] Yuri P. Tsentalovich, Leonid V. Kulik, Nina P. Gritsan, and Alexandra V. Yurkovskaya. Solvent effect on the rate of β-scission of the tert-butoxyl radical. *The Journal of Physical Chemistry A*, 102(41):7975–7980, 1998. doi: 10.1021/jp9822236. URL https://doi.org/10.1021/jp9822236.

[36] Torsten Zytowski and Hanns Fischer. Absolute rate constants for the addition of methyl radicals to alkenes in solution: New evidence for polar interactions. *Journal of the American Chemical Society*, 118(2):437–439, 1996. doi: 10.1021/ja953085q. URL https://doi.org/10.1021/ja953085q.

[37] Jacques Lalevée, Xavier Allonas, Jean Pierre Fouassier, Daniel Rinaldi, Manuel F. Ruiz Lopez, and Jean Louis Rivail. Solvent effect on the radical addition reaction to double bond: Experimental and quantum chemical investigations. *Chemical Physics Letters*, 415(4):202 – 205, 2005. ISSN 0009-2614. doi: https://doi.org/10.1016/j.cplett.2005.08.137. URL http://www.sciencedirect.com/science/article/pii/S0009261405013333.

[38] Roberto Peverati and Donald G. Truhlar. Quest for a universal density functional: the accuracy of density functionals across a broad spectrum of databases in chemistry and physics. *Philosophical Transactions of the Royal Society of London A: Mathematical, Physical and Engineering Sciences*, 372 (2011), 2014. ISSN 1364-503X. doi: 10.1098/rsta.2012.0476. URL http://rsta.royalsocietypublishing.org/content/372/2011/20120476.

[39] Amir Karton. A computational chemist's guide to accurate thermochemistry for organic molecules. *Wiley Interdisciplinary Reviews: Computational Molecular Science*, 6(3):292–310, 2016. doi: 10.1002/wcms.1249. URL https://onlinelibrary.wiley.com/doi/abs/10.1002/wcms.1249.

[40] Krishnan Raghavachari and Arjun Saha. Accurate composite and fragment-based quantum chemical models for large molecules. *Chemical Reviews*, 115(12):5643–5677, 2015. doi: 10.1021/cr500606e. URL https://doi.org/10.1021/cr500606e. PMID: 25849163.

[41] Antoine Osmont, Laurent Catoire, Iskender Gökalp, and Vigor Yang. Ab initio quantum chemical predictions of enthalpies of formation, heat capacities, and entropies of gas-phase energetic compounds. *Combustion and Flame*, 151(1):262–273, 2007. ISSN 0010-2180. doi: 10.1016/j.combustflame.2007.05.001. URL http://www.sciencedirect.com/science/article/pii/S0010218007001174.

[42] Detlev Conrad Mielczarek, Chourouk Nait Saidi, Patrice Paricaud, and Laurent Catoire. Generalized prediction of enthalpies of formation using dlpno-ccsd(t) ab initio calculations for molecules containing the elements h, c, n, o, f, s, cl, br. *Journal of Computational Chemistry*, 40(6):768–793, 2019. doi: 10.1002/jcc.25763. URL https://onlinelibrary.wiley.com/doi/abs/10.1002/jcc.25763.

[43] Shurong Wang, Gongxin Dai, Haiping Yang, and Zhongyang Luo. Lignocellulosic biomass pyrolysis mechanism: A state-of-the-art review. *Progress in Energy and Combustion Science*, 62:33 – 86, 2017. ISSN 0360-1285. doi: https://doi.org/10.1016/j.pecs.2017.05.004. URL http://www.sciencedirect.com/science/article/pii/S0360128517300266.

[44] Schlaf Marcel and Zhang Zonghcao. *Reaction pathways and mechanisms in thermocatalytic biomass conversion. II, Homogeneously catalyzed transformations, acrylics from biomass, theoretical aspects, Lignin valorization and pyrolysis pathways*. Springer, 2016. ISBN 978-981-287-769-7.

[45] Nikolaevich Kondratiev Victor. Combustion: Chemical reaction, 2018. URL https://www.britannica.com/science/combustion.

[46] Linghong Zhang, Chunbao (Charles) Xu, and Pascale Champagne. Overview of recent advances in thermo-chemical conversion of biomass. *Energy Conversion and Management*, 51(5):969 – 982, 2010. ISSN 0196-8904. doi: https://doi.org/10.1016/j.enconman.2009.11.038. URL http://www.sciencedirect.com/science/article/pii/S0196890409004889.

[47] Van Loo Sjaak and Koppejan Jaap. *The Handbook of Biomass Combustion and Co-firing*. Earthscan, 2008. ISBN 978-1-84971-104-3. doi: https://doi.org/10.4324/9781849773041.

[48] Esteban Chornet and Ralph P. Overend. *Biomass Liquefaction: An Overview*, pages 967–1002. Springer Netherlands, Dordrecht, 1985. ISBN 978-94-009-4932-4. doi: $10.1007/978-94-009-4932-4_54$. URL $https://doi.org/10.1007/978-94-009-4932-4_54$.

[49] Sibel Basakçılardan Kabakcı and Şeyma Hacıbektasoglu. Catalytic pyrolysis of biomass. In Mohamed Samer, editor, *Pyrolysis*, chapter 7. IntechOpen, Rijeka, 2017. doi: 10.5772/67569. URL https://doi.org/10.5772/67569.

[50] Ersan Pütün. Catalytic pyrolysis of biomass: Effects of pyrolysis temperature, sweeping gas flow rate and mgo catalyst. *Energy*, 35(7):2761 – 2766, 2010. ISSN 0360-5442. doi: https://doi.org/10.1016/j.energy.2010.02.024. URL http://www.sciencedirect.com/science/article/pii/S0360544210000782.

[51] Leiyu Zhou, Hongmin Yang, Hao Wu, Meng Wang, and Daqian Cheng. Catalytic pyrolysis of rice husk by mixing with zinc oxide: Characterization of bio-oil and its rheological behavior. *Fuel Processing Technology*, 106:385 – 391, 2013. ISSN 0378-3820. doi: https://doi.org/10.1016/j.fuproc.2012.09.003. URL http://www.sciencedirect.com/science/article/pii/S0378382012003190.

[52] H.B. Goyal, Diptendu Seal, and R.C. Saxena. Bio-fuels from thermochemical conversion of renewable resources: A review. *Renewable and Sustainable Energy Reviews*, 12(2):504 – 517, 2008. ISSN 1364-0321. doi: https://doi.org/10.1016/j.rser.2006.07.014. URL http://www.sciencedirect.com/science/article/pii/S1364032106001171.

[53] M. C. Samolada, A. Papafotica, and I. A. Vasalos. Catalyst evaluation for catalytic biomass pyrolysis. *Energy & Fuels*, 14(6):1161–1167, 2000. doi: 10.1021/ef000026b. URL https://doi.org/10.1021/ef000026b.

[54] Richard French and Stefan Czernik. Catalytic pyrolysis of biomass for biofuels production. *Fuel Processing Technology*, 91(1):25 – 32, 2010. ISSN 0378-3820. doi: https://doi.org/10.1016/j.fuproc.2009.08.011. URL http://www.sciencedirect.com/science/article/pii/S0378382009002392.

[55] Haiping Yang, Rong Yan, Hanping Chen, Dong Ho Lee, and Chuguang Zheng. Characteristics of hemicellulose, cellulose and lignin pyrolysis. *Fuel*, 86(12):1781 – 1788, 2007. ISSN 0016-2361. doi: https://doi.org/10.1016/j.fuel.2006.12.013. URL http://www.sciencedirect.com/science/article/pii/S001623610600490X.

[56] Lopamudra Devi, Krzysztof J Ptasinski, and Frans J.J.G Janssen. A review of the primary measures for tar elimination in biomass gasification processes. *Biomass and Bioenergy*, 24(2):125 – 140, 2003. ISSN 0961-9534. doi: https://doi.org/10.1016/S0961-9534(02)00102-2. URL http://www.sciencedirect.com/science/article/pii/S0961953402001022.

[57] K Maniatis and A.A.C.M Beenackers. Tar protocols. iea bioenergy gasification task. *Biomass and Bioenergy*, 18(1):1 – 4, 2000. ISSN 0961-9534. doi: https://doi.org/10.1016/S0961-9534(99)00072-0. URL http://www.sciencedirect.com/science/article/pii/S0961953499000720.

[58] A. Broido and Maxine A. Nelson. Char yield on pyrolysis of cellulose. *Combustion and Flame*, 24:263 – 268, 1975. ISSN 0010-2180. doi: https://doi.org/10.1016/0010-2180(75)90156-X. URL http://www.sciencedirect.com/science/article/pii/001021807590156X.

[59] Allan G. W. Bradbury, Yoshio Sakai, and Fred Shafizadeh. A kinetic model for pyrolysis of cellulose. *Journal of Applied Polymer Science*, 23(11): 3271–3280, 1979. doi: 10.1002/app.1979.070231112. URL https://onlinelibrary.wiley.com/doi/abs/10.1002/app.1979.070231112.

[60] R Chan and B B Krieger. Modeling of physical and chemical processes during pyrolysis of a large biomass pellet with experimental verification. *Prepr. Pap., Am. Chem. Soc., Div. Fuel Chem.; (United States)*, 28, 1 1983.

[61] Paulo Eduardo Amaral Debiagi, Giancarlo Gentile, Matteo Pelucchi, Alessio Frassoldati, Alberto Cuoci, Tiziano Faravelli, and Eliseo Ranzi. Detailed kinetic mechanism of gas-phase reactions of volatiles released from biomass pyrolysis. *Biomass and Bioenergy*, 93:60 – 71, 2016. ISSN 0961-9534. doi: https://doi.org/10.1016/j.biombioe.2016.06.015. URL http://www.sciencedirect.com/science/article/pii/S0961953416302173.

[62] Takeshi Nakamura, Haruo Kawamoto, and Shiro Saka. Condensation reactions of some lignin related compounds at relatively low pyrolysis temperature. *Journal of Wood Chemistry and Technology*, 27(2):121–133, 2007. doi: 10.1080/02773810701515143. URL https://doi.org/10.1080/02773810701515143.

[63] Arieh Ben-Naim. *Solvation Thermodynamics*. Springer Science+Business Media New York, 1987. ISBN 978-1-4757-6552-6. doi: 10.1007/978-1-4757-6550-2.

[64] Branko Ruscic and David H. Bross. Chapter 1 - thermochemistry. In Tiziano Faravelli, Flavio Manenti, and Eliseo Ranzi, editors, *Mathematical Modelling of Gas-Phase Complex Reaction Systems: Pyrolysis and Combustion*, volume 45 of *Computer Aided Chemical Engineering*, pages 3 – 114. Elsevier, 2019. doi: https://doi.org/10.1016/B978-0-444-64087-1.00001-2. URL http://www.sciencedirect.com/science/article/pii/B9780444640871000012.

[65] John A. Pople. Nobel lecture: Quantum chemical models. *Rev. Mod. Phys.*, 71:1267–1274, Oct 1999. doi: 10.1103/RevModPhys.71.1267. URL https://link.aps.org/doi/10.1103/RevModPhys.71.1267.

[66] Jan M. L. Martin and Glênisson de Oliveira. Towards standard methods for benchmark quality ab initio thermochemistry—w1 and w2 theory. *The Journal of Chemical Physics*, 111(5):1843–1856, 1999. doi: 10.1063/1.479454. URL https://doi.org/10.1063/1.479454.

[67] Srinivasan Parthiban and Jan M. L. Martin. Assessment of w1 and w2 theories for the computation of electron affinities, ionization potentials, heats of formation, and proton affinities. *The Journal of Chemical Physics*, 114(14):6014–6029, 2001. doi: 10.1063/1.1356014. URL https://doi.org/10.1063/1.1356014.

[68] A. Daniel Boese, Mikhal Oren, Onur Atasoylu, Jan M. L. Martin, Mihály Kállay, and Jürgen Gauss. W3 theory: Robust computational thermochemistry in the kj/mol accuracy range. *The Journal of Chemical Physics*, 120(9):4129–4141, 2004. doi: 10.1063/1.1638736. URL https://doi.org/10.1063/1.1638736.

[69] Andreas Köhn, Gareth W. Richings, and David P. Tew. Implementation of the full explicitly correlated coupled-cluster singles and doubles model ccsd-f12 with optimally reduced auxiliary basis dependence. *The Journal of Chemical Physics*, 129(20):201103, 2008. doi: 10.1063/1.3028546. URL https://doi.org/10.1063/1.3028546.

[70] Christof Hättig, David P. Tew, and Andreas Köhn. Communications: Accurate and efficient approximations to explicitly correlated coupled-cluster singles and doubles, ccsd-f12. *The Journal of Chemical Physics*, 132(23):231102, 2010. doi: 10.1063/1.3442368. URL https://doi.org/10.1063/1.3442368.

[71] John A. Pople, Martin Head-Gordon, Douglas J. Fox, Krishnan Raghavachari, and Larry A. Curtiss. Gaussian-1 theory: A general procedure for prediction of molecular energies. *The Journal of Chemical Physics*, 90(10):5622–5629, 1989. doi: 10.1063/1.456415. URL https://doi.org/10.1063/1.456415.

[72] Larry A. Curtiss, Christopher Jones, Gary W. Trucks, Krishnan Raghavachari, and John A. Pople. Gaussian-1 theory of molecular energies for second-row compounds. *The Journal of Chemical Physics*, 93(4):2537–2545, 1990. doi: 10.1063/1.458892. URL https://doi.org/10.1063/1.458892.

[73] Larry A. Curtiss, Krishnan Raghavachari, Gary W. Trucks, and John A. Pople. Gaussian-2 theory for molecular energies of first- and second-row compounds. *The Journal of Chemical Physics*, 94(11):7221–7230, 1991. doi: 10.1063/1.460205. URL https://doi.org/10.1063/1.460205.

[74] Larry A. Curtiss, Krishnan Raghavachari, Paul C. Redfern, Vitaly Rassolov, and John A. Pople. Gaussian-3 (g3) theory for molecules containing first and second-row atoms. *The Journal of Chemical Physics*, 109(18):7764–7776, 1998. doi: 10.1063/1.477422. URL https://doi.org/10.1063/1.477422.

[75] Henry Eyring. The activated complex in chemical reactions. *The Journal of Chemical Physics*, 3(2):107–115, 1935. doi: 10.1063/1.1749604. URL https://doi.org/10.1063/1.1749604.

[76] M. G. Evans and M. Polanyi. Some applications of the transition state method to the calculation of reaction velocities, especially in solution. *Trans. Faraday Soc.*, 31:875–894, 1935. doi: 10.1039/TF9353100875. URL http://dx.doi.org/10.1039/TF9353100875.

[77] Kun Wang and Anthony M. Dean. Chapter 4 - rate rules and reaction classes. In Tiziano Faravelli, Flavio Manenti, and Eliseo Ranzi, editors, *Mathematical Modelling of Gas-Phase Complex Reaction Systems: Pyrolysis and Combustion*, volume 45 of *Computer Aided Chemical Engineering*, pages 203 – 257. Elsevier, 2019. doi: https://doi.org/10.1016/B978-0-444-64087-1.00004-8. URL http://www.sciencedirect.com/science/article/pii/B9780444640871000048.

[78] Amrit Jalan, Robert W. Ashcraft, Richard H. West, and William H. Green. Predicting solvation energies for kinetic modeling. *Annu. Rep. Prog. Chem., Sect. C: Phys. Chem.*, 106:211–258, 2010. doi: 10.1039/B811056P. URL http://dx.doi.org/10.1039/B811056P.

[79] Andreas Klamt. *COSMO RS: From Quantum Chemistry to Fluid Phase Thermodynamics and Drug Design*. Elsevier, 2005. ISBN 978-0-444-51994-8.

[80] Andreas Klamt. Conductor-like screening model for real solvents: A new approach to the quantitative calculation of solvation phenomena. *The Journal of Physical Chemistry*, 99(7):2224–2235, 1995. doi: 10.1021/j100007a062.

[81] Andreas Klamt. Cosmo-rs: a novel and efficient method for the a priori prediction of thermophysical data of liquids. *Fluid Phase Equilibria*, 172: 43–72, 2000. doi: https://doi.org/10.1016/S0378-3812(00)00357-5.

[82] Chieh-Ming Hsieh and Stanley I.Sandler. Improvements of cosmo-sac for vapor-liquid and liquid-liquid equilibrium predictions. *Fluid Phase Equilibria*, 297(1):90–97, 2010. doi: https://doi.org/10.1016/j.fluid.2010.06.011.

[83] Chieh-Ming Hsieh, Stanley I. Sandler, and Shiang-Tai Lin. Improvements of cosmo-sac for vapor–liquid and liquid–liquid equilibrium predictions. *Fluid Phase Equilibria*, 297(1):90 – 97, 2010. ISSN 0378-3812. doi: https://doi.org/10.1016/j.fluid.2010.06.011. URL http://www.sciencedirect.com/science/article/pii/S0378381210003201.

[84] Robert Franke, Cornelia Borgmann, Dieter Hess, and Klaus-Diether Wiese. Density functional theory calculations of the barrier to atropisomerism of a dibenzo[d, f][1, 3, 2]dioxaphosphepin moiety: a tool for rational ligand design. *Zeitschrift für anorganische und allgemeine Chemie*, 629(14):2535–2538, 2003. doi: 10.1002/zaac.200300296. URL https://onlinelibrary.wiley.com/doi/abs/10.1002/zaac.200300296.

[85] Maria S. Contreras, Theodorus de Bruin, Pascal Mougin, and Hervé Toulhoat. Thermochemistry of 1-methylnaphthalene hydroconversion: Comparison of group contribution and ab initio models. *Energy & Fuels*, 27(9):5475–5482, 2013. doi: 10.1021/ef401064j. URL https://doi.org/10.1021/ef401064j.

[86] Amrit Jalan, Richard H. West, and William H. Green. An extensible framework for capturing solvent effects in computer generated kinetic models. *The Journal of Physical Chemistry B*, 117(10):2955–2970, 2013. doi: 10.1021/jp310824h. URL https://doi.org/10.1021/jp310824h. PMID: 23301874.

[87] Mohammad Hossein Keshavarz, Mehdi Zamani, Fariborz Atabaki, and Khadijeh Hosseini Monjezi. Reliable approach for prediction of heats of formation of polycyclic saturated hydrocarbons using recently developed density functionals. *Computational and Theoretical Chemistry*, 1011:30 – 36, 2013. ISSN 2210-271X. doi: https://doi.org/10.1016/j.comptc.2013.01.015. URL http://www.sciencedirect.com/science/article/pii/S2210271X13000479.

[88] John D. Watts and Rodney J. Bartlett. Triple excitations in coupled-cluster theory: Energies and analytical derivatives. *International Journal of Quantum Chemistry*, 48(S27):51–66, 1993. ISSN 1097-461X. doi: 10.1002/qua.560480809. URL http://dx.doi.org/10.1002/qua.560480809.

[89] Chr Møller and Milton S Plesset. Note on an approximation treatment for many-electron systems. *Physical review*, 46(7):618, 1934.

[90] Svein Saebo/ and Peter Pulay. Fourth-order mo/ller–plessett perturbation theory in the local correlation treatment. i. method. *The Journal of chemical physics*, 86(2):914–922, 1987.

[91] Larry A. Curtiss, Paul C. Redfern, and Krishnan Raghavachari. Gaussian-4 theory. *The Journal of Chemical Physics*, 126(8):084108, 2007. doi: 10.1063/1.2436888. URL https://doi.org/10.1063/1.2436888.

[92] F. Coester and H. Kümmel. Short-range correlations in nuclear wave functions. *Nuclear Physics*, 17:477 – 485, 1960. ISSN 0029-5582. doi: https://doi.org/10.1016/0029-5582(60)90140-1. URL http://www.sciencedirect.com/science/article/pii/0029558260901401.

[93] Axel D Becke. Density-functional thermochemistry. i. the effect of the exchange-only gradient correction. *The Journal of chemical physics*, 96(3): 2155–2160, 1992.

[94] Axel D. Becke. A new mixing of hartree–fock and local density-functional theories. *The Journal of Chemical Physics*, 98(2):1372–1377, 1993. doi: 10.1063/1.464304. URL https://doi.org/10.1063/1.464304.

[95] A. D. Becke. Density-functional exchange-energy approximation with correct asymptotic behavior. *Phys. Rev. A*, 38:3098–3100, Sep 1988. doi: 10.1103/PhysRevA.38.3098. URL https://link.aps.org/doi/10.1103/PhysRevA.38.3098.

[96] Chengteh Lee, Weitao Yang, and Robert G Parr. Results obtained with the correlation energy density functionals. *Phys. Rev. B: Condens. Matter Mater. Phys*, 37:785, 1988.

[97] S. H. Vosko, L. Wilk, and M. Nusair. Accurate spin-dependent electron liquid correlation energies for local spin density calculations: a critical analysis. *Canadian Journal of Physics*, 58(8):1200–1211, 1980. doi: 10.1139/p80-159. URL https://doi.org/10.1139/p80-159.

[98] Robin Fingerhut, Wei-Lin Chen, Andre Schedemann, Wilfried Cordes, Jürgen Rarey, Chieh-Ming Hsieh, Jadran Vrabec, and Shiang-Tai Lin. Comprehensive assessment of cosmo-sac models for predictions of fluid-phase equilibria. *Industrial & Engineering Chemistry Research*, 56(35):9868–9884, 2017. doi: 10.1021/acs.iecr.7b01360. URL https://doi.org/10.1021/acs.iecr.7b01360.

[99] Connie W. Gao, Joshua W. Allen, William H. Green, and Richard H. West. Reaction mechanism generator: Automatic construction of chemical kinetic mechanisms. *Computer Physics Communications*, 203:212 – 225, 2016. ISSN 0010-4655. doi: https://doi.org/10.1016/j.cpc.2016.02.013. URL http://www.sciencedirect.com/science/article/pii/S0010465516300285.

[100] M. J. Frisch, G. W. Trucks, and al. Gaussian 09 revision, 2009. Gaussian Inc. Wallingford CT 2009.

[101] Frank Neese. New developments in dlpno methods, 2017. Presentation, ORCA USer Group Meeting 2017.

[102] SÃ©bastien Canneaux, FrÃ©dÃ©ric Bohr, and Eric Henon. Kisthelp: A program to predict thermodynamic properties and rate constants from quantum chemistry results . *Journal of Computational Chemistry*, 35(1):82–93, 2014. doi: 10.1002/jcc.23470. URL https://onlinelibrary.wiley.com/doi/abs/10.1002/jcc.23470.

[103] Stanley I. Sandler. *An Introduction to Applied Statistical Thermodynamics*. John Wiley & Sons, Inc., first edition, DecJanuary 2010. ISBN 978-0-470-91347-5.

[104] Sidney W. Benson and Jerry H. Buss. Additivity rules for the estimation of molecular properties. thermodynamic properties. *The Journal of Chemical Physics*, 29(3):546–572, 1958. doi: 10.1063/1.1744539. URL https://doi.org/10.1063/1.1744539.

[105] Sidney W. Benson, F. R. Cruickshank, D. M. Golden, Gilbert R. Haugen, H. E. O'Neal, A. S. Rodgers, Robert Shaw, and R. Walsh. Additivity rules for the estimation of thermochemical properties. *Chemical Reviews*, 69(3):279–324, 1969. doi: 10.1021/cr60259a002. URL https://doi.org/10.1021/cr60259a002.

[106] N. Cohen and S. W. Benson. Estimation of heats of formation of organic compounds by additivity methods. *Chemical Reviews*, 93(7):2419–2438, 1993. doi: 10.1021/cr00023a005. URL https://doi.org/10.1021/cr00023a005.

[107] N. Cohen. Revised group additivity values for enthalpies of formation at 298K of carbon-hydrogen and carbon-hydrogen-oxygen compounds. *Journal of Physical and Chemical Reference Data*, 25(6):1411–1481, 1996. doi: 10.1063/1.555988. URL https://doi.org/10.1063/1.555988.

[108] Daniel R. Stull, Edgar F. Westrum, and Gerard C. Sinke. *The chemical thermodynamics of organic compounds*. J. Wiley (New York), 1969. ISBN 9780471834908.

[109] Eugene S. Domalski and Elizabeth D. Hearing. Estimation of the thermodynamic properties of c-h-n-o-s-halogen compounds at 298.15 k. *Journal of Physical and Chemical Reference Data*, 22(4):805–1159, 1993. doi: 10.1063/1.555927. URL https://doi.org/10.1063/1.555927.

[110] Eugene S. Domalski. *Estimation of Enthalpies of Formation of Organic Compounds at Infinite Dilution in Water at* 298.15 K. American Chemical Society, 1998. doi: 10.1021/bk-1998-0677.ch003. URL https://pubs.acs.org/doi/abs/10.1021/bk-1998-0677.ch003.

[111] Nicole Laurencelle and Philip D. Pacey. Simple electrostatic model for enthalpies of formation of singly substituted alkanes. *Journal of the American Chemical Society*, 115(2):625–631, 1993. doi: 10.1021/ja00055a035. URL https://doi.org/10.1021/ja00055a035.

[112] Z. J. Chen and S. B. Desu. The explicit expression for the enthalpy of formation of organometallic compounds of si, ge and sn. *Materials Chemistry and Physics*, 35(2):151 – 154, 1993. ISSN 0254-0584. doi: https://doi.org/10.1016/0254-0584(93)90191-N. URL http://www.sciencedirect.com/science/article/pii/025405849390191N.

[113] Derek W. Smith. Additive bond-energy scheme with geminal h-h terms applications to the enthalpies of formation of alkane derivatives. *J. Chem. Soc., Faraday Trans.*, 93:2037–2041, 1997. doi: 10.1039/A608288B. URL http://dx.doi.org/10.1039/A608288B.

[114] AndrÃ©s Mercader, Eduardo A. Castro, and Andrey A. Toropov. Maximum topological distances based indices as molecular descriptors for qspr. 4. modeling the enthalpy of formation of hydrocarbons from elements. *International Journal of Molecular Sciences*, 2(2):121–132, 2001. ISSN 1422-0067. doi: 10.3390/i2020121. URL https://www.mdpi.com/1422-0067/2/2/121.

[115] David Feller and David A. Dixon. Predicting the heats of formation of model hydrocarbons up to benzene. *The Journal of Physical Chemistry A*, 104 (13):3048–3056, 2000. doi: 10.1021/jp994340m. URL https://doi.org/10.1021/jp994340m.

[116] Olga V. Dorofeeva, Vladimir S. Yungman, and Pauline Saks. Enthalpies of formation for gaseous polychlorinated biphenyls: A modified group additivity scheme. *The Journal of Physical Chemistry A*, 105(27):6621–6629, 2001. doi: 10.1021/jp010082t. URL https://doi.org/10.1021/jp010082t.

[117] Olga V Dorofeeva and Natalia F Moiseeva. Computational study of the thermochemistry of organophosphorus (iii) compounds. *The Journal of Physical Chemistry A*, 110(28):8925–8932, 2006. doi: 10.1021/jp060982f.

[118] Otilia Mo, Manuel Yanez, Jose Elguero, Maria Victoria Roux, Pilar Jimenez, Juan Z. Davalos, Manuel A. V. Ribeiro da Silva, Maria das Dores M. C. Ribeiro da Silva, Pilar Cabildo, and Rosa Claramunt. Substituent effects on enthalpies of formation: Benzene derivatives. *The Journal of Physical Chemistry A*, 107(3):366–371, 2003. doi: 10.1021/jp0265790. URL https://doi.org/10.1021/jp0265790.

[119] Wim Klopper and Jozef Noga. Accurate quantum-chemical prediction of enthalpies of formation of small molecules in the gas phase. *ChemPhysChem*, 4(1):32–48, 2003. doi: 10.1002/cphc.200390006. URL https://chemistry-europe.onlinelibrary.wiley.com/doi/abs/10.1002/cphc.200390006.

[120] Chenzhong Cao and Shuo Gao. Estimating enthalpies of formation of monoalkenes by the bonding orbital-connecting matrix of molecular graphics and the steric effect of the cis/trans configuration. *Journal of Molecular Structure: THEOCHEM*, 718(1):153 – 163, 2005. ISSN 0166-1280. doi: https://doi.org/10.1016/j.theochem.2005.01.004. URL http://www.sciencedirect.com/science/article/pii/S0166128005000151.

[121] Paul C. Redfern, Peter Zapol, Larry A. Curtiss, and Krishnan Raghavachari. Assessment of gaussian-3 and density functional theories for enthalpies of formation of c1â^'c16 alkanes. *The Journal of Physical Chemistry A*, 104(24):5850–5854, 2000. doi: 10.1021/jp994429s. URL https://doi.org/10.1021/jp994429s.

[122] Ali Vatani, Mehdi Mehrpooya, and Farhad Gharagheizi. Prediction of standard enthalpy of formation by a qspr model. *International Journal of Molecular Sciences*, 8(5):407–432, 2007. ISSN 1422-0067. doi: 10.3390/i8050407. URL https://www.mdpi.com/1422-0067/8/5/407.

[123] Chenzhong Cao. Topological electronegativity index and its application 2. enthalpies of formation for monosubstituted alkanes rx. *QSAR & Combinatorial Science*, 27(5):555–562, 2008. doi: 10.1002/qsar.200730063. URL https://onlinelibrary.wiley.com/doi/abs/10.1002/qsar.200730063.

[124] Laurent Catoire, Mohammed Yahyaoui, Antoine Osmont, Iskender Gökalp, Meryl Brothier, Hélène Lorcet, and David Guénadou. Thermochemistry of compounds formed during fast pyrolysis of lignocellulosic biomass. *Energy & Fuels*, 22(6):4265–4273, 2008. doi: 10.1021/ef800418z. URL https://doi.org/10.1021/ef800418z.

[125] J. A. Montgomery, Jr., M. J. Frisch, J. W. Ochterski, and G. A. Petersson. A complete basis set model chemistry. vii. use of the minimum population localization method. *The Journal of Chemical Physics*, 112(15):6532–6542, 2000. doi: 10.1063/1.481224. URL https://doi.org/10.1063/1.481224.

[126] John M. Simmie and Kieran P. Somers. Benchmarking compound methods (cbs-qb3, cbs-apno, g3, g4, w1bd) against the active thermochemical tables: Formation enthalpies of radicals. *The Journal of Physical Chemistry A*, 119(33):8922–8933, 2015. ISSN 15205215. doi: 10.1021/acs.jpca.5b05448. URL http://dx.doi.org/10.1021/acs.jpca.5b05448. PMID: 26171842.

[127] Mohammad M. Ghahremanpour, Paul J. van Maaren, Jonas C. Ditz, Roland Lindh, and David van der Spoel. Large-scale calculations of gas phase thermochemistry: Enthalpy of formation, standard entropy, and heat capacity. *The Journal of Chemical Physics*, 145(11):114305, 2016. doi: 10.1063/1.4962627. URL https://doi.org/10.1063/1.4962627.

[128] Dimitrios G. Liakos and Frank Neese. Improved correlation energy extrapolation schemes based on local pair natural orbital methods. *The Journal of Physical Chemistry A*, 116(19):4801–4816, 2012. doi: 10.1021/jp302096v. URL http://dx.doi.org/10.1021/jp302096v. PMID: 22489633.

[129] Dimitrios G. Liakos and Frank Neese. Is it possible to obtain coupled cluster quality energies at near density functional theory cost? domain-based local pair natural orbital coupled cluster vs modern density functional theory. *Journal of Chemical Theory and Computation*, 11(9):4054–4063, 2015. ISSN 15499626. doi: 10.1021/acs.jctc.5b00359.

[130] Masaaki Saitow, Ute Becker, Christoph Riplinger, Edward F. Valeev, and Frank Neese. A new near-linear scaling, efficient and accurate, open-shell domain-based local pair natural orbital coupled cluster singles and doubles theory. *The Journal of Chemical Physics*, 146(16):164105, 2017. doi: 10.1063/1.4981521. URL https://doi.org/10.1063/1.4981521.

[131] Christoph Riplinger, Barbara Sandhoefer, Andreas Hansen, and Frank Neese. Natural triple excitations in local coupled cluster calculations with pair natural orbitals. *The Journal of Chemical Physics*, 139(13):134101, 2013. doi: 10.1063/1.4821834. URL https://doi.org/10.1063/1.4821834.

[132] Manuel Sparta and Frank Neese. Chemical applications carried out by local pair natural orbital based coupled-cluster methods. *Chem. Soc. Rev.*, 43: 5032–5041, 2014. doi: 10.1039/C4CS00050A. URL http://dx.doi.org/10.1039/C4CS00050A.

[133] Christoph Riplinger, Peter Pinski, Ute Becker, Edward F. Valeev, and Frank Neese. Sparse maps—a systematic infrastructure for reduced-scaling electronic structure methods. ii. linear scaling domain based pair natural orbital coupled cluster theory. *The Journal of Chemical Physics*, 144(2): 024109, 2016. doi: 10.1063/1.4939030. URL https://doi.org/10.1063/1.4939030.

[134] Christopher J Cramer. *Essentials of Computational Chemistry Theories and Models*. Wiley, 2004. ISBN 0470091819. doi: 10.1021/ci010445m. URL http://scholar.google.com/scholar?hl=en{&}btnG=Search{&}q=intitle:Essentials+of+computational+chemistry{#}0.

[135] D. A. Ponomarev and V. V. Takhistov. What are isodesmic reactions? *Journal of Chemical Education*, 74(2):201, 1997. doi: 10.1021/ed074p201. URL http://dx.doi.org/10.1021/ed074p201.

[136] Dirk Bakowies. Ab initio thermochemistry using optimal-balance models with isodesmic corrections: The atomic protocol. *Journal of Chemical Physics*, 130(14), 2009. ISSN 00219606. doi: 10.1063/1.3089241.

[137] Ingvar Arnason, Palmar I Gudnason, Ragnar Björnsson, and Heinz Oberhammer. Gas phase structures, energetics, and potential energy surfaces of disilacyclohexanes. *The Journal of Physical Chemistry A*, 115(35):10000–10008, 2011. doi: 10.1021/jp202722t. URL https://doi.org/10.1021/jp202722t. PMID: 21780826.

[138] S. R. Saraf, W. J. Rogers, M. S. Mannan, M. B. Hall, and L. M. Thomson. Theoretical thermochemistry: Ab initio heat of formation for hydroxylamine. *Journal of Physical Chemistry A*, 107(8):1077–1081, 2003. ISSN 10895639. doi: 10.1021/jp026027h.

[139] C. F. Wilcox and S. O. Russo. An improved protocol for the efficient ab initio calculation of accurate enthalpies of formation for c,h,n compounds. *International Journal of Chemical Kinetics*, 33(12):770–774, 2001. ISSN 1097-4601. doi: 10.1002/kin.10002. URL http://dx.doi.org/10.1002/kin.10002.

[140] Antoine Osmont, Laurent Catoire, and Iskender Gökalp. Physicochemical properties and thermochemistry of propellanes. *Energy & Fuels*, 22(4): 2241–2257, 2008. doi: 10.1021/ef8000423. URL http://dx.doi.org/10.1021/ef8000423.

[141] Attila Tajti, Peter G. Szalay, Attila G. Csaszar, Mihaly Kallay, Jurgen Gauss, Edward F. Valeev, Bradley A. Flowers, Juana Vazquez, and John F. Stanton. Heat: High accuracy extrapolated ab initio thermochemistry. *The Journal of Chemical Physics*, 121(23):11599–11613, 2004. doi: 10.1063/1.1811608. URL https://doi.org/10.1063/1.1811608.

[142] Attila G. Csaszar and Tibor Furtenbacher. From a network of computed reaction enthalpies to atom-based thermochemistry (neat). *Chemistry – A European Journal*, 16(16):4826–4835, 2010. doi: 10.1002/chem.200903252. URL https://chemistry-europe.onlinelibrary.wiley.com/doi/abs/10.1002/chem.200903252.

[143] Ilie Fishtik. Unique stoichiometric representation for computational thermochemistry. *The Journal of Physical Chemistry A*, 116(7):1854–1863, 2012. doi: 10.1021/jp211795s. URL https://doi.org/10.1021/jp211795s. PMID: 22225427.

[144] Dirk Bakowies. Ab initio thermochemistry using optimal-balance models with isodesmic corrections: The atomic protocol. *The Journal of Chemical Physics*, 130(14):144113, 2009. doi: 10.1063/1.3089241. URL https://doi.org/10.1063/1.3089241.

[145] Dirk Bakowies. Ab initio thermochemistry with high-level isodesmic corrections: Validation of the atomic protocol for a large set of compounds with first-row atoms (h, c, n, o, f). *The Journal of Physical Chemistry A*, 113(43):11517–11534, 2009. doi: 10.1021/jp9027782. URL https://doi.org/10.1021/jp9027782. PMID: 19848424.

[146] Dirk Bakowies. Assessment of density functional theory for thermochemical approaches based on bond separation reactions. *The Journal of Physical Chemistry A*, 117(1):228–243, 2013. doi: 10.1021/jp310735h. URL https://doi.org/10.1021/jp310735h. PMID: 23214917.

[147] Mark T. Swihart and Laurent Catoire. Thermochemistry of aluminum species for combustion modeling from ab initio molecular orbital calculations. *Combustion and Flame*, 121(1):210–222, 2000. ISSN 0010-2180. doi: 10.1016/S0010-2180(99)00128-5. URL http://www.sciencedirect.com/science/article/pii/S0010218099001285.

[148] Frank Neese. The orca program system. *Wiley Interdisciplinary Reviews: Computational Molecular Science*, 2(1):73–78, 2012. ISSN 1759-0884. doi: 10.1002/wcms.81. URL http://dx.doi.org/10.1002/wcms.81.

[149] Frank Neese. Software update: the orca program system, version 4.0. *Wiley Interdisciplinary Reviews: Computational Molecular Science*, pages n/a–n/a, 2017. ISSN 1759-0884. doi: 10.1002/wcms.1327. URL http://dx.doi.org/10.1002/wcms.1327.

[150] Stefan Grimme, Jens Antony, Stephan Ehrlich, and Helge Krieg. A consistent and accurate ab initio parametrization of density functional dispersion correction (dft-d) for the 94 elements h-pu. *The Journal of Chemical Physics*, 132(15):154104, 2010. doi: 10.1063/1.3382344. URL https://doi.org/10.1063/1.3382344.

[151] Stefan Grimme, Stephan Ehrlich, and Lars Goerigk. Effect of the damping function in dispersion corrected density functional theory. *Journal of Computational Chemistry*, 32(7):1456–1465, 2011. ISSN 1096-987X. doi: 10.1002/jcc.21759. URL http://dx.doi.org/10.1002/jcc.21759.

[152] Holger Kruse, Lars Goerigk, and Stefan Grimme. Why the standard b3lyp/6-31g* model chemistry should not be used in dft calculations of molecular thermochemistry: Understanding and correcting the problem. *Journal of Organic Chemistry*, 77(23):10824–10834, 2012. ISSN 00223263. doi: 10.1021/jo302156p.

[153] Stefan Grimme. Seemingly simple stereoelectronic effects in alkane isomers and the implications for kohn-sham density functional theory. *Angewandte Chemie - International Edition*, 45(27):4460–4464, 2006. ISSN 14337851. doi: 10.1002/anie.200600448.

[154] Matthew D. Wodrich, Clémence Corminboeuf, and P. V R Schleyer. Systematic errors in computed alkane energies using b3lyp and other popular dft functionals. *Organic Letters*, 8(17):3631–3634, 2006. ISSN 15237060. doi: 10.1021/ol061016i.

[155] Matthew D. Wodrich, Clémence Corminboeuf, Peter R. Schreiner, Andrey A. Fokin, and Paul Ragué Von Schleyer. How accurate are dft treatments of organic energies? *Organic Letters*, 9(10):1851–1854, 2007. ISSN 15237060. doi: 10.1021/ol070354w.

[156] Peter R. Schreiner. Relative energy computations with approximate density functional theory - a caveat! *Angewandte Chemie - International Edition*, 46(23):4217–4219, 2007. ISSN 14337851. doi: 10.1002/anie.200700386.

[157] Stephan N. Steinmann, Matthew D. Wodrich, and Clemence Corminboeuf. Overcoming systematic dft errors for hydrocarbon reaction energies. *Theoretical Chemistry Accounts*, 127(5):429–442, 2010. ISSN 1432881X. doi: 10.1007/s00214-010-0818-3.

[158] Aron J. Cohen, Paula Mori-Sánchez, and Weitao Yang. Challenges for density functional theory. *Chemical Reviews*, 112(1):289–320, 2012. doi: 10.1021/cr200107z.

[159] Julian Tirado-Rives and William L. Jorgensen. Performance of b3lyp density functional methods for a large set of organic molecules. *Journal of Chemical Theory and Computation*, 4(2):297–306, 2008. ISSN 15499618. doi: 10.1021/ct700248k.

[160] Lars Goerigk, Andreas Hansen, Christoph Bauer, Stephan Ehrlich, Asim Najibi, and Stefan Grimme. A look at the density functional theory zoo with the advanced gmtkn55 database for general main group thermochemistry, kinetics and noncovalent interactions. *Phys. Chem. Chem. Phys.*, pages –, 2017. doi: 10.1039/C7CP04913G. URL http://dx.doi.org/10.1039/C7CP04913G.

[161] Florian Weigend, Filipp Furche, and Reinhart Ahlrichs. Gaussian basis sets of quadruple zeta valence quality for atoms h–kr. *The Journal of Chemical Physics*, 119(24):12753–12762, 2003. doi: 10.1063/1.1627293. URL https://doi.org/10.1063/1.1627293.

[162] Florian Weigend and Reinhart Ahlrichs. Balanced basis sets of split valence, triple zeta valence and quadruple zeta valence quality for h to rn: Design and assessment of accuracy. *Phys. Chem. Chem. Phys.*, 7:3297–3305, 2005. doi: 10.1039/B508541A. URL http://dx.doi.org/10.1039/B508541A.

[163] Florian Weigend. Accurate coulomb-fitting basis sets for h to rn. *Phys. Chem. Chem. Phys.*, 8:1057–1065, 2006. doi: 10.1039/B515623H. URL http://dx.doi.org/10.1039/B515623H.

[164] Simone Kossmann and Frank Neese. Efficient structure optimization with second-order many-body perturbation theory: The rijcosx-mp2 method. *Journal of Chemical Theory and Computation*, 6(8):2325–2338, 2010. doi: 10.1021/ct100199k. URL https://doi.org/10.1021/ct100199k. PMID: 26613489.

[165] Róbert Izsák and Frank Neese. An overlap fitted chain of spheres exchange method. *The Journal of Chemical Physics*, 135(14):144105, 2011. doi: 10.1063/1.3646921. URL https://doi.org/10.1063/1.3646921.

[166] Arnim Hellweg, Christof Hättig, Sebastian Höfener, and Wim Klopper. Optimized accurate auxiliary basis sets for ri-mp2 and ri-cc2 calculations for the atoms rb to rn. *Theoretical Chemistry Accounts*, 117(4):587–597, Apr 2007. ISSN 1432-2234. doi: 10.1007/s00214-007-0250-5. URL https://doi.org/10.1007/s00214-007-0250-5.

[167] Florian Weigend and Reinhart Ahlrichs. Balanced basis sets of split valence, triple zeta valence and quadruple zeta valence quality for h to rn: Design and assessment of accuracy. *Phys. Chem. Chem. Phys.*, 7:3297–3305, 2005. doi: 10.1039/B508541A. URL http://dx.doi.org/10.1039/B508541A.

[168] Manoj K. Kesharwani, Brina Brauer, and Jan M. L. Martin. Frequency and zero-point vibrational energy scale factors for double-hybrid density functionals (and other selected methods): Can anharmonic force fields be avoided? *The Journal of Physical Chemistry A*, 119(9):1701–1714, 2015. doi: 10.1021/jp508422u. URL https://doi.org/10.1021/jp508422u. PMID: 25296165.

[169] R Core Team. *R: A Language and Environment for Statistical Computing*. R Foundation for Statistical Computing, Vienna, Austria, 2016. URL https://www.R-project.org/.

[170] Marie L. Laury, Matthew J. Carlson, and Angela K. Wilson. Vibrational frequency scale factors for density functional theory and the polarization consistent basis sets. *Journal of Computational Chemistry*, 33(30):2380–2387, 2012. ISSN 1096-987X. doi: 10.1002/jcc.23073. URL http://dx.doi.org/10.1002/jcc.23073.

[171] D.A. McQuarrie. *Statistical Thermodynamics*. Harper's chemistry series. University Science Books, 1973. ISBN 9780935702187. URL https://books.google.fr/books?id=l63vAAAAMAAJ.

[172] Steven G. Johnson. The nlopt nonlinear-optimization package. http://ab-initio.mit.edu/nlopt, 2008.

[173] T. Rowan. *Functional Stability Analysis of Numerical Algorithms*. PhD thesis, Department of Computer Sciences, University of Texas at Austin, 1990.

[174] W. L. Price. A controlled random search procedure for global optimisation. *The Computer Journal*, 20(4):367–370, 1977. doi: 10.1093/comjnl/20.4.367. URL +http://dx.doi.org/10.1093/comjnl/20.4.367.

[175] W. L. Price. Global optimization by controlled random search. *Journal of Optimization Theory and Applications*, 40(3):333–348, Jul 1983. ISSN 1573-2878. doi: 10.1007/BF00933504. URL https://doi.org/10.1007/BF00933504.

[176] Eligius M.T. Hendrix, P.M. Ortigosa, and I. García. On success rates for controlled random search. *Journal of Global Optimization*, 21(3):239–263, Nov 2001. ISSN 1573-2916. doi: 10.1023/A:1012387510553. URL https://doi.org/10.1023/A:1012387510553.

[177] Jelmer Ypma, Hans W. Borchers, and Dirk Eddelbuettel. https://cran.r-project.org/package=nloptr, 2014.

[178] A. R. H. Goodwin and M. R. Moldover. Thermophysical properties of gaseous refrigerants from speed of sound measurements. i. apparatus, model, and results for 1,1,1,2-tetrafluoroethane r134a. *The Journal of Chemical Physics*, 93(4):2741–2753, 1990. doi: 10.1063/1.458913. URL https://doi.org/10.1063/1.458913.

[179] W. Beekermann and F. Kohler. Acoustic determination of ideal-gas heat capacity and second virial coefficients of some refrigerants between 250 and 420 k. *International Journal of Thermophysics*, 16(2):455–464, Mar 1995. ISSN 1572-9567. doi: 10.1007/BF01441911. URL https://doi.org/10.1007/BF01441911.

[180] A. R. H. Goodwin and M. R. Moldover. Thermophysical properties of gaseous refrigerants from speed-of-sound measurements. ii. results for 1,1-dichloro-1-fluoroethane (ccl2fch3). *The Journal of Chemical Physics*, 95(7):5230–5235, 1991. doi: 10.1063/1.461694. URL https://doi.org/10.1063/1.461694.

[181] A. R. H. Goodwin and M. R. Moldover. Thermophysical properties of gaseous refrigerants from speed-of-sound measurements. iii. results for 1,1-dichloro-2,2,2-trifluoroethane (chcl2-cf3) and 1,2-dichloro-1,2,2-trifluoroethane (chclf-cclf2). *The Journal of Chemical Physics*, 95(7):5236–5242, 1991. doi: 10.1063/1.461831. URL https://doi.org/10.1063/1.461831.

[182] R Bender, K Bier, and G Maurer. Heat capacity at constant pressure and joule-thomson coefficient of monochloro-1,2,2,2-tetrafluoroethane. *The Journal of Chemical Thermodynamics*, 12(4):335–341, 1980. ISSN 0021-9614. doi: 10.1016/0021-9614(80)90145-7. URL http://www.sciencedirect.com/science/article/pii/0021961480901457.

[183] J. L. Hales, E. B. Lees, and D. J. Ruxton. Thermodynamic properties of organic oxygen compounds. part 18.-vapour heat capacities and heats of vaporization of ethyl ketone, ethyl propyl ketone, methyl isopropy1 ketone, and methyl phenyl ether. *Trans. Faraday Soc.*, 63:1876–1879, 1967. doi: 10.1039/TF9676301876. URL http://dx.doi.org/10.1039/TF9676301876.

[184] Kenneth S. Pitzer and Donald W. Scott. The thermodynamics and molecular structure of benzene and its methyl derivatives1. *Journal of the American Chemical Society*, 65(5):803–829, 1943. doi: 10.1021/ja01245a019. URL https://doi.org/10.1021/ja01245a019.

[185] W Barho. Die molwärme der fluor-chlor-derivate des methans im zustand idealer gase. *Kälte-Technik*, 17:219–222, 1965.

[186] G. Ernst and J. Büsser. Ideal and real gas state heat capacities cp of c3h8, i-c4h10, ch2clcf3, cf2clcfcl2, and chf2cl. *The Journal of Chemical Thermodynamics*, 2(6):787–791, 1970. ISSN 0021-9614. doi: 10.1016/0021-9614(70)90020-0. URL http://www.sciencedirect.com/science/article/pii/0021961470900200.

[187] Günter Esper, Wolfgang Lemming, Wilhelm Beckermann, and Friedrich Kohler. Acoustic determination of ideal gas heat capacity and second virial coefficient of small hydrocarbons. *Fluid Phase Equilibria*, 105(2):173–192, 1995. ISSN 0378-3812. doi: 10.1016/0378-3812(94)02608-4. URL http://www.sciencedirect.com/science/article/pii/0378381294026084.

[188] J. P. McCullough, R. E. Pennington, and Guy Waddington. A calorimetric determination of the vapor heat capacity and gas imperfection of water. *Journal of the American Chemical Society*, 74(17):4439–4442, 1952. doi: 10.1021/ja01137a061. URL https://doi.org/10.1021/ja01137a061.

[189] Samuel O. Colgate, Charles F. Sona, Kyle R. Reed, and A. Sivaraman. Experimental ideal gas reference state heat capacities of gases and vapors. *Journal of Chemical & Engineering Data*, 35(1):1–5, 1990. doi: 10.1021/je00059a001. URL https://doi.org/10.1021/je00059a001.

[190] M.B. Ewing and A.R.H. Goodwin. Thermophysical properties of alkanes from speeds of sound determined using a spherical resonator 4.2-methylpropane at temperatures in the range 251 k to 320 k and pressures in the range 5 kpa to 114 kpa. *The Journal of Chemical Thermodynamics*, 23 (12):1107–1120, 1991. ISSN 0021-9614. doi: 10.1016/S0021-9614(05)80141-7. URL http://www.sciencedirect.com/science/article/pii/S0021961405801417.

[191] J.P.M. Trusler and M.P. Zarari. Second and third acoustic virial coefficients of methane at temperatures between 125 k and 375 k. *The Journal of Chemical Thermodynamics*, 27(7):771–778, 1995. ISSN 0021-9614. doi: 10.1006/jcht.1995.0080. URL http://www.sciencedirect.com/science/article/pii/S0021961485700808.

[192] William Weltner and Kenneth S. Pitzer. Methyl alcohol: The entropy, heat capacity and polymerization equilibria in the vapor, and potential barrier to internal rotation. *Journal of the American Chemical Society*, 73(6):2606–2610, 1951. doi: 10.1021/ja01150a053. URL https://doi.org/10.1021/ja01150a053.

[193] S.J. Boyes, M.B. Ewing, and A.R.H. Goodwin. Heat capacities and second virial coefficients for gaseous methanol determined from speed-of-sound measurements at temperatures between 280 k and 360 k and pressures from 1.03 kpa to 80.5 kpa. *The Journal of Chemical Thermodynamics*, 24(11): 1151–1166, 1992. ISSN 0021-9614. doi: 10.1016/S0021-9614(05)80238-1. URL http://www.sciencedirect.com/science/article/pii/S0021961405802381.

[194] I.A. Hossenlopp and D.W. Scott. Vapor heat capacities and enthalpies of vaporization of five alkane hydrocarbons. *The Journal of Chemical Thermodynamics*, 13(5):415–421, 1981. ISSN 0021-9614. doi: 10.1016/0021-9614(81)90047-1. URL http://www.sciencedirect.com/science/article/pii/0021961481900471.

[195] M.B Ewing, M.L McGlashan, and J.P.M Trusler. The speed of sound in gases ii. acoustic virial coefficients and perfect-gas heat capacities for 2,2-dimethylpropane obtained using a cylindrical interferometer. *The Journal of Chemical Thermodynamics*, 18(6):511–517, 1986. ISSN 0021-9614. doi: 10.1016/0021-9614(86)90134-5. URL http://www.sciencedirect.com/science/article/pii/0021961486901345.

[196] Alexander Burcat. Thermodynamic properties of ideal gas nitro and nitrate compounds. *Journal of Physical and Chemical Reference Data*, 28(1): 63–130, 1999. doi: 10.1063/1.556033. URL https://doi.org/10.1063/1.556033.

[197] G. B. Kistiakowsky, J. R. Lacher, and W. W. Ransom. The low temperature gaseous heat capacities of certain c3 hydrocarbons. *The Journal of Chemical Physics*, 8(12):970–977, 1940. doi: 10.1063/1.1750612. URL https://doi.org/10.1063/1.1750612.

[198] M. B. Ewing and J. P. M. Trusler. Speeds of sound in cf4 between 175 and 300 k measured with a spherical resonator. *The Journal of Chemical Physics*, 90(2):1106–1115, 1989. doi: 10.1063/1.456165. URL https://doi.org/10.1063/1.456165.

[199] Lars Goerigk and Stefan Grimme. A general database for main group thermochemistry, kinetics, and noncovalent interactions - assessment of common and reparameterized (meta-)gga density functionals. *Journal of Chemical Theory and Computation*, 6(1):107–126, 2010. doi: 10.1021/ct900489g. URL http://dx.doi.org/10.1021/ct900489g. PMID: 26614324.

[200] Lars Goerigk and Stefan Grimme. Efficient and accurate double-hybrid-meta-gga density functionals—evaluation with the extended gmtkn30 database for general main group thermochemistry, kinetics, and noncovalent interactions. *Journal of Chemical Theory and Computation*, 7(2):291–309, 2011. doi: 10.1021/ct100466k. URL http://dx.doi.org/10.1021/ct100466k. PMID: 26596152.

[201] Lars Goerigk and Stefan Grimme. A thorough benchmark of density functional methods for general main group thermochemistry, kinetics, and nocovalent interactions. *Phys Chem Chem Phys*, pages 6670–6688, 2011. ISSN 15499618. doi: 10.1021/ct100466k.

[202] R. L. Montgomery, F. D. Rossini, and M Mansson. Enthalpies of combustion, vaporization, and formation of phenylbenzene, cyclohexylbenzene, and cyclohexylcyclohexane; enthalpy of hydrogenation of certain aromatic systems. *J. Chem. Eng. Data*, 23:125, 1978.

[203] D. J. Coleman and G Pilcher. Heats of combustion of biphenyl, bibenzyl, naphthalene, anthracene and phenanthrene. *Trans. Faraday Soc.*, 62:821, 1966.

[204] H. Mackle and P. A. G O'Hare. A high-precision aneroid semimicro combustion calorimeter. *Trans. Faraday Soc.*, 59:2693, 1963.

[205] G. S. Parks and L. M Vaughan. The heat of combustion of biphenyl. *J. Am. Chem. Soc.*, 73:2380, 1951.

[206] R. D. Chirico, S. E. Knipmeyer, A. Nguyen, and W. V Steele. The thermodynamic properties of biphenyl. *J. Chem. Thermodyn.*, 21:1307, 1989.

[207] T. Clark, T. Knox, H. Mackle, M. A. McKervey, and J. J Rooney. Heats of sublimation of some cage hydrocarbons by a temperature scanning technique. *J. Chem. Soc., Faraday Trans. 1*, 71:2107, 1975.

[208] E Morawetz. Enthalpies of vaporization for a number of aromatic compounds. *J. Chem. Thermodyn.*, 4:455, 1972.

[209] R. S. Bradley and T. G Cleasby. The vapour pressure and lattice energy of some aromatic ring compounds. *J. Chem. Soc.*, page 1690, 1953.

[210] Carl L. Yaws, editor. *Yaws' Handbook of Thermodynamic Properties for Hydrocarbons and Chemicals*. Knovel, 2009.

[211] Ericka C. Barnes, George A. Petersson, John A. Montgomery, Michael J. Frisch, and Jan M. L. Martin. Unrestricted coupled cluster and brueckner doubles variations of w1 theory. *Journal of Chemical Theory and Computation*, 5(10):2687–2693, 2009. doi: 10.1021/ct900260g. URL https://doi.org/10.1021/ct900260g. PMID: 26631782.

[212] D.R. Burgess, M.R. Zachariah, W. Tsang, and P.R. Westmoreland. Thermochemical and chemical kinetic data for fluorinated hydrocarbons. *Progress in Energy and Combustion Science*, 21(6):453–529, 1995. ISSN 0360-1285. doi: 10.1016/0360-1285(95)00009-7. URL http://www.sciencedirect.com/science/article/pii/0360128595000097.

[213] S. S. Chen, A. S. Rodgers, J. Choo, R. C. Wilhoit, and B. J. Zwolinski. Ideal gas thermodynamic properties of six fluoroethanes. *Journal of Physical and Chemical Reference Data*, 4(2):441–456, 1975. doi: 10.1063/1.555521. URL https://doi.org/10.1063/1.555521.

[214] David R. Lide, editor. *CRC Handbook of Chemistry and Physics*. CRC Press, Taylor & Francis, 90th edition, 2009.

[215] D.R. Burgess. Thermochemical data. In *NIST Chemistry WebBook, NIST Standard Reference Database Number 69*. National Institute of Standards and Technology, Gaithersburg MD, 20899, 2017.

[216] V.A. Platonov and Yu.N. Simulin. Experimental determination of the standard enthalpies of formation of polychlorobenzenes. ii. standard enthalpies of formation of dichlorobenzenes. *Russ. J. Phys. Chem. (Engl. Transl.)*, 58, 1984.

[217] V.A. Platonov and Yu.N. Simulin. Determination of the standard enthalpies of formation of polychlorobenzenes. iii. the standard enthalpies of formation of mono-1,2,4- and 1,3,5-tri-, and 1,2,3,4- and 1,2,3,5-tetrachlorobenzenes. *Russ. J. Phys. Chem. (Engl. Transl.)*, 59:179–181, 1985.

[218] Bernhard Hidding and Michael Pfitzner. Rocket propellant characteristics of silanes/o2. *Journal of Propulsion and Power*, 22:786–789, 07 2006.

[219] S.N. Hajiev and M.J. Agarunov. Thermochemical studies of organometallic compounds i. heats of formation of dimethylchlorosilane methyldichlorosilane and dimethyldichlorosilane. *Journal of Organometallic Chemistry*, 11:415–422, 1968. ISSN 0022-328X. doi: 10.1016/0022-328X(68)80065-8. URL http://www.sciencedirect.com/science/article/pii/0022328X68800658.

[220] Vladislav S Pervov and N S Nikolaev. Advances in fluorine calorimetry. *Russian Chemical Reviews*, pages 319–329, 1976.

[221] V. Ya. Leonidov and P. A. G. O'Hare. Fluorine combustion calorimetry: progress in recent years and possibilities of further development. *Pure and Applied Chemistry*, 64(1), 1992. doi: 10.1351/pac199264010103.

[222] P. A. G. O'Hare. Thermochemistry of silicon-containing materials. *Pure and Applied Chemistry*, 71(7):1243–1248, 1999. doi: 10.1351/pac199971071243.

[223] Milton Farber and Srivastava R.D. Enthalpies of formation of the silane chlorides. *The Journal of Chemical Thermodynamics*, 11(10):939–944, 1979. ISSN 0021-9614. doi: 10.1016/0021-9614(79)90041-7. URL http://www.sciencedirect.com/science/article/pii/0021961479900417.

[224] Alan M. Doncaster and Robin Walsh. Thermochemistry of silicon-containing compounds. part 2.-the enthalpies of formation of the methylsilanes, an experimental study and review. *J. Chem. Soc., Faraday Trans. 2*, 82:707–717, 1986. doi: 10.1039/F29868200707. URL http://dx.doi.org/10.1039/F29868200707.

[225] Robin Walsh. Thermochemistry of silicon-containing compounds. part 1.-silicon-halogen compounds, an evaluation. *J. Chem. Soc., Faraday Trans. 1*, 79:2233–2248, 1983. doi: 10.1039/F19837902233. URL http://dx.doi.org/10.1039/F19837902233.

[226] M W. Chase. *NIST-JANAF Thermochemical Tables 2 Volume-Set*. American Institute of Physics, 8 1998.

[227] M.G. Voronkov, V.P. Baryshok, V.A. Klyuchnikov, T.F. Danilova, V.I. Pepekin, A.N. Korchagina, and Yu.I. Khudobin. Thermochemistry of organosilicon compounds: I. triorganyl-, tetraorganyl-, organylorganoxy- and tetraorganoxy-silanes. *Journal of Organometallic Chemistry*, 345(1):27–38, 1988. ISSN 0022-328X. doi: 10.1016/0022-328X(88)80231-6. URL http://www.sciencedirect.com/science/article/pii/0022328X88802316.

[228] Jeffrey W. Keister, Päivi Tomperi, and Tomas Baer. Thermochemistry of gaseous ethylsilanes and their radical cations. *Journal of the American Society for Mass Spectrometry*, 9(6):597–605, 1998. ISSN 1044-0305. doi: 10.1016/S1044-0305(98)00026-9. URL http://www.sciencedirect.com/science/article/pii/S1044030598000269.

[229] James J. P. Stewart. Optimization of parameters for semiempirical methods ii. applications. *Journal of Computational Chemistry*, 10(2):221–264, 1989. doi: 10.1002/jcc.540100209. URL https://onlinelibrary.wiley.com/doi/abs/10.1002/jcc.540100209.

[230] DIPPR. Dippr project 801 [421], 2007 release. Technical report, Design Institute for Physical Properties (DIPPR) of the American Institute of Chemical Engineers AIChE, 2007.

[231] Tomohito Shimpo, Takeshi Yoshikawa, and Kazuki Morita. Thermodynamic study of the effect of calcium on removal of phosphorus from silicon by acid leaching treatment. *Metallurgical and Materials Transactions B*, 35(2):277–284, Apr 2004. ISSN 1543-1916. doi: 10.1007/s11663-004-0029-1. URL https://doi.org/10.1007/s11663-004-0029-1.

[232] G. GEISELER and J. SAWISTOWSKY. Cheminform abstract: Bldg.-enthalpien und mesomerieenergien von pi-bindungssyst. 4. mitt. bldg.-enthalpien einiger thiacyclanone. *Chemischer Informationsdienst*, 3(47):no–no, 1972. ISSN 2199-2924. doi: 10.1002/chin.197247107. URL http://dx.doi.org/10.1002/chin.197247107.

[233] Karl K. Irikura. Thermochemistry of disulfur decafluoride, s2f10. *The Journal of Chemical Physics*, 103(23):10162–10168, 1995. doi: 10.1063/1.469918. URL https://doi.org/10.1063/1.469918.

[234] Karl K. Irikura. Erratum: "thermochemistry of disulfur decafluoride, s2f10" [j. chem. phys. 103, 10162 (1995)]. *The Journal of Chemical Physics*, 115 (10):4966–4966, 2001. doi: 10.1063/1.1394746. URL https://doi.org/10.1063/1.1394746.

[235] Pass G. Thermodynamic functions of disulphur decafluoride. *Journal of Applied Chemistry*, 19(3):77–78, 1969. doi: 10.1002/jctb.5010190304. URL https://onlinelibrary.wiley.com/doi/abs/10.1002/jctb.5010190304.

[236] Gene A. Silvey and George H. Cady. Trifluoromethylsulfur pentafluoride. *Journal of the American Chemical Society*, 72(8):3624–3626, 1950. doi: 10.1021/ja01164a084. URL https://doi.org/10.1021/ja01164a084.

[237] W. T. Sturges, T. J. Wallington, M. D. Hurley, K. P. Shine, K. Sihra, A. Engel, D. E. Oram, S. A. Penkett, R. Mulvaney, and C. A. M. Brenninkmeijer. A potent greenhouse gas identified in the atmosphere: Sf5cf3. *Science*, 289(5479):611–613, 2000. ISSN 0036-8075. doi: 10.1126/science.289.5479.611. URL http://science.sciencemag.org/content/289/5479/611.

[238] Richard P. Tuckett. Chapter 3: Trifluoromethyl sulphur pentafluoride, sf5cf3: Atmospheric chemistry and its environmental importance via the greenhouse effect. In Alain Tressaud, editor, *Fluorine and the Environment*, volume 1 of *Advances in Fluorine Science*, pages 89–129. Elsevier, 2006. doi: 10.1016/S1872-0358(06)01003-7. URL http://www.sciencedirect.com/science/article/pii/S1872035806010037.

[239] Wen-Tien Tsai. The prediction of environmental fate for trifluoromethyl sulfur pentafluoride (sf5cf3), a potent greenhouse gas. *Journal of Hazardous Materials*, 149(3):747–751, 2007. ISSN 0304-3894. doi: 10.1016/j.jhazmat.2007.08.035. URL http://www.sciencedirect.com/science/article/pii/S0304389407012137. Pollution Prevention and Restoration of the Environment.

[240] Sebastian Kozuch and Jan M. L. Martin. Halogen bonds: Benchmarks and theoretical analysis. *Journal of Chemical Theory and Computation*, 9(4): 1918–1931, 2013. doi: 10.1021/ct301064t. URL https://doi.org/10.1021/ct301064t. PMID: 26583543.

[241] Yan Zhao and Donald G. Truhlar. The m06 suite of density functionals for main group thermochemistry, thermochemical kinetics, noncovalent interactions, excited states, and transition elements: two new functionals and systematic testing of four m06-class functionals and 12 other functionals. *Theoretical Chemistry Accounts*, 120(1):215–241, May 2008. ISSN 1432-2234. doi: 10.1007/s00214-007-0310-x. URL https://doi.org/10.1007/s00214-007-0310-x.

[242] Jeng-Da Chai and Martin Head-Gordon. Systematic optimization of long-range corrected hybrid density functionals. *The Journal of Chemical Physics*, 128(8):084106, 2008. doi: 10.1063/1.2834918. URL https://doi.org/10.1063/1.2834918.

[243] Yan Zhao, Nathan E. Schultz, and D. G. Truhlar. Exchange-correlation functional with broad accuracy for metallic and nonmetallic compounds, kinetics, and noncovalent interactions. *The Journal of Chemical Physics*, 123(16):161103, 2005. doi: 10.1063/1.2126975. URL https://doi.org/10.1063/1.2126975.

[244] Martin Walker, Andrew J. A. Harvey, Ananya Sen, and Caroline E. H. Dessent. Performance of m06, m06–2x, and m06–hf density functionals for conformationally flexible anionic clusters: M06 functionals perform better than b3lyp for a model system with dispersion and ionic hydrogen-bonding interactions. *The Journal of Physical Chemistry A*, 117(47):12590–12600, 2013. doi: 10.1021/jp408166m. URL https://doi.org/10.1021/jp408166m. PMID: 24147965.

[245] Edward G. Hohenstein, Samuel T. Chill, and C. David Sherrill. Assessment of the performance of the m05–2x and m06–2x exchange-correlation functionals for noncovalent interactions in biomolecules. *Journal of Chemical Theory and Computation*, 4(12):1996–2000, 2008. doi: 10.1021/ct800308k. URL https://doi.org/10.1021/ct800308k. PMID: 26620472.

[246] Daniela Josa, Jesús Rodríguez-Otero, Enrique M. Cabaleiro-Lago, and Marcos Rellán-Piñeiro. Analysis of the performance of dft-d, $m05-2x$ and $m06-2x$ functionals for studying $\pi-\pi$ interactions. *Chemical Physics Letters*, 557:170 – 175, 2013. ISSN 0009-2614. doi: https://doi.org/10.1016/j.cplett.2012.12.017. URL http://www.sciencedirect.com/science/article/pii/S0009261412014364.

[247] Steven E. Wheeler and K. N. Houk. Integration grid errors for meta-gga-predicted reaction energies: Origin of grid errors for the m06 suite of functionals. *Journal of Chemical Theory and Computation*, 6(2):395–404, 2010. doi: 10.1021/ct900639j. URL https://doi.org/10.1021/ct900639j.

[248] Narbe Mardirossian and Martin Head-Gordon. Thirty years of density functional theory in computational chemistry: an overview and extensive assessment of 200 density functionals. *Molecular Physics*, 115(19):2315–2372, 2017. doi: 10.1080/00268976.2017.1333644. URL https://doi.org/10.1080/00268976.2017.1333644.

[249] Manuel A.V. Ribeiro da Silva and Luísa M.P.F. Amaral. Standard molar enthalpies of formation of 2-furancarbonitrile, 2-acetylfuran, and 3-furaldehyde. *The Journal of Chemical Thermodynamics*, 41(1):26 – 29, 2009. ISSN 0021-9614. doi: https://doi.org/10.1016/j.jct.2008.08.004. URL http://www.sciencedirect.com/science/article/pii/S0021961408001894.

[250] P. Knauth and R. Sabbah. Combustion calorimetry on milligram samples of liquid substances with a crmt rocking bomb calorimeter. application to the study of ω-alkanediols at 298.15 k. *The Journal of Chemical Thermodynamics*, 21(2):203 – 210, 1989. ISSN 0021-9614. doi: https://doi.org/10.1016/0021-9614(89)90131-6. URL http://www.sciencedirect.com/science/article/pii/0021961489901316.

[251] David Feller and John M. Simmie. High-level ab initio enthalpies of formation of 2,5-dimethylfuran, 2-methylfuran, and furan. *The Journal of Physical Chemistry A*, 116(47):11768–11775, 2012. doi: 10.1021/jp3095984. URL https://doi.org/10.1021/jp3095984. PMID: 23121013.

[252] M. Agostinha R. Matos, Margarida S. Miranda, and Victor M. F. Morais. Thermochemical study of the methoxy- and dimethoxyphenol isomers. *Journal of Chemical & Engineering Data*, 48(3):669–679, 2003. doi: 10.1021/je025641j. URL https://doi.org/10.1021/je025641j.

[253] Branko Ruscic. Active thermochemical tables: Sequential bond dissociation enthalpies of methane, ethane, and methanol and the related thermochemistry. *The Journal of Physical Chemistry A*, 119(28):7810–7837, 2015. doi: 10.1021/acs.jpca.5b01346. URL http://dx.doi.org/10.1021/acs.jpca.5b01346. PMID: 25760799.

[254] María Victoria Roux, Manuel Temprado, James S. Chickos, and Yatsuhisa Nagano. Critically evaluated thermochemical properties of polycyclic aromatic hydrocarbons. *Journal of Physical and Chemical Reference Data*, 37(4):1855–1996, 2008. doi: 10.1063/1.2955570. URL https://doi.org/10.1063/1.2955570.

[255] Yang Meng-Yan and G. Pilcher. Enthalpies of combustion of succinic anhydride, glutaric anhydride, and glutarimide. *The Journal of Chemical Thermodynamics*, 22(9):893 – 898, 1990. ISSN 0021-9614. doi: https://doi.org/10.1016/0021-9614(90)90177-R. URL http://www.sciencedirect.com/science/article/pii/002196149090177R.

[256] R. A. Fletcher and G. Pilcher. Measurements of heats of combustion by flame calorimetry. part 6.-formaldehyde glyoxal. *Trans. Faraday Soc.*, 66: 794–799, 1970. doi: 10.1039/TF9706600794. URL http://dx.doi.org/10.1039/TF9706600794.

[257] G. B. Guthrie, D. W. Scott, W. N. Hubbard, C. Katz, J. P. McCullough, M. E. Gross, K. D. Williamson, and Guy Waddington. Thermodynamic properties of furan. *Journal of the American Chemical Society*, 74(18):4662–4669, 1952. doi: 10.1021/ja01138a063. URL https://doi.org/10.1021/ja01138a063.

[258] A. S. Pell and G. Pilcher. Measurements of heats of combustion by flame calorimetry. part 3.-ethylene oxide, trimethylene oxide, tetrahydrofuran and tetrahydropy. *Trans. Faraday Soc.*, 61:71–77, 1965. doi: 10.1039/TF9656100071. URL http://dx.doi.org/10.1039/TF9656100071.

[259] R. J. L. Andon, D. P. Biddiscombe, J. D. Cox, R. Handley, D. Harrop, E. F. G. Herington, and J. F Martin. Thermodynamic properties of organic oxygen compounds. part i. preparation and physical properties of pure phenol, cresols, and xylenols. *J. Chem. Soc.*, page 5246, 1960.

[260] Cox J. D. The heats of combustion of phenol and the three cresols. *Pure and Applied Chemistry*, 2, 1961. doi: 10.1351/pac196102010125.

[261] D. Ambrose, J.E. Connett, J.H.S. Green, J.L. Hales, A.J. Head, and J.F. Martin. Thermodynamic properties of organic oxygen compounds 42. physical and thermodynamic properties of benzaldehyde. *The Journal of Chemical Thermodynamics*, 7(12):1143 – 1157, 1975. ISSN 0021-9614. doi: https://doi.org/10.1016/0021-9614(75)90035-X. URL http://www.sciencedirect.com/science/article/pii/002196147590035X.

[262] W. V. Steele, R. D. Chirico, A. Nguyen, I. A. Hossenlopp, and N. K Smith. Determination of ideal-gas enthalpies of formation for key compounds. aiche symp. *Ser.*, 86:138, 1990.

[263] Raphaël Sabbah and Marc Laffitte. Etude thermodynamique de la molécule de benzophénone. *Thermochimica Acta*, 23(1):196 – 198, 1978. ISSN 0040-6031. doi: https://doi.org/10.1016/0040-6031(78)85128-4. URL http://www.sciencedirect.com/science/article/pii/0040603178851284.

[264] R Sabbah. Thermodynamic study of fluorene and dibenzofuran, 1991.

[265] WV Steele and RD Chirico. Thermodynamics and the hydrodeoxygenation of 2, 3-benzofuran. Technical report, National Inst. for Petroleum and Energy Research, Bartlesville, OK (USA), 1990.

[266] J. O. Fenwick, D. Harrop, and A. J Head. Thermodynamic properties of organic oxygen compounds 41 enthalpies of formation of eight ethers. *J. Chem. Thermodyn.*, 7:943, 1975.

[267] John Desmond Cox and Geoffrey Pilcher. *Thermochemistry of Organic and Organometallic Compounds*. Academic Press, 1970. URL https://books.google.fr/books?id=_QbwAAAAMAAJ.

[268] Dimitrios M. Speros and Frederick D. Rossini. Heats of combustion and formation of naphthalene, the two methylnaphthalenes, cis and trans-decahydronaphthalene, and related compounds1. *The Journal of Physical Chemistry*, 64(11):1723–1727, 1960. doi: 10.1021/j100840a029. URL https://doi.org/10.1021/j100840a029.

[269] Sylvio Canuto. *Solvation Effects on Molecules and Biomolecules: Computational Methods and Applications*. Springer Netherlands, 2008. ISBN 978-90-481-7826-1.

[270] Tohid N. Borhani, Salvador García-Muñoz, Carla Vanesa Luciani, Amparo Galindo, and Claire S. Adjiman. Hybrid qspr models for the prediction of the free energy of solvation of organic solute/solvent pairs. *Phys. Chem. Chem. Phys.*, 21:13706–13720, 2019. doi: 10.1039/C8CP07562J. URL http://dx.doi.org/10.1039/C8CP07562J.

[271] Christopher J. Cramer and Donald G. Truhlar. Implicit solvation models: Equilibria, structure, spectra, and dynamics. *Chemical Reviews*, 99(8): 2161–2200, 1999. doi: 10.1021/cr00031a013. URL https://doi.org/10.1021/cr960149m.

[272] Christopher J. Cramer and Donald G. Truhlar. A universal approach to solvation modeling. *Accounts of Chemical Research*, 41(6):760–768, 2008. doi: 10.1021/ar800019z. URL https://doi.org/10.1021/ar800019z.

[273] Aleksandr V. Marenich, Christopher J. Cramer, and Donald G. Truhlar. Universal solvation model based on solute electron density and on a continuum model of the solvent defined by the bulk dielectric constant and atomic surface tensions. *The Journal of Physical Chemistry B*, 113(18):6378–6396, 2009. doi: 10.1021/jp810292n. URL https://doi.org/10.1021/jp810292n.

[274] Aleksandr V. Marenich, Christopher J. Cramer, and Donald G. Truhlar. Generalized born solvation model sm12. *Journal of Chemical Theory and Computation*, 9(1):609–620, 2013. doi: 10.1021/ct300900e. URL https://doi.org/10.1021/ct300900e.

[275] Jacopo Tomasi, Benedetta Mennucci, and Roberto Cammi. Quantum mechanical continuum solvation models. *Chemical Reviews*, 105(8):2999–3094, 2005. doi: 10.1021/cr9904009. URL https://doi.org/10.1021/cr9904009. PMID: 16092826.

[276] Jacopo Tomasi and Maurizio Persico. Molecular interactions in solution: An overview of methods based on continuous distributions of the solvent. *Chemical Reviews*, 94(7):2027–2094, 1994. doi: 10.1021/cr00031a013. URL https://doi.org/10.1021/cr00031a013.

[277] Maurizio Cossi, Nadia Rega, Giovanni Scalmani, and Vincenzo Barone. Energies, structures, and electronic properties of molecules in solution with the c-pcm solvation model. *Journal of Computational Chemistry*, 24(6):669–681, 2003. doi: 10.1002/jcc.10189. URL https://onlinelibrary.wiley.com/doi/abs/10.1002/jcc.10189.

[278] Guilherme Duarte Ramos Matos, Daisy Y. Kyu, Hannes H. Loeffler, John D. Chodera, Michael R. Shirts, and David L. Mobley. Approaches for calculating solvation free energies and enthalpies demonstrated with an update of the freesolv database. *Journal of Chemical & Engineering Data*, 62 (5):1559–1569, 2017. doi: 10.1021/acs.jced.7b00104. URL https://doi.org/10.1021/acs.jced.7b00104.

[279] AAGE Fredenslund, JÜRGEN Gmehling, and PETER Rasmussen. *Vapor-liquid Equilibria Using Unifac*. Elsevier, 1977. ISBN 978-0-444-41621-6.

[280] Jürgen Gmehling, Jürgen Lohmann, Antje Jakob, Jiding Li, and Ralph Joh. A modified unifac (dortmund) model. 3. revision and extension. *Industrial & Engineering Chemistry Research*, 37(12):4876–4882, 1998. doi: 10.1021/ie980347z. URL https://doi.org/10.1021/ie980347z.

[281] R.C. Reid, J.M. Prausnitz, and B.E. Poling. *The properties of gases and liquids*. Mcgraw-Hill New York, 1 1987.

[282] Simon Dufal, Vasileios Papaioannou, Majid Sadeqzadeh, Thomas Pogiatzis, Alexandros Chremos, Claire S. Adjiman, George Jackson, and Amparo Galindo. Prediction of thermodynamic properties and phase behavior of fluids and mixtures with the saft-γ mie group-contribution equation of state. *Journal of Chemical & Engineering Data*, 59(10):3272–3288, 2014. doi: 10.1021/je500248h. URL https://doi.org/10.1021/je500248h.

[283] Sofiane Tamouza, J.-Philippe Passarello, Pascal Tobaly, and J.-Charles de Hemptinne. Group contribution method with saft eos applied to vapor liquid equilibria of various hydrocarbon series. *Fluid Phase Equilibria*, 222-223:67 – 76, 2004. ISSN 0378-3812. doi: https://doi.org/10.1016/j.fluid.2004.06.038. URL http://www.sciencedirect.com/science/article/pii/S0378381204002560. Proceedings of the Fifteenth Symposium on Thermophysical Properites.

[284] Moine Edouard, Privat Romain, Jaubert Jean-Noël, Sirjean Baptiste, Novak Nefeli, Voutsas Epaminondas, and Boukouvalas Christos. Can we safely predict solvation gibbs energies of pure and mixed solutes with a cubic equation of state? *Pure and Applied Chemistry*, 91(8):1295 – 1307, 2019. doi: https://doi.org/10.1515/pac-2018-1112. URL https://www.degruyter.com/view/journals/pac/91/8/article-p1295.xml.

[285] Andrew R. Leach. *Molecular Modelling: Principles and Applications*. Person Education Limited, 2001. ISBN 0-582-38210-6.

[286] Jay W. Ponder, Chuanjie Wu, Pengyu Ren, Vijay S. Pande, John D. Chodera, Michael J. Schnieders, Imran Haque, David L. Mobley, Daniel S. Lambrecht, Robert A. DiStasio, Martin Head-Gordon, Gary N. I. Clark, Margaret E. Johnson, and Teresa Head-Gordon. Current status of the amoeba polarizable force field. *The Journal of Physical Chemistry B*, 114(8):2549–2564, 2010. doi: 10.1021/jp910674d. URL https://doi.org/10.1021/jp910674d. PMID: 20136072.

[287] Tai-Sung Lee, David S. Cerutti, Dan Mermelstein, Charles Lin, Scott LeGrand, Timothy J. Giese, Adrian Roitberg, David A. Case, Ross C. Walker, and Darrin M. York. Gpu-accelerated molecular dynamics and free energy methods in amber18: Performance enhancements and new features. *Journal of Chemical Information and Modeling*, 58(10):2043–2050, 2018. doi: 10.1021/acs.jcim.8b00462. URL https://doi.org/10.1021/acs.jcim.8b00462. PMID: 30199633.

[288] Karl T. Debiec, David S. Cerutti, Lewis R. Baker, Angela M. Gronenborn, David A. Case, and Lillian T. Chong. Further along the road less traveled: Amber ff15ipq, an original protein force field built on a self-consistent physical model. *Journal of Chemical Theory and Computation*, 12(8):3926–3947, 2016. doi: 10.1021/acs.jctc.6b00567. URL https://doi.org/10.1021/acs.jctc.6b00567. PMID: 27399642.

[289] Shujie Fan, Bogdan I. Iorga, and Oliver Beckstein. Prediction of octanol-water partition coefficients for the sampl6-log^P $logp$ molecules using molecular dynamics simulations with opls-aa, amber and charmm force fields. *Journal of Computer-Aided Molecular Design*, 34(291):1573–4951, 2020. doi: 10.1007/s10822-019-00267-z. URL https://doi.org/10.1007/s10822-019-00267-z.

[290] Tohid Nejad Ghaffar Borhani, Mohammadhossein Saniedanesh, Mehdi Bagheri, and Jeng Shiun Lim. Qspr prediction of the hydroxyl radical rate constant of water contaminants. *Water Research*, 98:344 – 353, 2016. ISSN 0043-1354. doi: https://doi.org/10.1016/j.watres.2016.04.038. URL http://www.sciencedirect.com/science/article/pii/S0043135416302378.

[291] Michael H. Abraham, James A. Platts, Anne Hersey, Albert J. Leo, and Robert W. Taft. Correlation and estimation of gas–chloroform and water–chloroform partition coefficients by a linear free energy relationship method. *Journal of Pharmaceutical Sciences*, 88(7):670–679, 1999. doi: 10.1021/js990008a. URL https://onlinelibrary.wiley.com/doi/abs/10.1021/js990008a.

[292] Jean-Claude Bradley, Michael H Abraham, Jr Acree, William E, and Andrew Sid Lang. Predicting abraham model solvent coefficients. *Chemistry Central journal*, 9(12):12–12, 2015. doi: 10.1186/s13065-015-0085-4. URL https://www.ncbi.nlm.nih.gov/pubmed/25798192.

[293] A. Ben-Naim and R. Lovett. Solvation free energy of a hard sphere solute in a square well solvent as a function of solute size. *The Journal of Physical Chemistry B*, 101(49):10535–10541, 1997. doi: 10.1021/jp962811o. URL https://doi.org/10.1021/jp962811o.

[294] Arieh Ben-Naim and M. Mazo Robert. Size dependence of the solvation free energies of large solutes. *journal of physical Chemistry*, 97(41):10829–10834, 1993. doi: DOI:10.1021/j100143a050.

[295] R. Rowley, W. Wilding, J. Oscarson, Y. Yang, and N. Giles. Dippr data compilation of pure chemical properties (design institute for physical properties). *American Institute of Chemical Engineers, AIChe,New York*, 2010. doi: 10.1007/BF01448224. URL https://doi.org/10.1007/BF01448224.

[296] Christina Mintz, Michael Clark, William E. Acree, and Michael H. Abraham. Enthalpy of solvation correlations for gaseous solutes dissolved in water and in 1-octanol based on the abraham model. *Journal of Chemical Information and Modeling*, 47(1):115–121, 2007. doi: 10.1021/ci600402n. URL https://doi.org/10.1021/ci600402n. PMID: 17238256.

[297] Shu Wang, Stanley I. Sandler, and Chau-Chyun Chen. Refinement of cosmo-sac and the applications. *Industrial & Engineering Chemistry Research*, 46(22):7275–7288, 2007. doi: 10.1021/ie070465z. URL https://doi.org/10.1021/ie070465z.

[298] Ruichang Xiong, Stanley I. Sandler, and Russell I. Burnett. An improvement to cosmo-sac for predicting thermodynamic properties. *Industrial & Engineering Chemistry Research*, 53(19):8265–8278, 2014. doi: 10.1021/ie404410v. URL https://doi.org/10.1021/ie404410v.

[299] Mqondisi Nala, Eric Auger, Ibrahim Gedik, Nicolas Ferrando, Moussa Dicko, Patrice Paricaud, Fabien Volle, Jean Philippe Passarello, Jean-Charles de Hemptinne, Pascal Tobaly, Paolo Stringari, Christophe Coquelet, Deresh Ramjugernath, Paramespri Naidoo, and Rafael Lugo. Vapour-liquid equilibrium (vle) for the systems $furan + n - hexane$ and furan+toluene. measurements, data treatment and modeling using molecular models. *Fluid Phase Equilibria*, 337:234 – 245, 2013. ISSN 0378-3812. doi: https://doi.org/10.1016/j.fluid.2012.08.005. URL http://www.sciencedirect.com/science/article/pii/S0378381212003585.

[300] Charlie Stephan, Moussa Dicko, Paolo Stringari, and Christophe Coquelet. Liquid-liquid equilibria of waterÂ + solutes (acetic acid/ acetol/furfural/guaiacol/methanol/phenol/propanal)Â + solvents (isopropyl acetate/toluene) ternary systems for pyrolysis oil fractionation. *Fluid Phase Equilibria*, 468:49 – 57, 2018. ISSN 0378-3812. doi: https://doi.org/10.1016/j.fluid.2018.04.016. URL http://www.sciencedirect.com/science/article/pii/S0378381218301638.

[301] John P. Perdew. Density-functional approximation for the correlation energy of the inhomogeneous electron gas. *Phys. Rev. B*, 33:8822–8824, Jun 1986. doi: 10.1103/PhysRevB.33.8822. URL https://link.aps.org/doi/10.1103/PhysRevB.33.8822.

[302] Yu Takano and K. N. Houk. Benchmarking the conductor-like polarizable continuum model (cpcm) for aqueous solvation free energies of neutral and ionic organic molecules. *Journal of Chemical Theory and Computation*, 1(1):70–77, 2005. doi: 10.1021/ct049977a. URL https://doi.org/10.1021/ct049977a. PMID: 26641117.

[303] J. L. Pascual-ahuir, E. Silla, and I. Tunon. Gepol: An improved description of molecular surfaces. iii. a new algorithm for the computation of a solvent-excluding surface. *Journal of Computational Chemistry*, 15(10):1127–1138, 1994. doi: 10.1002/jcc.540151009. URL https://onlinelibrary.wiley.com/doi/abs/10.1002/jcc.540151009.

[304] Aage Fredenslund, Russell L. Jones, and John M. Prausnitz. Group-contribution estimation of activity coefficients in nonideal liquid mixtures. *AIChE Journal*, 21(6):1086–1099, 1975. doi: 10.1002/aic.690210607. URL https://onlinelibrary.wiley.com/doi/abs/10.1002/aic.690210607.

[305] A. Frassoldati, A. Cuoci, A. Stagni, T. Faravelli, R. Calabria, and P. Massoli. Thermo-physical characterization of fpbo and preliminary surrogate definition, 2017. This project has received funding from the European Union's Horizon 2020 research and innovation programme under grant agreement No. 654650.

[306] J.P. Diebold. A review of the chemical and physical mechanisms of the storage stability of fast pyrolysis bio-oils, 2002. URL https://www.nrel.gov/docs/fy00osti/27613.pdf. This report was prepared as an account of work sponsored by an agency of the United States government.

[307] Takeo Kotake, Haruo Kawamoto, and Shiro Saka. Pyrolysis reactions of coniferyl alcohol as a model of the primary structure formed during lignin pyrolysis. *Journal of Analytical and Applied Pyrolysis*, 104:573 – 584, 2013. ISSN 0165-2370. doi: https://doi.org/10.1016/j.jaap.2013.05.011. URL http://www.sciencedirect.com/science/article/pii/S0165237013001022.

[308] Mark Saeys, Marie-Françoise Reyniers, Guy B. Marin, Veronique Van Speybroeck, and Michel Waroquier. Ab initio calculations for hydrocarbons: Enthalpy of formation, transition state geometry, and activation energy for radical reactions. *The Journal of Physical Chemistry A*, 107(43):9147–9159, 2003. doi: 10.1021/jp021706d. URL https://doi.org/10.1021/jp021706d.

[309] Takeshi Nakamura, Haruo Kawamoto, and Shiro Saka. Condensation reactions of some lignin related compounds at relatively low pyrolysis temperature. *Journal of Wood Chemistry and Technology*, 27(2):121–133, 2007. doi: 10.1080/02773810701515143. URL https://doi.org/10.1080/02773810701515143.

[310] Haruo Kawamoto. Lignin pyrolysis reactions. *Journal of Wood Science*, 63(2):117–132, 2017. doi: 10.1007/s10086-016-1606-z. URL https://doi.org/10.1007/s10086-016-1606-z.

[311] Donald G. Truhlar and Yan Zhao. The m06 suite of density functionals for main group thermochemistry, thermochemical kinetics, noncovalent interactions, excited states, and transition elements: two new functionals and systematic testing of four m06-class functionals and 12 other functionals. *Theoretical Chemistry Accounts*, 120:215–241, 2008. doi: 10.1007/s00214-007-0310-x. URL https://doi.org/10.1007/s00214-007-0310-x.

[312] E. P. Wigner and Arthur S. Wightman. *On the Quantum Correction for Thermodynamic Equilibrium*, pages 110–120. Springer Berlin Heidelberg, Berlin, Heidelberg, 1997. ISBN 978-3-642-59033-7. doi: 10.1007/978-3-642-59033-7. URL https://doi.org/10.1007/978-3-642-59033-7.

[313] Carl Eckart. The penetration of a potential barrier by electrons. *Phys. Rev.*, 35:1303–1309, Jun 1930. doi: 10.1103/PhysRev.35.1303. URL https://link.aps.org/doi/10.1103/PhysRev.35.1303.

[314] Sebastien Canneaux, Frederic Bohr, and Eric Henon. Kisthelp: A program to predict thermodynamic properties and rate constants from quantum chemistry results . *Journal of Computational Chemistry*, 35(1):82–93, 2014. doi: 10.1002/jcc.23470. URL https://onlinelibrary.wiley.com/doi/abs/10.1002/jcc.23470.

[315] Reinhart Ahlrichs, Michael Bär, Marco Häser, Hans Horn, and Christoph Kölmel. Electronic structure calculations on workstation computers: The program system turbomole. *Chemical Physics Letters*, 162(3):165 – 169, 1989. ISSN 0009-2614. doi: https://doi.org/10.1016/0009-2614(89)85118-8. URL http://www.sciencedirect.com/science/article/pii/0009261489851188.

[316] Hans-Heinrich Carstensen and Anthony M Dean. Development of detailed kinetic models for the thermal conversion of biomass via first principle methods and rate estimation rules. In *Computational modeling in lignocellulosic biofuel production*, pages 201–243. ACS Publications, 2010.

[317] C. Cavallotti, A. Cuoci, T. Faravelli, A. Frassoldati, M. Pelucchi, and E. Ranzi. Detailed kinetics of pyrolysis and combustion of catechol and guaiacol, as reference components of bio-oil from biomass. *Chemical Engineering Transactions*, 65:79–84, Jun. 2018. doi: 10.3303/CET1865014. URL https://www.cetjournal.it/index.php/cet/article/view/CET1865014.

[318] Julia Gebhardt, Matthias Kiesel, Sereina Riniker, and Niels Hansen. Combining molecular dynamics and machine learning to predict self-solvation free energies and limiting activity coefficients. *Journal of Chemical Information and Modeling*, 0(0):null, 0. doi: 10.1021/acs.jcim.0c00479. URL https://doi.org/10.1021/acs.jcim.0c00479. PMID: 32786697.

[319] J.B. Pedley. *Thermochemical Data and Structures of Organic Compounds*. Number vol. 1 in TRC data series. Taylor & Francis, 1994. ISBN 9781883400019. URL https://books.google.fr/books?id=ap0Pc0xrN0cC.

[320] M. Colomina, M. V. Roux, and C Turrion. Thermochemical properties of naphthalene compounds ii. enthalpies of combustion and formation of the 1-and 2-naphthols. *J. Chem. Thermodyn.*, 6:571, 1974.

[321] M. A. V. Ribeiro da Silva, M. D. M. C. Ribeiro da Silva, and G Pilcher. Enthalpies of combustion of 1-hydroxynaphthalene, 2-hydroxynaphthalene, and 1,2-, 1,3-, 1,4-, and 2,3-dihydroxynaphthalenes. *J. Chem. Thermodyn.*, 20:969, 1988.

[322] R. D. Chirico, W. V. Steele, and A. F Kazakov. Thermodynamic properties of 1-naphthol: Mutual validation of experimental and computational results. *J. Chem. Thermodyn.*, 86:106, 2015.

[323] C. M. Anderson and E. C Gilbert. The apparent energy of the nn bond as calculated from heats of combustion. *J. Am. Chem. Soc.*, 64:2369, 1942.

[324] L. G. Cole and E. C Gilbert. The heats of combustion of some nitrogen compounds and the apparent energy of the n-n bond. *J. Am. Chem. Soc.*, 73: 5423, 1951.

[325] W. E. Hatton, D. L. Hildenbrand, G. C. Sinke, and D. R Stull. Chemical thermodynamic properties of aniline. *J. Chem. Eng. Data*, 7:229, 1962.

[326] W. V. Steele, R. D. Chirico, S. E. Knipmeyer, and A Nguyen. Vapor pressure, heat capacity, and density along the saturation line: Measurements for benzenamine, butylbenzene, sec-butylbenzene, tert-butylbenzene, 2,2-dimethylbutanoic acid, tridecafluoroheptanoic acid, 2-butyl-2-ethyl-1,3-propanediol, 2,2,4-trimethyl-1,3-pentanediol, and 1-chloro-2-propanol. *J. Chem. Eng. Data*, 47:648, 2002.

[327] K. Kusano and I Wadso. Enthalpy of vaporization of some organic substances at 25 ∘c and test of calorimeter. *Bull. Chem. Soc. Jpn.*, 44:1705, 1971.

[328] R. G. Simoões, F. Agapito, H. P. Diogo, and M. E. M da Piedade. Enthalpy of formation of anisole: Implications for the controversy on the o-h bond dissociation enthalpy in phenol. *J. Phys. Chem. A*, 118:11026, 2014.

[329] M. M Badoche. Chaleurs de combustion du phe nol, du m-cre sol et de leurs e thers. *Bull. Soc. Chim. Fr.*, 8:212, 1941.

[330] N. D. Lebedeva and Yu. A. Katin. Heats of combustion of monosubstituted benzenes. *Russ. J. Phys. Chem.*, 46:1088, 1972.

[331] T. G. Kalugina and E. G Kiparisova. Enthalpies of combustion and of formation of derivatives of carbamide. *Russ. J. Phys. Chem.*, 61:261, 1987.

[332] L. A. T. Gomez and R Sabbah. Thermodynamique de substances azotees. ix. etude thermochimique de la benzamide comparaison des grandeurs energetiques liees a la structure de quelques amides et thioamides. *Thermochim. Acta*, 58:311, 1982.

[333] A. R. R. P. Almeida and M. J. S Monte. Thermodynamic study of benzamide, n-methylbenzamide, and n, n-dimethylbenzamide: vapor pressures, phase diagrams, and hydrogen bond enthalpy. *J. Chem. Eng. Data*, 55:3507, 2010.

[334] S. P. Verevkin, V. N. Emel'yanenko, and R. N Nagrimanov. Nearest-neighbor and non-nearest-neighbor interactions between substituents in the benzene ring. experimental and theoretical study of functionally substituted benzamides. *J. Phys. Chem. A*, 120:9867, 2016.

[335] J.D. Cox, D.D. Wagman, and V.A. Medvedev. *CODATA key values for thermodynamics*. CODATA series on thermodynamic properties. Hemisphere Pub. Corp., 1989. ISBN 9780891167587. URL `https://books.google.fr/books?id=rTpRAAAAMAAJ`.

[336] A. Labbauf and F. D. Rossini. Heats of combustion, formation, and hydrogenation of 14 selected cyclomonoölefin hydrocarbons. *J. Phys. Chem.*, 65: 476, 1961.

[337] W. D. Good and N. K. Smith. Enthalpies of combustion of toluene, benzene, cyclohexane, cyclohexene, methylcyclopentane, 1-methylcyclopentene, and n-hexane. *J. Chem. Eng. Data*, 14:102, 1969.

[338] W. V. Steele, R. D. Chirico, S. E. Knipmeyer, A. Nguyen, N. K. Smith, and I. R. Tasker. Thermodynamic properties and ideal-gas enthalpies of formation for cyclohexene, phthalan (2,5-dihydrobenzo-3,4-furan), isoxazole, octylamine, dioctylamine, trioctylamine, phenyl isocyanate, and 1,4,5,6-tetrahydropyrimidine. *J. Chem. Eng. Data*, 41:1269, 1996.

[339] H. Pines, B. Kvetinskas, L. S. Kassel, and V. N. Ipatieff. Determination of equilibrium constants for butanes and pentanes. *J. Am. Chem. Soc.*, 67: 631, 1945.

[340] E. J. Prosen, F. W. Maron, and F. D. Rossini. Heats of combustion, formation, and isomerization of ten c4 hydrocarbons. *J. Res. Natl. Bur. Stand.*, 46:106, 1951.

[341] D. A. Pittam and G. Pilcher. Measurements of heats of combustion by flame calorimetry. part 8 methane, ethane, propane, n-butane and 2-methylpropane. *J. Chem. Soc., Faraday Trans. 1*, 68:2224, 1972.

[342] N. D. Lebedeva, Yu. A. Katin, and G. Akhmedova. Ya. *Standard Enthalpy of Formation for Nitrobenzene. Dep. VINITI*, page 2945, 1971.

[343] S. P. Verevkin, V. N. Emel'yanenko, V. Diky, and O. V Dorofeeva. Enthalpies of formation of nitromethane and nitrobenzene: New experiments vs. quantum chemical calculations. *J. Chem. Thermodyn.*, 73:163, 2014.

[344] M. P. Kozina, L. V. Bychikhina, G. L. Galchenko, E. M. Milvitskaya, M. Ordubadi, and A. F. Plate. Enthalpies of nortricyclene and norbornene formation. *Doklady Akad. Nauk SSSR*, 226:1105, 1976.

[345] W. V. Steele, R. D. Chirico, S. E. Knipmeyer, A. Nguyen, and N. K. Smith. Thermodynamic properties and ideal-gas enthalpies of formation for butyl vinyl ether, 1,2-dimethoxyethane, methyl glycolate, bicyclo[2.2.1]hept-2-ene, 5-vinylbicyclo[2.2.1]hept-2-ene, trans-azobenzene, butyl acrylate, di-tert-butyl ether, and hexane-1,6-diol. *J. Chem. Eng. Data*, 41:1285, 1996.

[346] R. Jochems, H. Dekker, C. Mosselman, and G. Somsen. The use of the lkb 8721–3 vaporization calorimeter to measure enthalpies of sublimation. the enthalpies of sublimation of bicyclo[2.2.1]hept-2-ene (norbornene), bicyclo[2.2.1]heptane (norbornane), and tricyclo[3.3.1.13,7]decane (adamantane). *J. Chem. Thermodyn.*, 14:395, 1982.

[347] G. S. Parks, K. E. Manchester, and L. M Vaughan. Heats of combustion and formation of some alcohols, phenols, and ketones. *J. Chem. Phys.*, 22: 2089, 1954.

[348] E. W Balson. Studies in vapour pressure measurement, part ii. a new all-glass manometer sensitive to 0.001 mm. *Trans. Faraday Soc.*, 43:48, 1947.

[349] I. Nitta and S Seki. Vapor pressure of phenol. *Nippon Kagaku Zasshi*, 69:143, 1948.

[350] D. P. Biddiscombe and J. F Martin. Vapour pressures of phenol and the cresols. *Trans. Faraday Soc.*, 54:1316, 1958.

[351] G. H. Parsons, C. H. Rochester, and C. E. C Wood. Effect of 4- substitution on the thermodynamics of hydration of phenol and the phenoxide anion. *J. Chem. Soc. B*, page 533, 1971.

[352] A. F. Bedford, A. E. Beezer, and C. T Mortimer. Heats of formation and bond energies. part x. 1,2,5,6-tetrahydropyridine, piperidine, and piperazine. *J. Chem. Soc.*, page 2039, 1963.

[353] W. D Good. Enthalpies of combustion of nine organic nitrogen compounds related to petroleum. *J. Chem. Eng. Data*, 17:28, 1972.

[354] A. G. Osborn and D. R Douslin. Vapor pressure relations of 13 nitrogen compounds related to petroleum. *J. Chem. Eng. Data*, 13:534, 1968.

[355] J. F. Messerly, S. S. Todd, H. L. Finke, W. D. Good, and B. E Gammon. Condensed-phase heat-capacity studies and derived thermodynamic properties for six cyclic nitrogen compounds. *J. Chem. Thermodyn.*, 20:209, 1988.

[356] I. A. Hossenlopp and D. G Archer. Enthalpies of vaporization of piperidine and 1,2-dimethylbenzene; gas-phase isobaric heat capacities of piperidine. *J. Chem. Thermodyn.*, 20:1061, 1988.

[357] D. D. Wagman, J. E. Kilpatrick, K. S. Pitzer, and F. D. Rossini. Heats, equilibrium constants, and free energies of formation of the acetylene hydrocarbons through the pentynes, to 1500K. *J. Res. Natl. Bur. Stand.*, 35:467, 1945.

[358] J. B. Conn, G. B. Kistiakowsky, and E. A. Smith. Heats of organic reactions. viii some further hydrogenations, including those of some acetylenes. *J. Am. Chem. Soc.*, 61:1868, 1939.

[359] H. M Huffman. Thermal data. xii the heats of combustion of urea and guanidine carbonate and their standard free energies of formation. *J. Am. Chem. Soc.*, 62:1009, 1940.

[360] W. H Johnson. Enthalpies of combustion and formation of acetanilide and urea. *J. Res. Natl. Bur. Stand., Sect. A*, 79A:487, 1975.

[361] M. Månsson and S. Sunner. Heat of formation of sulphuric acid. *Acta Chem. Scand.*, 17:723, 1963.

[362] I. Aleksandrov, Yu, T. R. Osipova, V. F. Yushkevich, S. V. Murashova, and B. N Oleinik. Study of urea as a reference compound for combustion calorimetry. *Termodin. Org. Soedin.*, page 65, 1979.

[363] G. Ya. Kabo, E. A. Miroshnichenko, M. L. Frenkel', A. A. Kozyro, V. V. Simirskii, A. P. Krasulin, and Yu. A Vorob'eva, V. P. ans Lebedev. Thermochemistry of alkyl derivatives of urea. *Doklady Akad. Nauk SSSR Ser. Khim.*, page 750, 1990.

[364] H. P. Diogo and M. E. M de Piedade. A micro-combustion calorimeter suitable for samples of mass 10 mg to 50 mg application to solid compounds of c, h, and o, and of c, h, o, and n. *J. Chem. Thermodyn.*, 27:197, 1995.

[365] M. D. M. C. Ribeiro da Silva, L. M. N. B. F. Santos, A. L. R. Silva, O . Fernandes, W. E. Acree, and Jr Energetics. the dissociation enthalpy of the (n-o) bond. *J. Chem. Thermodyn.*, 35:1093, 2003.

[366] Dz Zaitsau, G. J. Kabo, A. A. Kozyro, and V. M. Sevruk. The effect of the failure of isotropy of a gas in an effusion cell on the vapor pressure and enthalpy of sublimation for alkyl derivatives of carbamide. *Thermochim. Acta*, 406:17, 2003.

[367] V. N. Emel'yanenko, G. J. Kabo, and S. P Verevkin. Measurement and prediction of thermochemical properties: improved increments for the estimation of enthalpies of sublimation and standard enthalpies of formation of alkyl derivatives of urea. *J. Chem. Eng. Data*, 51:79, 2006.

[368] Douglas Bond. Computational methods in organic thermochemistry. 2. enthalpies and free energies of formation for functional derivatives of organic hydrocarbons. *The Journal of Organic Chemistry*, 72(19):7313–7328, 2007. doi: 10.1021/jo071213a. URL http://dx.doi.org/10.1021/jo071213a. PMID: 17713954.

[369] R. D. Johnson. Nist computational chemistry comparison and benchmark data- base, 2005. URL http://srdata.nist.gov/cccbdb. III, Ed.; NIST Standard Reference Database No. 101,Release 11, May 2005.

[370] David Lokhat, Deresh Ramjugernath, and Maciej Starzak. Gas-phase equilibrium constants for the thermally initiated oxidation of hexafluoropropene with molecular oxygen. *Journal of Physical Organic Chemistry*, 28(7):460–471, 2015. ISSN 1099-1395. doi: 10.1002/poc.3437. URL http://dx.doi.org/10.1002/poc.3437. POC-14-0209.R1.

[371] W. D. Good, J. L. Lacina, D. W. Scott, and J. P. McCullough. Combustion calorimetry of organic fluorine compounds. the heats of combustion and formation of the difluorobenzenes, 4-fluorobenzenes, 4-fluorotoluene and m-trifluorotoluic acid. *The Journal of Physical Chemistry*, 66(8):1529–1532, 1962. doi: 10.1021/j100814a035. URL https://doi.org/10.1021/j100814a035.

[372] J.D. Cox, H.A. Gundry, D. Harrop, and A.J. Head. Thermodynamic properties of fluorine compounds 9. enthalpies of formation of some compounds containing the pentafluorophenyl group. *The Journal of Chemical Thermodynamics*, 1(1):77–87, 1969. ISSN 0021-9614. doi: 10.1016/0021-9614(69)90038-X. URL http://www.sciencedirect.com/science/article/pii/002196146990038X.

[373] James J. P. Stewart. Comparison of the accuracy of semiempirical and some dft methods for predicting heats of formation. *Journal of Molecular Modeling*, 10(1):6–12, Feb 2004. ISSN 0948-5023. doi: 10.1007/s00894-003-0157-6. URL https://doi.org/10.1007/s00894-003-0157-6.

[374] HK YAN, JG GU, XW An, and RH HU. Standard enthalpies of formation and enthalpies of isomerization of trichlorobenzenes. *ACTA CHIMICA SINICA*, 45(12):1184–1187, 1987.

[375] V.A. Platonov and Yu.N. Simulin. Standard enthalpies of formation of 1,2,3-trichlorobenzene, 1,2,4,5-tetrachlorobenzene, and hexachlorobenzene. *Russ. J. Phys. Chem. (Engl. Transl.)*, 57, 1983.

[376] Yu.N. Platonov, V.A.; Simulin and M.M. Rozenberg. Standard heat of formation of pentachlorobenzene. calculation of ΔH_c°(g) and ΔE_s°(g) of polychlorobenzenes by the tatevskii method. *Russ. J. Phys. Chem. (Engl. Transl.)*, 59, 1985.

[377] J.D. Cox, D.D. Wagman, and V.A. Medvedev. *CODATA key values for thermodynamics*. CODATA series on thermodynamic properties. Hemisphere Pub. Corp., 1984.

[378] Peter Fowell, J. R. Lacher, and J. D. Park. Reaction heats of organic compounds. part 3.-heats of hydrogenation of methyl bromide and ethyl bromide. *Trans. Faraday Soc.*, 61:1324–1327, 1965. doi: 10.1039/TF9656101324. URL http://dx.doi.org/10.1039/TF9656101324.

[379] G. P. Adams, A. S. Carson, and P. G. Laye. Thermochemistry of reductions caused by lithium aluminium hydride. part 4.-heat of formation of methyl bromide. *Trans. Faraday Soc.*, 62:1447–1449, 1966. doi: 10.1039/TF9666201447. URL http://dx.doi.org/10.1039/TF9666201447.

[380] K. C. Ferguson, E. N. Okafo, and E. Whittle. Bond dissociation energies from equilibrium studies. part 4.-the equilibrium br2+ ch4[right left harpoons] hbr + ch3br. determination of d(ch3-br) and [capital delta]h(ch3br, g). *J. Chem. Soc., Faraday Trans. 1*, 69:295–301, 1973. doi: 10.1039/F19736900295. URL http://dx.doi.org/10.1039/F19736900295.

[381] M. R. Lane, J. W. Linnett, and H. G. Oswin. A study of the c2h4+hcl=c2h5cl and c2h4+hbr=c2h5br equilibria. *Proceedings of the Royal Society of London A: Mathematical, Physical and Engineering Sciences*, 216(1126):361–374, 1953. ISSN 0080-4630. doi: 10.1098/rspa.1953.0027. URL http://rspa.royalsocietypublishing.org/content/216/1126/361.

[382] S. J. Ashcroft, A. S. Carson, W. Carter, and P. G. Laye. Thermochemistry of reductions caused by lithium aluminium hydride. part 3.-the c-halogen bond dissociation energies in ethyl iodide and ethyl bromide. *Trans. Faraday Soc.*, 61:225–229, 1965. doi: 10.1039/TF9656100225. URL http://dx.doi.org/10.1039/TF9656100225.

[383] S. A. Kudchadker and A. P. Kudchadker. Ideal gas thermodynamic properties of selected bromoethanes and iodoethane. *Journal of Physical and Chemical Reference Data*, 8(2):519–526, 1979. doi: 10.1063/1.555601. URL https://doi.org/10.1063/1.555601.

[384] B. Ruscic and D. H. Bross. Active thermochemical tables (atct) values based on ver. 1.122 of the thermochemical network, 2016.

[385] J. R. Lacher, A. Kianpour, P. Montgomery, H. Knedler, and J. D. Park. Reaction heats of organic halogen compounds. ix. the catalytic hydrogenation of vinyl and perfluorovinyl bromide. *The Journal of Physical Chemistry*, 61(8):1125–1126, 1957. doi: 10.1021/j150554a020. URL http://dx.doi.org/10.1021/j150554a020.

[386] J Davies, JR Lacher, and JD Park. Reaction heats of organic compounds. part 4.—heats of hydrogenation of n-and iso-propyl bromides and chlorides. *Transactions of the Faraday Society*, 61:2413–2416, 1965.

[387] Lars Bjellerup. On the accuracy of heat of combustion data obtained with a precision moving-bomb calorimetric method for organic bromine compounds. *Acta Chemica Scandinavica*, 15(15):121–140, 1961.

[388] D. N. Andreevskii A. M. Rozhnov. Equilibrium of the $C_3H_7Br \leftrightarrows C_3H_6$ + HBr reaction. *Dokl. Akad. Nauk SSSR*, 147:388–391, 1962. URL http://mi.mathnet.ru/dan27231.

[389] O. H. Gellner and H. A. Skinner. 244. dissociation energies of carbon-halogen bonds. the bond strengths allyl-x and benzyl-x. *J. Chem. Soc.*, pages 1145–1148, 1949. doi: 10.1039/JR9490001145. URL http://dx.doi.org/10.1039/JR9490001145.

[390] John C. Traeger. A study of the allyl cation thermochemistry by photoionization mass spectrometry. *International Journal of Mass Spectrometry and Ion Processes*, 58:259–271, 1984. ISSN 0168-1176. doi: 10.1016/0168-1176(84)80034-8. URL http://www.sciencedirect.com/science/article/pii/0168117684800348.

[391] Lars Bjellerup. Heats of combustion and formation of the 1-bromoalkanes from c4 through c8. *Acta Chemica Scandinavica*, 15(2):231–241, 1961.

[392] Allan Lord, C. A. Goy, and Huw O. Pritchard. The heats of formation of trifluoromethyl chloride and bromide. *The Journal of Physical Chemistry*, 71 (8):2705–2707, 1967. doi: 10.1021/j100867a048. URL http://dx.doi.org/10.1021/j100867a048.

[393] J. W. Coomber and E. Whittle. Bond dissociation energies from equilibrium studies. part 1.-d(cf3-br), d(c2f5-br) and d(n-c3f7-br). *Trans. Faraday Soc.*, 63:608–619, 1967. doi: 10.1039/TF9676300608. URL http://dx.doi.org/10.1039/TF9676300608.

[394] G. Lord and A. A. Woolf. The cyanogen halides. part iii. their heats of formation and free energies. *J. Chem. Soc.*, pages 2546–2551, 1954. doi: 10.1039/JR9540002546. URL http://dx.doi.org/10.1039/JR9540002546.

[395] TS Papina, VP Kolesov, and Yu G Golovanova. The standard enthalpy of formation of bromoform. *Russ. J. Phys. Chem*, 56:1666–1172, 1982.

[396] D. W. Scott, D. R. Douslin, H. L. Finke, W. N. Hubbard, J. F. Messerly, I. A. Hossenlopp, and J. P. McCullough. 2-methyl-2-butanethiol: Chemical thermodynamic properties and rotational isomerism. *The Journal of Physical Chemistry*, 66(7):1334–1341, 1962. doi: 10.1021/j100813a028. URL http://dx.doi.org/10.1021/j100813a028.

[397] M Mansson and S Sunner. Heats of combustion and formation of the n-alkane-$\alpha\omega$-dithiols from ethane through pentane,. *ACTA CHEMICA SCANDINAVICA*, 16:1863–1869, 1962.

[398] W. D. Good and B. L. DePrater. The enthalpies of combustion and formation of the 1-alkanethiols. the methylene increment to the enthalpy of formation1. *The Journal of Physical Chemistry*, 70(11):3606–3609, 1966. doi: 10.1021/j100883a041. URL http://dx.doi.org/10.1021/j100883a041.

[399] Ward N. Hubbard, Charles Katz, and Guy Waddington. A rotating combustion bomb for precision calorimetry. heats of combustion of some sulfur-containing compounds. *The Journal of Physical Chemistry*, 58(2):142–152, 1954. doi: 10.1021/j150512a010. URL http://dx.doi.org/10.1021/j150512a010.

[400] S Sunner, Leslie Leifer, and Örjan Wiberg. Corrected heat of combustion and formation values for a number of organic sulphur compounds. *Acta Chemica Scandinavica*, 17:728–730, 01 1963.

[401] Ward N. Hubbard, William D. Good, and Guy Waddington. The heats of combustion, formation and isomerization of the seven isomeric c4h10s alkane thiols and sulfides. *The Journal of Physical Chemistry*, 62(5):614–617, 1958. doi: 10.1021/j150563a024. URL http://dx.doi.org/10.1021/j150563a024.

[402] Ward N. Hubbard and Guy Waddington. The heats of combustion, formation and isomerization of propanethiol-1, propane-thiol-2 and 2-thiabutane. *Recueil des Travaux Chimiques des Pays-Bas*, 73(11):910–923, 1954. ISSN 0165-0513. doi: 10.1002/recl.19540731107. URL http://dx.doi.org/10.1002/recl.19540731107.

[403] William D. Good. Enthalpies of combustion of 18 organic sulfur compounds related to petroleum. *Journal of Chemical & Engineering Data*, 17(2): 158–162, 1972. doi: 10.1021/je60053a049. URL http://dx.doi.org/10.1021/je60053a049.

[404] J.B. Pedley. *Thermochemical Data of Organic Compounds*. Springer Netherlands, 1986. ISBN 9780412271007. URL https://books.google.fr/books?id=dTRmQgAACAAJ.

[405] H. Mackle and R. T. B. McClean. Studies in the thermochemistry of organic sulphides. part 4.-heat of formation of the mercaptyl radical. *Trans. Faraday Soc.*, 58:895–899, 1962. doi: 10.1039/TF9625800895. URL http://dx.doi.org/10.1039/TF9625800895.

[406] D. W. Scott and G. A. Crowder. Cyclohexanethiol and 2,4-dimethyl-3-thiapentane: Molecular vibrations, conformational analyses, and chemical thermodynamic properties. *The Journal of Chemical Physics*, 46(3):1054–1062, 1967. doi: 10.1063/1.1840768. URL https://doi.org/10.1063/1.1840768.

[407] W. T. Berg, D. W. Scott, W. N. Hubbard, S. S. Todd, J. F. Messerly, I. A. Hossenlopp, Ann Osborn, D. R. Douslin, and J. P. McCullough. The chemical thermodynamic properties of cyclopentanethiol1. *The Journal of Physical Chemistry*, 65(8):1425–1430, 1961. doi: 10.1021/j100826a035. URL http://dx.doi.org/10.1021/j100826a035.

[408] J. P. McCullough, W. N. Hubbard, F. R. Frow, I. A. Hossenlopp, and Guy Waddington. Ethanethiol and 2-thiapropane: Heats of formation and isomerization; the chemical thermodynamic properties from 0 to 1000 k. *Journal of the American Chemical Society*, 79(3):561–566, 1957. doi: 10.1021/ja01560a017. URL http://dx.doi.org/10.1021/ja01560a017.

[409] W. D. Good, J. L. Lacina, and J. P. McCullough. Methanethiol and carbon disulfide: Heats of combustion and formation by rotating-bomb calorimetry1. *The Journal of Physical Chemistry*, 65(12):2229–2231, 1961. doi: 10.1021/j100829a031. URL http://dx.doi.org/10.1021/j100829a031.

[410] J. Peter Guthrie. Hydration of thioesters. evaluation of the free-energy changes for the addition of water to some thioesters, rate-equilibrium correlations over very wide ranges in equilibrium constants, and a new mechanistic criterion. *Journal of the American Chemical Society*, 100(18): 5892–5904, 1978. doi: 10.1021/ja00486a048. URL http://dx.doi.org/10.1021/ja00486a048.

[411] J. P. McCullough, D. W. Scott, H. L. Finke, W. N. Hubbard, M. E. Gross, C. Katz, R. E. Pennington, J. F. Messerly, and Guy Waddington. The thermodynamic properties of 2-methyl-2propanethiol from 0 to 1000 k. *Journal of the American Chemical Society*, 75(8):1818–1824, 1953. doi: 10.1021/ja01104a011. URL http://dx.doi.org/10.1021/ja01104a011.

[412] James V. Davies and Stig Sunner. Heats of combustion and formation of thiolane and of the thiolenes. *Acta Chemica Scandinavica*, 16:1870–1876, 1962. doi: 10.3891/acta.chem.scand.16-1870.

[413] W. N. Hubbard, D. W. Scott, F. R. Frow, and G. Waddington. Thiophene: Heat of combustion and chemical thermodynamic properties1. *Journal of the American Chemical Society*, 77(22):5855–5857, 1955. doi: 10.1021/ja01627a023. URL http://dx.doi.org/10.1021/ja01627a023.

[414] George E. Moore, Melvin L. Renquist, and George S. Parks. Thermal data on organic compounds. xx. modern combustion data for two methylnonanes, methyl ethyl ketone, thiophene and six cycloparaffins. *Journal of the American Chemical Society*, 62(6):1505–1507, 1940. doi: 10.1021/ja01863a049. URL http://dx.doi.org/10.1021/ja01863a049.

[415] Guy. Waddington, J. W. Knowlton, D. W. Scott, G. D. Oliver, S. S. Todd, W. N. Hubbard, J. C. Smith, and Hugh M. Huffman. Thermodynamic properties of thiophene. *Journal of the American Chemical Society*, 71(3):797–808, 1949. doi: 10.1021/ja01171a010. URL http://dx.doi.org/10.1021/ja01171a010.

[416] M Zaheeruddin and ZH Lodhi. Enthalpies of formation of some cyclic compounds. *Phys. Chem.(Peshawar, Pak.)*, 10:111–118, 1991.

[417] D. W. Scott, J. P. McCullough, W. N. Hubbard, J. F. Messerly, I. A. Hossenlopp, F. R. Frow, and Guy Waddington. Benzenethiol: Thermodynamic properties in the solid, liquid and vapor states; internal rotation of the thiol group1. *Journal of the American Chemical Society*, 78(21):5463–5468, 1956. doi: 10.1021/ja01602a002. URL http://dx.doi.org/10.1021/ja01602a002.

[418] Geoffrey Pilcher, M. Luisa P. Leitao, Yang Meng-Yan, and Robin Walsh. Standard enthalpy of formation of hexamethyldisilane. *J. Chem. Soc., Faraday Trans.*, 87:841–845, 1991. doi: 10.1039/FT9918700841. URL http://dx.doi.org/10.1039/FT9918700841.

[419] Domenico Simone, Claudio Bruno, and Bernhard Hidding. Silanes as fuel for aerospace propulsion. *Transactions of the Japan Society for Aeronautical and Space Sciences, Space Technology Japan*, 7(ists26):33–39, 2009.

[420] S.N. Hajiev and M.J. Agarunov. Thermochemical studies of organometallic compounds ii. thermochemistry of methylchlorosilanes. *Journal of Organometallic Chemistry*, 22:305–311, 1970.

[421] W.Vincent Wilding, Richard L Rowley, and John L Oscarson. Dippr® project 801 evaluated process design data. *Fluid Phase Equilibria*, 150-151: 413–420, 1998. ISSN 0378-3812. doi: 10.1016/S0378-3812(98)00341-0. URL http://www.sciencedirect.com/science/article/pii/S0378381298003410.

INSTITUT POLYTECHNIQUE DE PARIS

Titre : Modélisation de la conversion thermique de carburants verts de type bio-huiles

Mots clés : Biomasse, Solvatation, Cinétique chimique de la phase liquide, Enthalpies de formation

Résumé : La production de bio-huiles par conversion thermochimique de la biomasse est un procédé prometteur pour le bioraffinage. Alors que la cinétique en phase gazeuse de la conversion de la bio-huile est bien avancée, sa réactivité en phase liquide reste mal connue. L'objectif de cette thèse est de comprendre le mécanisme cinétique détaillé de la décomposition thermochimique de la biomasse à basse température en phase liquide. Une phase liquide est observée pendant la première étape de la pyrolyse de la biomasse. Dans cette étude, nous tenterons de modéliser le premier stade de la pyrolyse de la biomasse. A notre connaissance, aucune étude de modélisation de la réactivité en phase liquide n'a été proposée pour la pyrolyse de la biomasse. L'étude des réactions en phase liquide de ces systèmes complexes nécessite une bonne connaissance de l'influence du solvant sur la cinétique. Nous avons en premier temps comparé la prédiction des modèles COSMO-SAC avec celles du modèle de solvatation Abraham, en considérant la base de données COMPSOL comme référence. Nous avons ensuite proposé une re-paramétrisation de ces modèles COSMO-SAC qui conduit à de bien meilleures prédictions et nous permets d'étendre ces modèles à l'utilisation des cavitées CPCM. Les méthodes prédictives basées sur des calculs ab initio peuvent être très précises pour prédire les propriétés thermochimiques en phase gazeuse et sont généralement plus polyvalentes que les méthodes de contribution de groupe. Une extension de la méthode ab initio de prédiction des enthalpies de formation de Paulechka et Kazakov a été proposée dans ce travail et utilisée pour les composés de la biomasse. A l'aide du générateur de mécanismes réactionnels (RMG) nous avons prédit les différents chemins réactionnels possibles de la décomposition des composés représentatifs de la partie lignine de la biomasse. Les composés choisis sont le créosol, le gaïacol et le méthoxyvinylphénol. Ce travail peut être considéré comme une extension du mécanisme en phase gazeuse de la pyrolyse proposé par Ranzi et ses colaborateurs en considérant la recombinaison radicalaire et la polymérisation qui se produit à basse température entre 100 °C et 300 °C. Pour modéliser la cinétique des réactions clés, nous les avons étudiés par l'approche des états de transition à l'aide de Gaussian 09 et d'ORCA. L'estimation des paramètres cinétiques est ensuite déterminé par la théorie des états de transition et de l'approche Green de la cinétique en phase liquide.

Title : Multiscale modeling of thermochemical conversion of bio-oils

Keywords : Biomass, Solvation, Chemical kinetics of liquid phase, Enthalpies of Formation

Abstract : Production of bio-oils through thermochemical biomass conversion is a promising process for biorefining. While gas-phase kinetics of bio-oil conversion has been improving, its liquid phase reactivity is currently poorly understood. The aim work of my thesis is about the understanding of detailed kinetics mechanism of biomass thermochemical decomposition at low temperature range in the liquid phase. A liquid phase is observed during the first stage of biomass pyrolysis. In this study we will try to model the first stage of biomass pyrolysis. To our knowledge, no modelling study of the rate of reactions in the liquid phase has been proposed for biomass pyrolysis. The investigation of liquid phase reactions of such complex systems requires a good knowledge of solvent effects. We compared the prediction capabilities of COSMO-SAC with those of the Abraham solvation model, by considering the COMPSOL database as the reference data. We then proposed a re-parametrization of these COSMO-SAC models that leads to much better predictions, and extend these models to CPCM cavities. Predictive methods based on ab initio calculations can be very accurate for predicting gas phase thermochemical properties and are usually more versatile than group contribution methods. An extension of Paulechka and Kazakov ab initio prediction method of enthalpies of formation was proposed in our study and used for biomass compounds. We then used Reaction Mechanism Generator (RMG) to investigate the possible reaction mechanism of different Tar surrogate compounds of biomass decomposition. The surrogate compounds that we chose are Creosol, guaiacol and methoxy vinylphenol to model the lignin. This work can be considered as an extension of the gas phase reaction mechanism of pyrolysis proposed by Ranzi and co-workers taking in consideration the primary tar recombination/polymerisation reaction that occur in the temperature range 100 °C to 300 °C. To model the kinetics of the key reaction, we investigated the Transitional state using Gaussian 09 and ORCA. We then estimated the kinetics parameters using Transitional State Theory with Kisthelp tool and Green's liquid phase kinetics approach based on the gas phase kinetics and solvation free energies correction.

Institut Polytechnique de Paris
91120 Palaiseau, France